Universitat Autònoma de Barcelona

Modern NMR Methodologies for the Measurement of Homo- and Heteronuclear Coupling Constants in Small Molecules

Josep Saurí i Jiménez

Doctoral Thesis

PhD in Chemistry
Director: Dr. Teodor Parella i Coll
Chemistry Department
Faculty of Sciences
2014

Universitat Autònoma de Barcelona

Chemistry Department
Faculty of Sciences

Memòria presentada per aspirar al Grau de Doctor per Josep Saurí i Jiménez

Vist i plau,

Dr. Teodor Parella i Coll **Josep Saurí i Jiménez**

Bellaterra, a 3 d'abril de 2014

A la meva àvia i al meu avi, que descansa.
També als meus pares.

A la Carol.

INDEX

ACKNOWLEDGMENTS

I would like to thank the financial support for this research provided by the following institutions:

- Project: "Nuevas metodologías en Resonancia Magnética Nuclear (part III)" CTQ2009-08328. MICINN, IP: Dr. Teodor Parella Coll

- Project: "Nuevas metodologías en Resonancia Magnética Nuclear (Part IV)" CTQ2012-32436. MINECO, IP: Dr. Teodor Parella Coll

I also want to express my personal gratitude for a grant received from MICINN:

- Beca Predoctoral FPI BES-2010-035106

A la primera persona que vull agrair és a en Teo. Li agraeixo tot el que he après durant els anys de tesi. Sempre m'he sentit molt afortunat de recaure en un grup de recerca liderat per algú que domina tant àmpliament el seu tema. Al principi no te'n adones, ho vas esbrinant amb el pas del temps. Al final, com a doctorand que esta de pas, he intentat treure el màxim profit de la possibilitat de treballar amb ell. Estic segur que el futur més immediat fent un post-doc a Merck amb en Gary Martin és gràcies a ell en gran part. A més a més considero que sap molt bé com portar un doctorand, com donar-li llibertat de maniobra i ajudar-lo quan cal. Finalment també agrair-li tots els congressos als que m'ha permès anar, on vam poder guanyar inclús un premi al millor pòster!

També vull agrair molt a en Miquel, figura indispensable al SeRMN. Personalment penso que si en Teo és el pare, en Miquel és la mare, si en Teo mana, en Miquel dirigeix. No la meva feina diària, però sí la rutina del dia a dia del Servei. M'ha ajudat en cada contratemps de caràcter tècnic de manera impecable. Agrair també als companys del laboratori. A en Sergi, que em va ajudar molt quan jo vaig començar i ell estava acabant. Quan comences a introduir-te al mon de la Ressonància Magnètica Nuclear al principi és difícil (després també però ja hi estàs més familiaritzat) i ell em va ajudar molt. Després especialment també a en Pau, que en sap molt de ressonància, i que sempre m'ha ajudat, sobretot també al principi. Evidentment a la resta dels companys també, la Míriam, la Sílvia, la Eva, la Laura i l'Albert, tots collonuts. Amb en Pau, la Laura i l'Albert trobaré a faltar les birres dels divendres al bar de ciències, on s'hi arribava a reunir molta gent. No em vull deixar l'Albert Virgili, que sempre que ha baixat al Servei ha estat una alegria.

Agrair al meu cercle d'amics més pròxim, que ja fa molts anys que ens coneixem, en Dani, la Laura, l'Aloa i Jordi, Esther i David, Mercè i Joan també... I a qui més a la Carol, la meva amiga, la meva parella... la meva millor conquesta i amb qui ja fa més de deu anys que estem junts, la que serà la meva dona i que m'acompanyarà a la nova aventura que ens espera i a qui estimo molt. I sense oblidar que va ser ella qui em va convèncer per iniciar el doctorat en RMN! El que pugui dir aquí es quedarà curt... li agraeixo infinites coses.

Finalment, a les meves germanes i als meus pares, la meva família, que sé que estan molt contents per mi.

LIST OF ACRONYMS

AP	**A**nti-**P**hase
BIRD	**BI**linear **R**otation **D**ecoupling
CLIP	**CL**ean **I**n-**P**hase
COSY	**CO**rrelation **S**pectroscop**Y**
CPMG	**C**arr-**P**urcell-**M**einboom-**G**ill
CTP	**C**oherence **T**ransfer **P**athway
DQ	**D**ouble **Q**uantum
ECOSY	**E**xclusive **CO**rrelation **S**pectroscop**Y**
EXSIDE	**EX**citation **S**culptured **I**ndirect **D**etection **E**xperiment
FID	**F**ree **I**nduction **D**ecay
GBIRD	**G**radient **BI**linear **R**otation **D**ecoupling
HECADE	**HE**teronuclear **C**ouplings from **A**SSCI-**D**omain with **E**.COSY-type cross peaks
HETLOC	**HET**eronuclear **LO**ng-Range **C**oupling
HMBC	**H**eteronuclear **M**ultiple **B**ond **C**orrelation
HMQC	**H**eteronuclear **M**ultiple **Q**uantum **C**oherence
HSQC	**H**eteronuclear **S**ingle **Q**uantum **C**oherence
HSQMBC	**H**eteronuclear **S**ingle **Q**uantum **M**ultiple-**B**ond **C**orrelation
INEPT	**I**nsensitive **N**uclei **E**nhanced by **P**olarization**T**ransfer
IP	**I**n-**P**hase
IPAP	**I**n-**P**hase **A**nti-**P**hase
MQ	**M**ultiple **Q**uantum
NMR	**N**uclear **M**agnetic **R**esonance
NOE	**N**uclear **O**verhauser **E**ffect
p	Coherence order
PEP	**P**reservation of **E**quivalent **P**athways
PFG	**P**ulse **F**ield **G**radient
RDC	**R**esidual **D**ipolar **C**oupling
R-INEPT	**R**efocused **I**nsensitive **N**uclei **E**nhanced by **P**olarization**T**ransfer
S^3	Spin State Selective
SNR	**S**ignal-to-**N**oise **R**atio
SQ	**S**ingle **Q**uantum
TOCSY	**TO**tal **C**orrelation **S**pectroscop**Y**
TROSY	**T**ransverse **R**elaxation **O**ptimized **S**pectroscop**Y**
TS	**T**ime **S**hared
ZQ	**Z**ero **Q**uantum

THESIS OUTLINE

This thesis is presented as a compendium of publications. The structure has been organized in five sections.

I. Introduction

This section contains a brief general explanation of some of the most fundamental NMR concepts that are needed to understand 2D NMR heteronuclear shift correlation NMR experiments. In turn, a general overview describing the main features of existing NMR methods for the measurement of heteronuclear coupling constants is also introduced.

II. Objectives

The main goals that led to the development of this thesis are detailed.

III. Results and Discussion

All new modern NMR methods developed during my PhD aimed to the measurement of coupling constants in small molecules are presented as *Original Research Papers* (Publications) in separate chapters.

IV. Appendixes

In this section, additional related works that have not been published yet and therefore they could not be included as *Original Research Papers* are reported.

V. Conclusions

A summary on the major conclusions extracted from this thesis are described.

I. INTRODUCTION

1. Fundamental aspects of 2D heteronuclear shift correlation NMR experiments

Proton–carbon coupling constants (J(CH)), as well as proton–proton coupling constants (J(HH)) and Nuclear Overhauser Effect (NOE), play an important role in molecules containing basically proton and carbon atoms, such as any type of organic-based compounds, natural products and biomolecules[1]. They can provide information about structure, conformation and dynamics of rigid and flexible molecules in solution, as well as they can serve as structural validation methods, determine multiple-conformation states in cyclic and acyclic spin systems or to be useful for the measurement of Residual Dipolar Couplings (RDCs) in molecules dissolved in weakly aligned media.

As this work is basically focused in the development of novel Nuclear Magnetic Resonance (NMR) methodologies for the measurement of several coupling constants, it is important to introduce two of the most fundamental NMR concepts that have been used in the design of novel pulse sequences: a) the inverse detection technique implemented in heteronuclear chemical–shift correlation experiments and b) the incorporation of Pulsed Field Gradients (PFGs) as a tool for coherence selection into such pulse sequences.

1.1 Inverse detection in NMR experiments

It is well known that sensitivity is one of the main problems in NMR. That fact is especially evident in heteronuclear correlation experiments, where the low natural abundance of the ^{13}C nucleus (1.1%) introduces an additional sensitivity penalty. In such NMR experiments the relative signal-to-noise ratio (SNR) is proportional to

$$\gamma_{exc}\gamma_{det}^{3/2}$$

Equation 1

where γ_{exc} and γ_{det} stands for the the gyromagnetic ratio (γ) of the excited and detected nuclei, respectively[2].

Four general schemes can be devised to perform a heteronuclear correlation experiment, according to which spin is used as the initial magnetization source and which is detected (**Fig. 1.01**).

[1] a) J. L. Marshall, Carbon–Carbon and Carbon–Proton NMR Couplings: Applications to Organic Stereochemistry and Conformational Analysis (Methods in Stereochemical Analysis) Verlag Chemie International. **1982**. b) W. A. Thomas. *Prog. Nucl. Magn. Reson. Spectrosc*. **1997**, 30, 183. c) N. Matsumori, D. Kaneno, M. Murata, H. Nakamura, K. Tachibana. *J. Org. Chem.*, **1999**, 64, 866. d) M. Tafazzoli, M. Ghiasi. *Carbohydr. Res*. **2007**, 342, 2086.

[2] T. D.W. Claridge. High-resolution NMR techniques in organic chemistry, Elsevier, Orford, UK. **1982**.

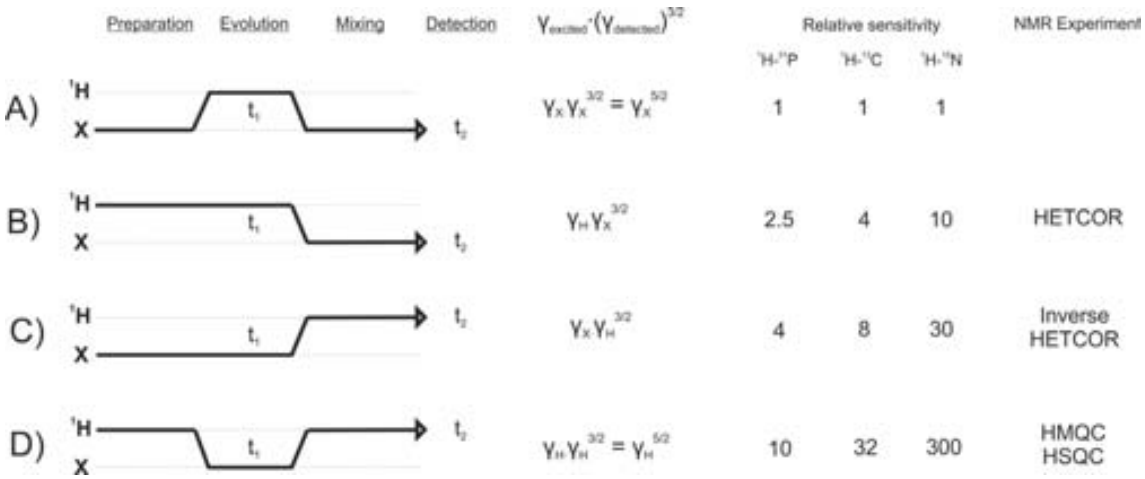

	$\gamma_{excited} \cdot (\gamma_{detected})^{3/2}$	^1H-^{31}P	^1H-^{13}C	^1H-^{15}N	NMR Experiment
A)	$\gamma_X \gamma_X^{3/2} = \gamma_X^{5/2}$	1	1	1	
B)	$\gamma_H \gamma_X^{3/2}$	2.5	4	10	HETCOR
C)	$\gamma_X \gamma_H^{3/2}$	4	8	30	Inverse HETCOR
D)	$\gamma_H \gamma_H^{3/2} = \gamma_H^{5/2}$	10	32	300	HMQC HSQC

Figure 1.01. General approaches to record 2D heteronuclear correlation spectra as a function of the excited and detected nuclei. The relative sensitivities of each approach is compared for ^{1}H correlation experiments with ^{31}P, ^{13}C or ^{15}N.

Fig. 1.01D uses the well-known inverse detection technique, initially proposed in 1979 by Morris and Freeman[3]. Taking into account that $\gamma_H/\gamma_C = 4$, inverse detection enhances the relative SNR by a factor of 32 in ^{1}H-^{13}C correlation experiments when compared with those experiments that use direct detection of the heteronucleus (**Fig. 1.01A** vs **Fig. 1.01D**). The enhancement arises from the transfer of nuclear spin polarization from spins with large Boltzmann population differences (usually protons) to spins with smaller Boltzmann population differences. The SNR increases as the γ of the heteronucleus has a lower value and the absolute sensitivity also depends of the natural abundance of the heteronucleus. Keeping in mind these important features, the proton-detected inverse-correlation method has become the universal adoption whenever possible in both chemical and biological NMR spectroscopy, being extensible to 3D and higher multidimensional experiments of proteins and nucleic acids.

1.1.1 The INEPT sequence

An important building block in modern NMR spectroscopy is the INEPT[3] (Insensitive Nuclei Enhanced by Polarization Transfer) pulse train (**Fig. 1.02**).

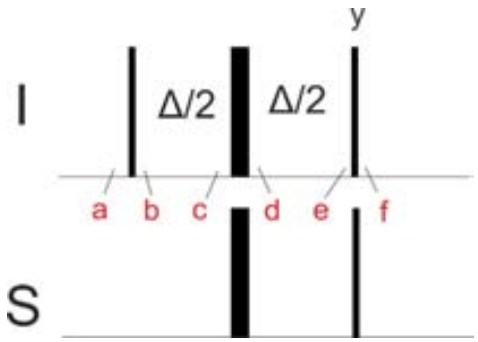

Figure 1.02. Basic INEPT pulse sequence. Narrow and wide bars indicate 90º and pulses 180º pulses, respectively. The inter-pulse Δ delay is set to $\Delta=1/(2\cdot J_{IS})$

[3] G. A. Morris, R. Freeman. *J. Am. Chem. Soc.* **1979**, 233, 760.

In what follows, an extensive analysis using the Product Operator Formalism[4] is made to understand the way how INEPT works. Let us consider a IS spin system where I nucleus (usually ^{1}H) is coupled to a heteronuclear S spin (usually ^{13}C or ^{15}N), with a J(IS) coupling value:

- Initially, at point a, magnetization is at its equilibrium position along the z-axis (I_z)
- The 90º(x) I pulse rotates the magnetization of the I spin from z-axis to the transverse xy-plane (point b)

$$I_z \xrightarrow{90_x^I} -I_y$$

- Then, during the evolution Δ/2 delay (Δ=1/(2J_{IS})) the magnetization components evolve simultaneously under both chemical shift and coupling constant effects. For clarity, these effects are shown separately. Thus, at point c we have

$$-I_y \xrightarrow{2\pi J_{IS}\Delta} -I_y\cos(\pi J_{IS}\Delta)+2I_xS_z\sin(\pi J_{IS}\Delta)$$

$$-I_y \xrightarrow{\Omega_I\Delta} -I_y\cos(\Omega_I\Delta) + I_x\sin(\Omega_I\Delta)$$

- Then, the 180º(x) I pulse (point d) inverts the I magnetization along the x-axis

$$-I_y\cos(\pi J_{IS}\Delta)+2I_xS_z\sin(\pi J_{IS}\Delta) \qquad -I_y\cos(\Omega_I\Delta)+I_x\sin(\Omega_I\Delta)$$

$$\downarrow 180_x^I \qquad \downarrow 180_x^I$$

$$+I_y\cos(\pi J_{IS}\Delta)+2I_xS_z\sin(\pi J_{IS}\Delta) \qquad +I_y\cos(\Omega_I\Delta)+I_x\sin(\Omega_I\Delta)$$

whereas the 180º(x) S pulse inverts the α/β- labels of the doublet I component

$$+I_y\cos(\pi J_{IS}\Delta)+2I_xS_z\sin(\pi J_{IS}\Delta) \qquad +I_y\cos(\Omega_I\Delta)+I_x\sin(\Omega_I\Delta)$$

$$\downarrow 180_x^S \qquad \downarrow 180_x^S$$

$$+I_y\cos(\pi J_{IS}\Delta)-2I_xS_z\sin(\pi J_{IS}\Delta) \qquad +I_y\cos(\Omega_I\Delta)+I_x\sin(\Omega_I\Delta)$$

- At the end of the second Δ/2 delay (point e), the chemical shift of I has been refocused to its original position

[4] O. W. Sorensen, G. W. Eich, M. H. Levitt, G. Bodenhausen, R. R. Ernst. *Prog. Nucl. Magn. Reson. Spectrosc.* **1983**, 16, 163.

$$+I_y\cos(\Omega_I\Delta)+I_x\sin(\Omega_I\Delta) \xrightarrow{\Omega_I\Delta} \begin{matrix} +I_y\cos(\Omega_I\Delta)\cos(\Omega_I\Delta) - I_x\cos(\Omega_I\Delta)\sin(\Omega_I\Delta) \\ + I_x\sin(\Omega_I\Delta)\cos(\Omega_I\Delta) - I_y\sin(\Omega_I\Delta)\sin(\Omega_I\Delta) \end{matrix}$$

$$\downarrow$$

$$+I_y\cos^2(\Omega_I\Delta) - I_y\sin^2(\Omega_I\Delta)$$

$$\downarrow \quad \cos^2\theta + \sin^2\theta = 1$$

$$\boxed{-I_y}$$

whereas the components of the heteronuclear J(IS) coupling constant are in anti-phase (AP) mode along the x-axis, in the form of $2I_xS_z$.

$$+I_y\cos(\pi J_{IS}\Delta)-2I_xS_z\sin(\pi J_{IS}\Delta) \xrightarrow{2\pi J_{IS}\Delta} \begin{matrix} +I_y\cos(\pi J_{IS}\Delta)\cos(\pi J_{IS}\Delta) \\ - 2I_xS_z\cos(\pi J_{IS}\Delta)\sin(\pi J_{IS}\Delta) \\ -2I_xS_z\sin(\pi J_{IS}\Delta)\cos(\pi J_{IS}\Delta) \\ - I_y\sin(\pi J_{IS}\Delta)\sin(\pi J_{IS}\Delta) \end{matrix}$$

$$\downarrow$$

$$+I_y[\cos^2(\pi J_{IS}\Delta)-\sin^2(\pi J_{IS}\Delta)] - 2I_xS_z[2\cos(\pi J_{IS}\Delta)\sin(\pi J_{IS}\Delta)]$$

$$\downarrow \quad \begin{matrix} \cos2(\theta)= \cos^2\theta - \sin^2\theta \\ \sin2(\theta)= 2\cos\theta\sin\theta \end{matrix}$$

$$+I_y\cos(2\pi J_{IS}\Delta) - 2I_xS_z\sin(2\pi J_{IS}\Delta)$$

- Finally, at point f, a 90º(y) I pulse generates zz-magnetization in the form of $2I_zS_z$

$$+I_y\cos(2\pi J_{IS}\Delta) - 2I_xS_z\sin(2\pi J_{IS}\Delta) \xrightarrow{90^I_y} +I_y\cos(2\pi J_{IS}\Delta)-2I_zS_z\sin(2\pi J_{IS}\Delta)$$

and a 90º(x) S pulse returns the magnetization to the xy-plane but now converted into S anti-phase magnetization with respect to the I spin, in the form of $2I_zS_y$.

$$+I_y\cos(2\pi J_{IS}\Delta)-2I_zS_z\sin(2\pi J_{IS}\Delta) \xrightarrow{90^S_x} +I_y\cos(2\pi J_{IS}\Delta)-2I_zS_y\sin(2\pi J_{IS}\Delta)$$

Nowadays, the INEPT pulse train constitutes a key block in most of modern multidimensional NMR experiments.

1.2 Pulse Field Gradients in NMR experiments

1.2.1 Fundamentals

In the early 90s, another major step was made after the incorporation of Pulsed Field Gradients (PFGs) as a method for coherence selection in high-resolution NMR spectroscopic techniques[5]. During a PFG (applied for a short period of some milliseconds) a spatial inhomogeneity along a specific axis of the static B_0 field is created in such a way that the magnetization is dephased. This spatially dependent phase created is given by

$$\Phi(r,\tau) = sB_g(r)\tau\sum_j p_j\gamma$$

Equation 2

where *s* is a shape factor, B_g is the spatially dependent (r) magnetic field and *p* and *γ* are the coherence order and the gyromagnetic ratio, respectively, of the individual *j* nuclear spins involved. It is assumed that in modern NMR spectrometers gradients are applied preferably along z-axis, so that the magnetic field produced by the PFG varies linearly along z-axis according to

$$B_g(r) = Gz$$

Equation 3

where G is the gradient expressed in $G{\cdot}cm^{-1}$. As a result, all the magnetization that is not located along the z-axis is dephased during the gradient and apparently lost. However, this loss can be further recovered by properly applying another PFG, restoring thus part of the magnetization (**Fig. 1.03**).

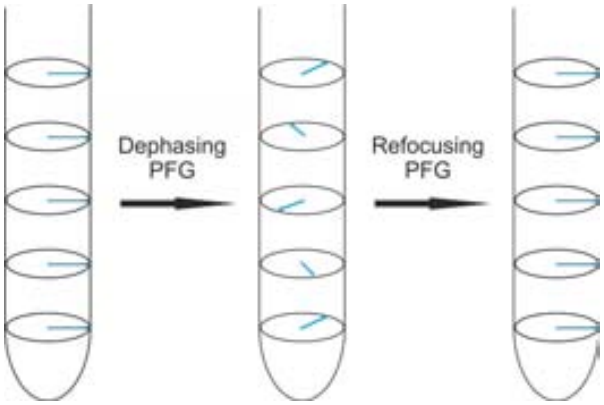

Figure 1.03. General strategy followed in gradient-based NMR experiments. First, a dephasing gradient is applied to generate a spatially-dependent phase. Then, in another part of the pulse sequence, a refocusing gradient is applied to recover the selected signal, as a function of the involved coherence orders.

To describe the effects of PFGs, it is convenient to convert the Cartesian operators I_x and I_y in terms of raising and lowering operators I^+ and I^-, respectively

[5] T. Parella. *Magn. Reson. Chem*. **1998**, 36, 467.

$$I^{+} = I_x + iI_y$$
$$I^{-} = I_x - iI_y$$

Equation 4

The evolution of the magnetization during a pulse sequence can be followed using the Coherence Transfer Pathway (CTP) (**Fig. 1.04**), which shows how the coherence orders (p) change during a pulse sequence. The coherence orders can be classified as:

- Single quantum coherences have p = ±1.
- Double quantum coherences have p = ±2.
- …
- Zero quantum coherence, as well as z-magnetization and zz-terms, have p = 0.

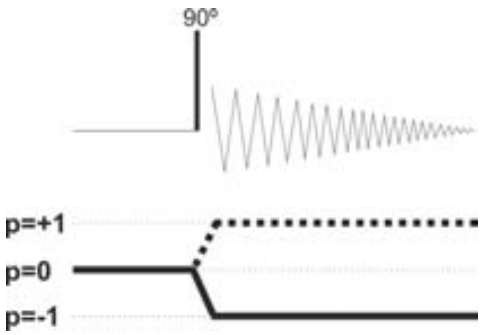

Figure 1.04. CTP diagram for a single pulse 1D experiment. The solid line represents the selected CTP of the detected magnetization. The dotted line represents the mirror-image pathway that is rejected.

When building a CTP diagram there are some arbitrary rules that we have to take into account for a proper analysis and interpretation:

- The starting point for any pulse sequence is always p = 0 (I_z).
- By convention, the receiver detects single quantum (SQ) coherences p = -1.
- The coherence order can only be changed by the application of pulses. p does not change during inter-pulse delays.
- The evolution under chemical shift generates the corresponding sine/cosine modulations:

$$I^{p} \xrightarrow{\Omega_i t} I^{p}\cos(p\Omega_i t) - I^{p}\sin(p\Omega_i t)$$

whereas evolution under scalar J-coupling effects generates in-phase/anti-phase terms:

$$I^{+} \xrightarrow{\pi Jt} I^{+}\cos(\pi Jt) - 2iI^{+}S_z\sin(\pi Jt)$$
$$2iI^{+}S_z \xrightarrow{\pi Jt} 2iI^{+}S_z\cos(\pi Jt) - I^{+}\sin(\pi Jt)$$

- The initial 90º pulse only creates SQ coherence with p = ±1 (**Fig. 1.04**).

$$I_z \xrightarrow{90^{\circ}_{x}} -I_y = i/2(I^{+} - I^{-})$$

- A second 90º pulse applied on transverse magnetization can create any coherence order.
- A pulse applied on the nucleus I only changes the coherence order of this specific nucleus, and not those of any other nucleus.
- A 180º pulse changes the coherence order from +p to –p, or vice versa.
- When PFGs are applied to select a specific CTP, only those CTPs in which the sum of the dephasing effects of each individual PFG applied throughout the entire sequence is zero just prior to acquisition will be detected. This is the so-called refocusing condition:

$$\sum_{i=1}^{n} s_i G_i \tau_i \left(\sum_j p_{ij} \gamma_{ij}\right) = 0$$

Equation 5

Assuming that all the gradients have the same shape and the same length, the refocusing condition can be simplified to:

$$\sum_{i=1}^{n} G_i \left(\sum_j p_{ij} \gamma_{ij}\right) = 0$$

Equation 6

1.2.2 Usage of PFGs

PFGs are used with two basic objectives:

a) <u>For purging purposes:</u>

- **Phase errors**. To minimize the phase errors originated by chemical shift evolution during the application of a gradient, PFGs are usually inserted into spin echo blocks.

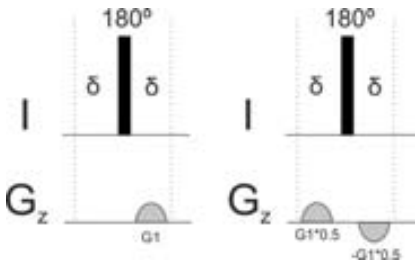

- As a **z-filter**, by including a PFG into two 90º pulses so that any coherence p=0 is selected whereas any transverse magnetization will be efficiently dephased.

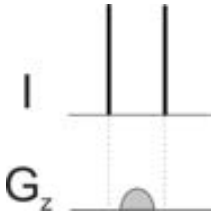

- For **refocusing purposes**. Inherent imperfections of 180º pulses will be removed when two equal gradients flanked it. Transverse magnetization that does not experience the 180º pulse will be also dephased.

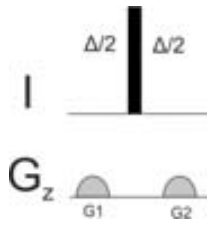

- For **inversion purposes** when a 180º pulse inverts magnetization from I_z to $-I_z$, or vice versa. Dephased undesired coherences will be refocused if the second gradient is applied in the opposite sense to the first gradient, so that any residual transverse magnetization created by imperfect 180º pulses will be efficiently removed.

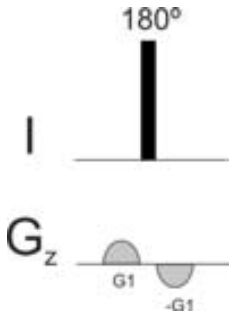

- **During heteronuclear magnetization transfer**, as an easy way to remove unwanted magnetization when a pair of simultaneous 90º pulses is applied to transfer magnetization between two J-coupled heternonuclei. Such particular state is known as zz-filter.

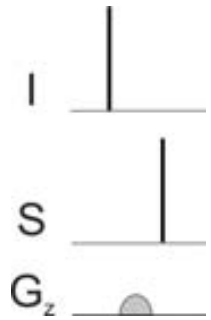

b) For selection of a coherence transfer pathway

- **For coherence selection**, as an alternative to use extensive phase cycling strategies. The goal is to select the magnetization that has followed a desired pathway and remove those that have followed any other pathway.

1.2.3 Advantages and drawbacks of PFGs

Regarding the use of PFGs for coherence selection it is worth it to highlight a complete set of different features:

a) A reduction in the number of phase cycling steps needed for the suppression of unwanted artifacts.
b) They can lead to a significant decrease in experiment acquisition times.
c) Reduction of t_1 noise in 2D NMR spectra.
d) Achievement of clean spectra.
e) Efficient suppression of undesired signals. The best example is the suppression of ^{1}H-^{12}C magnetization in inverse NMR experiments of natural abundant molecules.
f) Better solvent suppression.
g) A reduction in the dynamic range.
h) Higher versatility in pulse sequence design.
i) New experiments, like the measurement of translational diffusion coefficients and DOSY application.
j) As an inconvenient, the use of PFGs for coherence selection produces a theoretical decrease in terms of SNR with respect to the original phase-cycled experiment because only one pathway can be selected. In multidimensional experiments this factor can be of √2.

1.3 The HSQC experiment

1.3.1 Basic pulse scheme

The Heteronuclear Single Quantum Coherence (HSQC) experiment[6] (**Fig. 1.05**) can be considered as one of the most emblematic pulse sequences because it is widely used to get chemical-shift correlation maps for both small chemical compounds and bio-molecules. The experiment yields a 2D spectrum presenting a cross-peak for each proton attached to the heteronucleus being considered (most often ^{13}C or ^{15}N).

[6] G. Bodenhauser, D.J. Ruben. *Chem. Phys. Lett*. **1980**, 69, 185.

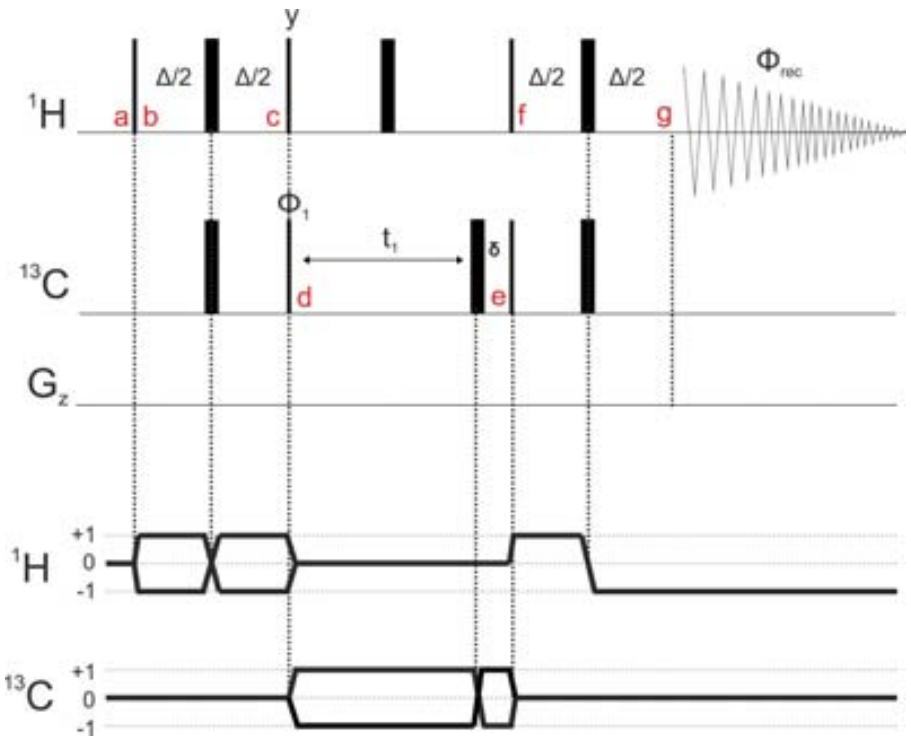

Figure 1.05. Basic ^{1}H-^{13}C-HSQC pulse sequence and its coherence level diagram below. $\Delta=1/(2\cdot{}^{1}J(CH))$. Φ_1= x,-x. Φ_{rec}= x,-x.

From an academic point of view, the HSQC pulse scheme represents an ideal experiment to understand what is really happening during a pulse sequence[7]. Let's consider a proton-carbon correlation where I nucleus stands for ^{1}H and S nucleus stands for ^{13}C. In the first part of the sequence the initial I_z magnetization (point a) is transferred to AP single quantum $2I_zS_y$ heteronuclear coherence (point d), thanks to the INEPT block:

$$I_z \xrightarrow{\text{INEPT}} +I_y\cos(2\pi J_{IS}\Delta)-2I_zS_y\sin(2\pi J_{IS}\Delta)$$

Then, the heteronuclear magnetization freely evolves during the t_1 period being frequency-labeled according to the heteronuclear chemical shift that generates the second non-detected dimension. By applying a 180º ^{1}H pulse at the middle of the t_1 period, the evolution of the heteronuclear coupling constant is refocused. At the end of t_1 there are two orthogonal components, $2I_zS_x$ and $2I_zS_y$ (point e):

$$+I_y\cos(2\pi J_{IS}\Delta)-2I_zS_y\sin(2\pi J_{IS}\Delta) \xrightarrow{t_1} \begin{matrix} -2I_zS_y\cos(\Omega_s t_1)\sin(2\pi J_{IS}\Delta) \\ +2I_zS_x\sin(\Omega_s t_1)\sin(2\pi J_{IS}\Delta) \end{matrix}$$

Finally, a refocused INEPT (R-INEPT) converts the AP $2I_zS_y$ term into IP proton magnetization (I_x) while the other AP $2I_zS_x$ term is converted into $2I_yS_x$ MQ coherence that is not observed (point g):

[7] P. K. Mandal, A. Majumdar. *Concepts Magn. Reson.* **2004**, 20A, 1.

$$\begin{matrix} -2I_zS_y\cos(\Omega_S t_1)\sin(2\pi J_{IS}\Delta) \\ +2I_zS_x\sin(\Omega_S t_1)\sin(2\pi J_{IS}\Delta) \end{matrix} \xrightarrow{\text{R-INEPT}} \begin{matrix} I_x\cos(\Omega_S t_1)\sin(2\pi J_{IS}\Delta)\sin(2\pi J_{IS}\Delta_1) \\ +2I_yS_x\sin(\Omega_S t_1)\sin(2\pi J_{IS}\Delta) \end{matrix}$$

The experiment requires a basic two-step phase cycle to remove unwanted magnetization from protons attached to ^{12}C. By inverting the phase of the Φ_1 pulse in alternate acquisitions, the $^1J(^{13}C\text{-}H)$ satellite lines are inverted while the $^1J(^{12}C\text{-}H)$ line remains unaffected. If the phase of the receiver (Φ_{rec}) is simultaneously inverted, $^1J(^{13}C\text{-}H)$ lines are coherently added and therefore detected, while the $^1J(^{12}C\text{-}H)$ line is removed each two scans. However, a perfect removal of the unwanted signals is difficult to achieve by phase cycling alone, and undesired t_1 noise is usually present in the final spectrum. The use of PFGs represents a nice approach to suppress unwanted signals in a single scan.

1.3.2 PFGs in the HSQC experiment. The Echo/Anti-echo method

PFGs are able to select a specific coherence transfer pathway removing all the others. One of the most widely methodologies used to achieve coherence selection using PGFs is the Echo/Anti-echo method[7,8]. For a successful implementation of such methodology two different PFGs must be properly inserted in the pulse sequence: the encoding G1 gradient, and the decoding G2 gradient (**Fig. 1.06**).

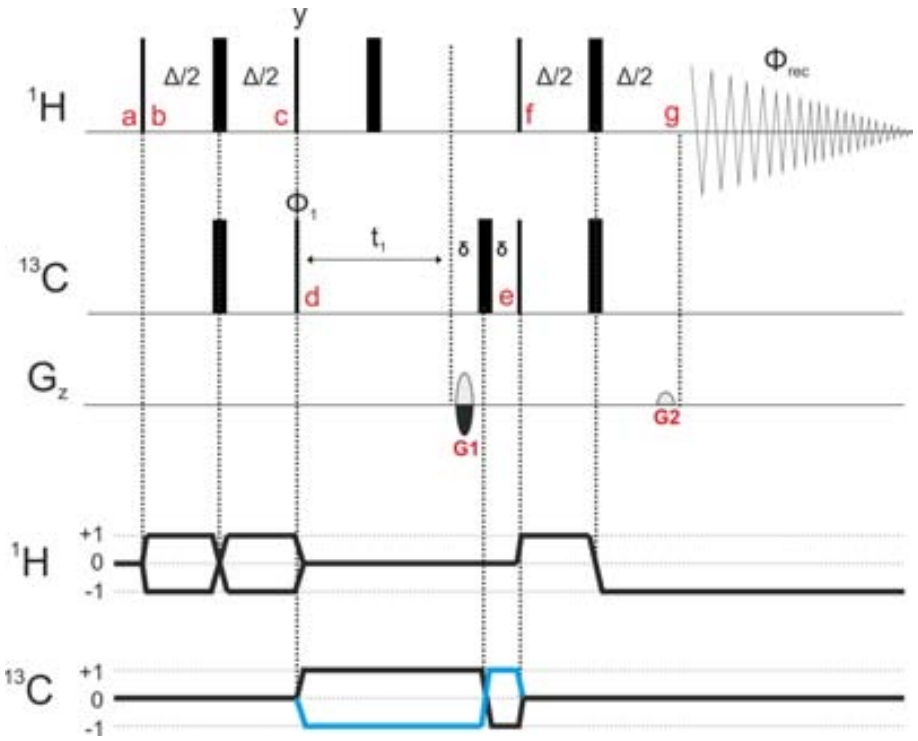

Figure 1.06. ^1H-^{13}C-HSQC pulse sequence using the Echo/Anti-echo method. $\Delta=1/(2\cdot{}^1J(CH))$. Φ_1= x,-x. Φ_{rec}= x,-x. G1:G2=80:20.1. Below it is shown the corresponding coherence level diagram: blue line stands for N-type magnetization (Echo), while black line stands for P-type magnetization (Anti-echo).

G1 will select coherence pathways in which the magnetization of the S spin is in the transverse plane during the free evolution t_1 period, and G2 will select coherence pathways in which the magnetization of the I spin is in the transverse plane during the detection t_2 period.

[8] J. Keeler, J. "Understanding NMR spectroscopy", John Wiley and Sons, Ltd, England. **2007**.

An important aspect that we have to take into account when using PFGs during t_1 is that the signal obtained is not sine/cosine amplitude-modulated[9] but phase modulated, which means that is modulated according to the rotation sense of the magnetization (S^+, echo; or S^-, anti-echo). This results in P-type data selection (anti-echo), in which the sense of the frequency modulation is the same in t_1 and t_2:

$$S(t_1,t_2)_{antiecho} = \gamma \cdot \exp(i\Omega_x t_1) \cdot \exp(i\Omega_x t_2)$$

Equation 7

and N-type data selection (echo), in which the sense is opposite:

$$S(t_1,t_2)_{echo} = \gamma \cdot \exp(-i\Omega_x t_1) \cdot \exp(i\Omega_x t_2)$$

Equation 8

That signal phase encoding makes the gradient only able to select one of the two desired CTP in each scan. Therefore, the spectrum will present cross peaks with undesirable phase-twisted lineshapes. To solve that problem the acquisition of the Echo/Anti-echo pathways has to be done in alternate acquisitions and then combine them in a proper way during the processing step. Both signals will be phase-modulated, but by addition and subtraction they will be amplitude-modulated as well, so that phase-sensitive spectra can be obtained.

The gradient strength has to be adjusted so that

$$G1/G2 = \gamma_I/\gamma_S$$

Equation 9

In the case of proton-carbon correlation experiments such ratio is $\gamma_H/\gamma_C = 4$. Therefore, gradients strength ratios are usually set up to G1:G2 = 4:1.

To achieve a proper coherence selection in HSQC experiments the encoding G1 gradient must label the transverse N-type (Echo) and P-type (Anti-echo) coherences in alternate scans, while the decoding G2 gradient must refocus the proton magnetization. To do that, the gradients ratio should satisfy the refocusing condition. In the case of proton-carbon correlation experiment, N-type coherence (blue line in **Fig. 1.06**) is selected using G1:G2 = 4 (typical ratio of 80:20.1), while P-type coherence (black line in **Fig. 1.06**) is selected by G1:G2 = -4 (typical ratio of -80:20.1). In terms of sensitivity, the use of PFGs during t_1 produces a SNR decrease by a factor of √2 with respect to the original experiment because only one pathway can be selected. This is the main drawback of the Echo/Anti-echo method. Nonetheless, the main advantages are that higher quality spectra are obtained, strong solvent signals (water) are efficiently suppressed, t_1 noise is better cleaned, and a considerable decrease in the overall acquisition time is achieved if the use of an extended phase cycle is avoided.

[9] It is important to make a point here: in a HSQC experiment without using PFGs for coherence selection the obtained signal is sine/cosine amplitude-modulated which means that a discrimination of the positive/negative frequencies with respect to the offset is not feasible. To solve it, an alternate acquisition where 90º the phase of the Φ_1 pulse is dephased accordingly to the phase of the receiver must be done. In this way, the complementary sine amplitude-modulated signal is also obtained and a positive/negative frequency's discrimination reached.

1.3.3 Improvements in HSQC experiments

Since its first appearance, the basic HSQC pulse sequence has been largely modified in order to improve its performance on a variety of conditions:

i. HSQC with heteronuclear decoupling during acquisition:

Broadband decoupling, or composite pulse decoupling (CPD), achieves an excitation of a large frequency range using a train of short pulses (which are able to excite a large bandwidth) applied in rapid succession so that fast $\alpha \rightarrow \beta$ and $\beta \rightarrow \alpha$ transitions takes place, making the lifetime of any particular spin in any given state shorter. In this way, broadband excitation of all frequencies corresponding to a particular nucleus type (^{13}C in this case) leads to multiplet collapse and simplification of the spin-spin splitting patterns of the signals.

ii. HSQC using adiabatic pulses:

Typically, the carrier frequency of a pulse remains constant and is applied at the center of the spectral region of interest. Adiabatic pulses are frequency-swept pulses in which the carrier frequency varies with time during the pulse. They invert spins by a slow passage of a chirped pulse through resonance so that spins having different resonance frequencies will be inverted at different times. Adiabatic pulses result to be very tolerant against field inhomogeneities and they are very effective within a large spectral bandwidth, being capable of invert/refocus heteronuclear spins having a large chemical shift range and, therefore, offering better excitation/inversion profiles than hard pulses[10]. This is especially convenient when working with ^{13}C nucleus in high-field spectrometers.

iii. HSQC with a trim pulse:

These kinds of pulses (also known as spin-lock pulses) are rather used for purging purposes[11]. They are placed at the end of a heteronuclear spin-echo (just before magnetization transfer from proton to carbon nucleus takes place) due to its ability to dephase undesired magnetization. They are commonly used in HSQC pulse sequences to suppress the strong water signal when working with proteins in aqueous solutions[12] or to reduce t_1 noise.

iv. Preservation of Equivalent Pathways methodology (PEP) in HSQC :

This methodology is based on the implementation of a second R-INEPT (shifted 90º) in the regular HSQC pulse sequence[13], which allows to obtain a sensitivity enhancement by a factor of C for IS groups (**Fig. 1.07**).

[10] E. Kupce, R. Freeman. *J. Magn. Reson. A*. **1996**, 118, 299.

[11] W. R. Croasmun, R. M. K. Carlson, "Two-dimensional NMR spectroscopy. Applications for chemist and biochemist", VCH publishers, Inc. New York, USA. **1994**.

[12] B. A. Messerle, G. Wider, G. Otting, C. Weber, K. Wütrich. *J. Magn. Reson.* **1989**, 85, 608.

[13] a) L. E. Kay, P. Keifer, T. Saarinen. *J. Am. Chem. Soc*. **1992**, 114, 10663. b) J. Schleucher, M. Schwendinger, M. Satller, P. Schmidt, O. Schedletzky, S. J. Glaser, O. W. Sorensen, C. Griesinger. *J. Biomol. NMR*, **1994**, 4, 301.

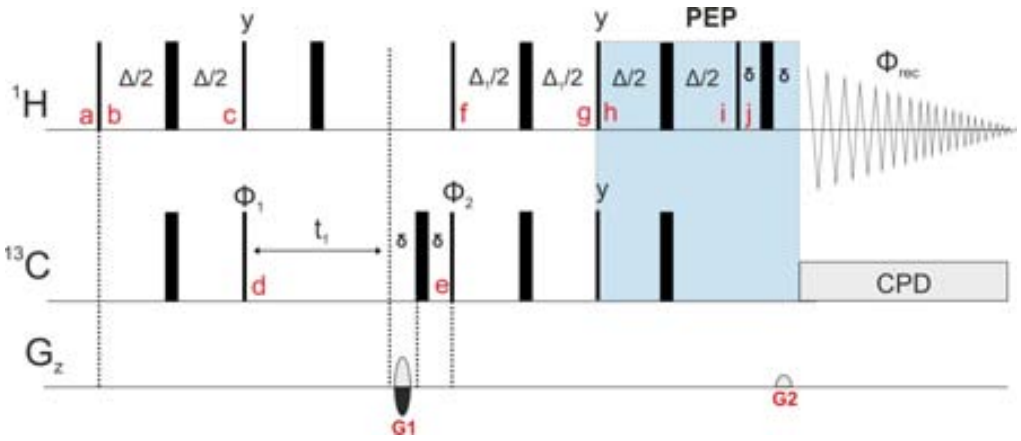

Figure 1.07. ^{1}H-^{13}C-HSQC-PEP pulse sequence using the Echo/Anti-echo method. Δ=1/(2·^{1}J(CH)), Δ$_1$= Δ for CH multiplicities, Δ1=1/(4·^{1}J(CH)) for all multiplicities. Φ$_1$= x,-x. Φ$_{rec}$= x,-x. G1:G2=80:20.1.

Let's consider a proton-carbon correlation where I nucleus stands for ^{1}H and S nucleus stands for ^{13}C. In the original HSQC experiment the conventional refocused INEPT converts the anti-phase term $2I_zS_y$ into detectable in-phase proton magnetization I_x, while the other $2I_zS_x$ anti-phase term is converted into $2I_yS_x$ multiple quantum coherence being consequently lost (see section 1.3.1) (g point):

$$\begin{matrix}-2I_zS_y\cos(\Omega_s t_1)\sin(2\pi J_{IS}\Delta) \\ +2I_zS_x\sin(\Omega_s t_1)\sin(2\pi J_{IS}\Delta)\end{matrix} \xrightarrow{\text{R-INEPT}} \begin{matrix}I_x\cos(\Omega_s t_1)\sin(2\pi J_{IS}\Delta)\sin(2\pi J_{IS}\Delta_1) \\ +2I_yS_x\sin(\Omega_s t_1)\sin(2\pi J_{IS}\Delta)\end{matrix}$$

At this point, a second R-INEPT is added to recover the MQ coherence. The strategy is based on keeping momentarily away the detected magnetization I_x, which is transferred to the z-axis as I_z magnetization, while the $2I_yS_x$ MQ term is converted into anti-phase $2I_yS_z$ magnetization (h point):

$$\begin{matrix}I_x\cos(\Omega_s t_1)\sin(2\pi J_{IS}\Delta)\sin(\pi 2J_{IS}\Delta_1) \\ +2I_yS_x\sin(\Omega_s t_1)\sin(2\pi J_{IS}\Delta)\end{matrix} \xrightarrow{90^I_y,\ 90^S_y} \begin{matrix}I_z\cos(\Omega_s t_1)\sin(2\pi J_{IS}\Delta)\sin(2\pi J_{IS}\Delta_1) \\ +2I_yS_z\sin(\Omega_s t_1)\sin(2\pi J_{IS}\Delta)\end{matrix}$$

After the second R-INEPT (i point), the $2I_yS_z$ term is converted into in-phase magnetization in the form of I_x, while I_z term is still kept along z-axis:

$$\begin{matrix}I_z\cos(\Omega_s t_1)\sin(2\pi J_{IS}\Delta)\sin(2\pi J_{IS}\Delta_1) \\ +2I_yS_z\sin(\Omega_s t_1)\sin(2\pi J_{IS}\Delta)\end{matrix} \xrightarrow{\Delta/2 - 180^{I,S}_x - \Delta/2} \begin{matrix}I_z\cos(\Omega_s t_1)\sin(2\pi J_{IS}\Delta)\sin(2\pi J_{IS}\Delta_1) \\ +I_x\cos(\Omega_s t_1)\sin^2(2\pi J_{IS}\Delta)\end{matrix}$$

Finally, a 90º ^{1}H pulse applied from x-axis put the I_z term along the transvers plane as I_y magnetization (j point):

$$\begin{matrix}I_z\cos(\Omega_s t_1)\sin(2\pi J_{IS}\Delta)\sin(2\pi J_{IS}\Delta_1) \\ +I_x\cos(\Omega_s t_1)\sin^2(2\pi J_{IS}\Delta)\end{matrix} \xrightarrow{90^I_x} \begin{matrix}I_y\cos(\Omega_s t_1)\sin(2\pi J_{IS}\Delta)\sin(2\pi J_{IS}\Delta_1) \\ +I_x\cos(\Omega_s t_1)\sin^2(2\pi J_{IS}\Delta)\end{matrix}$$

Because two orthogonal magnetization terms with sine and cosine modulation are retained in each acquisition, the obtained signal is sine/cosine phase-modulated and therefore, a sensitivity enhancement of √2 is obtained when compared with the most conventional HSQC pulse sequence[9]. Very importantly, such gain is retained even by the use the Echo/Anti-echo method because the experiment is fully compatible with the phase-modulated nature of the signals.

Nevertheless, it is not possible to completely refocus both magnetization terms for all spin systems[14] so that the Δ_1 delay must be adjusted accordingly to the maximum sensitivity enhancement that can be reached for a given spin system. When only IS pairs are to be observed, the INEPT delays should be optimized to $\Delta = \Delta_1 = 1/2(J_{IS})$, whereas for the detection of all multiplicities (IS, I_2S and I_3S) the Δ_1 period should be reduced to $1/4(J_{IS})$.

v. HSQC using the CLIP technique:

A simple way to measure $^1J(CH)$ is from a F2-coupled HSQC experiment. The range of $^1J(CH)$ coupling constants generally falls between 120-210 Hz. This fact might cause the appearance of signal distortions when the Δ delay is not perfectly optimized to the real $^1J(CH)$ value. In order to solve this drawback the CLIP (**CL**ean **I**n-**P**hase) technique offers the possibility to obtain better quality spectra in HSQC pulse sequences by incorporating an additional 90º ^{13}C pulse inserted after the refocusing INEPT transfer, just prior to the acquisition, so that AP components are converted into multiple quantum coherences and IP multiplets are expected to be obtained.

Let's consider a proton-carbon correlation where I nucleus stands for ^1H and S nucleus stands for ^{13}C. The magnetization just prior to the beginning of a R-INEPT block is found in the form of:

$$2I_yS_z\sin(2\pi J_{IS}\Delta)\cos(\Omega_S t_1)$$

If there is a significant mismatch between the Δ delay used and the real $^1J(CH)$ value, and inefficiency occurs during the INEPT transfer so that not the whole AP component is transferred to IP component making possible that a part of that AP component still remain at the end of the refocusing period:

$$-2I_yS_z\sin(2\pi J_{IS}\Delta)\cos(\Omega_S t_1)\cos(2\pi J_{IS}\Delta) + I_x\sin^2(2\pi J_{IS}\Delta)\cos(\Omega_S t_1)$$

By inserting at this point a 90º ^{13}C pulse applied from x-axis, the AP $2I_yS_z$ component is converted into MQ $2I_yS_y$ magnetization:

$$-2I_yS_y\sin(2\pi J_{IS}\Delta)\cos(\Omega_S t_1)\cos(2\pi J_{IS}\Delta) + I_x\sin^2(2\pi J_{IS}\Delta)\cos(\Omega_S t_1)$$

In this way, only the in-phase I_x component will be detected. A comparison between the conventional HSQC and the related CLIP-HSQC experiment[15] on the strychnine molecule is shown in **Fig. 1.08.**

[14] J. Schleucher, M. Schwendinger, M. Satller, P. Schmidt, O. Schedletzky, S.J. Glaser, O.W. Sorensen, C. Griesinger. *J. Biomol. NMR.* **1994**, 4, 301.

[15] A. Enthart, J. C. Freudenberger, J. Furrer, H. Kessler, B. Luy. *J. Magn. Reson*. **2008**, 192, 314.

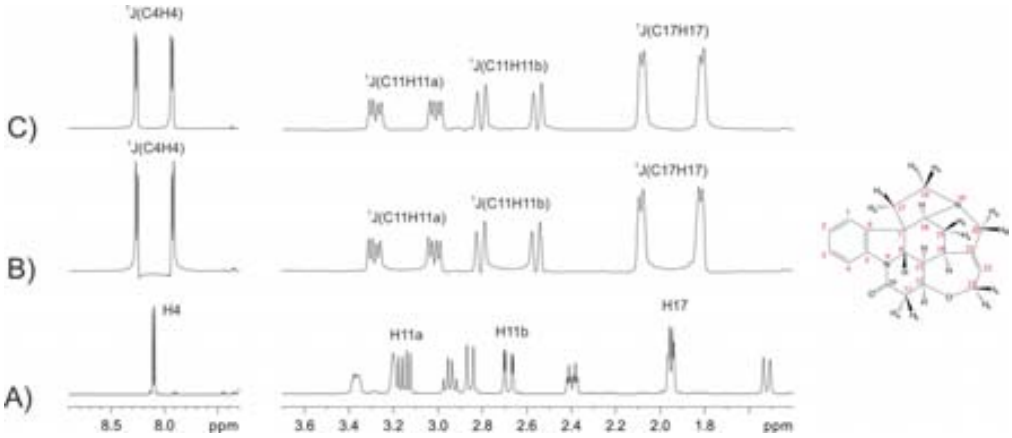

Figure 1.08. A) ^{1}H NMR spectra, B-C) 1D slices from the conventional HSQC and CLIP-HSQC spectra, respectively.

vi. <u>HSQC with PFGs for purging purposes:</u>

PFGs can be used as purging filters without modifying too much the sensitivity of a particular NMR experiment[16]. In HSQC-like sequences the most important ones are PFGs for refocusing purposes and as zz-filters (see section 1.2.2).

1.4 The HMQC experiment

The Heteronuclear Multiple Quantum Coherence (HMQC) experiment[17] is the most ancient experiment using inverse detection technique. It achieves similar results as HSQC experiment. The basic pulse scheme only contains four pulses, making it a more robust experiment in terms of radiofrequency pulse homogeneities (**Fig. 1.09**).

[16] A. Bax, S. Pochapsky. *J. Magn. Reson*. **1992**, 99, 638.

[17] L. Muller. *J. Am. Chem*. **1979**, 101, 4481.

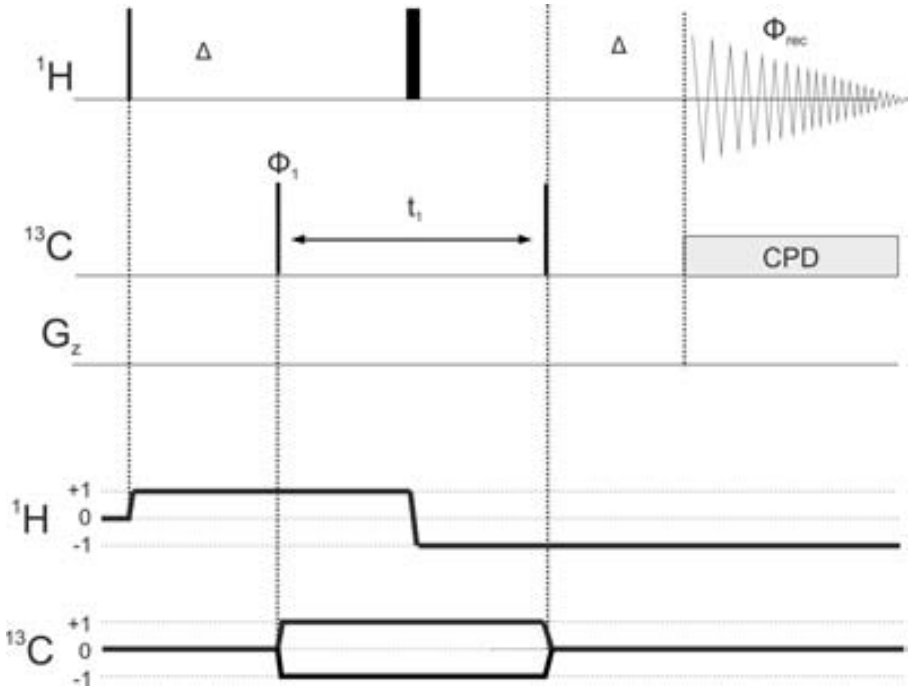

Figure 1.09. Basic ^{1}H-^{13}C-HMQC pulse sequence. Δ=1/(2·^{1}J(CH)). Φ_1= x,-x. Φ_{rec}= x,-x. Below it is shown the corresponding coherence level diagram.

Let's consider a proton-carbon correlation where I nucleus stands for ^{1}H and S nucleus stands for ^{13}C. The sequence starts with a proton magnetization transfer from z-axis to the xy-plane thanks to a 90º ^{1}H pulse. Then, transverse magnetization evolve under coupling constants effects during the Δ delay, which is adjusted to Δ=1/(2·^{1}J(CH)). After such delay, proton AP magnetization with respect to the ^{1}J(CH) is obtained.

$$I_z \xrightarrow{\Delta} 2I_xS_z$$

By a 90º ^{13}C pulse the AP magnetization is converted into MQ magnetization that freely evolve during the t_1 period under the effects of carbon chemical shift. Because of the 180º ^{1}H pulse placed at the middle of the sequence, proton chemical shift and heteronuclear J(CH) evolutions are refocused.

$$2I_xS_z \xrightarrow{90^{S}_{x}} -2I_xS_y \xrightarrow[180^{I}_{x}]{\Omega_S t_1} -2I_xS_y\cos(\Omega_S t_1) + 2I_xS_x\sin(\Omega_S t_1)$$

After that, the last 90º ^{13}C pulse returns one of the MQ terms to AP proton magnetization, which is detected as IP magnetization after the second Δ delay.

$$-2I_xS_y\cos(\Omega_S t_1) + 2I_xS_x\sin(\Omega_S t_1) \xrightarrow{90^{S}_{x}} -2I_xS_z\cos(\Omega_S t_1) \xrightarrow{\Delta} -I_y\cos(\Omega_S t_1)$$

Analogously to the HSQC experiment, a basic two-step phase cycle to remove unwanted magnetization from protons attached to ^{12}C is required. PFGs can also be used to achieve a better suppression of undesired signals. Although there are several ways to implement such PFGs, here it is only illustrated the Echo/Anti-echo version of the HMQC with PFGs during the t_1 period (**Fig. 1.10**).

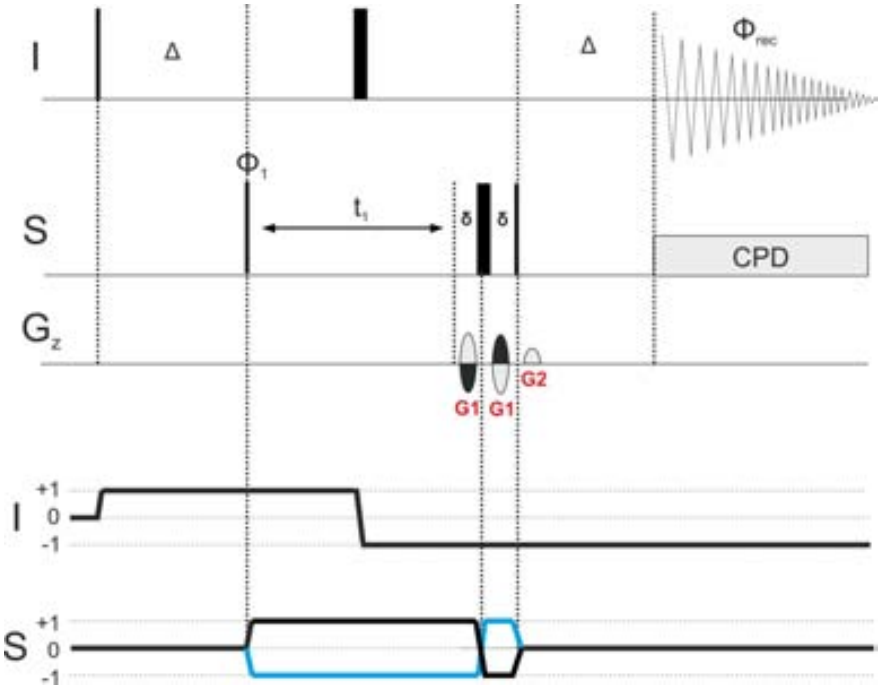

Figure 1.10. ^{1}H-^{13}C-HMQC pulse sequence using the Echo/Anti-echo method. Δ=1/(2·^{1}J(CH)), Φ_1= x,-x. Φ_{rec}= x,-x. G1:G2=80:40.2. Below it is shown the corresponding coherence level diagram: blue line stands for N-type magnetization (Echo), while black line stands for P-type magnetization (Anti-echo).

In this case the gradient strength has to be adjusted so that

$$G1/G2 = \gamma_I/2\gamma_S$$

Equation 10

For proton-carbon correlation experiments the gradient ratio is set to G1:G2=2:1.

Main downside of the HMQC experiment is that J(HH) evolution takes place during t_1 that generates tilting cross-peaks along the indirect F1 dimension. Finally, it is worth it to mention that a sensitivity-enhanced HMQC experiment[18] using the PEP methodology can be also used in order to recover one of the unobservable MQ terms that otherwise is lost.

[18] A. Plamer I, J. Cavanagh, P. Wright, M. Rance. *J. Magn. Reson.* **1991**, 93, 151.

2. NMR Methods for the measurement of long-range heteronuclear coupling constants

2.1 The cross-peak nature vs NMR experiment

The nature of a cross-peak coupling pattern obtained from a particular NMR experiment is a very important factor that must be taken into account when measuring quantitatively long-range heteronuclear coupling constants ($^{n}J(CH)$). This is directly related to both the simplicity and the accuracy of the measurement[19]. Different methodologies to extract $^{n}J(CH)$ values according to their coupling pattern can be devised, as illustrated in **Fig. 1.11**.

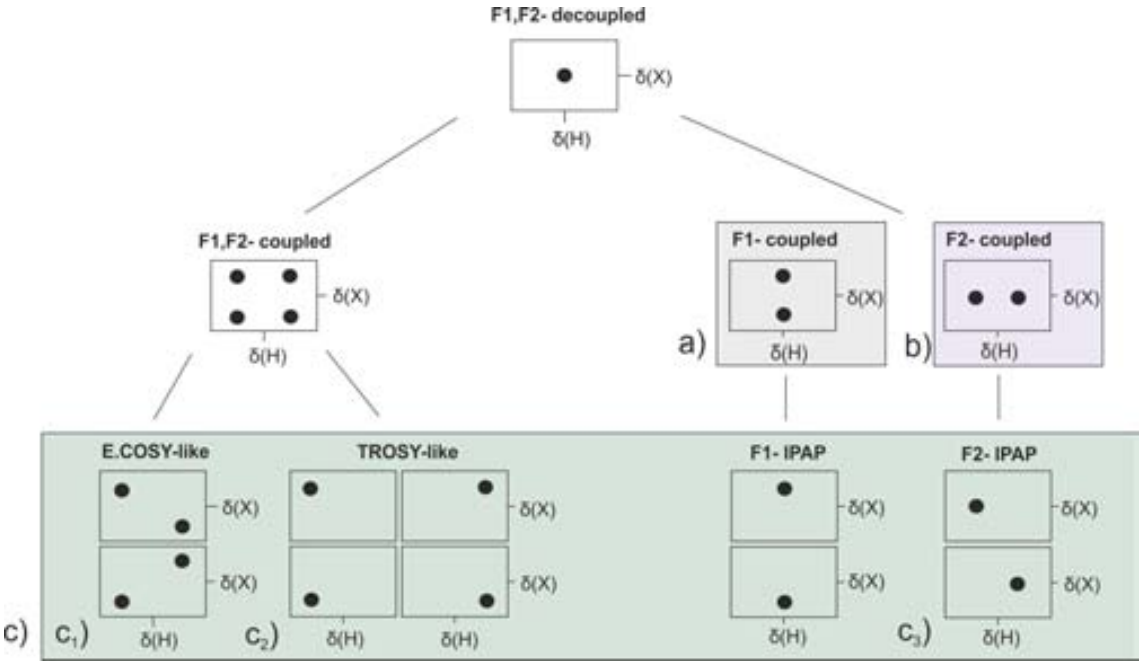

Figure 1.11. Schematic coupling patterns obtained for a CH cross-peak in 2D NMR experiments.

a) From an additional splitting along the indirect F1 dimension

This kind of cross-peak coupling pattern can be reached by allowing both the X chemical shift and the heteronuclear coupling constant evolve independently using the J-resolved technique[20]. The main drawback of this time-consuming methodology is the need of acquiring a large number of t_1 increments to get a high resolution along the indirect F1 dimension. To partially solve this problem the use of scaling k factors in the indirect dimension can be advisable. Other possibilities are spectra-folding, non-linear sampling or zero-filling and linear prediction in the processing step. J-HMBC[21] and EXSIDE[22] pulse schemes are the most important experiments using this technique.

---

[19] T. Parella, J.F. Espinosa. *Prog. Nucl. Magn. Reson. Spectrosc.* **2007**, 50, 179.

[20] G. A. Morris, J. W. Emsley (Eds.), Multidimensional NMR Methods for the Solution State, Two-Dimensional J-Resolved Spectroscopy, John Wiley & Sons Ltd., Chichester, **2010**. (pp. 145−159).

[21] a) C. H. Gotfredsen, A. Meissner, J. Ø. Duus, O. W. Sørensen. *Magn. Reson. Chem*. **2000**, 38, 692. b) A. Meissner, O. W. Sørensen. *Magn. Reson. Chem*. **2001**, 39, 49.

[22] V. V. Krishnamurthy. J. Magn. Reson. A. **1996**, 121, 33.

b) From an additional splitting along the direct F2 dimension

Such cross-peak coupling pattern is achieved by omitting heteronuclear decoupling during proton acquisition. In this way, an additional splitting along the direct F2 dimension is reached. Depending on the pulse scheme used the splitted multiplets can present pure IP properties with respect to both J(HH) and J(CH) couplings, or, on the contrary, they can present AP properties. In the first case, J couplings can be measured by the direct analysis of outer peaks frequency separation, or from fitting procedures with a reference cross-peak. Anyway, obtaining pure IP cross-peaks is not an easy task. In the second case, a direct measurement of the coupling constant is almost impossible to achieve in terms of peak separation and a individualized fitting procedure for each cross-peak is required in most of the cases so that the process may become a time-consuming task. Several solutions have been proposed for an accurate measurement of $^{n}J(CH)$ from AP multiplets[23]. The analysis of AP cross-peaks may suffer from partial/full signal cancellation, peak distortion, or shifted peak maxima. Conventional HMBC[24] and HSQMBC[25] pulse schemes are the most typical experiments using this approach.

c) From spin-state selective (S^3) techniques

This approach is based on the manipulation of the magnetization in such a way that the α- and β- ^{13}C multiplet components are separated in two different spectra. The $^{n}J(CH)$ value can be extracted by analyzing the relative displacement of the α/β cross-peaks components. There are several spin-state selective (S^3) techniques to take into account:

c1) E.COSY pattern

The E.COSY[26] technique allows the measurement of non-resolved couplings between spins I and Y, as long as spin Y is also coupled with a third spin S. This coupling constant, J(YS), allows the resolution of the unresolved desired coupling constant J(IY). As a requirement, during the magnetization transference between I spin and S spin, the spin-state of the spin Y cannot be disturbed. Main advantages of the E.COSY pattern are: i) very easy interpretation, ii) they are equally well suited for the measurement of small and large coupling values, iii) they provide information about the sign by analyzing the relative positive/negative tilting of cross peak components, iv) the method allows the measurement of coupling values smaller than the line width, and v) J values are extracted from the F2 dimension, where good resolution requirements are more easily reached. HETLOC[27] and HECADE[28] experiments provide E.COSY-like multiplets.

[23] a) J.J. Titman, D. Neuhaus, J. Keeler. *J. Magn. Reson.* **1989**, 85, 111., b) J.M. Richardson, J.J. Titman, J. Keeler, D. Neuhaus. *J. Magn. Reson.* **1991**, 93, 533.

[24] A. Bax, M. Summers. *J. Am. Chem. Soc*. **1986**, 108, 2093.

[25] a) R. Marek, L. Kralik, V. Sklenar. *Tetrahedron Lett.* **1997**, 38, 665. b) R.T. Williamson, B.L. Marquez, W.H. Gerwick, K.E. Kover. *Magn. Reson. Chem.* **2000**, 38, 265.

[26] a) C. Griesinger, O. W. Sorensen, R. R. Ernst. *J. Am. Chem. Soc*. *1985*, 107, 6394, b) C. Griesinger, O. W. Sorensen, R. R. Ernst. *J. Chem. Phys*. **1986**, 852, 6837.

[27] M. Kurz, P. Schmieder, H. Kessler. *Angew. Chem. Int. Ed*. **1991**, 30, 1329.

[28] W. Kozminski, D. Nanz. *J. Magn. Reson*. **2000**, 142, 294.

c2) TROSY pattern

TROSY/Anti-TROSY[29] spectra can separate the two α/β- E.COSY components in two separate spectra, minimizing overlapping problems since the number of cross-peaks is reduced from two to one. This technique is widely used for the structural elucidation of large biomolecules where is very common to have overlapped signals.

c3) IPAP Principle applied along the F2 dimension

IPAP methodology[30] allows us to obtain the α/β components from two separate, but complementary, spectra along the same F2 or F1 dimension. The first spectrum is acquired such that we get pure IP multiplets, while the second one is acquired such that we get complementary AP multiplets. After addition and subtraction of these two spectra, two new sub-spectra are obtained corresponding to the high- and low frequency multiplet, α- and β-, respectively. The coupling constant value can be easily extracted by analyzing their relative displacements (**Fig.1.12**).

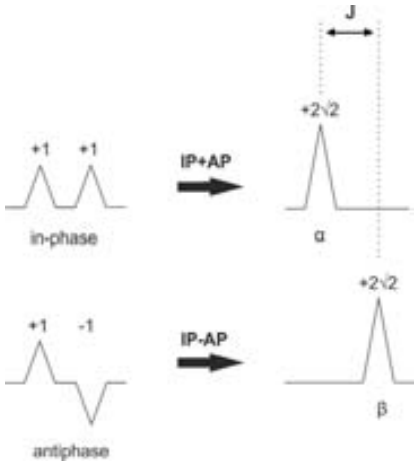

Figure 1.12. Schematic representation of the IPAP methodology.

Very importantly, IP and AP pulse sequences cannot show large differences between them and must be kept as equivalent as possible in order to avoid an extensive cross-talk in the resulting multiplets that may introduce errors in the measurement. Cross-talk is defined as the percentage of the undesired components remaining due to a non-perfect subtraction procedure. Main sources that cause these unwanted effects are J-mismatch, off-resonance effects, and the different relaxation between IP and AP data. Because no passive spins are involved and splittings are measured along the detected dimension, there is no need for large numbers of t_1 increments or high resolution in the indirect dimension. HSQC-TOCSY IPAP[31] is one of the most common experiments using this technique.

[29] K. Pervushin, R. Riek, G. Wider, K. Wuthrich. *Proc. Natl. Acad. Sci. USA*. **1997**, 94, 12366. b) D. Yang, L. E. Kay. *J. Biomol. NMR*. **1999**, 13, 3. c) K. Ding, A. M. Gronenborn. *J. Magn. Reson*. **2003**, 163, 208.

[30] M. Ottiger, F. Delaglio, A. Bax. *J. Magn. Reson*. **1998**, 131, 373.

[31] P. Nolis, J. F. Espinosa, T. Parella, *J. Magn. Reson*. **2006**, 180, 39.

2.2 NMR experiments vs transfer mechanisms

Two general approaches can be described for the measurement of $^{n}J(CH)$ as a function of the transfer mechanism used in a 2D heteronuclear shift correlation NMR experiment

- NMR experiments based on the $^{1}J(CH)$ + J(HH) transfer mechanism. Some examples are: HETLOC, HECADE, HSQC-TOCSY IPAP

- NMR experiments based on a direct long-range ^{1}H-^{13}C transfer mechanism. Some examples are: HMBC, HSQMBC, EXSIDE

There is no intention here to explain in detail some of these widely used NMR pulse schemes, which have been analyzed by former members of our NMR research group[32]. In order to situate the reader for the different pulse schemes that will be introduced in further sections of this thesis work, it was considered appropriate to merely describe the HSQC-TOCSY experiment as well as the HMBC and HSQMBC experiments because they contain enough information to understand the experiments that will be described later.

2.2.1 The HSQC-TOCSY experiment

2.2.1.1 The basic scheme

The HSQC-TOCSY pulse sequence is derived from the basic HSQC experiment by inserting a TOCSY block at the end of the sequence. Phase-sensitive HSQC-TOCSY data can be acquired using the same principles discussed for the HSQC experiment, as, for instance, using the Echo/Anti-echo approach (**Fig. 1.13**).

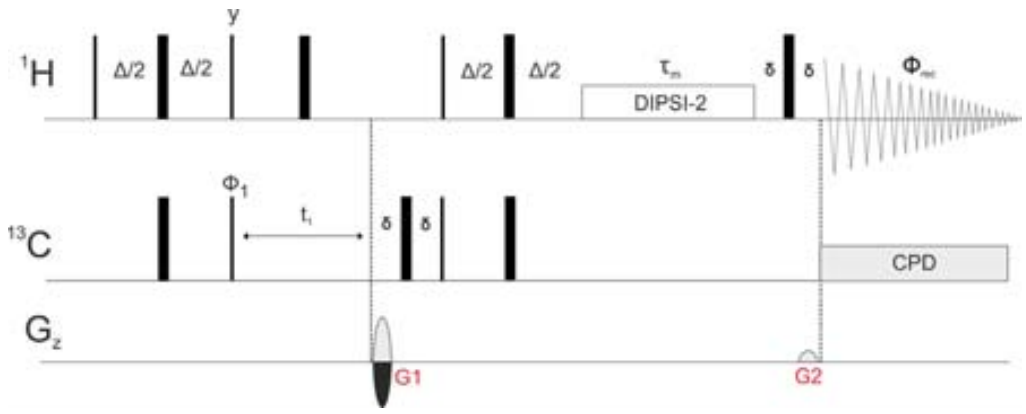

Figure 1.13. ^{1}H-^{13}C-HSQC-TOCSY pulse sequence using the Echo/Anti-echo method. $\Delta=1/(2\cdot{}^{1}J(CH))$. Φ_1= x,-x. Φ_{rec}= x,-x. G1:G2=80:20.1.

The experiment can be described in two stages: in the first stage each proton directly attached to ^{13}C is labeled according to ^{13}C chemical shift in an "out and back" process (**Fig. 1.14**) thanks to the ^{1}H-^{13}C HSQC block (green and red arrows). Then, in the second stage, a

[32] a) P. Nolis. *Disseny i aplicació de nous mètodes de RMN: Avenços en polarització creuada heteronuclear, mètodes d'estat de spin selectius i adquisició simultània de diferents espectres.* PhD thesis. Director: T. Parella. Barcelona: Autonomus University of Barcelona. Chemistry Department. **2007**. b) S. Gil. *Diseño de nuevas metodologías en RMN basadas en la secuencia de pulsos HSQC*. PhD thesis. Director: T. Parella. Barcelona: Autonomus University of Barcelona. Chemistry Department. **2011**.

homonuclear transfer block extends the labeled component to the others protons belonging to the same spin system via J(HH) (black arrows).

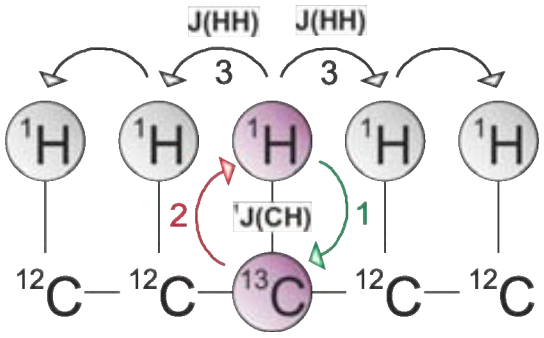

Figure 1.14. Magnetization transfer scheme for the HSQC-TOCSY experiment.

2.2.1.2 The HSQC-TOCSY-PEP experiment

As well as in HSQC experiment, a sensitivity enhancement can be reached by using the PEP methodology[13] (**Fig. 1.15**). Such methodology allows us to obtain a sensitivity enhancement by a factor of √2 in IS spin systems with respect to the conventional HSQC-TOCSY experiment.

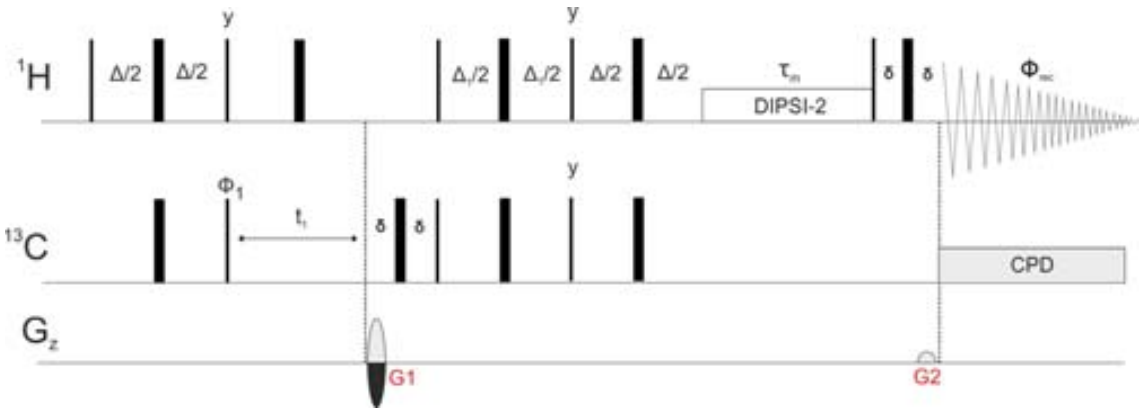

Figure 1.15. ^{1}H-^{13}C-HSQC-TOCSY-PEP pulse sequence using the Echo/Anti-echo method. Δ=1/(2·^{1}J(CH)), Δ_1= Δ for CH multiplicities, Δ_1=1/(4·^{1}J(CH)) for all multiplicities. Φ_1= x,-x. Φ_{rec}= x,-x. G1:G2=80:20.1.

Both HSQC-TOCSY and HSQC-TOCSY PEP experiments can be used to measure heteronuclear coupling constants[33]. The method involves the acquisition of separate coupled and decoupled HSQC-TOCSY experiments. The coupling constants are measured by taking two slices from the direct dimension through the correlation of interest and horizontally shifting one of the two spectra by a trial amount. By adding the two spectra together a new spectrum is obtained which is directly compared with an F2-slice taken from the ^{13}C decoupled HSQC-TOCSY. When an appropriate match is observed, one can extract the coupling constant by simply noting the horizontal displacement used in the trial fit.

[33] K.E. Kover, V.J. Hruby, D. Uhrin. *J. Magn. Reson.* **1997**, 129, 125.

2.2.1.3 Implementing IPAP into the HSQC-TOCSY-PEP experiment

By using the IPAP principle a more accurate measurement of $^{n}J(CH)$ coupling constants is achieved since the potential overlapping of the satellite α- and β- signals can be avoided. Two spectra are acquired, one of them showing pure IP multiplets, and the other one showing AP multiplets. After addition and subtraction of these two complementary spectra, two new sub-spectra are obtained, one of them showing the α- component of the satellite and the other one the β- component. It is important to highlight that the measurement is performed along the proton dimension where good resolution requirements are easily achieved, so that an accurate measurement of $^{n}J(CH)$ is reached. In addition, because the TOCSY block preserves the α/β-^{13}C spin state information, the relative sign of $^{n}J(CH)$ can be measured by analyzing the relative displacement between α- and β- spectra. The pulse sequence for the acquisition of the IP data is of the same length as for the AP data, having the same pulses and therefore minimizing possible J cross-talk effects. The only difference is the phase of the last 90º ^{1}H pulses: for IP data ϕ_2=x and ϕ_3=y, while for AP data ϕ_2=y and ϕ_3=x (**Fig. 1.16**). An example of the HSQC-TOCSY IPAP experiment on the strychnine molecule is shown in Fig. **1.17**.

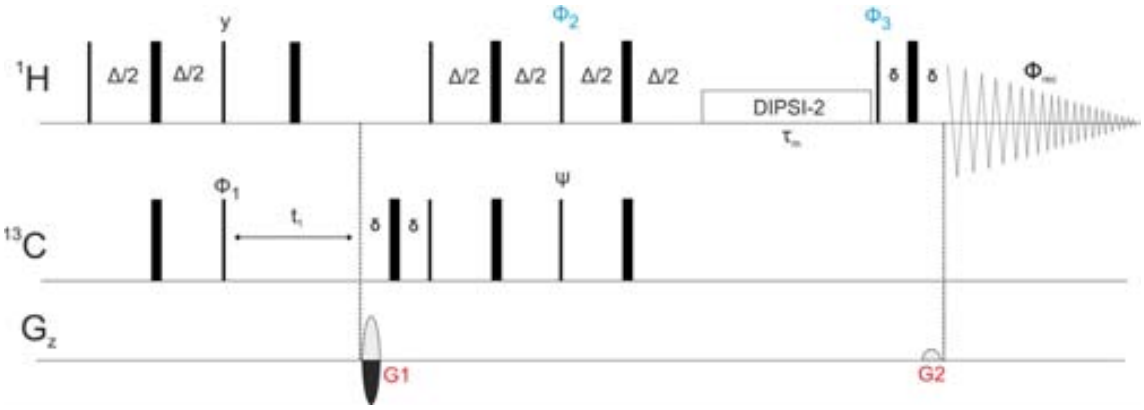

Figure 1.16. ^{1}H-^{13}C-HSQC-TOCSY IPAP pulse sequence using PEP methodology. Δ=1/(2^{n}J(CH)). Φ_1= x,-x. Φ_{rec}= x,-x. IP: Φ_2=x, Φ_3=y. AP: Φ_2=y, Φ_3=x. G1:G2 = 80:20.1

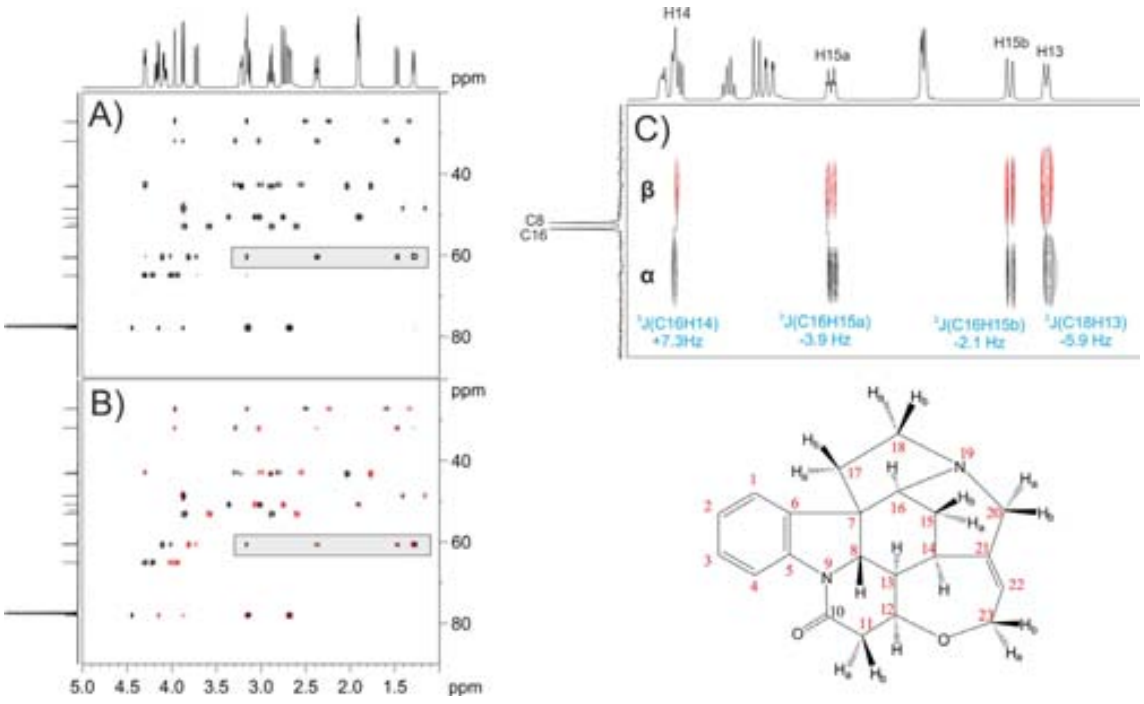

Figure 1.17. A) IP HSQC-TOCSY, B) AP HSQC-TOCSY, and C) Superimposed α- (IP+AP) and β- (IP-AP) spectra showing an expanded area corresponding to C8 and C16 carbon frequencies in strychnine. An accurate measurement of the magnitude and the sign of $^{n}J(CH)$ is made by analyzing the relative displacement between α- and β- multiplets.

In the case that J(HH) is close to zero (which means that no TOCSY transfer is reached), the experiment fails due to the fact that the double magnetization transfer mechanism, in the form of $^{1}J(CH)+J(HH)$, is not fulfilled. Another inconvenient is that the experiment does not provide signal for non-protonated carbons. Other versions of the HSQC-TOCSY using the CLIP technique (See section 1.3.3, paragraph v., of this thesis work) or zero-quantum filters have been reported to measure $^{n}J(CH)$.

The use of Zero-Quantum filters:

Zero-quantum (ZQ) coherences are a form of transverse magnetization and, although they are not detected, they can be transferred into observables signals producing AP dispersive components in the final spectrum. For instance, ZQ contributions lead to lineshape distortions in TOCSY spectra. Some years ago, Keeler and co-workers[34] proposed the use of an adiabatic 180º ^{1}H pulse and a soft PFG simultaneously applied in order to remove ZQ contributions (**Fig. 1.18**).

[34] M. Thrippleton, J. Keeler. *Angew. Chem. Int. Ed*. **2003**, 42, 3938.

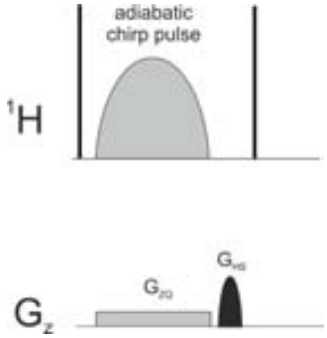

Figure 1.18. ZQ-filter scheme that consists of a simultaneous CHIRP 180º ^{1}H pulse and a purging gradient followed by a single short gradient, all they placed between two 90º ^{1}H pulses.

The frequency-swept pulse flips the spins in different positions of the sample producing different evolutions for the ZQ terms. If the new phases created are enough, an efficient cancelation of ZQ terms is achieved. In **Fig. 1.19** it is shown the better performance of a 1D selective TOCSY experiment using the ZQ filter. The results can be extrapolated into the HSQC-TOCSY experiment where the application of ZQ filters is highly advisable to obtain better quality spectra.

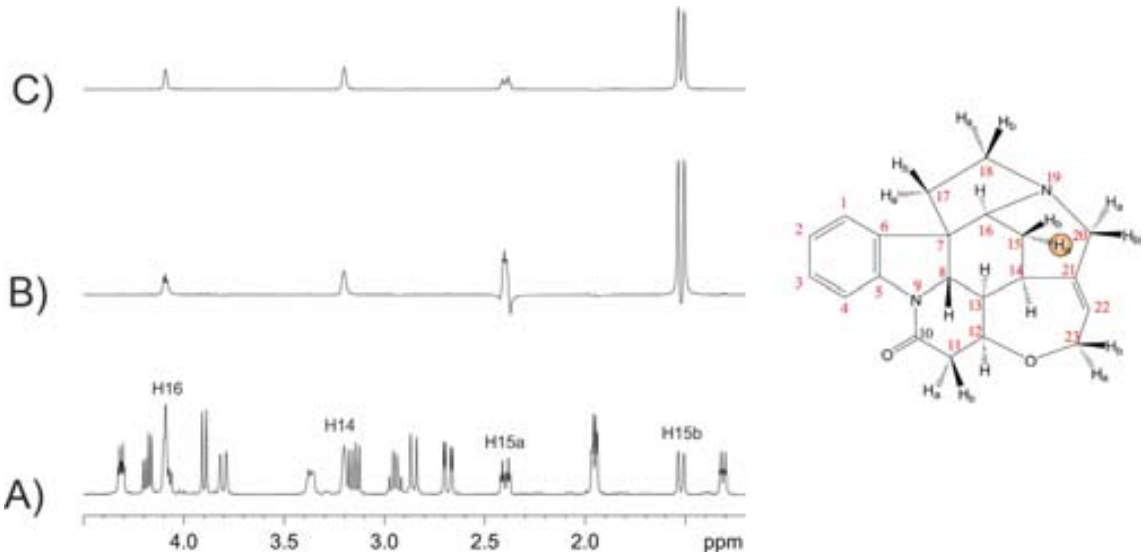

Figure 1.19. A) ^{1}H NMR spectrum of strychnine, B-C) conventional and ZQ filter version of the 1D-selective TOCSY experiment after selective inversion of the H15a proton, respectively. Notice that pure in-phase lineshapes are obtained in C) after a successful removal of ZQ contributions.

2.2.2 The HMBC experiment

The Heteronuclear Multiple Bond Correlation (HMBC) experiment[24] can be considered as the long-range correlation version of the HMQC experiment. It usually provides two- and three-bond correlations with non-protonated nuclei. **Fig. 1.20** shows the most basic HMBC pulse scheme that uses PFGs, so that the undesired signals from protons attached to ^{12}C are efficiently removed. The rules to optimize the gradient ratios are similar as discussed for HMQC.

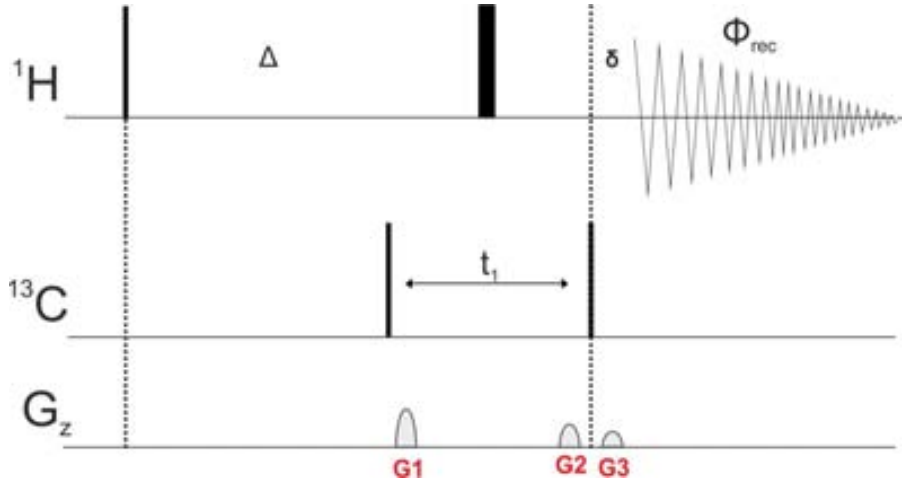

Figure 1.20. Basic ^{1}H-^{13}C-HMBC pulse sequence. Δ=1/(2^{n}J(CH)). G1:G2:G3=50:30:20.

Because long-range carbon-proton coupling constants (^{n}J(CH); n>1) values cover a range from 0 to 15 Hz, the experiment is usually acquired with a Δ period optimized to 5-8 Hz, which means that the inter-pulse delay lasts about 60-70 ms, whereas in HSQC/HMQC pulse sequences such delay lasts about 3.5 ms (usually optimized to ^{1}J(CH)=140 Hz). For that reason, the normal refocusing period is avoided, otherwise the pulse sequence becomes too large and relaxation losses are more severe. As a result, the proton signal is acquired as AP $2I_xS_z$ magnetization; therefore, the experiment must be recorded without carbon decoupling.

^{n}J(CH) and J(HH) coupling constants evolve simultaneously and similarly during the inter-pulse delay because their typical values are covered by the same range, so that the signals appear highly phase-twisted and therefore the determination of ^{n}J(CH) values is not an easy task. For clarity purposes, a processing step in magnitude mode is usually advisable for a qualitative analysis of HMBC spectra. Another important factor to take into account is that signal intensities in HMBC experiments depend on ^{n}J(CH) values and on the inter-pulse delay as

$$\alpha \sin(2\pi J_{(CH)}\Delta)$$

Thus, some expected cross-peaks having a small ^{n}J(CH) value could be missing or they could present very low intensity. Over the years, different improvements have been implemented in HMBC experiment in order to obtain better results[35], like for instance low-pass J-filters to remove one-bond correlation, or constant-time periods to achieve better peak appearance along the indirect dimension.

2.2.3 The HSQMBC experiment

2.2.3.1 The basic pulse scheme

The HSQMBC experiment[25] is a long-range optimized version of the HSQC experiment. It is based on the heteronuclear polarization transfer through ^{n}J(CH), via SQ coherences during the Δ delay as well as during t_1. Similarly to the HMBC experiment, its transfer mechanism allows to obtain correlations between protons and both protonated and non-protonated

[35] a) J. Furrer. *Concepts Magn. Reson*. **2012**, 40A, 101. b) J. Furrer. *Concepts Magn. Reson*. **2012**, 40A, 146.

carbon atoms separated by more than one bond (**Fig. 1.21**). The signal intensity will also depend on the nJ(CH) value and the Δ delay, as a function of $\sin(\pi {}^{n}J(CH)\Delta)$.

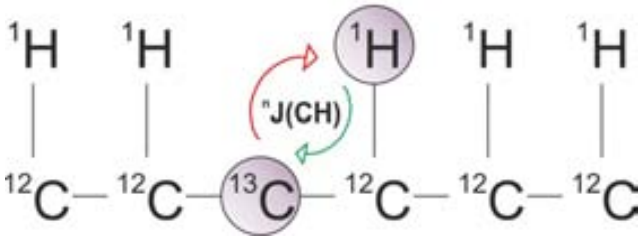

Figure 1.21. Magnetization transfer scheme for the HSQMBC experiment.

HSQMBC has a great advantage with respect to the HMBC experiment because J(HH) evolution is not present during the t_1 period. In addition, data can be presented in a phase-sensitive mode with pure absorption lineshapes which means that is perfectly suitable for the measurement of $^{n}J(CH)$. Hovewer, since J(HH) and $^{n}J(CH)$ values have similar sizes, simultaneous evolution of J(HH) and $^{n}J(CH)$ during the inter-pulse delay can cause the appearance of phase distortored cross-peaks and/or producing an important decrease of signal intensities. Since no refocused INEPT is applied for the same reasons as in HMBC experiments, the final magnetization is recorded in AP mode with respect to the active $^{n}J(CH)$ (**Fig. 1.22**).

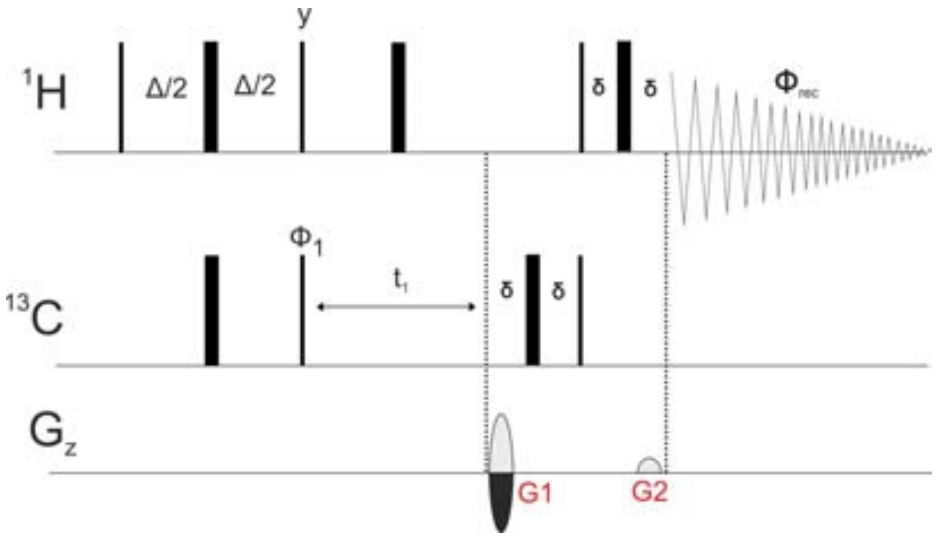

Figure 1.22. Basic pulse scheme of the ^{1}H-^{13}C-HSQMBC experiment. $\Delta=1/(2{}^{n}J(CH))$. Φ_1= x,-x. Φ_{rec}= x,-x. G1:G2 = 80:20.1

This fact might cause partial cancelation of long-range correlation cross-peaks or a maxima peak shifted. When the correlation cross-peaks appear as a singlets or doublets, a direct analysis from the AP signals can be done in a rather simple way. Nonetheless, in cases where the correlation cross-peaks appears as a more complex multiplet or when the $^{n}J(CH)$ value is small, a tedious and time-consuming fitting procedure is mandatory[36]. Such procedure requires an individualized fitting analysis for each cross-peak in which a reference peak is needed. To extract the heteronuclear coupling constant two signals from the ^{1}H NMR spectrum must be added in the following way: the first one in its conventional shape, and the

[36] R. A. E. Edden, J. Keeler. *J. Magn. Reson*. **2004**, 166, 53.

second one inverted and shifted until a similar pattern to the heteronuclear correlation is reached. The performed relative shift until a perfect fitting is achieved will indicate the magnitude of the $^{n}J(CH)$ (**Fig. 1.23**). If the original ^{1}H NMR signal appears overlapped it is also possible to use the 1D projection of a 2D HSQC cross-peak as a reference.

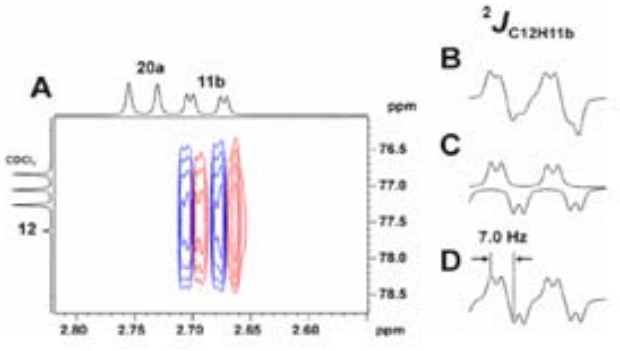

Figure 1.23. Fitting procedure to extract $^{n}J(CH)$ from HSQMBC multiplet patterns: A) expanded area showing the two-bond H11b-C12 cross-peak. B) 1D trace. C) two identical shifted multiplets (one of them inverted) obtained from the conventional ^{1}H NMR spectrum. D) $^{2}J(C12H11b)$ adjusted signal.

Due to the problems associated to the simultaneous evolution of J(HH) and $^{n}J(CH)$ coupling constants, several improvements has been proposed in the original HSQMBC pulse sequence. The most important are a) the implementation of BIRD block and b) the use of a 180º pulse train known as Carr-Purcell-Meiboom-Gil (CPMG) block.

2.2.3.2 The BIRD block: HSQMBC-BIRD experiment

The BIRD block[37] is generally used for two main purposes: a) to selectively observe the protons bound to ^{13}C and suppress those bound to ^{12}C after an inversion recovery period, and b) to differentiate direct ($^{1}J(CH)$) from long-range heteronuclear correlations ($^{n}J(CH)$) thanks to the large difference in their values (120-210 Hz vs. 0-12 Hz, respectively). Two different BIRD blocks are available: the $BIRD^{x}$ block, which is able to invert $^{1}J(CH)$ correlations while $^{n}J(CH)$ are unaffected; and the $BIRD^{y}$ block, which has the opposite effect (**Fig 1.24**).

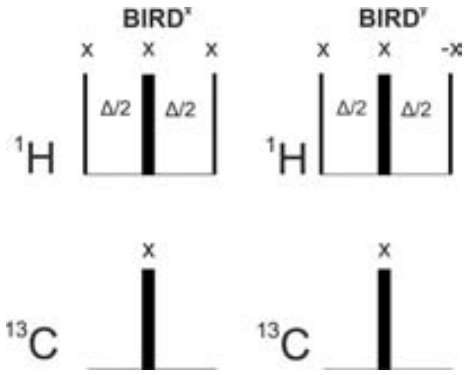

Figure 1.24. The BIRDx (right) and BIRDy (left) blocks. Δ is adjusted according to the $^{1}J(CH)$ value.

[37] D. Uhrín, T. Liptaj, K. E. Kövér. *J. Magn. Reson. A*. **1993**, 101, 41.

The BIRD^{y} block is able to refocuse the magnetization of the spin system into spin-echo periods, so that both chemical shift and homonuclear scalar coupling constants between I spins do not evolve during the Δ delay (**Fig. 1.25**).

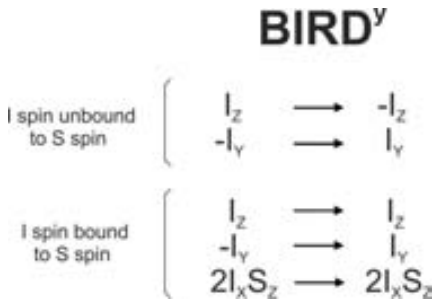

Figure 1.25. Magnetization transfer for the BIRD^{y} block. I nucleus stands for ^{1}H and S nucleus stands for ^{13}C.

In addition, the BIRD^{y} block is able to differentiate protons attached to ^{13}C nucleus from those attached to ^{12}C. Since ^{12}C-bound protons have no one-bond heteronuclear coupling, only their chemical shifts evolve during the Δ delay. These are subsequently refocused by the 180º ^{1}H pulse so that at the end of the second Δ period, the second 90º ^{1}H pulse places magnetization along the –z-axis producing the desired inversion of the ^{1}H–^{12}C resonances. For those spins that possess a heteronuclear coupling, chemical shifts will be refocused as well, so only the effect of the coupling has to be taken into account. After the second Δ delay, the magnetization lies along y-axis and is finally returned to +z-axis by the action of the final proton pulse, in such a way that it is as if the BIRD has never appeared for them.

As an application of the BIRD^{y} module, **Fig. 1.26** shows the pulse scheme for the HSQMBC-BIRD experiment[38] which is an HSQMBC experiment where the direct $^{1}J(CH)$ responses are minimized and J(HH) are partially refocused (except for $^{2}J(HH)$).

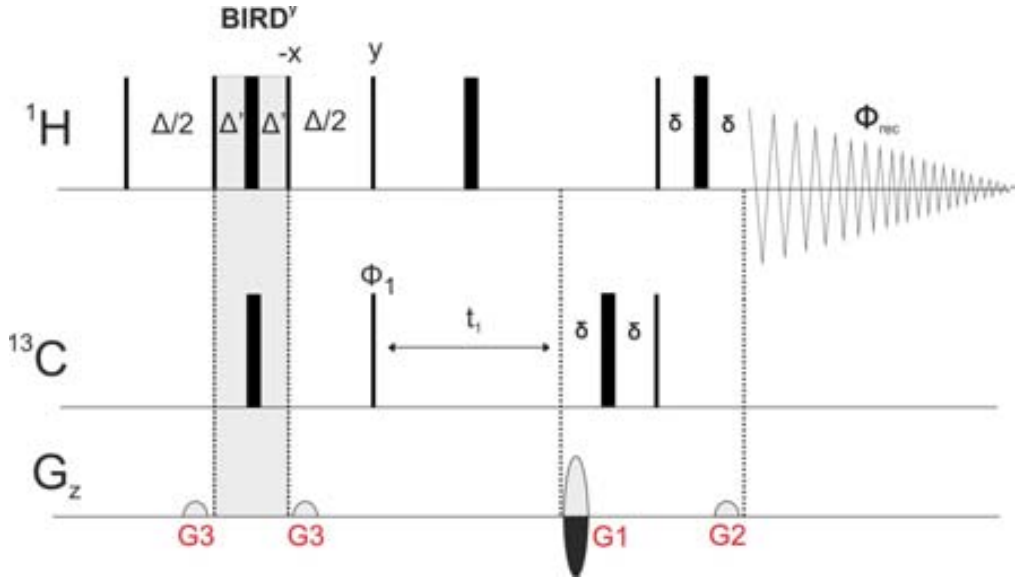

Figure 1.26. ^{1}H-^{13}C HSQMBC-BIRD experiment. $\Delta=1/(2^{n}J(CH))$. Φ_1= x,-x. Φ_{rec}= x,-x. G1:G2:G3 = 80:20.1:17.

[38] B.L. Marquez, W.H. Gerwick, R.T. Williamson. *Magn. Reson. Chem*. **2001**, 39, 499.

2.2.3.3 The CPMG pulse train: HSQMBC-CPMG experiment

It has been also reported that by applying a CPMG pulse train using composite π pulses and optimized inter-pulse delays (τ) within the CPMG cycle[39], the effect of undesired homonuclear J(HH) modulation from HSQMBC-like sequences could be minimized (**Fig. 1.27**). In theory, IP multiplets with respect to J(HH) should be obtained so that $^{n}J(CH)$ could be efficiently extracted from the resulting cross-peaks because no phase distortions should be expected. In this way the accuracy of the $^{n}J(CH)$ value would be mainly limited by the SNR of the corresponding cross-peak.

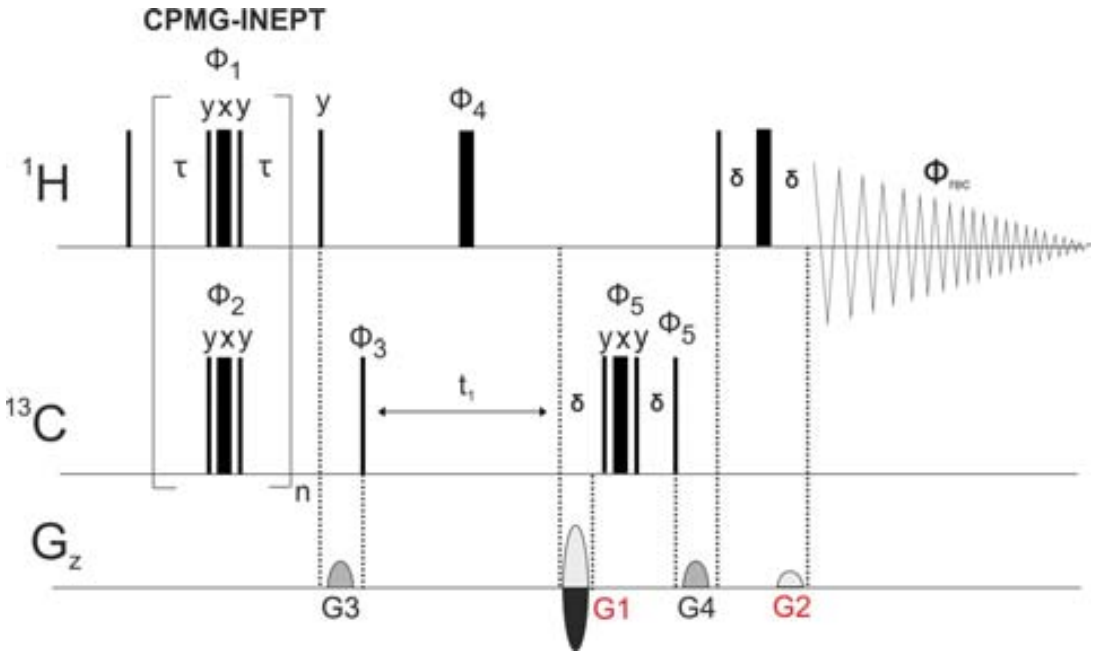

Figure 1.27. ^{1}H-^{13}C-CPMG-HSQMBC pulse sequence. The inter-pulse delay τ is usually adjusted around 200-400 μs, and the overall evolution period (2n*τ) is adjusted for long-range correlations (typically about 60-70 ms). Φ_1 and Φ_2 are incremented according to XY-16 cycles within the CPMG sequence. Φ_3= x,-x. Φ_4= x,x,-x,-x. Φ_5= x,x,x,x,-x,-x,-x,-x. Φ_{rec}= x,-x,x,-x,-x,x,-x,x. G1:G2:G3:G4 = 80:20.1:15:10.

It has been accepted that J(HH) coupling constants cannot be completely removed for all spin systems using CPMG and the use of very short inter-pulse delays (τ ≤ 400 μs) can put in serious troubles the limits of the probehead due to sample heating effects. In addition, homonuclear TOCSY transfer can be also effective during the CPMG period.

2.2.3.4 The combined GBIRD-CPMG-HSQMBC experiment

Williamson and co-workers published the GBIRD-CPMG-HSQMBC experiment[40] where the concepts of BIRD and CPMG were implemented into the same pulse sequence (**Fig. 1.28**). In theory, HSQMBC spectra with minimum distortions should be obtained (**Fig. 1.29**).

[39] K. E. Kövér, G. Batta, K. Fehér. *J. Magn. Reson*. **2006**, 181, 89.

[40] L. Valdemar Jr, V. Gil, M. G. Constantino, C. F. Tormena, R. T. Williamson, B. Marquez. *Magn. Reson. Chem.* **2006**, 44, 95.

2. Measurement of $^{n}J(CH)$

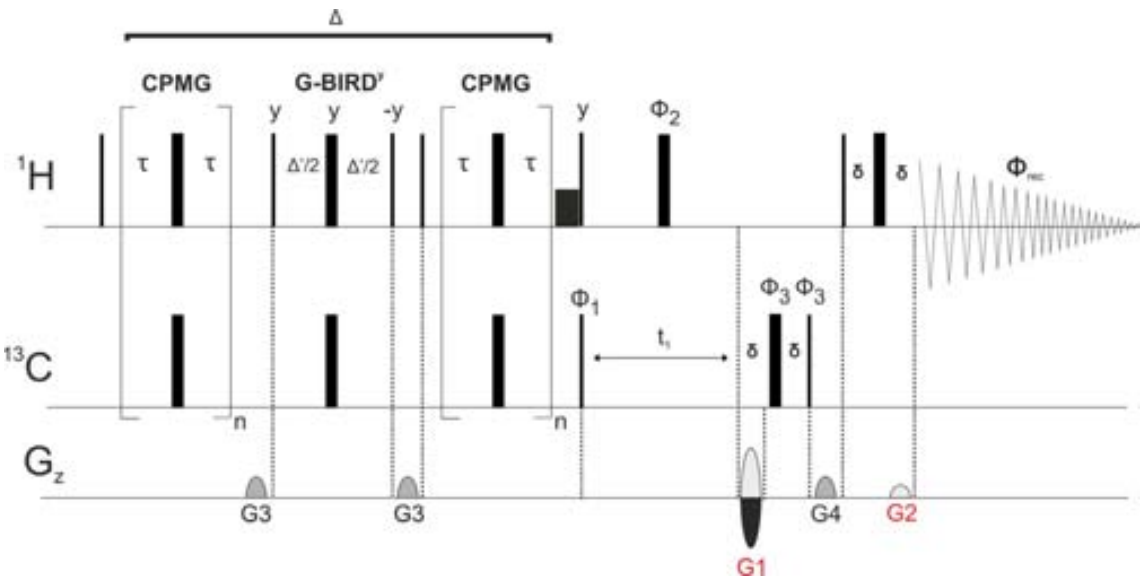

Figure 1.28. ^{1}H-^{13}C-GBIRD-CPMG-HSQMBC pulse sequence. $\Delta'=1/(2^{n}J(CH))$, τ=200 µs. Φ_1= x,-x. Φ_{rec}= x,-x. G1:G2:G3:G4 = 8:2:2.5:2.5:1

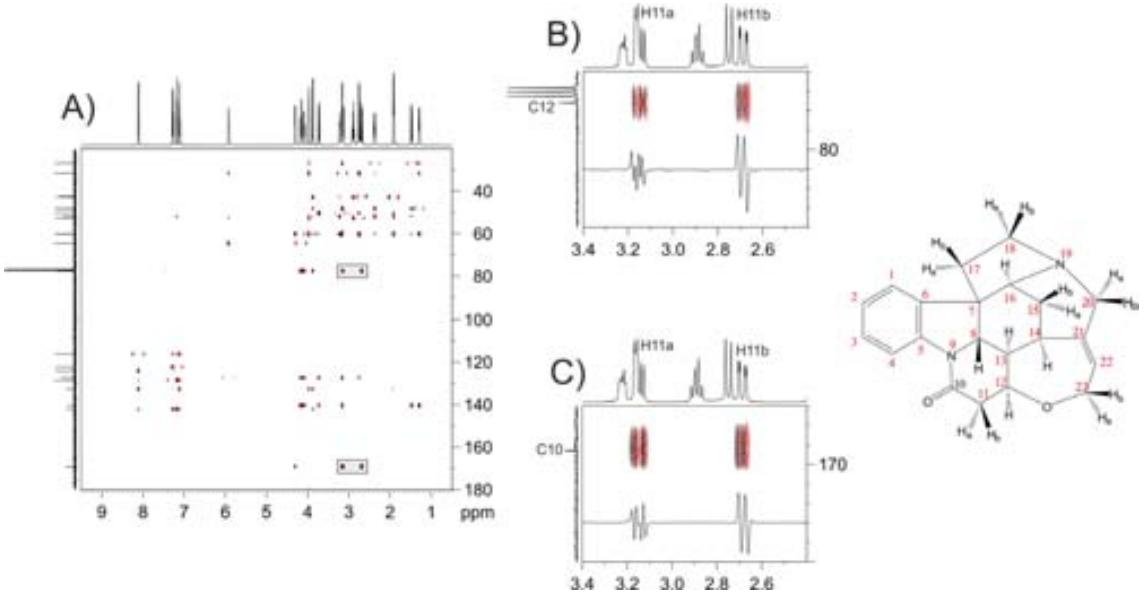

Figure 1.29. A) GBIRD-CPMG HSQMBC spectrum of strychnine, B) expanded area of the H11a-C12 and H11b-C12 cross-peaks, C) expanded area of the H11a-C10 and H11b-C10 cross-peaks.

Nevertheless, the experiment still has certain problems that prevent its general implementation in routine protocols:

- Strong dependence with the heteronuclear offset.
- Sample heating effects due to the short delays used in the CPMG pulse train.
- TOCSY signals coming from the CPMG pulse train.
- Lower sensitivity than other approaches due to t_1(rho) relaxation.
- Non perfect J(HH) refocusing.
- A fitting procedure is still required for the measurement of heteronuclear coupling constants from AP coupling patterns. An external reference is also required.

2.2.3.5 Implementing the IPAP methodology in HSQMBC-like sequence

The implementation of the IPAP methodology into the HSQMBC experiment was carried out by our research group[41] in order to avoid what very often tends to be a tedious and time-consuming analysis of AP multiplets for the extraction of $^{n}J(CH)$ coupling constants. The first idea was to use the HSQMBC-IPAP as it is done in the HSQC-TOCSY IPAP experiment. For a successful implementation of such methodology it is very important to keep IP signals with similar intensities as for the AP signals to avoid the use of scaling k factors and to minimize J cross-talk effects.

The HSQMBC IPAP experiment

When a refocused INEPT is inserted after the free evolution period t_1 of a HSQMBC experiment, the AP $2I_zS_x$ component is converted into IP I_y magnetization. An easy way to obtain AP multiplets without changing too much the pulse sequence can be reached by using a proton spin echo period instead of a R-INEPT transfer (**Fig. 1.30**). This is achieved by omitting the 180º heteronuclear pulse (marked with ε) and by changing the phase of the last 90º ^{1}H pulse (marked with Ψ) so that heteronuclear coupling constant refocusing does not take place.

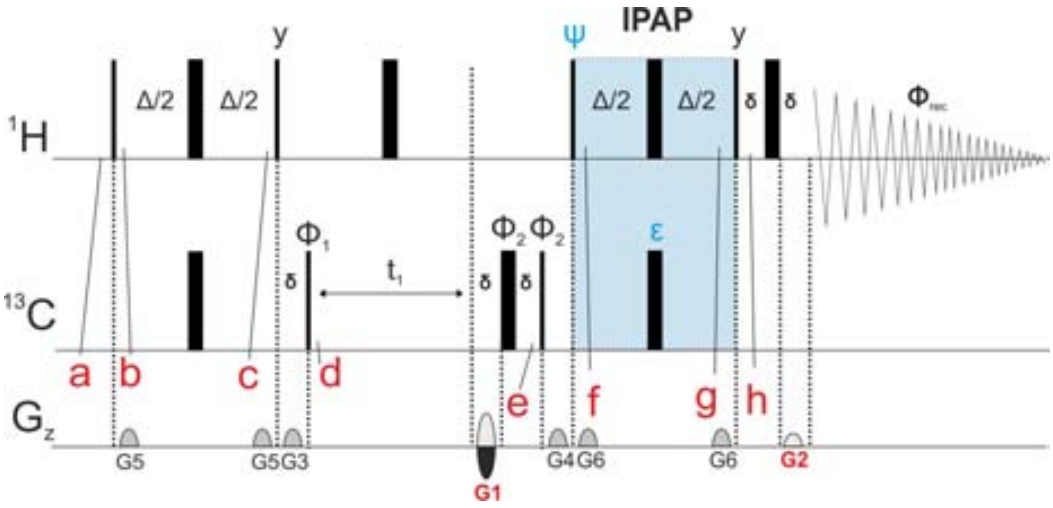

Figure 1.30. ^{1}H-^{13}C-HSQMBC IPAP pulse sequence. $\Delta=1/(2^{n}J(CH))$. Φ_1= x,-x. Φ_2= x,x,-x,-x. Φ_{rec}= x,-x,-x,x. IP: Ψ= y, ε= on. AP: Ψ= x, ε= off. G1:G2:G3:G4:G5:G6= 80:20.1:33:50:17:11

In what follows, an extensive analysis using the product operator formalism is made in order to completely understand what is happening with the magnetization components during the entire pulse sequence, and how IP and AP data are obtained. Such analysis is performed here because most of the sequences that will be introduced in further sections are based in the refocused version of the HSQMBC pulse scheme containing the IPAP methodology.

Let us consider a I nucleus (^{1}H) long-range coupled with a heteronuclear S spin (^{13}C), with a small $^{n}J(IS)$ coupling value. It is clear that simultaneous J(HH) evolution will take place during the inter-pulse Δ delays but, for clarity purposes, all the magnetization components due to such simultaneous evolution will be neglected. From the

[41] S. Gil, J. F. Espinosa, T. Parella. *J. Magn. Reson*. **2010**, 207, 312.

beginning of the pulse sequence (a point in **Fig. 1.30**) until the G1 encoding gradient is applied after the t_1 period (e point in **Fig. 1.30**), the evolution of the magnetization has already been analyzed[42] (see previous sections 1.1.1 and 1.3.1 of this thesis work). Until that point, and even after applying the subsequent 90º ^{13}C pulse, the pulse sequence, and thus, the evolution of the magnetization is exactly the same for both IP and AP data.

$$I_z \xrightarrow{\text{INEPT}} \xrightarrow{\Omega_S t_1} \xrightarrow{90^S_x} -2I_zS_z\sin(2\pi J_{IS}\Delta)\cos(\Omega_S t_1) + 2I_zS_x\sin(2\pi J_{IS}\Delta)\sin(\Omega_S t_1)$$

Henceforth, IP and AP data will follow different pathways and they are analyzed separately:

IP data: ψ=y, ε=on

$$-2I_zS_z\sin(2\pi J_{IS}\Delta)\cos(\Omega_S t_1) \xrightarrow{90^I_y\ (\psi=y)} -2I_xS_z\sin(2\pi J_{IS}\Delta)\cos(\Omega_S t_1) + \boxed{2I_xS_x\sin(2\pi J_{IS}\Delta)\sin(\Omega_S t_1)}$$

($2I_xS_x$ is MQ coherence and is not detected in the FID)

$$\xrightarrow{2\pi J_{IS}\Delta} -2I_xS_z\sin(2\pi J_{IS}\Delta)\cos(\Omega_S t_1)\cos(\pi J_{IS}\Delta) - I_y\sin(2\pi J_{IS}\Delta)\cos(\Omega_S t_1)\sin(\pi J_{IS}\Delta)$$

$$\xrightarrow{180^I_x} -2I_xS_z\sin(2\pi J_{IS}\Delta)\cos(\Omega_S t_1)\cos(\pi J_{IS}\Delta) + I_y\sin(2\pi J_{IS}\Delta)\cos(\Omega_S t_1)\sin(\pi J_{IS}\Delta)$$

$$\xrightarrow{180^S_x\ (\varepsilon=on)} +2I_xS_z\sin(2\pi J_{IS}\Delta)\cos(\Omega_S t_1)\cos(\pi J_{IS}\Delta) + I_y\sin(2\pi J_{IS}\Delta)\cos(\Omega_S t_1)\sin(\pi J_{IS}\Delta)$$

$$\xrightarrow{2\pi J_{IS}\Delta} \begin{aligned} &+ 2I_xS_z\sin(2\pi J_{IS}\Delta)\cos(\Omega_S t_1)\cos(\pi J_{IS}\Delta)\cos(\pi J_{IS}\Delta) \\ &+ I_y\sin(2\pi J_{IS}\Delta)\cos(\Omega_S t_1)\cos(\pi J_{IS}\Delta)\sin(\pi J_{IS}\Delta) \\ &+ I_y\sin(2\pi J_{IS}\Delta)\cos(\Omega_S t_1)\sin(\pi J_{IS}\Delta)\cos(\pi J_{IS}\Delta) \\ &- 2I_xS_z\sin(2\pi J_{IS}\Delta)\cos(\Omega_S t_1)\sin(\pi J_{IS}\Delta)\sin(\pi J_{IS}\Delta) \end{aligned} \rightarrow$$

$$\begin{aligned} &+ 2I_xS_z[\sin(2\pi J_{IS}\Delta)\cos(\Omega_S t_1)]\cdot[\cos^2(\pi J_{IS}\Delta)-\sin^2(\pi J_{IS}\Delta)] \\ &+ I_y\sin[(2\pi J_{IS}\Delta)\cos(\Omega_S t_1)]\cdot[2\sin(\pi J_{IS}\Delta)\cos(\pi J_{IS}\Delta)] \end{aligned} \quad \begin{matrix} \cos2(\theta)=\cos^2\theta-\sin^2\theta \\ \Rightarrow \\ \sin2(\theta)=2\cos\theta\sin\theta \end{matrix}$$

$$+ 2I_xS_z[\sin(2\pi J_{IS}\Delta)\cos(\Omega_S t_1)]\cdot[\cos(2\pi J_{IS}\Delta)] + I_y\sin[(2\pi J_{IS}\Delta)\cos(\Omega_S t_1)]\cdot[\sin(2\pi J_{IS}\Delta)] \xrightarrow{90^I_y} + 2I_zS_z[\sin(2\pi J_{IS}\Delta)\cos(\Omega_S t_1)]\cdot[\cos(2\pi J_{IS}\Delta)] \boxed{+ I_y\sin^2(2\pi J_{IS}\Delta)\cos(\Omega_S t_1)}$$

[42] Although such analysis was performed for the HSQC pulse sequence, same rules are applicable here since the only difference is related to the optimized Δ delay (one-bond optimized vs. long-range optimized).

AP data: ψ=x, ε=off

$$-2I_zS_z\sin(2\pi J_{IS}\Delta)\cos(\Omega_S t_1) \xrightarrow{90^{\circ}_{x}(\psi=x)} -2I_yS_z\sin(2\pi J_{IS}\Delta)\cos(\Omega_S t_1) + \boxed{2I_yS_x\sin(2\pi J_{IS}\Delta)\sin(\Omega_S t_1)}$$

(2I$_y$S$_x$ is MQ coherence and is not detected in the FID)

$$\xrightarrow{2\pi J_{IS}\Delta} -2I_yS_x\sin(2\pi J_{IS}\Delta)\cos(\Omega_S t_1)\cos(\pi J_{IS}\Delta) + I_x\sin(2\pi J_{IS}\Delta)\cos(\Omega_S t_1)\sin(\pi J_{IS}\Delta)$$

$$\xrightarrow{180^{\circ}_{x}} +2I_yS_z\sin(2\pi J_{IS}\Delta)\cos(\Omega_S t_1)\cos(\pi J_{IS}\Delta) + I_x\sin(2\pi J_{IS}\Delta)\cos(\Omega_S t_1)\sin(\pi J_{IS}\Delta)$$

$$\xrightarrow{2\pi J_{IS}\Delta} \begin{aligned} &+ 2I_yS_x\sin(2\pi J_{IS}\Delta)\cos(\Omega_S t_1)\cos(\pi J_{IS}\Delta)\cos(\pi J_{IS}\Delta) \\ &- I_x\sin(2\pi J_{IS}\Delta)\cos(\Omega_S t_1)\cos(\pi J_{IS}\Delta)\sin(\pi J_{IS}\Delta) \\ &+ I_x\sin(2\pi J_{IS}\Delta)\cos(\Omega_S t_1)\sin(\pi J_{IS}\Delta)\cos(\pi J_{IS}\Delta) \\ &+ 2I_yS_z\sin(2\pi J_{IS}\Delta)\cos(\Omega_S t_1)\sin(\pi J_{IS}\Delta)\sin(\pi J_{IS}\Delta) \end{aligned} \longrightarrow$$

$$+ 2I_yS_z[\sin(2\pi J_{IS}\Delta)\cos(\Omega_S t_1)]\cdot[\cos^2(\pi J_{IS}\Delta)+\sin^2(\pi J_{IS}\Delta)] \xrightarrow{\cos^2\theta + \sin^2\theta = 1}$$

$$+ 2I_yS_z\sin(2\pi J_{IS}\Delta)\cos(\Omega_S t_1) \xrightarrow{90^{\circ}_{y}} \boxed{+ 2I_yS_z\sin(2\pi J_{IS}\Delta)\cos(\Omega_S t_1)}$$

After addition and subtraction of the IP and AP data, two new α- and β- sub-spectra, are obtained, where the magnetization components are parallel with respect to the I spin magnetization:

α (IP+AP): $[I_y\sin(2\pi J_{IS}\Delta)+2I_yS_z]\,[\sin(2\pi J_{IS}\Delta)\cos(\Omega_S t_1)]$
β (IP-AP): $[I_y\sin(2\pi J_{IS}\Delta)-2I_xS_z]\,[\sin(2\pi J_{IS}\Delta)\cos(\Omega_S t_1)]$

When considering not only a I nucleus long-range coupled with a S spin, but also coupled with other nucleus I by means of J(II), the final expressions change to:

IP: $+ I_y\sin^2(2\pi J_{IS}\Delta)\cos(\Omega_S t_1)\mathbf{\cos^2(\pi\Pi J_{II}\Delta)}$
AP: $+ 2I_yS_x\sin(2\pi J_{IS}\Delta)\cos(\Omega_S t_1)\mathbf{\cos^2(\pi\Pi J_{II}\Delta)}$

Very importantly, the percentage of cross-talk generated in such addition/subtraction (IP ± AP) procedures due to the non equivalence between IP and AP data is an important issue to evaluate. Ignoring important relaxation differences in small molecules, the amount the cross-talk in a given multiplet will be proportional to the $\sin^2(2\pi J_{IS}\Delta)$ - $\sin(2\pi J_{IS}\Delta)$ factor and the percentage of cross-talk with respect to the overall multiplet sensitivity is defined by:

$$\%\text{cross-talk} = [\sin(2\pi J_{IS}\Delta)-1]/[\sin(2\pi J_{IS}\Delta)+1]$$

Equation 11

As an example, if the Δ delay is optimized to 6 Hz with a J_{IS} = 4.0 Hz, the percentage of cross talk would be 7,2%.

2.2.3.6 The GBIRD-HSQMBC IPAP experiment

In order to minimize the effects of J(HH) evolution, as well as $^{1}J(CH)$ responses, a GBIRD filter can be inserted into the INEPT block giving as a result the GBIRD-HSQMBC IPAP experiment[41] (**Fig. 1.31**).

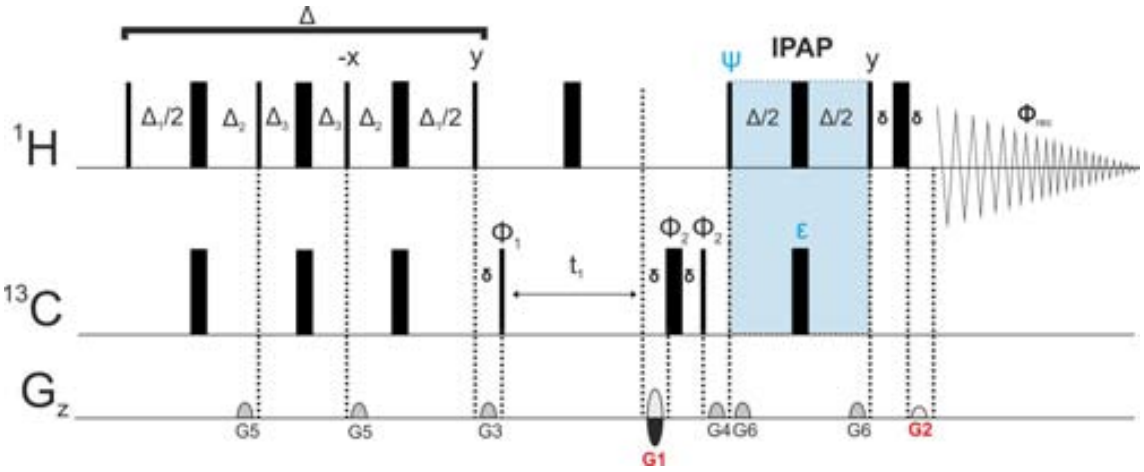

Figure 1.31. ^{1}H-^{13}C-GBIRD-HSQMBC IPAP pulse sequence. $\Delta=1/(2^{n}J(CH))=2\Delta_1+2\Delta_2+2\Delta_3$; where $\Delta_1=1/(8^{n}J(CH))$, $\Delta_2=\Delta_1-\Delta_3$ and $\Delta_3=1/(2^{1}J(CH))$. Φ_1= x,-x. Φ_2= x,x,-x,-x. Φ_{rec}= x,-x,-x,x. IP: Ψ= y, ε= on. AP: Ψ= x, ε= off. G1:G2:G3:G4:G5:G6= 80:20.1:33:50:17:11.

Any J(HH) evolution that modifies the shape of the IP and AP cross-peak patterns is produced in a complementary way in both experiments. That modulation is equally preserved in the α- and β- spectra and therefore they would present the same phase distortions, allowing the measurement of $^{n}J(CH)$ in a simple manner by analyzing the relative α/β- displacement along the detected dimension (**Fig. 1.32**).

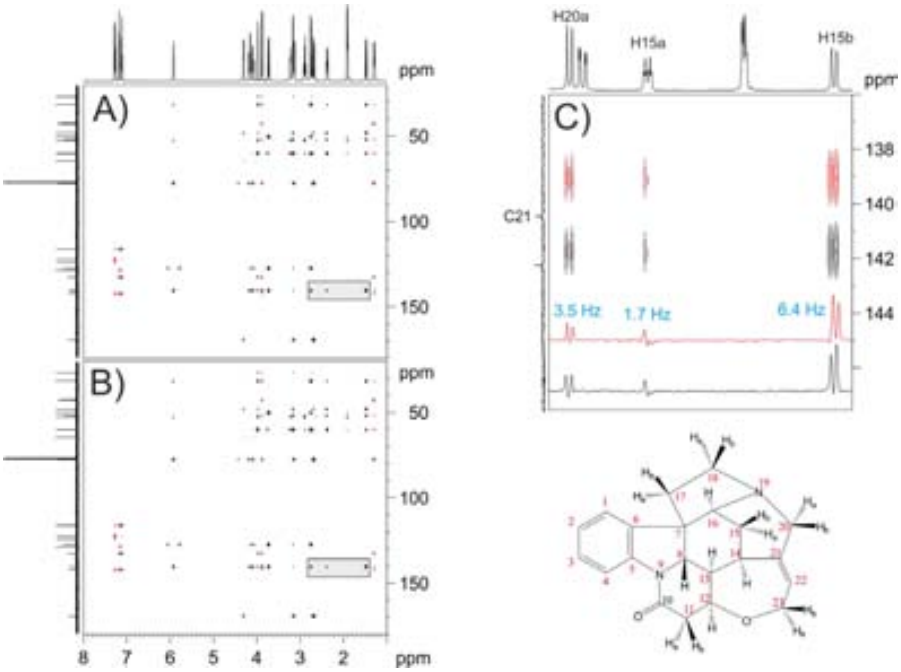

Figure 1.32. A) GBIRD-HSQMBC IP data, B) GBIRD-HSQMBC AP data, and C) expanded area at the C21 carbon frequency showing some of the α-/β- cross-peaks. Note that the extraction of the magnitude of the coupling constant is performed from the 1D slices.

2.3 Implementing frequency-selective 180º ^{1}H pulses: the selHSQMBC IPAP experiment

Despite the fact that GBIRD-HSQMBC IPAP experiment has proved efficient for the measurement of ^{n}J(CH) in both protonated and non-protonated carbon atoms, the modulation of the intensity by the homonuclear J(HH) couplings still remain as the most important drawback to overcome. A very simple solution to avoid such J(HH) interferences in HSQMBC pulse schemes was proposed by our research group[43]. It is based on the implementation of frequency-selective 180º ^{1}H pulses during the INEPT blocks. Although that idea can be implemented in the original non-refocused HSQMBC experiment where the resulting cross-peaks would present AP coupling pattern with respect to the active ^{n}J(CH) and pure IP pattern with respect to all passive J(HH), accidental line cancelation and/or complex analysis of AP multiplets could still remain, meaning that tedious and time-consuming fitting procedures would be required. To solve that problem a powerful approach for the simple, direct and accurate determination of ^{n}J(CH) has been described, denoted as selHSQMBC IPAP experiment[43]. It is based on the incorporation of the IPAP principle into the selHSQMBC pulse scheme (**Fig. 1.33**), and combines the features of the selHSQMBC-IP and selHSQMBC-AP experiments. The IP data, generated using Ψ= y and ε = on, present a $\sin^2(\pi^n J(CH)\Delta)$ intensity dependence, whereas the AP data, obtained using Ψ= x and omitting the last 180º ^{13}C pulse to avoid J(CH) refocusing (ε = off), present a simple $\sin(\pi^n J(CH)\Delta)$ intensity dependence. These time-domain data are added/subtracted to afford pure-phase α/β-selHSQMBC spectra.

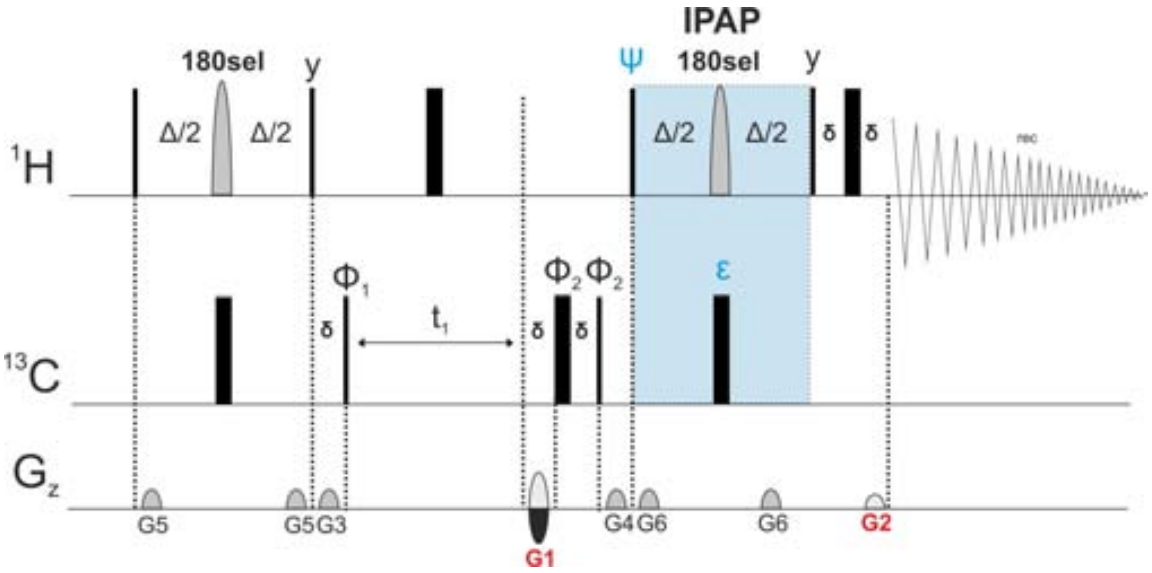

Figure 1.33. ^{1}H-^{13}C-selHSQMBC IPAP pulse sequence. Δ=1/(2^{n}J(CH)). Φ_1= x,-x. Φ_2= x,x,-x,-x. Φ_{rec}= x,-x,-x,x. IP: Ψ= y, ε= on. AP: Ψ= x, ε= off. G3 and G4 gradients act as zz-purge gradient filters, G5 and G6 are used for refocused heteronuclear gradient echo and G1 and G2 are used for coherence selection. G1:G2:G3:G4:G5:G6= 80:20.1:33:50:17:11.

The ^{n}J(CH) coupling constant value can be extracted by direct analysis of the relative frequency displacement between α/β- cross peaks (**Fig. 1.34**). As a very important point to highlight, the measurement is performed along the detected dimension, which is not a practical problem because the frequency-selective nature of the experiment allows the use of

[43] S. Gil, J.F. Espinosa, T. Parella. *J. Magn. Reson.* **2011**, 213, 145.

reduced spectral widths and the relatively long acquisition time needed to reach high levels of digitalization can be compensated by the use of short pre-scan delays for an optimal relaxation. Therefore, the number of t_1 increments is only dependent on the degree of signal congestion in the ^{13}C dimension.

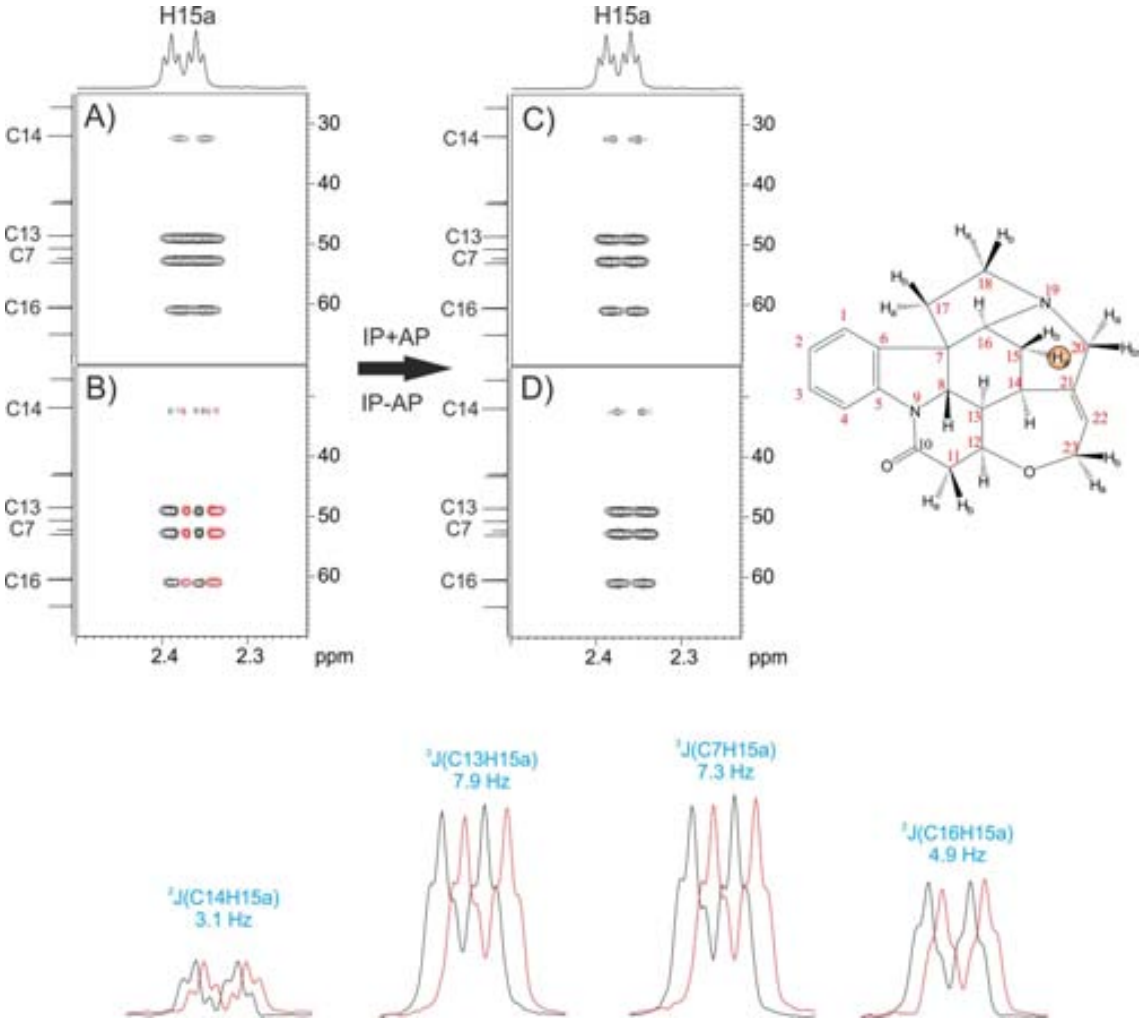

Figure 1.34. selHSQMBC IPAP after selective inversion of H15a in strychnine. A) IP data, B) AP data, C) α-spectrum (IP+AP) and D) β-spectrum (IP-AP). Note that the magnitude of $^{n}J(CH)$ can be extracted with high accuracy by analyzing the relative displacements of α- and β- spectra from their 1D projections.

II. OBJECTIVES

Evaluation of existing experiments

The first objective of this thesis was to evaluate and to compare the existing NMR methods developed to measure long-range heteronuclear coupling constants, in order to better understand the advantages/drawbacks of each methodology.

Design of new NMR methods

A second general objective was to design new NMR methods to overcome the different drawbacks found when measuring such coupling constants. They can be resumed as:

- How to obtain an accurate measurement of small long-range proton-carbon coupling constants ($^{n}J(CH)$), with special emphasis to magnitudes smaller than 2-3 Hz.
- How to perform such measurements for both protonated and non-protonated carbon atoms.
- How to determine the relative sign information of $^{n}J(CH)$.
- How to measure $^{n}J(CH)$ for any type of multiplet pattern, independent of its complexity and degree of signal overlapping.

Pursuing the ideal situation

Another main objective was the development of NMR techniques that yield the maximum spectroscopic information with the minimum experimental time, and if possible, in a single-shot NMR experiment. Such experiment should be easy to implement and should be as robust and accurate as possible. In addition, the extraction of the relevant NMR parameters (mainly focused on coupling constants) should be done in a straightforward way, without extensive and sophisticated post-processing tasks.

Experimental aspects to take into account

Some key features that would define a specific NMR method as an ideal tool to measure coupling constants can be explained in terms of experimental aspects (resolution, sensitivity and general applicability of the method) and further data manipulation (simplicity and accuracy of the measurement). We wanted to concentrate our efforts to develop new methods that should meet a number of basic conditions:

- Good sensitivity to obtain NMR data in a reasonable experimental time.
- Optimal spectral resolution in both detected and indirect dimensions.
- General applicability covering a wide range of conditions and situations (spectral complexity of the molecule and its degree of accidental signal overlap, the number and nature of cross-peaks to be analyzed from a single NMR spectrum, etc.).

- The method should be simple in terms of data acquisition, data analysis, processing, and spectral interpretation.

- The method should provide an accurate and precise measurement, if possible, through a simple and direct analysis of cross-peaks, and without complex post-processing data manipulation.

Most of the times the ideas came to us as the new NMR methods were being developed. The starting point was the prior knowledge and experience of our research group and some of our previous developed NMR techniques, with special emphasis to the selHSQMBC experiment and the IPAP methodology.

III. RESULTS AND DISCUSSION

This section contains the results obtained during my PhD that have been published in different scientific journals as eight individual original research papers. In each publication a different experiment is described either for the measurement of long-range heteronuclear coupling constants or for the simultaneous measurement of both heteronuclear and homonuclear coupling constants.

Since every published paper has gone through a review process by NMR experts, not much attention is devoted to the discussion of the results beyond what is discussed in each publication. Nevertheless, a little introduction is presented for each one of the published papers, as well as an expansion of the results in some cases.

It has been considered appropriate to introduce the publications in such a way that a logical thread is followed, instead of presenting them in a chronological order. Therefore, the publications have been divided as follows:

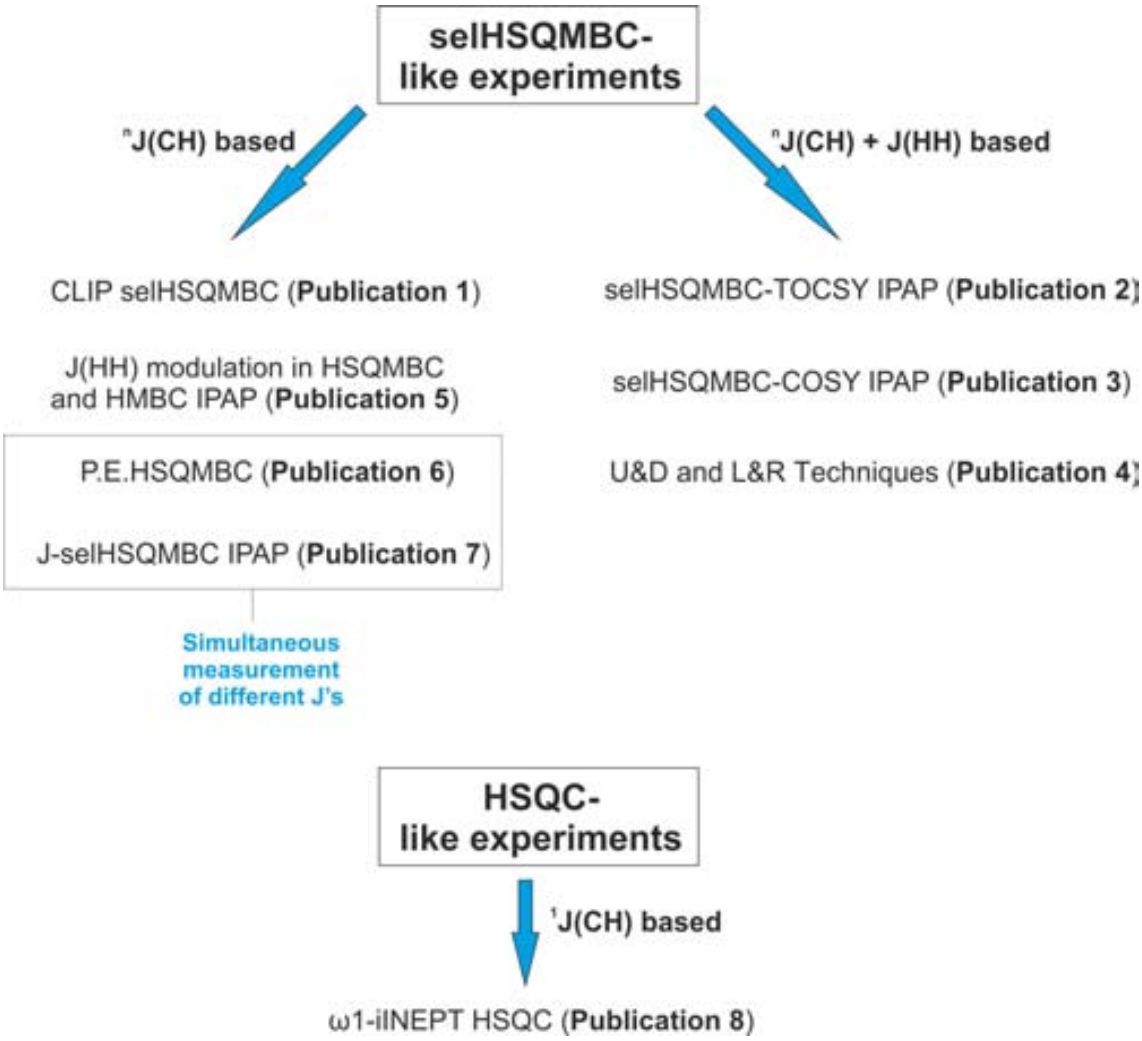

PUBLICATION 1

CLIP-HSQMBC: Easy measurement of small proton-carbon coupling constants in organic molecules

J. Saurí, T. Parella, J. F. Espinosa. ***Org. Biomol. Chem.*** **2013, 11, 4473-4478**

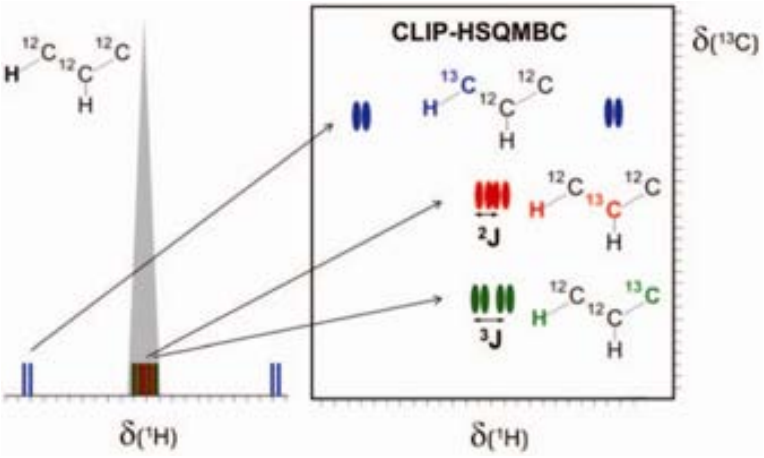

1. Introduction

A very simple experiment for the measurement of the magnitude of $^{n}J(CH)$ coupling constants, denoted as CLIP-selHSQMBC (where CLIP stands for CLean In-Phase) is presented.

The pulse sequence is closely related to the selHSQMBC IPAP experiment to obtain IP data[1] but with a slight modification: a 90º carbon purge pulse is inserted at the end of the pulse sequence, just prior to the acquisition, in order to remove unwanted AP components that would difficult the extraction of $^{n}J(CH)$[2]. The paper evaluates how the presence/absence of such purge pulse can affect the accuracy of the measurement of heteronuclear coupling constants in HSQMBC-like sequences. In the resulting CLIP-HSQMBC spectra, $^{n}J(CH)$ values are directly measured from pure in-phase multiplets patterns. The extraction is performed by analyzing the additional splitting due to the heteronuclear coupling constant with respect to those multiplets from the conventional ^{1}H NMR spectrum. In cases of resolved signals the measurement can be made in terms of peak separation or from the difference of the outer peaks with respect to those of the multiplets from the conventional ^{1}H NMR spectrum. For non-resolved multiplets a fitting procedure taking the internal satellite line obtained from a $^{1}J(CH)$ cross-peak as a reference, is required.

In HSQMBC-like experiments the signal intensity is directly correlated to the magnitude of the heteronuclear coupling constant. In order to measure small $^{n}J(CH)$ values, a TOCSY block can be inserted at the end of the pulse sequence to extend the information along the complete spin system. Thanks to the application of ZQ-filters, non-distorted pure IP TOCSY multiplets are reached and the measurement can efficiently be performed[3].

[1] See section 2.3 of this thesis work.

[2] See section 1.3.3, paragraph v., of this thesis work.

[3] See section 2.2.1.3 of this thesis work.

Organic & Biomolecular Chemistry

RSCPublishing

PAPER

View Article Online
View Journal | View Issue

Cite this: Org. Biomol. Chem., 2013, 11, 4473

CLIP-HSQMBC: easy measurement of small proton–carbon coupling constants in organic molecules†

Josep Saurí,[a] Teodor Parella[a] and Juan F. Espinosa*[b]

A user-friendly 2D NMR approach denoted as CLIP-HSQMBC is proposed for the very easy, direct and accurate measurement of long-range proton–carbon coupling constants in organic molecules and natural products. The *J* value can be extracted directly from the analysis of resolved in-phase ^{1}H multiplets that show an additional splitting arising from the proton–carbon coupling. In cases of unresolved peaks, a simple fitting analysis using the internal satellite lines as a reference is performed. Addition of a spin-lock period results in a CLIP-HSQMBC-TOCSY experiment that is suitable for the measurement of very small coupling values or to observe correlations from overlapped resonances.

Received 4th April 2013,
Accepted 9th May 2013

DOI: 10.1039/c3ob40675j

www.rsc.org/obc

Introduction

The increasing use of proton–carbon coupling constants over more than one bond in structural elucidation and conformational analysis of organic molecules[1] has been paralleled by the development of many different pulse sequences for their measurement in small molecules at natural abundance.[2] One of the major problems encountered by those who want to apply these couplings in organic chemistry is the analysis of the resulting signals. The methodology used depends on whether the carbon involved in the coupling is protonated or non-protonated. For protonated carbons, sequences that start with an HSQC step to separate proton signals showing the α and the β state of the attached carbon, followed by a TOCSY element to propagate the magnetization to the protons of the same spin system, represent the preferred solution, and NMR experiments such as HECADE[3] or α/β-HSQC-TOCSY[4] are widely used. These experiments provide 2D spectra where accurate values of the magnitude and sign of the proton–carbon couplings can be easily measured from signal displacement along the F2-dimension of higher resolution.

In contrast, when the carbon is non-protonated or when magnetization transfer *via* TOCSY is not possible because of a vanishingly small proton–proton coupling constant, this type of sequence cannot be applied and a variety of solutions based on HSQMBC[5] or HMBC[6] schemes with interpulse delays optimized to long-range proton–carbon couplings have been developed. In these experiments, the measurement of the coupling constants along the detected F2 dimension is not simple due to the anti-phase character of the heteronuclear coupling that may lead to partial or complete cancellation of peaks, complicating the analysis especially for complex multiplets. In addition, evolution of homonuclear coupling constants causes additional phase distortions in the final multiples. Although some solutions have been proposed such as the use of CPMG pulse trains to "decouple" the homonuclear couplings[7] a complete suppression of signal distortion is not always achieved. Alternatively, the heteronuclear couplings can be determined *via J*-resolved spectroscopy, although the couplings are measured with less precision due to the lower resolution along the indirect F1 dimension.[8]

Organic chemists routinely measure proton–proton coupling constants as the difference in frequency between the relevant peaks within a multiplet in conventional ^{1}H spectra. The proton–carbon coupling constants can be also measured in terms of peak separation in ^{13}C-labeled compounds in which protons coupled to the ^{13}C-nucleus exhibit an extra splitting. These multiplets showing a proton–carbon coupling are also present in ^{1}H spectra of unlabeled molecules, arising from the ^{13}C-isotopomer that accounts for 1.1% of the total compound; however, the signals are very weak and they are obscured by the strong signals of the ^{12}C-isotopomer. Only the ^{13}C-satellites of protons attached to a ^{13}C-nucleus may be visible because they appear well separated from the major ^{12}C-isotopomer signals, but they merely provide one-bond proton–carbon couplings.

Here we report a 2D-NMR sequence based on the HSQMBC experiment (Fig. 1) that allows the clean observation of the ^{13}C-isotopomer signals without the interference of the ^{12}C-isotopomer signals. In contrast to the conventional HSQMBC, the

[a]Servei de Ressonància Magnética Nuclear, Universitat Autònoma de Barcelona, 08193-Bellaterra, Barcelona, Spain
[b]Centro de Investigación Lilly S.A., Avda. de la Industria 30, 28108-Alcobendas, Madrid, Spain. E-mail: jfespinosa@lilly.com; Fax: +34 91 6233561; Tel: +34 91 6633435

†Electronic supplementary information (ESI) available. See DOI: 10.1039/c3ob40675j

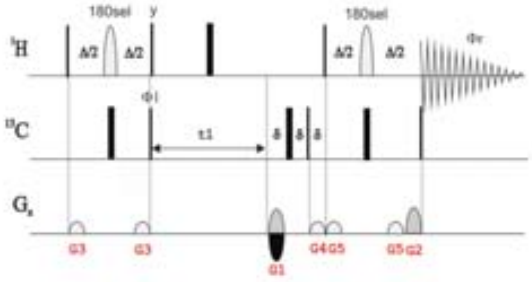

Fig. 1 Pulse scheme for the CLIP-HSQMBC experiment. Narrow and wide rectangular bars represent 90° and 180° pulses. A ^{1}H-selective 180° pulse marked as a shaped bar is applied in the middle of the INEPT blocks ($\Delta' = 1/(2^nJ(CH)) = \Delta$ + p180 where p180 is the duration of the selective 180° ^{1}H pulse) and ^{1}H data are acquired without ^{13}C decoupling. All pulses have phase x, unless otherwise noted. A minimum two-step phase cycle is applied: $\phi_1 = x, -x$ and $\phi_r = x, -x$. Gradients G1 and G2 are used for coherence selection using the echo-antiecho protocol, G4 acts as a zz-filter, and G3 and G5 flank the inversion proton pulses to generate pure refocusing elements. δ stands for the duration of the pulsed-field gradient and the corresponding recovery delay.

heteronuclear and the homonuclear couplings exhibit pure in-phase character and therefore the proton–carbon coupling can be easily measured in terms of peak separation in the same manner as proton–proton couplings are measured.

Results and discussion

The new 2D pulse sequence is a proton-selective HSQMBC experiment with the hard 180° proton pulses in the INEPT periods replaced with selective 180° pulses to completely eliminate homonuclear coupling modulation and avoid signal distortion.[9] The removal of homonuclear coupling modulation is crucial to assure pure absorptive lineshapes from which accurate couplings can be determined. These principles were first applied in a 1D doubly-selective experiment that included selective shaped-pulses on both proton and carbon resonances for determination of the heteronuclear coupling constant for a specific proton–carbon pair.[10] The second key point of the pulse sequence is the application of a 90° carbon pulse before acquisition to convert residual antiphase $2I_yS_z$ components to non-observable $2I_yS_y$ multiple-quantum coherences. The experiment leads to full in-phase multiplets in the form of $I_x\sin^2(\pi^nJ_{CH}\Delta')$ that are acquired without carbon decoupling. The selection of a 90° carbon pulse as a purge element was based on the comparative analysis performed by Luy and coworkers,[11] who examined three different modifications of the HSQC experiment for antiphase removal and concluded that the best clean in-phase spectra were obtained when a 90° carbon pulse was applied prior to detection. This approach was first proposed by Sorensen and coworkers in DEPT+ experiments.[12] In analogy to the CLIP-HSQC experiment developed by Luy and coworkers for the measurement of one-bond heteronuclear couplings from pure absorptive spectra, we have denoted this pulse sequence as CLIP-HSQMBC, where the term CLIP refers to CLean IN-Phase multiplets and HSQMBC stands for Heteronuclear Single Quantum Multiple Bond Correlation (HSQMBC) as in the original sequence.

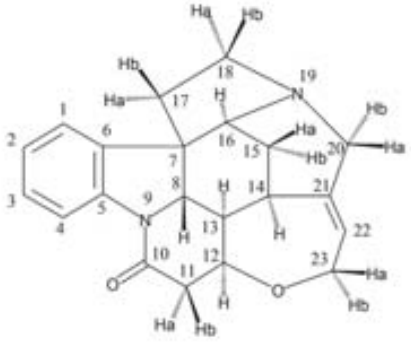

Fig. 2 Molecular structure of strychnine (**1**).

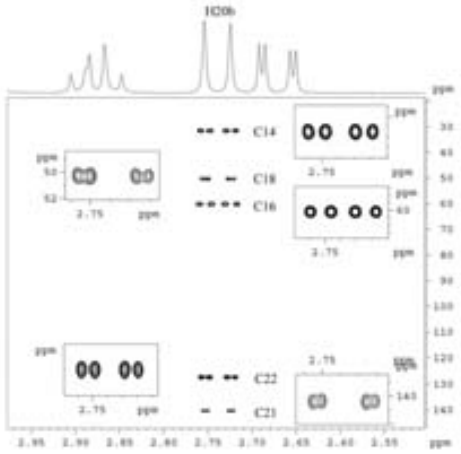

Fig. 3 2D CLIP-HSQMBC spectrum of **1** after selective pulsing on H20b with a 20 ms Gaussian-shaped 180° ^{1}H pulse. The inter-pulse Δ' delay was optimized to 62.5 ms (corresponding to $^nJ(CH) = 8$ Hz).

The pulse sequence was tested for strychnine (**1**, Fig. 2). The ^{1}H-selective HSQMBC spectrum corresponding to the H20b proton is shown in Fig. 3 along with the corresponding expansions. All expected two-bond and three-bond correlation signals appear at the H20b frequency in the F2-dimension and at different carbon frequencies in the F1-dimension. Each signal corresponds to a ^{13}C isotopomer in which the ^{13}C nucleus is located at a different position on the molecule and it is long-range coupled to H20b. As depicted in the graphical abstract, these peaks are not directly visible in the conventional ^{1}H spectrum due to the overlap with the strong ^{12}C isotopomer signals. H20b appears as a doublet in the ^{1}H spectrum and as a clear doublet of doublets in each CLIP-HSQMBC cross-peak, from which the proton–carbon coupling value can be easily extracted from signal splitting.

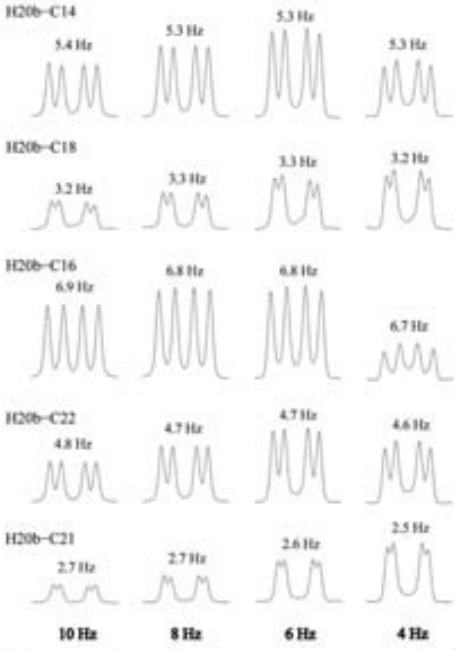

Fig. 4 Measurement of several H20b–Cx coupling constants as a function of the experiment optimization (in bold) when a purge 90° carbon pulse prior to acquisition is used. Note that all measurements present an experimental deviation of ≤0.2 Hz, independently of experiment optimization.

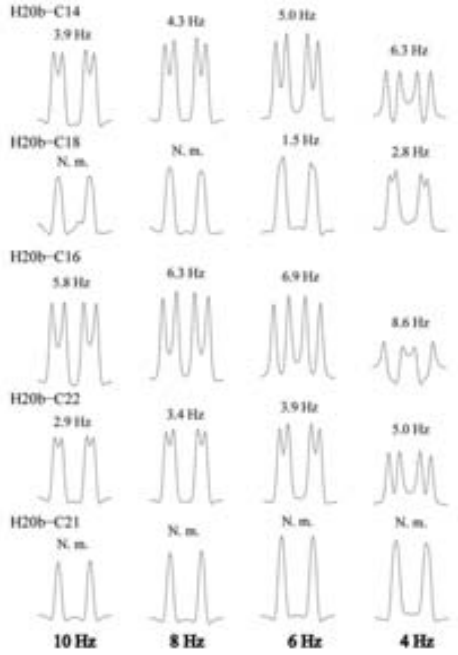

Fig. 5 Measurement of several H20b–Cx coupling constants as a function of the experiment optimization (in bold) when a purge 90° carbon pulse prior to acquisition is not used. Note the important errors introduced in all measurements when compared with Fig. 4.

In the original CLIP-HSQC sequence the experimental one-bond proton–carbon coupling constants deviate from the nominal coupling constants to which the INEPT delays are adjusted by approximately up to 20–30% and therefore the signal only contained a relatively small contribution of the antiphase component. However, removal of the antiphase term is more demanding in HSQMBC experiments where a significant deviation between the smallest nominal coupling and the actual value may exist. Thus, we investigated as to whether the 90° carbon pulse was capable to eliminate undesired antiphase terms for a set of INEPT delays optimized to a range of coupling constants (Fig. 4). The signals were compared with those obtained with a similar pulse sequence that lacked the additional carbon pulse (Fig. 5). It can be noted that, when the purge 90° carbon pulse was applied, the absorptive in-phase character of the signals was preserved for all the delays and the value of the coupling constant was practically not affected. In contrast, the signals obtained with the sequence without the 90° carbon pulse exhibited dispersive antiphase distortions that often precluded an accurate and precise measurement of the heteronuclear coupling constant. Thus, a perfect match between ^{n}J(CH) and the delay is not critical and a wide range of J values can be measured in a single experiment. The $\sin^2(\pi J_{CH}\Delta)$ dependence of the signal intensity with the delay optimization can be noted and the strongest intensity is obtained when the INEPT inter-pulse delay is optimized to a value close to the experimental coupling constant.

In the case of more complex multiplets, a direct measurement of the ^{n}J(CH) in the conventional HSQMBC experiment is usually not recommended due to the anti-phase character of the heteronuclear couplings that may result in partial or full cancellation of peaks and shifted peak maxima. In contrast, a CLIP-HSQMBC cross-peak presents a pure in-phase pattern and if the outer peaks of a multiplet are well resolved, the proton–carbon couplings can be measured in terms of peak separation irrespective of the complexity of the multiplet. In a complex multiplet, identification of two peaks whose difference in frequency corresponds to the proton–carbon coupling is not simple; however, the proton–carbon coupling can be determined by means of measuring the separation between the outer peaks of the multiplet and subtracting the value to the equivalent separation in the ^{1}H spectrum. As the procedure involves peak maxima, the differences in line width between the HSQMBC and the ^{1}H signals do not affect the accuracy of the measurement as long as the outer peaks are well defined. The simplicity of the procedure is shown for H13, which is coupled to three protons and appears as an apparent doublet of triplets (ΣJ = 16.8 Hz) in the ^{1}H spectrum (Fig. 6). The signal becomes more complex in the CLIP-HSQMBC spectra acquired with a selective 180° proton pulse on H13 owing to the additional splitting caused by the extra proton–carbon

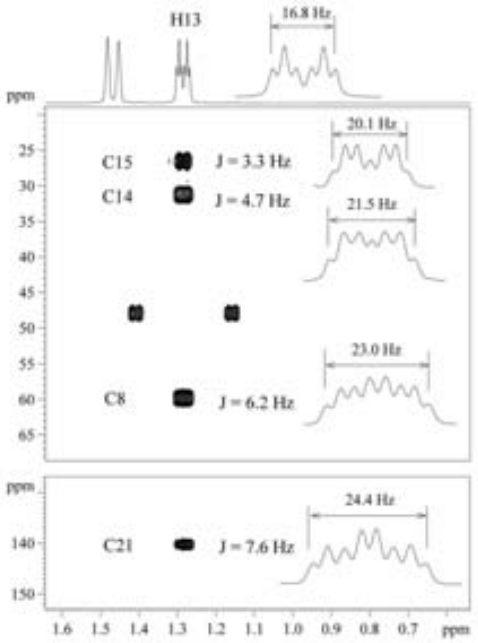

Fig. 6 Measurement of proton–carbon coupling constants in terms of peak separation in the 8 Hz optimized CLIP-HSQMBC spectrum after selective refocusing of the H13 proton with a 20 ms Gaussian-shaped 180° ^{1}H pulse. The 1D expansions are not scaled.

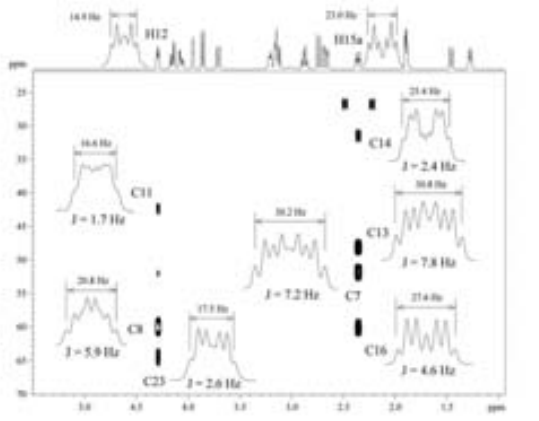

Fig. 7 Measurement of proton–carbon coupling constants in terms of peak separation in a 6 Hz optimized CLIP-HSQMBC spectrum after doubly-selective excitation on H12 and H15a protons using a Gaussian-shaped shifted laminar pulse of 20 ms. The 1D expansions are not scaled.

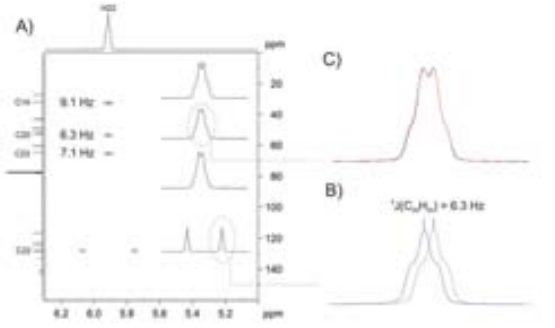

Fig. 8 (A) 8 Hz optimized 2D CLIP-HSQMBC spectrum after selective refocusing of the broad olefinic H22 proton of **1** using a 20 ms Gaussian-shaped pulse; (B) fitting procedure based on the left/right displacement of the low-field in-phase component of the internal $^{1}J_{CH}$ direct response; (C) perfect matching achieved between the simulated multiplet obtained in B with the experimental cross-peak corresponding to the H22–C20 correlation.

coupling. Despite the complexity of the multiplets, proton–carbon coupling constants in the range 3–8 Hz were easily measured by outer peak separation as shown in Fig. 6.

The proposed experiment is a proton selective 2D scheme and therefore several experiments would be needed for a complete determination of all the heteronuclear coupling constants of a molecule. However, the measurement of heteronuclear coupling constants from multiple protons can be achieved with only one experiment using band-selective or multiple-frequency selective pulses for simultaneous excitation of several protons under the condition that mutually coupled protons are not excited. As an example, Fig. 7 shows the CLIP-HSQMBC spectrum in which H15a and H12 were simultaneously excited using a doubly-selective 180° proton pulse and the coupling constants of these two protons and their coupled carbons were measured in a single experiment.

When the signals are broad and the outer peaks of the multiplets are not resolved, the measurement of the coupling constants cannot be achieved from peak separation and a simple fitting procedure is required. This approach has been traditionally performed for HSQMBC- and HMBC-based experiments. The original procedure involves a template signal for the proton under analysis, which can be taken from the conventional ^{1}H or the one-bond HSQC spectra, and summed to an identical but inverted signal, shifted by a trial coupling constant, until a match with the experimental signal is achieved. In our case, the fitting procedure is easier because pure in-phase multiplets are targeted. A similar procedure was described for the extraction of ^{n}J(CH) in a coupled/decoupled HSQC-TOCSY experiment,[13] where an external reference from a second experiment was needed. Here we propose to use the satellite cross-peak as an internal "decoupled" reference. As an example, this protocol is illustrated for the measurement of coupling constants involving the olefinic H22 proton (Fig. 8). Its proton resonance appears as a broad triplet in the ^{1}H spectrum and the additional splitting due to ^{n}J(CH) resulted in a somewhat broad signal in the CLIP-HSQMBC cross-peaks. In this case direct measurement in terms of peak separation is not possible and the satellite lines were used for the fitting procedure. Experimentally this is easily done by shifting left/right this satellite component and the excellent in-phase

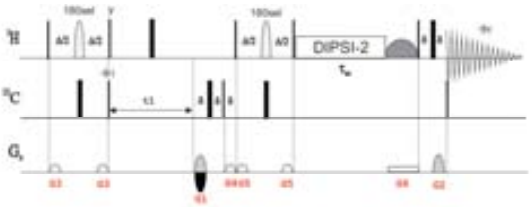

Fig. 9 Pulse scheme for the 2D CLIP-HSQMBC-TOCSY experiment. A *z*-filtered DIPSI-2 pulse train is used for the TOCSY mixing transfer with an overall duration of t_{tx}. All other experimental conditions as described in Fig. 1.

properties of multiplets ensure a perfect matching between the simulated and experimental cross-peaks.

Another important drawback of conventional HMBC and HSQMBC experiments is that the sine dependence of cross-peak intensities and their anti-phase nature usually preclude the observation of cross-peaks when the proton–carbon coupling is small. The HSQMBC experiment can be combined with a TOCSY period to extend the measurement in areas where selective excitation is not feasible and to efficiently measure very small *J* values.[14] Similarly, we propose to append a TOCSY element to the CLIP-HSQMBC experiment for an effective magnetization transfer to other protons of the same spin system and additional pure in-phase multiplets for other protons of the ^{13}C-isotopomer would be detected. These cross-peaks are not obtained through a direct proton–carbon magnetization transfer, however they are accessible *via* a two-step procedure that relies on a sequential $^{n}J(CH) + J(HH)$ transfer mechanism in which the initial proton exhibits a larger coupling constant to the specific ^{13}C nucleus. Thus, from this CLIP-HSQMBC-TOCSY experiment (Fig. 9) it is possible to obtain cross-peaks showing small *J* values because the intensities of relayed cross-peaks depend on the original proton–carbon coupling.

Fig. 10 shows an extremely challenging measurement obtained from the CLIP-HSQMBC-TOCSY spectrum after selection of the abovementioned olefinic H22 proton. Additional cross-peaks for the relayed H23a and H23b methylene protons (they form a typical AB spin system) are clearly observed when compared with the analog spectrum of Fig. 8. Apparently, the resulting C14–H23a and C14–H23b cross-peaks showed the same multiple pattern as in the ^{1}H spectrum (Fig. 10B) but a closer look at the cross-peak suggested a slightly broader line width for the H23b proton. Fitting analysis using the satellite lines as a template (Fig. 10C) and further matching with the experimental multiplet (Fig. 10D) yielded a *J* value of 0.8 Hz which is in strong agreement with the value obtained with other methods. Following the same procedure, the H23a–C14 coupling value is <0.2 Hz (expansions not shown).

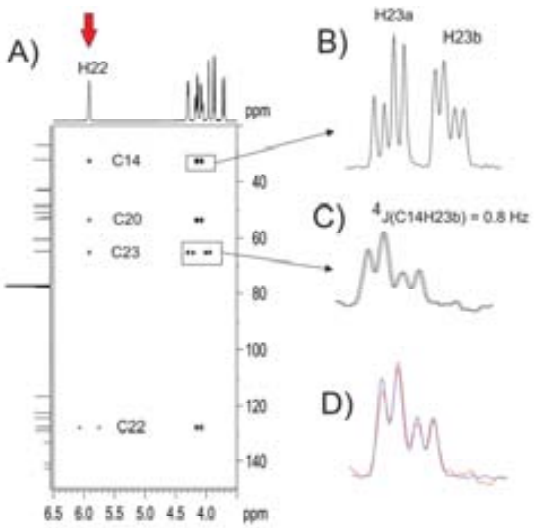

Fig. 10 2D CLIP-HSQMBC-TOCSY spectrum after selective excitation of the H22 proton. The experiment was optimized to 8 Hz and TOCSY mixing time was set to 40 ms. All other experimental conditions as described in Fig. 8. In (D) it is shown the perfect matching between the simulated (obtained from the fitting of the satellite lines of the relayed H23b proton; see (C)) and the experimental multiplet (see B) allows the measurement of the small 0.8 Hz coupling.

Materials and methods

The NMR experiments were recorded with a sample of 0.1 M of strychnine (**1**) in $CDCl_3$ on a Bruker Avance 500 instrument equipped with an inverse TCI cryo-probe incorporating a *z*-gradient coil at 25 °C. Data were acquired and processed using the TOPSPIN software package. The pulse schemes for CLIP-HSQMBC and CLIP-HSQMBC-TOCSY are shown in Fig. 1 and 9 respectively. Sine bell-shaped gradients of 1 ms were used, followed by a recovery delay of 200 μs. The proportionality between gradient strengths for G1 : G2 : G3 : G4 : G5 shows the 80 : 20.1 : 33 : 50 : 17 ratio. Gradient strengths are given as percentages of the absolute gradient strength of approximately 53.5 G cm^{-1}. Adiabatic CHIRP shapes with a sweep width of 60 kHz are used for inversion (0.5 ms) and refocusing (2 ms) 180° carbon pulses. The acquisition times t_2 and t_1 were 1.02 s (spectral width 2000 Hz, 4k complex data points) and 4 ms (spectral width 16 000 Hz, 128 real data points) respectively. The relaxation delay was 1 s and 2 scans were accumulated per t_1 increment. Zero filling to 1024 points in F1, 8096 points in F2 and sine-squared window function in both F1 and F2 dimensions were applied before Fourier transformation of 2D data. CLIP-HSQMBC-TOCSY spectra were recorded and processed exactly under the same conditions using 4 scans per t_1 increment. A zero-quantum filter consisting of a CHIRP-shaped ^{1}H pulse (30 ms) applied simultaneously with a G6 gradient (3%) is incorporated into the TOCSY element to remove unwanted antiphase contributions.[15]

Conclusions

In summary, we have developed a new 2D experiment referred to as CLIP-HSQMBC for the easy measurement of long-range

proton–carbon coupling constants. The resulting pure in-phase multiplets exhibit an extra splitting and the proton–carbon coupling can be measured along the detected dimension as the difference in frequency between two peaks in the same natural way as the proton–proton couplings are determined. We show that the measurement in terms of peak separation is also possible even for complex multiplets. The method ensures good accuracy, reproducibility and resolution as the measurement is made in the direct dimension. In the case of unresolved signals the coupling constants are determined through a fitting procedure that uses the satellite line as an internal reference. Finally, it has been shown that a related CLIP-HSQMBC-TOCSY experiment opens the door for determining very small coupling constants and to observe correlations from overlapped protons where selective excitation cannot be feasible. The proposed method avoids the tedious analysis of twisted-phase multiplets associated with traditional experiments and also the uncertainty on the percentage of unwanted cross-talk in IPAP experiments.[14]

Acknowledgements

Financial support for this research provided by MICINN (projects CTQ2009-08328 and CTQ2012-32436) and by a Bruker-Lilly agreement is gratefully acknowledged.

Notes and references

1 (*a*) J. L. Marshall, *Carbon–Carbon and Carbon–Proton NMR Couplings: Applications to Organic Stereochemistry and Conformational Analysis (Methods in Stereochemical Analysis)* Verlag Chemie International, 1982; (*b*) W. A. Thomas, *Prog. Nucl. Magn. Reson. Spectrosc.*, 1997, **30**, 183–207; (*c*) N. Matsumori, D. Kaneno, M. Murata, H. Nakamura and K. Tachibana, *J. Org. Chem.*, 1999, **64**, 866–876; (*d*) M. Tafazzoli and M. Ghiasi, *Carbohydr. Res.*, 2007, **342**, 2086–2096.

2 (*a*) B. L. Márquez, W. H. Gerwick and R. T. Williamson, *Magn. Reson. Chem.*, 2001, **39**, 499–530; (*b*) T. Parella, in *Multidimensional NMR Methods for the Solution State, 2D Methods for the Measurement of Long-Range Proton–Carbon Coupling Constants*, ed. G. A. Morris and J. W. Emsley, John Wiley & Sons Ltd, Chichester, 2010, pp. 305–314; (*c*) N. Nath, Lokesh and N. Suryaprakash, *ChemPhysChem*, 2012, **13**, 645–660.

3 W. Koźmiński and D. Nanz, *J. Magn. Reson.*, 1997, **124**, 383–392.

4 (*a*) W. Koźmiński, *J. Magn. Reson.*, 1999, **137**, 408–412; (*b*) M. D. Sørensen, A. Meissner and O. W. Sørensen, *J. Magn. Reson.*, 1999, **137**, 237–242; (*c*) P. Nolis, J. F. Espinosa and T. Parella, *J. Magn. Reson.*, 2006, **179**, 295–306.

5 R. T. Williamson, B. L. Márquez, W. H. Gerwick and K. E. Kövér, *Magn. Reson. Chem.*, 2000, **38**, 265–273.

6 (*a*) J. J. Titman, D. Neuhaus and J. Keeler, *J. Magn. Reson.*, 1989, **85**, 111–131; (*b*) J. M. Richardson, J. J. Titman, J. Keeler and D. Neuhaus, *J. Magn. Reson.*, 1991, **93**, 533–553; (*c*) R. A. E. Edden and J. Keeler, *J. Magn. Reson.*, 2004, **166**, 53–68.

7 (*a*) K. Kövér, G. Batta and K. Fehér, *J. Magn. Reson.*, 2006, **181**, 89–97; (*b*) S. Boros and K. E. Kövér, *Magn. Reson. Chem.*, 2011, **49**, 106–110.

8 (*a*) V. V. Krishnamurthy, *J. Magn. Reson., Ser. A*, 1996, **121**, 33–41; (*b*) A. Meissner and O. W. Sørensen, *Magn. Reson. Chem.*, 2001, **39**, 49–52; (*c*) M. Findeisen and S. Berger, *Magn. Reson. Chem.*, 2003, **41**, 431–434; (*d*) K. Furihata, M. Tashiro and H. Seto, *Magn. Reson. Chem.*, 2009, **47**, 814–818.

9 A. Bax, K. A. Farley and G. S. Walker, *J. Magn. Reson., Ser. A*, 1996, **119**, 134–138.

10 J. F. Espinosa, P. Vidal, T. Parella and S. Gil, *Magn. Reson. Chem.*, 2011, **49**, 502–507.

11 A. Enthart, J. C. Freudenberger, J. Furrer, H. Kessler and B. Luy, *J. Magn. Reson.*, 2008, **192**, 314–322.

12 O. W. Sorensen and R. R. Ernst, *J. Magn. Reson.*, 1983, **51**, 477–489.

13 K. E. Kövér, V. J. Hruby and D. Uhrín, *J. Magn. Reson.*, 1997, **129**, 125–129.

14 J. Saurí, J. F. Espinosa and T. Parella, *Angew. Chem., Int. Ed.*, 2012, **51**, 3919–3922.

15 M. J. Thrippleton and J. Keeler, *Angew. Chem., Int. Ed.*, 2003, **42**, 3938–3941.

PUBLICATION 2

A definitive NMR solution for a simple and accurate measurement of the magnitude and the sign of small heteronuclear coupling constants on protonated and non-protonated carbons

J. Saurí, J. F. Espinosa, T. Parella. *Angew. Chem. Int. Ed.*, 2012, 51, 3919 –3922

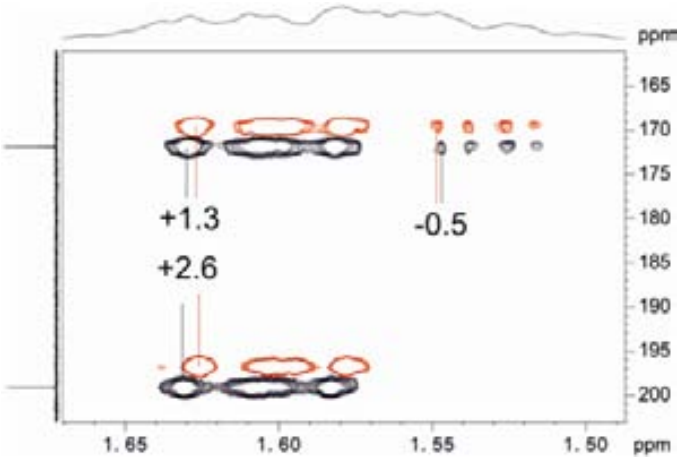

1. Introduction

In this publication, a powerful NMR experiment for the measurement of the magnitude and the sign of small $^{n}J(CH)$ coupling constants on protonated and non-protonated carbon atoms is introduced, denoted as selHSQMBC-TOCSY IPAP, solving thus one of the most important challenges that still remained. As it has been mentioned in the Introduction section, two transfer mechanisms can be feasible when measuring the magnitude of $^{n}J(CH)$:

a) HSQC-TOCSY-like experiments based on $^{1}J(CH)$ + J(HH)
b) HMBC or HSQMBC-like experiments based on the direct $^{n}(JCH)$ transfer.

A new experiment based on the additive $^{n}J(CH)$ + J(HH) coupling transfer mechanism is introduced (**Fig. 3.01**). This concept came to us with the idea to design an NMR experiment able to extend the $^{n}J(CH)$ information obtained in HSQMBC-like sequences to a given spin system via J(HH) transfer mechanism. In addition, a preservation of the α/β ^{13}C spin state information is expected, obtaining thus the relative sign information of the $^{n}J(CH)$, as occurs in conventional HSQC-TOCSY-like experiment.

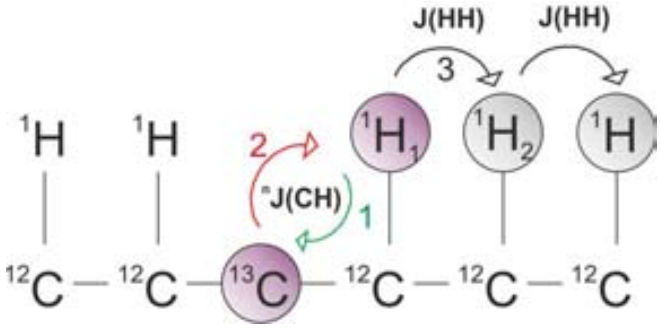

Figure 3.01. Basic magnetization transfer scheme for the selHSQMBC-TOCSY experiment.

In HSQC and HSQC-TOCSY experiments there is an important difference between the magnitudes of $^{1}J(CH)$ and J(HH) values, and therefore the undesired effects on J(HH) modulation can be neglected during the INEPT transfers. However, both $^{n}J(CH)$ and J(HH) have similar values and they simultaneously evolve during INEPT transfers found in HSQMBC-like sequences. The result is phase-distorted cross-peaks, making difficult the analysis of the multiplets and preventing an easy and accurate extraction of the $^{n}J(CH)$ value.

To overcome such drawback, selective 180º ^{1}H pulses in HSQMBC-like sequences are used in order to avoid any J(HH) evolution[1,2]. At the same time, it will be shown how the addition of a J(HH) transfer block is perfectly suitable to extend the information through a given spin system, as well as how the use of the IPAP methodology leads to an accurate measurement of the magnitude and the sign of small $^{n}J(CH)$ coupling constants.

The method uses a ZQ-filter element, consisting of an adiabatic chirp pulse applied simultaneously with a weak PFG, which converts undesired ZQ contributions into non-

[1] S. Gil, J. F. Espinosa, T. Parella. *J. Magn. Reson*. **2011**, 213, 145.
[2] See section 2.3 of this thesis work.

observable MQ coherences,[3] so that cleaner spectra showing pure phase multiplet patterns are obtained (**Fig. 3.02**).

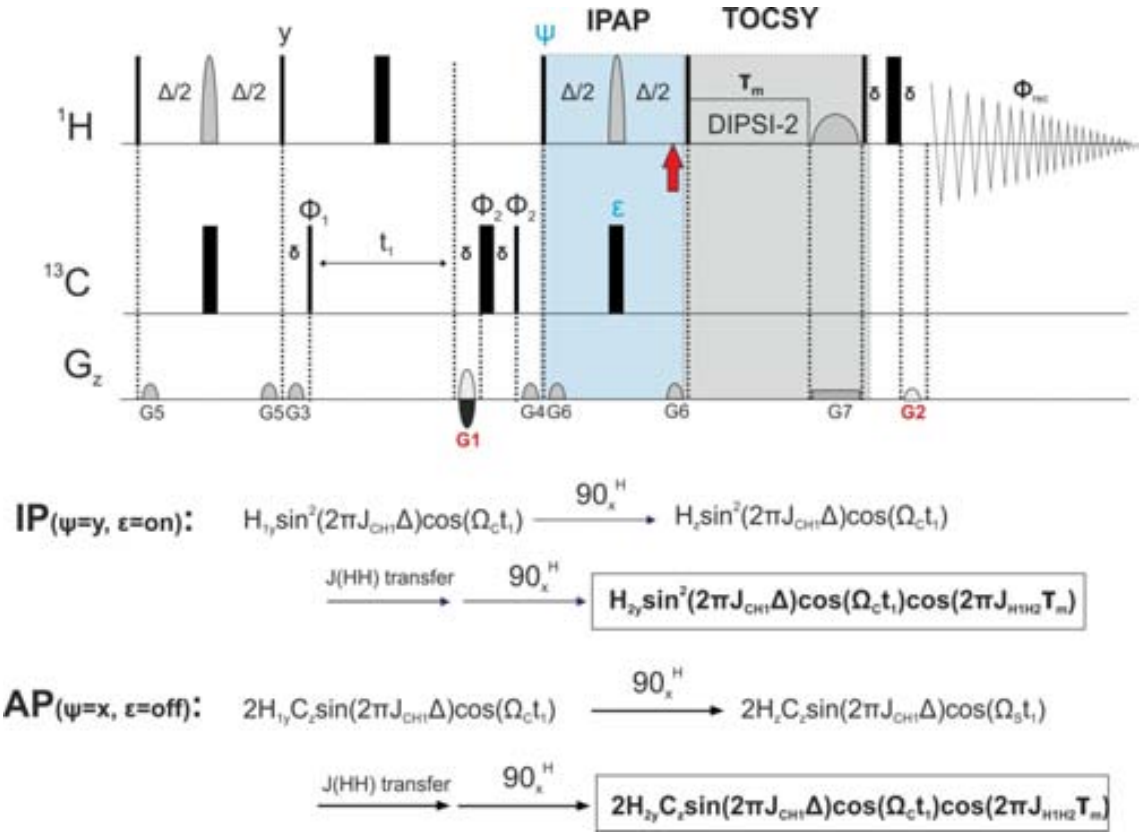

Figure 3.02. Basic description of the IP and AP data in selHSQMBC-TOCSY experiment.

Very importantly, the signal intensity of the relayed ^nJ(C-H2) cross peak (displayed in **Fig. 3.01**) not depends on its own value but on the initial ^nJ(C-H1)+J(H1-H2) transfer.

[3] See section 2.2.1.3 of this thesis work

NMR Spectroscopy

DOI: 10.1002/anie.201108959

A Definitive NMR Solution for a Simple and Accurate Measurement of the Magnitude and the Sign of Small Heteronuclear Coupling Constants on Protonated and Non-Protonated Carbon Atoms**

*Josep Saurí, Juan Félix Espinosa, and Teodor Parella**

For many years the practical use and measurement of long-range proton–carbon coupling constants (^nJ(CH); $n>1$) in natural abundant molecules have been a timely topic in NMR spectroscopy and there are still a number of unresolved issues in this area.[1] There have always been doubts about the correct choice of the best NMR method to be used and many discussions have focused on the accuracy, reliability, and simplicity of the data analysis and determination of the ^nJ(CH) coupling constant. Despite the extensive number of NMR techniques that have been developed, there are still two unsolved experimental problems pertaining basically to non-protonated carbon atoms, namely, a) an accurate measurement of very small coupling constants (less than 2–3 Hz) and b) the absence of a general and robust approach to determine the sign of the coupling constant. Widely used pulse sequences like α/β-HSQC-TOCSY,[2] HETLOC,[3] or HECADE[4] that consist of a dual-step HSQC-type block followed by a TOCSY transfer (^1J(CH)+J(HH), Scheme 1A) provide the magnitude and the sign of $^nJ_{CH}$ coupling constants irrespective of their values (0–10 Hz) but only for protonated carbons. On the other hand, long-range correlation schemes such as HSQMBC,[5] EXSIDE,[6] or J-HMBC[7] experiments based on a direct ^nJ(CH) transfer (Scheme 1B), typically fail to measure very small coupling constants (0–3 Hz) as well as they do not provide information about the sign.

We show here that all these drawbacks can be solved by a slightly modified HSQC-TOCSY method in which the 180°(^{1}H) pulses in the INEPT blocks are applied selectively to one or several nonmutually coupled ^{1}H resonances and the delays are adjusted to the ^nJ(CH) values (Figure 1). The

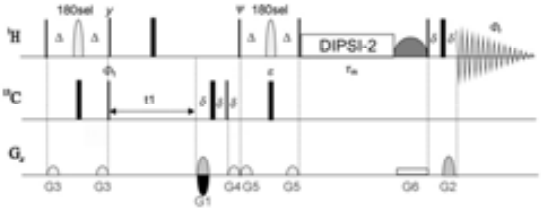

Figure 1. Pulse scheme of the 2D ^{1}H-selective HSQMBC-TOCSY experiment. Proton 180° pulses applied in the middle of the evolution periods ($(\Delta+p(180°sel)/2)=1/(4\,^nJ(CH))$) can be selective for the frequency, region, or for multiple frequencies. Two independent IP ($\Psi=y$, $\varepsilon=$ on) and AP ($\Psi=x$, $\varepsilon=$ off) data sets are initially collected and further combined to provide complementary α and β data (IP ± AP) in separate spectra.

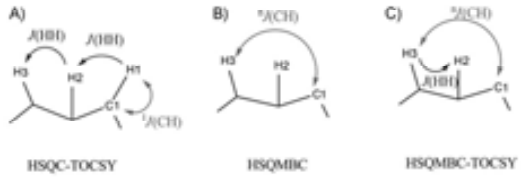

Scheme 1. The pathway transfer mechanisms involved in A) HSQC-TOCSY, B) HSQMBC, and C) HSQMBC-TOCSY experiments dedicated to the measurement of $^nJ_{CH}$.

selHSQMBC-TOCSY scheme generates α/β multiplets by recording two separate and complementary in-phase (IP) and anti-phase (AP) data sets followed by a basic addition/subtraction data processing.[8] The behavior of both J(HH) and ^nJ(CH) evolution throughout the entire pulse sequence yields pure-phase multiplets and, in addition, the TOCSY period preserves the α/β ^{13}C spin-state information. The method allows the efficient measurement of the magnitude and the sign of ^nJ(CH) by analyzing the relative displacement of α/β cross-peaks in the detected dimension with high resolution and accuracy even for very small values.

The proposed selHSQMBC-TOCSY experiment consists of a two-step procedure based on a sequential ^nJ(CH)+J(HH) transfer mechanism (Scheme 1C). The success of the method relies on the presence of a large coupling constant between the initial H3 and the intermediate C1 spins and, secondly, on the effective magnetization transfer to the third H2 spin through a TOCSY process. Thus, starting from a selected H3 proton, the signal intensity for a relayed H2-C1

[*] J. Saurí, Dr. T. Parella
SeRMN, Universitat Autònoma de Barcelona
08193 Bellaterra, Barcelona (Spain)
E-mail: teodor.parella@uab.cat
Dr. J. F. Espinosa
Centro de Investigación Lilly SA
Av. De la Industria 30, 28101 Alcobendas (Spain)

[**] Financial support for this research was provided by the MICINN (project number CTQ2009-08328 and Consolider Ingenio-2010 CSD2007-00006) and by a Bruker-Lilly agreement. We also thank the Servei de Ressonància Magnètica Nuclear, Universitat Autònoma de Barcelona, for allocating instrument time to this project.

Supporting information for this article is available on the WWW under http://dx.doi.org/10.1002/anie.201108959.

α/β cross-peak will depend on a $\sin(2\pi^n J(\mathrm{C1H3})\Delta)\cos(\pi J(\mathrm{H2H3})r_m)[1+\sin(2\pi^n J(\mathrm{C1H3})\Delta)]$ function as a result of an additive $^nJ(\mathrm{H3\text{-}C1})+J(\mathrm{H2\text{-}H3})$ transfer mechanism, so it is completely independent of the $^nJ(\mathrm{H2\text{-}C1})$ value and also of the C1 carbon multiplicity.

The benefits to append a TOCSY transfer in selHSQMBC experiments[8] are evident comparing the spectra of Figure 2A vs. 2B. The number of cross-peaks is notoriously

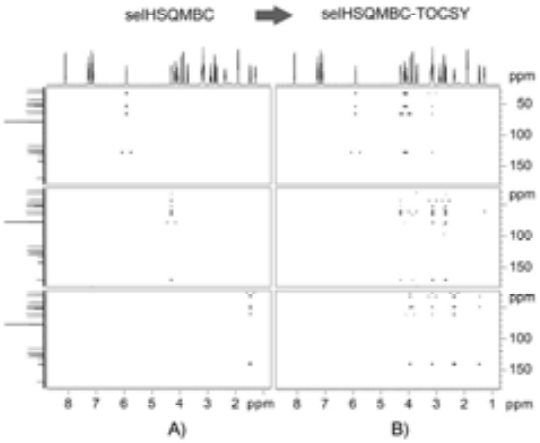

Figure 2. In-phase A) selHSQMBC and B) selHSQMBC-TOCSY spectra after selective refocusing of H22, H12, and H15a protons in strychnine (**1**).

increased thanks to the combination of selective proton excitation and TOCSY transfer highlighting very much its superior information content. While in the selHSQMBC experiment only the largest coupling constants of the excited proton can be determined, the additional TOCSY cross-peaks allow the measurement between these carbon atoms and all other protons belonging to the same spin system of the excited proton. The magnitude and the sign of $^nJ(\mathrm{CH})$ in selHSQMBC-TOCSY experiments are easily determined by analyzing the relative sense of the displacement of the α/β components, which are generated by a linear combination of the IP ± AP data. For protonated carbon atoms, the sense of the corresponding direct $^1J_{CH}$ correlation (positive sign) can be used as the reference. In the absence of this direct correlation or for non-protonated centers, the comparison of the relative sense between cross-peaks is necessary. Assuming that a large three-bond correlation will have a positive value, such direction of the displacement can be taken as the reference for sign determination of other cross-peaks in the same row. Thus, if a cross-peak defined as positive shows a left/right pattern, other cross-peaks having the same left/right pattern will be positive whereas those peaks having an opposite right/left pattern will be negative. For instance, the simple analysis of the relative displacement for the carbonyl C10 carbon cross-peaks at 169.3 ppm (Figure 3) after simultaneous excitation of the three overlapped, nonmutually coupled H14, H11, and H18a protons of the alkaloid

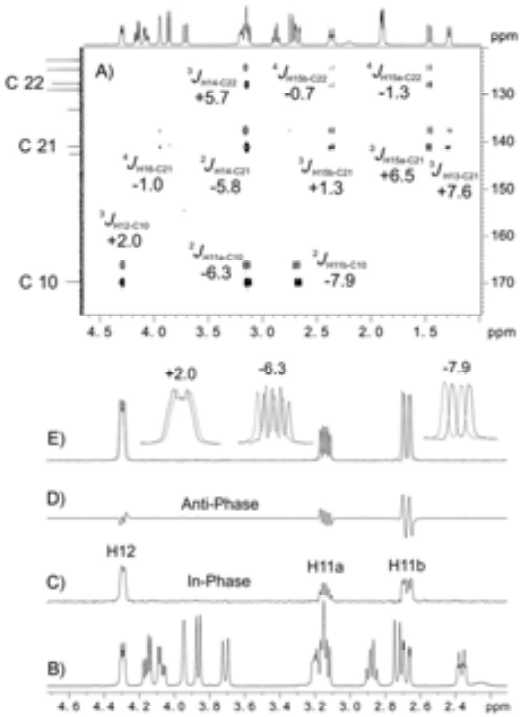

Figure 3. A) Expanded area showing the overlayed α/β selHSQMBC-TOCSY spectra (visualized here as vertically shifted red/black peaks) after selective refocusing of the overlapped H14, H11, and H18a protons resonating close to the 3.15 ppm signal of strychnine. B) Conventional 1D ^{1}H NMR spectrum and C–E) 1D slices taken at the carbonyl C10 chemical shift corresponding to the C) IP, D) AP and E) α/β spectra. The determination of the magnitude and the sign of the coupling value are made in a very straightforward way by analyzing the relative displacement between relayed α/β cross-peaks.

strychnine, **1**, all of them resonating around 3.15 ppm, clearly shows large negative values for H11a and H11b (−6.3 and −7.9 Hz, respectively) and a small positive value for H12 (+2.0 Hz). On the other hand, the olefinic C21 carbon at 140.5 ppm (see Figure 3A) presents positive values for H13 (+7.6 Hz), H15a (+6.5 Hz), and H15b (+1.3 Hz) and negative values for the two-bond H14 (−5.8 Hz) and even for the tiny four-bond H16 (−1.0 Hz) correlations.

The proposed IPAP methodology successfully works even for nonresolved, broad, or complex resonances and the accuracy of the measurement can be further validated by comparing the $^nJ(\mathrm{CH})$ values obtained from the α/β data analysis with those of the recorded IP and AP data. On the other hand, the complementarity between selHSQMBC-TOCSY experiments with different proton excitations is displayed in Figure 4. Thus, whereas the selHSQMBC experiment on the H13 proton only shows some correlations corresponding to the most intense coupling values (Figure 4A), the complementary selHSQMBC-TOCSY experiment on the adjacent H8 proton provides up to six additional cross-peaks for this relayed H13 proton from which coupling

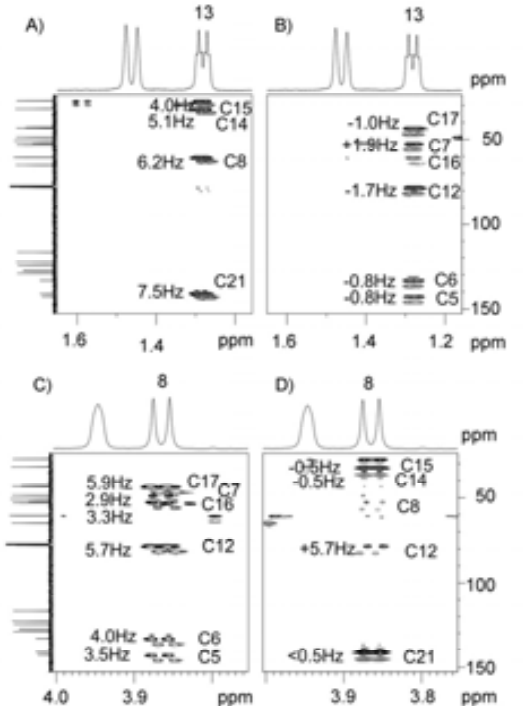

Figure 4. 2D expanded plots showing the complementarity between the selHSQMBC experiments of A) H13 and C) H8 and between selHSQMBC-TOCSY experiments of B) H8 and D) H13. Note that relayed cross-peaks in selHSQMBC-TOCSY spectra make it possible to measure the very small coupling values that are missing in the original selHSQMBC spectra.

values smaller than 2 Hz can be determined (Figure 4B). The opposite reasoning can also be done for the H8 proton (compare Figure 4C vs. 4D).

The enormous versatility of the method can be further enhanced by simultaneously selection of multiple, nonmutually coupled protons located in different parts of the molecular skeleton by region- or multiple-site selective excitation (see the Supporting Information for examples). This can represent a good strategy to simultaneously map out independent coupling topologies and different structural environments.

The steroid progesterone is a challenging example demostrating that the method succesfully works on complicated NMR spectra with an elevated degree of signal overlap including highly complex multiplets. Thus, many different long-range correlations are obtained when all protons resonating at 1.75–2.1 ppm (H21, H15, H12eq, H1eq, and H7eq protons) are simultaneously inverted. For instance, whereas the H1eq proton shows strong correlations with C2 (4.0 Hz), C3 (9.5 Hz), C10(4.0 Hz), C5(7.7 Hz), and C9(4 Hz) carbon atoms in the selHSQMBC spectrum, the TOCSY transfer allows the additional measurement of ^{n}J(CH) for all these carbon atoms and the relayed H1ax, H2eq, and H2ax protons (Figure 5). For instance, coupling values of +1.3 and +2.6 Hz

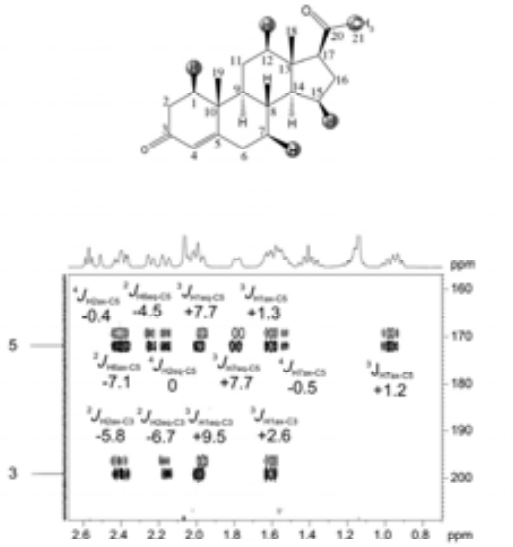

Figure 5. Expanded area of the α/β-selHSQMBC-TOCSY spectra of progesterone after selective inversion of all protons resonating in the region of 1.75–2.1 ppm.

are measured for the three-bond correlation between H1ax, C5, and C3, respectively, as well as a very small and negative −0.5 Hz for the four-bond H11eq-C5 correlation. Such measurements are practically impossible to be done using conventional HSQMBC and HSQC-TOCSY experiments.

In conclusion, a robust NMR method for the measurement of ^{n}J(CH) of general applicability and high versatility solves the major problems encountered in the original HSQC-TOCSY and HSQMBC experiments while the most important advantages are retained: a) both protonated and non-protonated carbon atoms can be observed, b) the magnitude and the sign of $^{n}J_{CH}$ are directly determined from the analysis of the relative displacement of α/β multiplets avoiding the need of complex and time-consuming analysis and individualized fitting procedures, c) the measurement is made in the detected dimension and therefore a great number of t_1 increments is not a requisite, d) pure-phase multiplets are obtained that allow the easy and accurate extraction of ^{n}J(CH) even for broad, unresolved or highly complex multiplets, e) coupling values smaller than the line width can be determined, and f) the combination of different forms of selective proton excitation and TOCSY editing offers an excellent versatility to clean overlapped regions and make reliable measurements even in congested areas or with the presence of mixtures of compounds.

The method can be understood as a way to obtain a ^{1}H TOCSY spectrum from a quaternary carbon chemical shift and this can also be interesting for structural elucidation and chemical assignment purposes. The method is equally applicable for the measurement of other heteronuclear coupling constants and, in particular, can be of enormeous interest in the measurement of residual dipolar coupling constants where the sign information is mandatory. The relative

simplicity in the experimental setup, the multiplet analysis, and the data interpretation will make this versatil HSQMBC-TOCSY experiment an essential tool for a reliable determination of $^nJ_{CH}$ in the structural and conformational studies of organic and natural products, even for inexperienced NMR users.

Experimental Section

All NMR experiments were recorded on a BRUKER DRX-500 spectrometer equiped with a three-channel 5 mm cryoprobe incorporating a *z*-gradient coil. The test samples were strychnine (**1**, 25 mg) in $CDCl_3$ (0.6 mL) and progesterone (**4**, 25 mg) in [D_6]DMSO (0.6 mL). ^1H–^{13}C IP and AP-HSQMBC experiments were separately recorded as described in Figure 1 using a recycle delay of 1 s, the interpulse delay ($\Delta + p(180°sel)/2 = 1/4\,^nJ_{CH}$) was optimized to 8 Hz, and the duration and shape of the selective proton 180° ^1H pulse (p(180°sel)) was set accordingly to the required selectivity in each case. A basic two-step phase cycle was applied: $\phi_1 = x,-x$ and $\phi_{rec} = x,-x$. Gradients G1 and G2 are used for coherence selection using echo-antiecho, G4 acts as a *zz*-filter, G3 and G5 flank the inversion proton pulses to generate pure refocusing elements, and G6 is applied simultaneously to a chirp pulse (30 ms) to remove undesired zero-quantum (ZQ) contributions.[9] This last element can be optionally incorporated into the TOCSY building block of 20–40 ms (τ_m) of duration consisting of a *z*-filtered DIPSI-2 scheme. The duration of each gradient was $\delta = 1$ ms and the proportionality between gradients G1:G2:G3:G4:G5:G6 were set to 80:20.1:33:50:17:3. The IP and AP data were acquired with $128 t_1$ increments of 4056 data points for each one, and then added/subtracted in the time domain. Prior to Fourier transformation of the data, zero filling to 1024 points in F1, 8192 points in F2, and a sine-squared function in both dimensions were applied. The data were finally obtained without any scaling factor to provide two separate α/β data sets.

Received: December 19, 2011
Revised: February 6, 2012
Published online: March 12, 2012

Keywords: coupling constants · NMR spectroscopy · structure elucidation

[1] a) R. T. Williamson, B. L. Márquez, W. H. Gerwick, K. E. Kövér, *Magn. Reson. Chem.* **2000**, *38*, 265–273; b) T. Parella in *Multidimensional NMR Methods for the Solution State* (Eds.: G. A. Morris, J. W. Emsley), Wiley, Chichester, **2010**, pp. 305–314.
[2] a) P. Nolis, J. F. Espinosa, T. Parella, *J. Magn. Reson.* **2006**, *180*, 39–50; b) W. Koźmiński, *J. Magn. Reson.* **1999**, *137*, 408–412; c) K. Kobzar, B. Luy, *J. Magn. Reson.* **2007**, *186*, 131–141.
[3] D. Uhrín, G. Batta, V. J. Hruby, P. N. Barlow, K. E. Kövér, *J. Magn. Reson.* **1998**, *130*, 155–161.
[4] W. Koźmiński, D. Nanz, *J. Magn. Reson.* **2000**, *142*, 294–321.
[5] a) B. L. Marquez, W. H. Gerwick, R. T. Williamson, *Magn. Reson. Chem.* **2001**, *39*, 499–530; b) K. E. Kövér, G. Batta, K. Fehér, *J. Magn. Reson.* **2006**, *181*, 89–97.
[6] V. Krishnamurthy, *J. Magn. Reson. Ser. A* **1996**, *121*, 33–41.
[7] A. Meissner, O. W. Sorensen, *Magn. Reson. Chem.* **2001**, *39*, 49–52.
[8] a) S. Gil, J. F. Espinosa, T. Parella, *J. Magn. Reson.* **2010**, *207*, 312–313; b) S. Gil, J. F. Espinosa, T. Parella, *J. Magn. Reson.* **2011**, *213*, 145–150.
[9] M. J. Thrippleton, J. Keeler, *Angew. Chem.* **2003**, *115*, 4068–4071; *Angew. Chem. Int. Ed.* **2003**, *42*, 3938–3941.

Angewandte Chemie
Eine Zeitschrift der Gesellschaft Deutscher Chemiker

Supporting Information

69451 Weinheim, Germany

A Definitive NMR Solution for a Simple and Accurate Measurement of the Magnitude and the Sign of Small Heteronuclear Coupling Constants on Protonated and Non-Protonated Carbon Atoms**

*Josep Saurí, Juan Félix Espinosa, and Teodor Parella**

anie_201108959_sm_miscellaneous_information.pdf

Experimental Section

Pulse Program code.

Scheme S1. Structures used as in this work: Strychnine (1), progesterone (2), taxol (3) and cyclosporine (4).

Figure S1. Comparison between selHSQMBC vs selHSQMBC-TOCSY spectra after selective excitation of a single frequency

Figure S2. Example of selHSQMBC vs selHSQMBC-TOCSY after selective excitation of multiple resonances by a shifted laminarpulse

Figure S3. Example showing the easy extraction of $^{n}J_{CH}$ in broads, non-resolved multiplet.

Figure S4. HSQMBC-TOCSY spectra resulting of the addition of 16 individualized selective

Figure S5. Comparison between a conventional 2D HSQC-TOCSY spectrum (only working for protonated carbons) with a selHSQMBC-TOCSY spectrum (working for any type of carbon)

Figure S6. Examples on the natural product taxol, 3, showing the advantage to use multiple-site excitation in a single HSQMBC-TOCSY experiment

Figure S7. HSQMBC-TOCSY spectra on the undecapeptide cyclosporine, 4, showing the advantage to use region-selective excitation in a single experiment.

Figure S8. selHSQMBC vs selHSQMBC-TOCSY spectra in progesterone, 2. Enlarged figures clearly showing the relative displacement between IPAP signals.

Figure S9: Enlarged Figures of the figure 4 of the main manuscript.

Experimental Section

All NMR experiments were recorded on a BRUKER DRX-500 spectrometer equiped with a 3-channel 5-mm cryoprobe incorporating a z-gradient coil. The test samples were 25mg of Strychnine (**1**) in 0.6 ml of $CDCl_3$, 25mg of cyclosporine (**2**) in benzene, 20mg of Taxol (**3**) in 0.6 ml of $CDCl_3$, 25mg of Progesterone (**4**) in 0.6 ml of DMSO-d_6. All data were acquired and processed with TOPSPIN v2.1. ^{1}H-^{13}C IP and AP-HSQMBC experiments were separately recorded as described in Fig. 1 using a recycle delay of 1 s, the interpulse delay (Δ+p(180°sel)/2=$1/4*^{n}J_{CH}$) was optimized to 8 Hz and the duration and shape of the selective proton 180° ^{1}H pulse (p(180°sel)) was set accordingly to the required selectivity in each case: A gaussian-shaped pulse with a duration of 20-80ms was used for single-frequency, a shifted laminar pulse generated from a gaussian shaped with a duration of 20-60ms was used for multiple-site excitation, and a reburp-shaped pulse with a duration of 5-10ms was used for band-selective-excitation. All shapes were generated using the shape tool utility included into the Topspin software package. A basic two-step phase cycle was applied: ϕ_1=x,-x and ϕ_{rec}=x,-x. Gradients G1 and G2 are used for coherence selection using echo-antiecho, G4 acts as a zz-filter, G3 and G5 flank the inversion proton pulses to generate pure refocusing elements, and G6 is applied simultaneously to a Chirp pulse (30ms) to remove undesired ZQ contributions.[9] This last element can be optionally incorporated into the TOCSY building block of 20-40ms (τ_m) of duration consisting of a z-filtered DIPSI-2 scheme. The duration of each gradient was δ=1ms and the proportionality between gradients G1:G2:G3:G4:G5:G6 were set to 80:20.1:33:50:17:3. IP and AP data were added/subtracted in the time-domain without any scaling factor to provide two separate α/β data which were analyzed directed on the display. Data were acquired with 128 t_1 increments of 4056 data points each one. Prior to Fourier-transformation of each data, zero filling to 1024 in F1, 8192 points in F2 and a sine squared function in both dimensions were applied.

Pulse Program Code for Bruker:

```
;teo_selhsqmbcto
;2D proton-selective HSQMBC-TOCSY experiment
;for the measurement of the smagnitude and the sign of long-range
;proton-carbon coupling constants

#include <Avance.incl>
#include <Grad.incl>
#include <Delay.incl>


"p2=p1*2"
"d4=1s/(cnst2*4)"
"d11=30m"
"d20=p3"
"d0=3u"
;"in0=inf1/2"
"DELTA1=50u+p16+d16"
"DELTA2=d4-larger(p12,p14)/2-50u-p16-d16"
"DELTA=p16+d16+50u+p2+d0*2+50u"

"FACTOR1=(d9/(p6*115.112))/2+0.5"
"l1=FACTOR1*2"

1 ze
  d11 pl12:f2
2 d1 pl1:f1
3 (p1 ph1)
  50u UNBLKGRAD
  p16:gp6
  d16
  DELTA2 pl0:f2 pl0:f1
  4u
  (center (p12:sp2 ph1) (p14:sp3 ph6):f2 )
  4u
  DELTA2 pl2:f2 pl1:f1
  50u
  p16:gp6
  d16
  p28 ph1
  (p1 ph2)
  (p3 ph3):f2
  d0
  (p2 ph5)
  d0
  50u
  p16:gp1*EA
  d16 pl0:f2
  d12
  (p24:sp7 ph14):f2
   DELTA pl2:f2
  (p3 ph4):f2
  50u
  p16:gp4
  d16
```

```
  if "cnst25==0"
      {
      (p1 ph2):f1
      }
      else
      {
      (p1 ph1):f1
  }

  50u
  p16:gp5
  d16
  DELTA2 pl0:f2 pl0:f1

  if "cnst25==0"
      {
      (center (p12:sp2 ph1) (p14:sp3 ph1):f2 )
      }
      else
      {
      (p12:sp2 ph1)
  }

  4u
  DELTA2 pl2:f2 pl1:f1
  50u
  p16:gp5
  d16
  (p1 ph1):f1

;starts tocsy

  d12 pl10:f1

4 p6*3.556 ph22
  p6*4.556 ph24
  p6*3.222 ph22
  p6*3.167 ph24
  p6*0.333 ph22
  p6*2.722 ph24
  p6*4.167 ph22
  p6*2.944 ph24
  p6*4.111 ph22

  p6*3.556 ph24
  p6*4.556 ph22
  p6*3.222 ph24
  p6*3.167 ph22
  p6*0.333 ph24
  p6*2.722 ph22
  p6*4.167 ph24
  p6*2.944 ph22
  p6*4.111 ph24

  p6*3.556 ph24
  p6*4.556 ph22
  p6*3.222 ph24
  p6*3.167 ph22
  p6*0.333 ph24
  p6*2.722 ph22
  p6*4.167 ph24
```

```
  p6*2.944 ph22
  p6*4.111 ph24

  p6*3.556 ph22
  p6*4.556 ph24
  p6*3.222 ph22
  p6*3.167 ph24
  p6*0.333 ph22
  p6*2.722 ph24
  p6*4.167 ph22
  p6*2.944 ph24
  p6*4.111 ph22
  lo to 4 times l1

  5u pl0:f1
  300u gron0
  pl3:sp4:f1 ph7
  100u groff
  d16

;end tocsy

  4u pl1:f1
  p1 ph1
  DELTA1
  (p2 ph1):f1
  50u
  pl6:gp2
  d16 BLKGRAD

  if "cnst25==0"
      {
      (p3 ph1):f2
      }
      else
      {
      d20
      }

  go=2 ph31
  d1 mc #0 to 2
     F1EA(igrad EA, id0 & ip3*2 & ip6*2 & ip31*2)
exit


ph1=0
ph2=1
ph3=0 2
ph4=0 0 2 2
ph5=0
ph6=0
ph7=0
ph14=0 0 2 2
ph22=3
ph24=1
ph31=0 2 2 0


;pl0 : 120dB
;pl1 : f1 channel - power level for pulse (default)
;pl2 : f2 channel - power level for pulse (default)
```

```
;pl10: f1 channel - power level for TOCSY-spinlock
;sp2: f1 channel - shaped pulse for selective proton refocussing
;sp3: f2 channel - shaped pulse (180degree inversion)
;spnam3: Crp60,0.5,20.1
;sp7: f2 channel - shaped pulse (180degree refocussing)
;spnam7: Crp60comp.4
;sp29: f1 channel - shaped pulse (adiabatic)
;p1 : f1 channel -  90 degree high power pulse
;p2 : f1 channel - 180 degree high power pulse
;p3 : f2 channel -  90 degree high power pulse
;p6 : f1 channel -  90 degree low power pulse
;p12: f1 channel - 180 degree shaped pulse     [20-80ms]
;p13: f1 channel - 180 degree shaped pulse (adiabatic)    [20 msec]
;     smoothed chirp (sweepwidth, 20% smoothing, 10000 points)
;p14: f2 channel - 180 degree shaped pulse for inversion
;     = 500usec for Crp60,0.5,20.1
;p24: f2 channel - 180 degree shaped pulse for refocussing
;     = 2msec for Crp60comp.4
;p16: homospoil/gradient pulse
;p28: f1 channel - trim pulse
;d0 : incremented delay (2D)                          [3 usec]
;d1 : relaxation delay; 1-5 * T1
;d4 : 1/(4J)XH
;d9 : TOCSY mixing time
;d11: delay for disk I/O                              [30 msec]
;d16: delay for homospoil/gradient recovery
;l1: loop for DIPSI cycle: ((p6*115.112) * l1) = mixing time
;cnst2: = J(XH)                                        [6-8 Hz]
;cnst17: = -0.5 for Crp60comp.4
;cnst25: = 0 (IP)
;        = 1 (AP)
;inf1: 1/SW(X) = 2 * DW(X)
;in0: 1/(2 * SW(X)) = DW(X)
;nd0: 2
;NS: 2 * n
;DS: >= 8
;td1: number of experiments
;FnMODE: echo-antiecho

;use gradient ratio:
;gpz0: ca. 3%
;gpz1: 80%
;gpz2: 20.1% for C-13
;gpz4: 50%
;gpz5: 17%
;gpz6: 33%

;use gradient files:
;gpnam1: SINE.100
;gpnam2: SINE.100
;gpnam3: SINE.100
;gpnam4: SINE.100
;gpnam5: SINE.100
;gpnam6: SINE.100
```

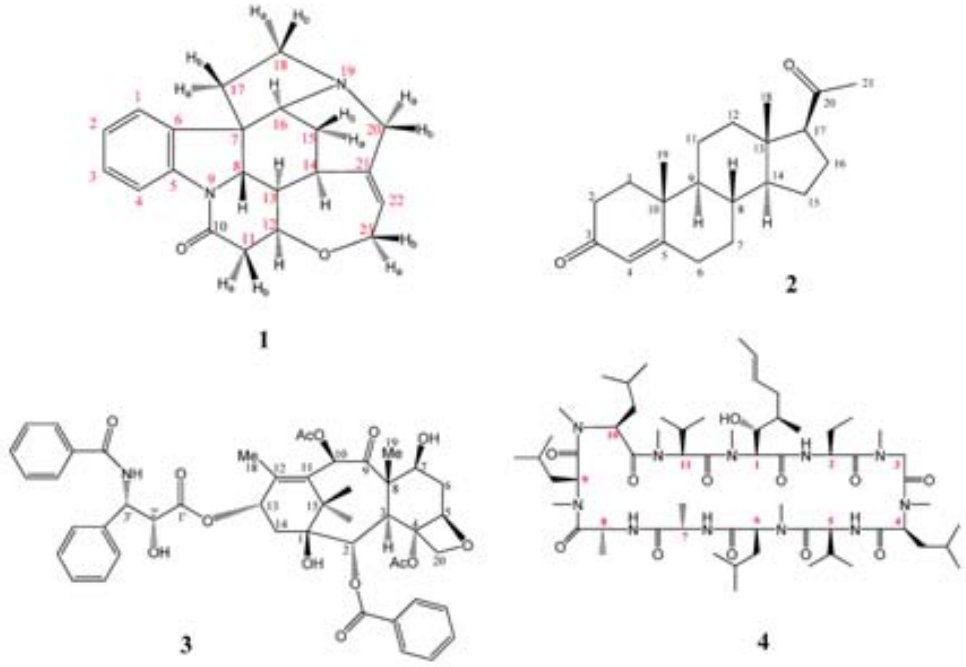

Scheme S1. Structures used in this work: Strychnine (1), progesterone (2), taxol (3) and cyclosporine (4).

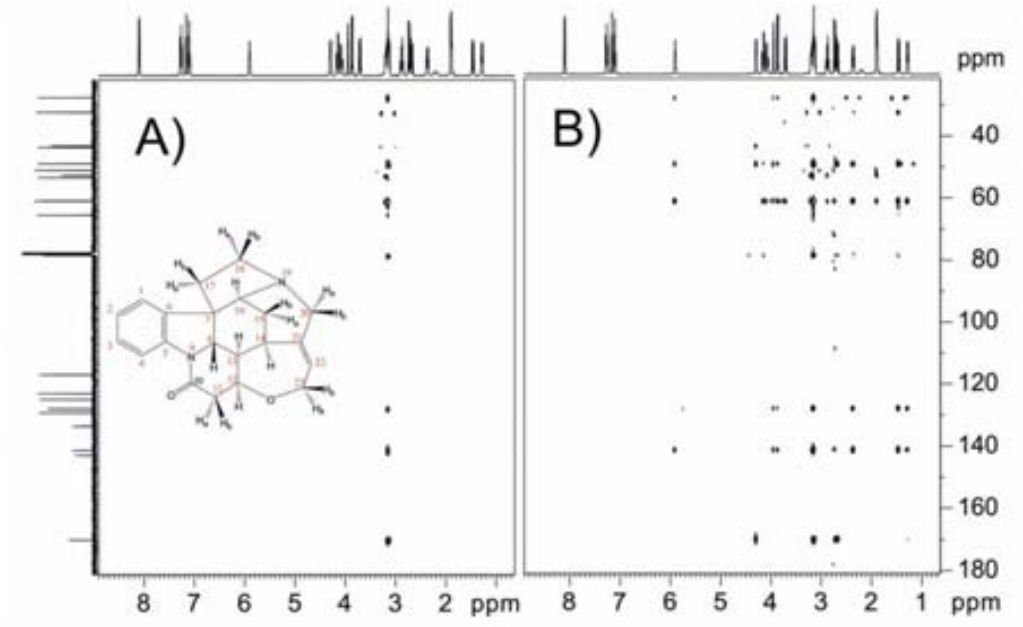

Figure S1. A) selHSQMBC and B) selHSQMBC-TOCSY spectra after selective refocusing of the overlapped H14, H11 and H18a protons of strychnine resonating near 3.15ppm. We can see in Fig. 3 of the manuscript an expanded 2D resgion of the resulting α,β-selHSQMBC-TOCSY subspectra. In Fig. 4 of the main manuscript, 1D slices showing pure phase IP, AP, and IPAP multiplets of the quaternary C10 carbon can be observed.

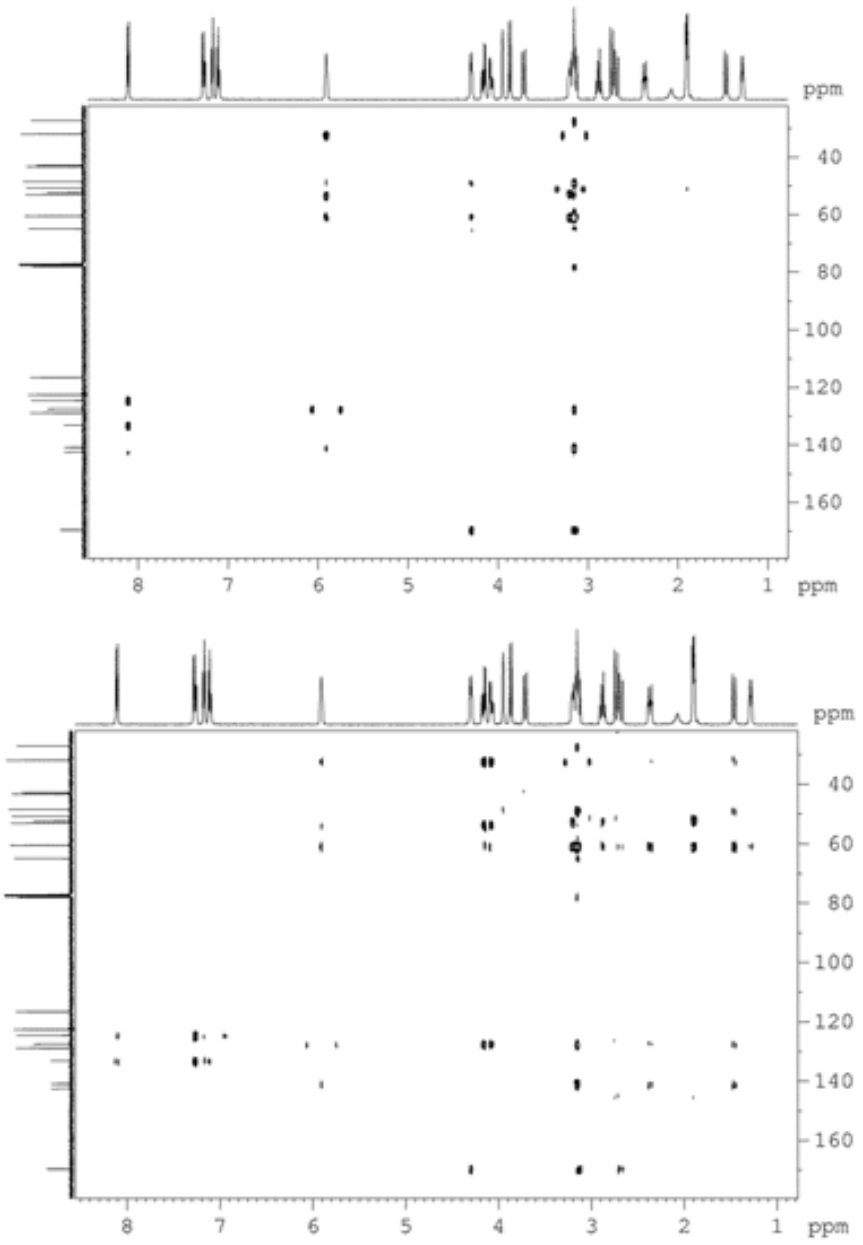

Figure S2. Example showing the implementation of multiple-site excitation using shifted laminar pulses: (top) selHSQMBC spectrum after selective excitation of H1, H22, H13 and the three protons corresponding at 3.15ppm, and (bottom) the equivalent selHSQMBC-TOCSY spectrum.

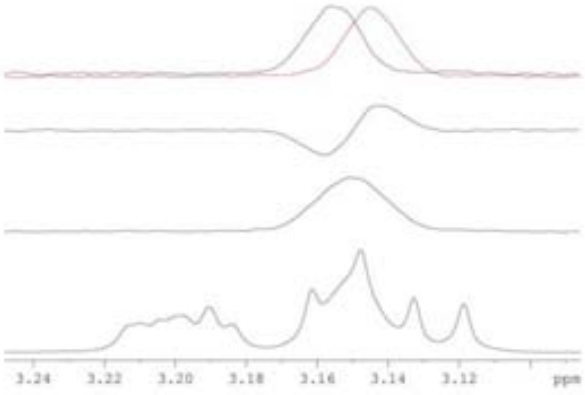

Figure S3. 1D slices showing the IP, AP and α/β multiplets corresponding to the H14-C21 cross peak. The tremendous benefits of the IPAP methodology can also be exemplified in the analysis of non-resolved, broad or complex resonances. For comparison, fig. 6 shows the diferent IP, AP and α/β multiplets corresponding to the H14-C21 cross-peak of 1. The expected additional splitting in the IP multiplet is not resolved whereas an overestimation of the direct measurement is made in the AP multiplet (8.8 Hz). Clearly, the analysis of the relative displacement of α/β components allows a reliable measurement of 6.2 Hz.

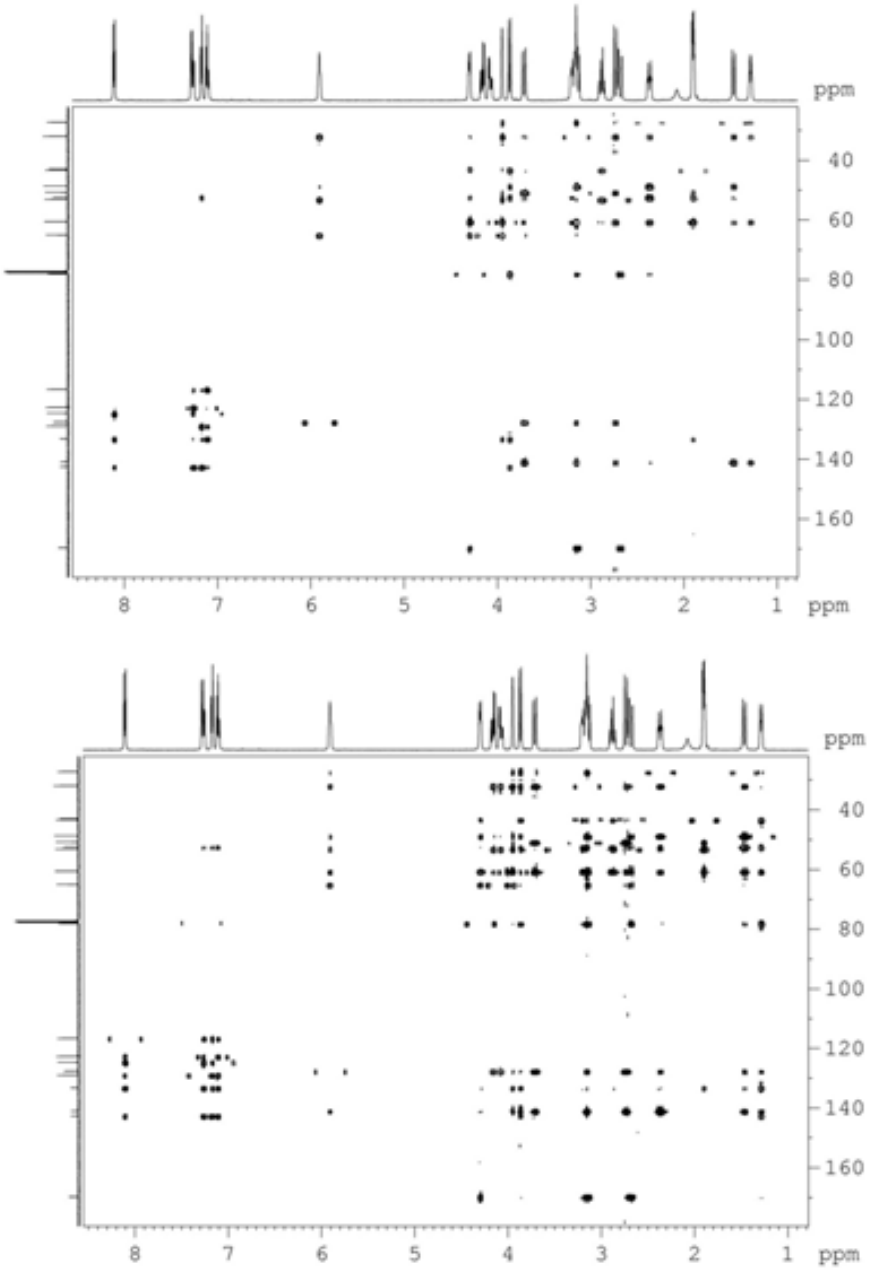

Figure S4. (top) HSQMBC and (botton) HSQMBC-TOCSY spectra resulting of the addition of 16 individualized selective experiments in strychnine

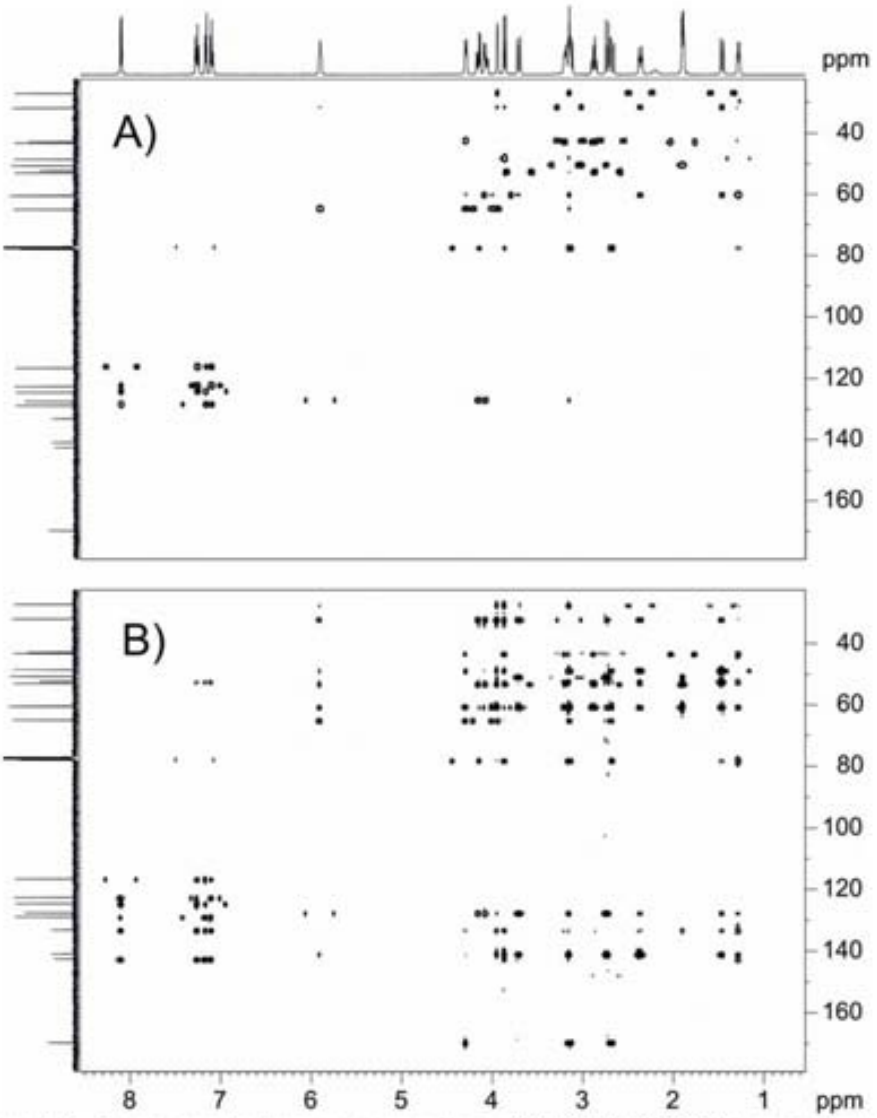

Figure S5. Comparison between a conventional 2D HSQC-TOCSY spectrum with a selHSQMBC-TOCSY spectrum resulting of the superposition of sixteen independent single-frequency experiments.

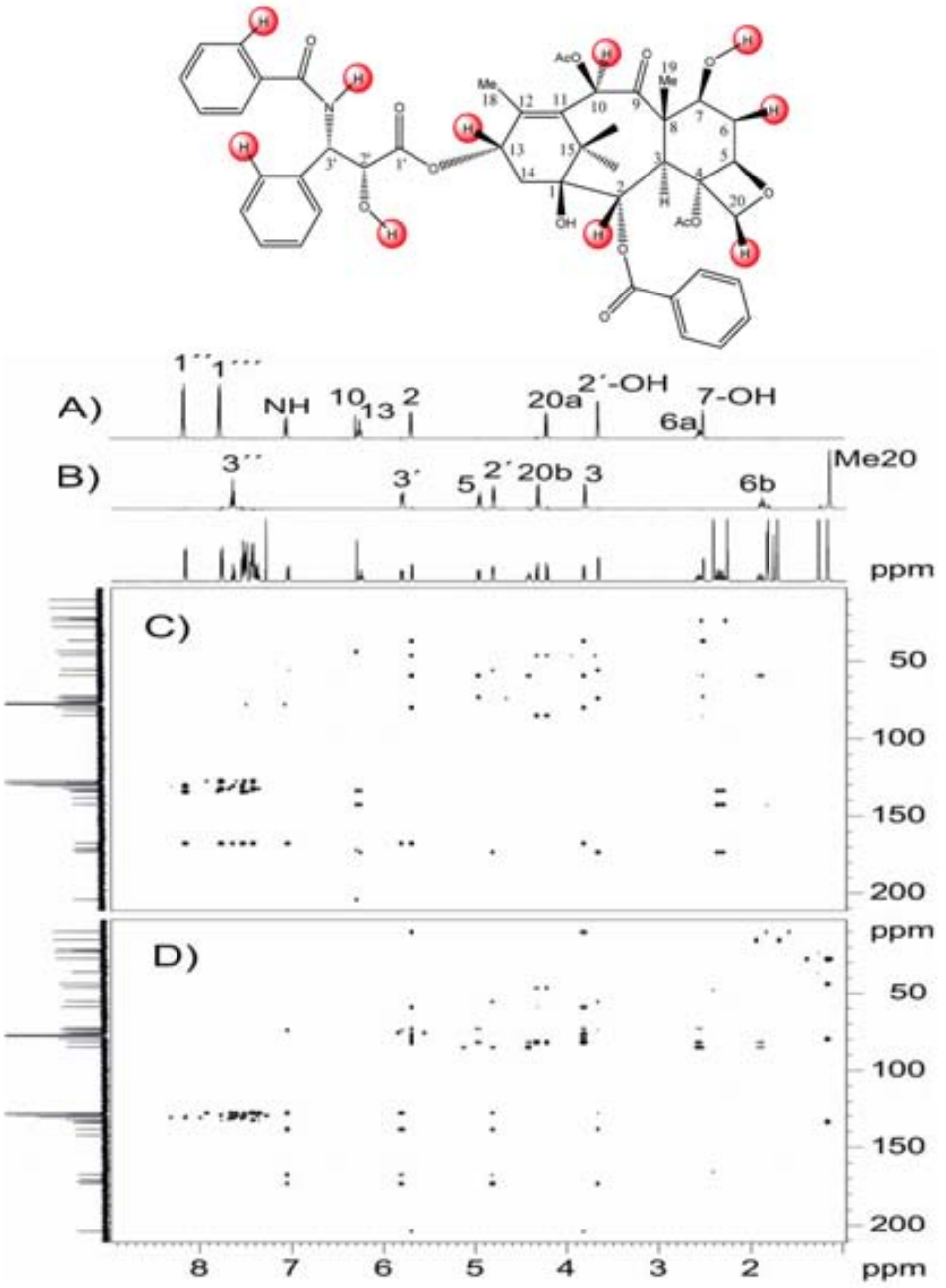

Figure S6. A-B) 1D proton spectra after simultaneous eight-site excitation in the natural product taxol, **3**. Protons excited in spectrum A) are marked in red in the chemical structure; C-D) Corresponding 2D selHSQMBC-TOCSY spectra after apply the selection described before.

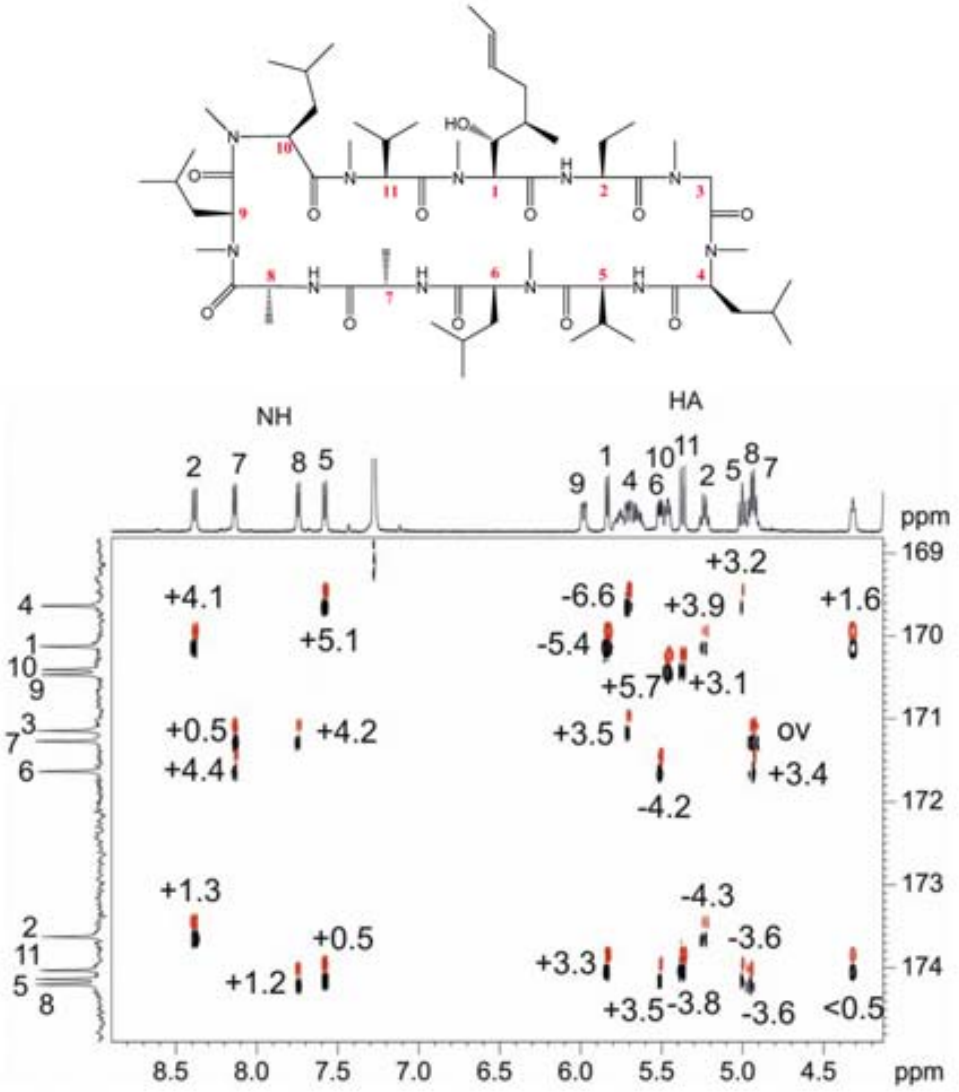

Figure S7. Expanded carbonyl region extracted from the Hα-band-selective HSQMBC-TOCSY experiment of the cyclic undecapeptide cyclosporine, **2**. All intraresidue ^{2}J(Hα-CO) and ^{3}J(NH-CO) and inter-residue ^{3}J(Hα-CO) and ^{2}J(NH-CO) coupling values can be determined. Although not shown here, practically the magnitude and the sign of all backbone and sidechain ^{n}J(CH) can be measured analyzing the whole 2D spectrum.

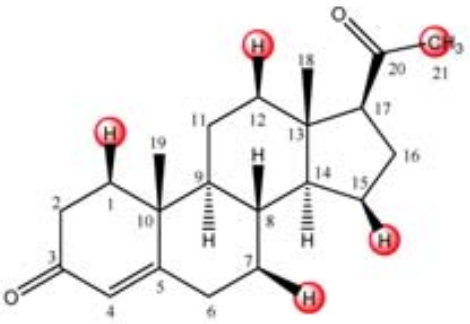
O
H
CH3
18
20
21
17
11
12
13
16
19
H
9
14
15
2
1
10
8
H
H
H
3
7
O
5
4
6

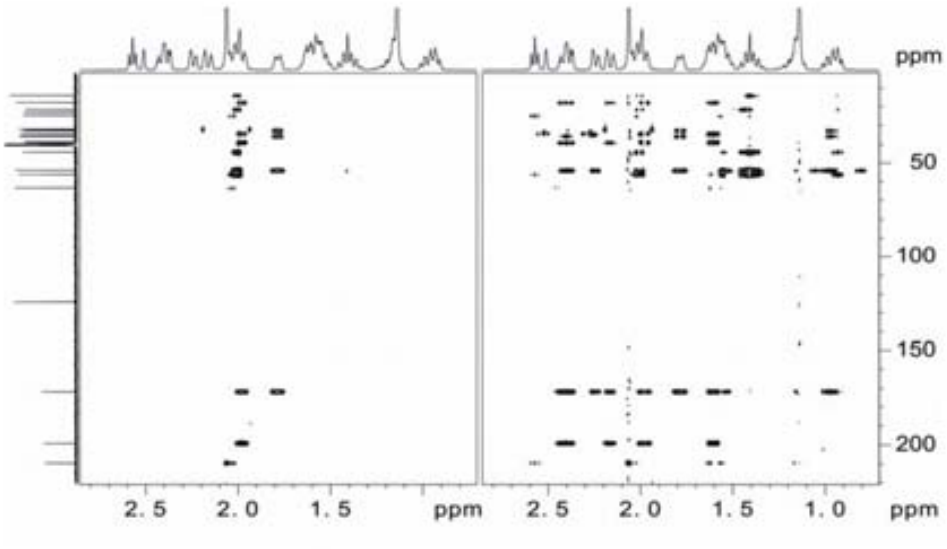
ppm
50
100
150
200
2.5
2.0
1.5
ppm
2.5
2.0
1.5
1.0
ppm

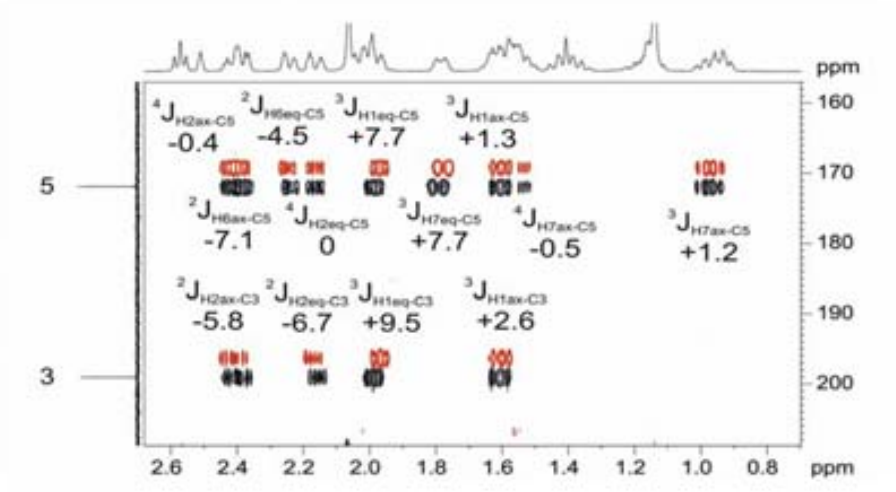
ppm
160
170
180
190
200
5
3
4J H2ax-C5 -0.4
2J H6eq-C5 -4.5
3J H1eq-C5 +7.7
3J H1ax-C5 +1.3
2J H6ax-C5 -7.1
4J H2eq-C5 0
3J H7eq-C5 +7.7
4J H7ax-C5 -0.5
3J H7ax-C5 +1.2
2J H2ax-C3 -5.8
2J H2eq-C3 -6.7
3J H1eq-C3 +9.5
3J H1ax-C3 +2.6
2.6
2.4
2.2
2.0
1.8
1.6
1.4
1.2
1.0
0.8
ppm

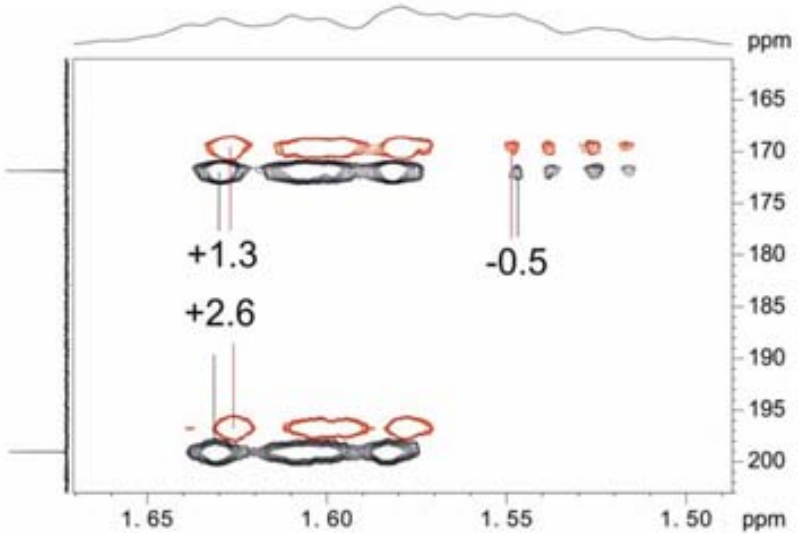

Figure S8. A) In-phase selHSQMBC and selHSQMBC-TOCSY spectra of progesterone after selective inversion of protons resonating in the region of 1.8-2.0 ppm. B) Expanded area of the α/β-selHSQMBC-TOCSY covering the quaternary C3, C5 and C20 carbons showing that the sign and magnitude can be directly measured from the relative signal displacement of each cross-peak. C) Expanded area showing that smaller values than 2 Hz and the corresponding can be measured from relayed cross-peaks .

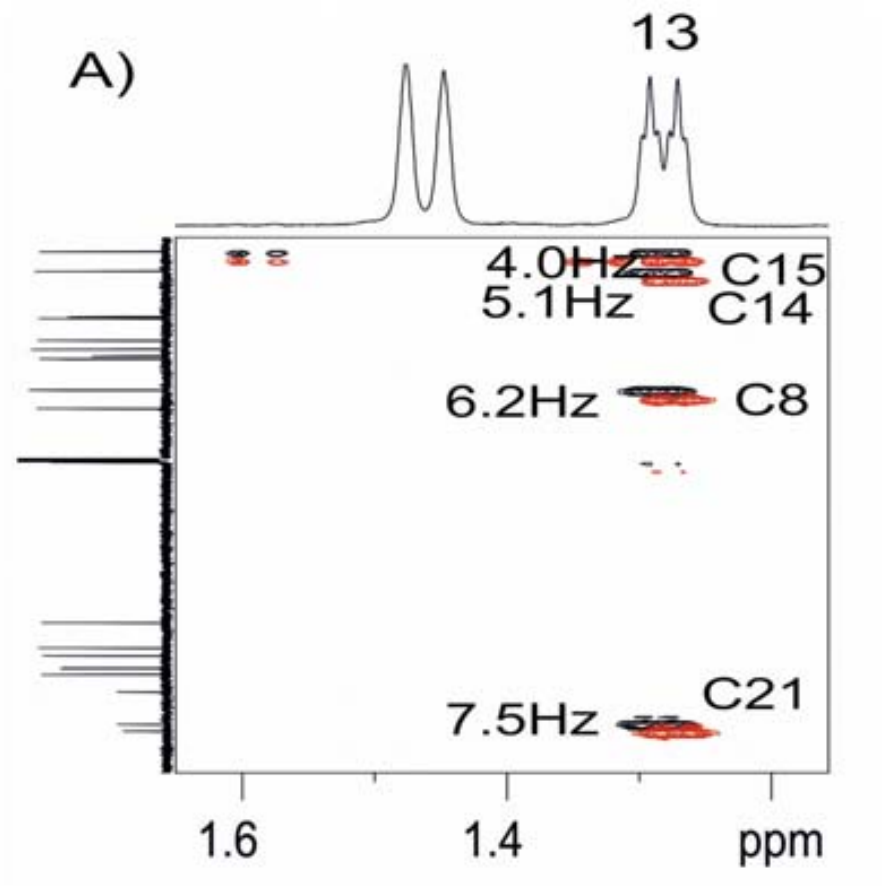
A)
13
4.0Hz
C15
5.1Hz
C14
6.2Hz
C8
C21
7.5Hz
1.6
1.4
ppm

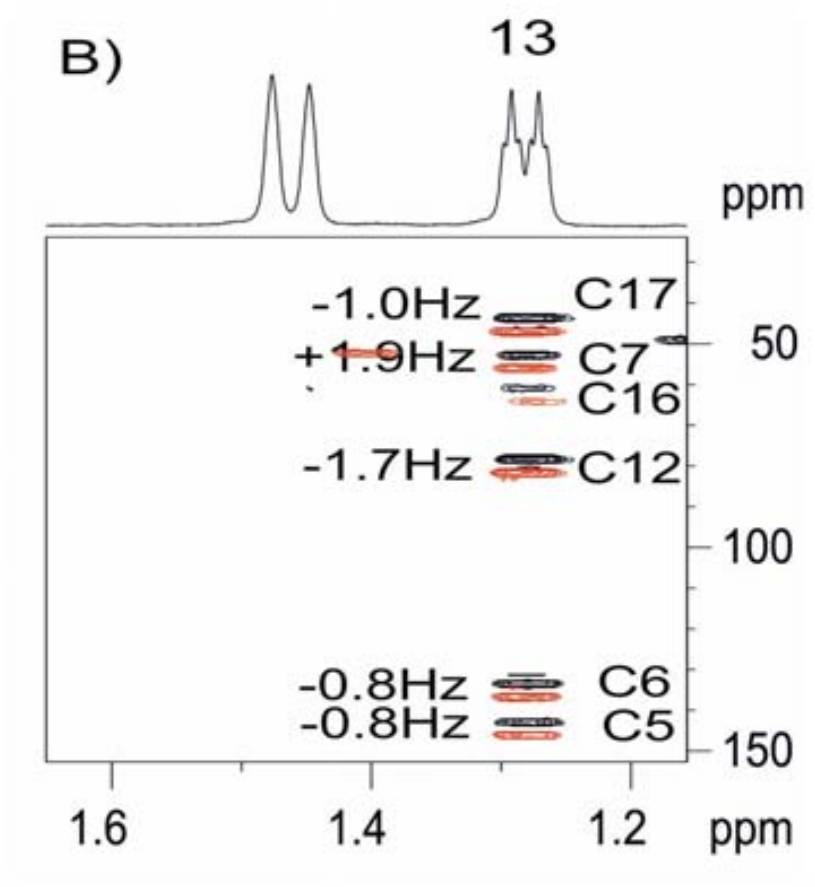
B)
13
ppm
-1.0Hz
C17
+1.9Hz
C7
C16
-1.7Hz
C12
50
100
-0.8Hz
C6
-0.8Hz
C5
150
1.6
1.4
1.2
ppm

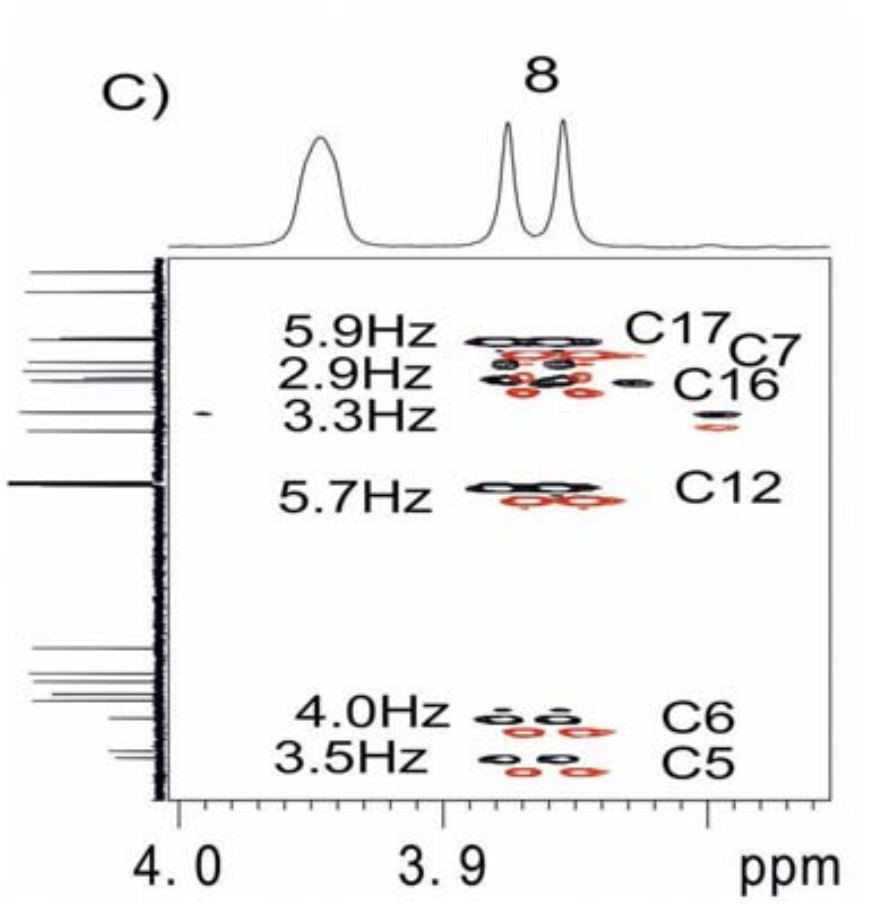
C)
8
5.9Hz
2.9Hz
3.3Hz
5.7Hz
4.0Hz
3.5Hz
C17
C7
C16
C12
C6
C5
4. 0
3. 9
ppm

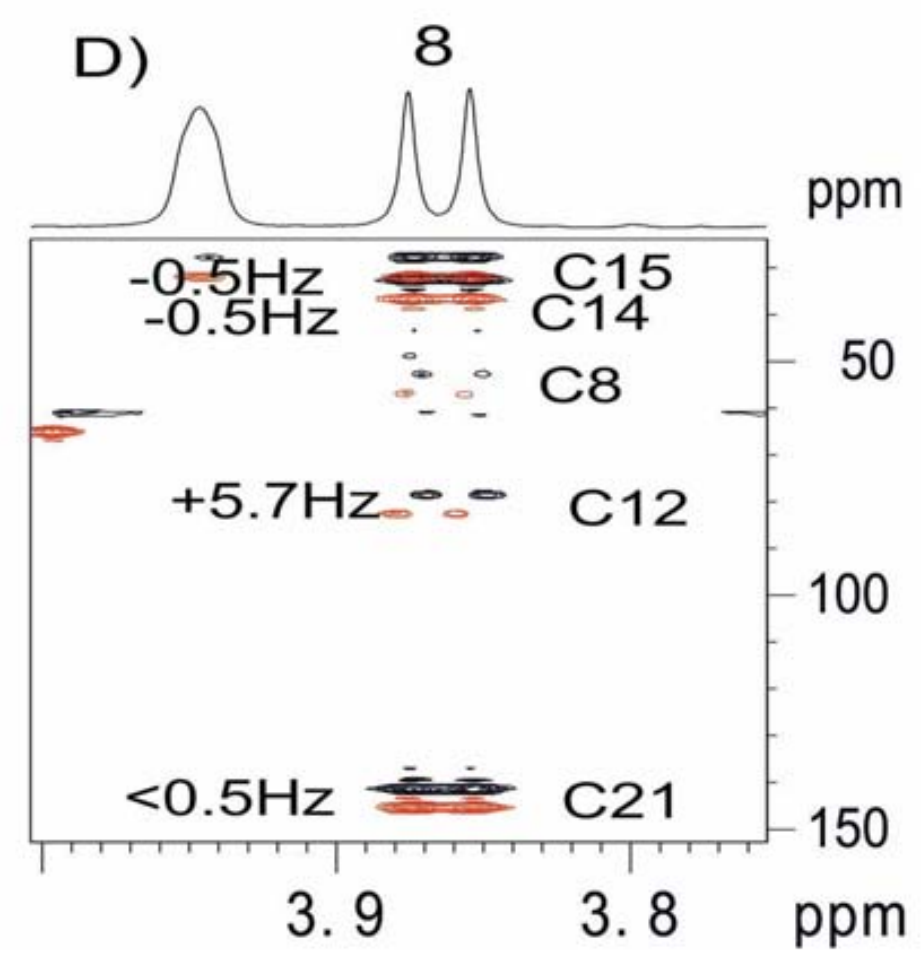

Figure S9: Amplified Figures of the figure 4 of the main manuscript.

PUBLICATION 3

Efficient measurement of the sign and the magnitude of long-range proton-carbon coupling constants from a spin-state-selective HSQMBC-COSY experiment

J. Saurí, T. Parella. *Magn. Reson. Chem*. 2012, 50, 717–721

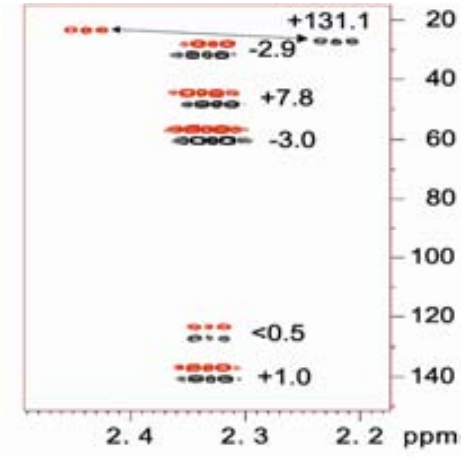

1. Introduction

In this publication, an hybrid selHSQMBC-COSY experiment is presented, in where the information obtained in a standard selHSQMBC experiments is extended to neighbouring ^{1}H nuclei by a COSY transfer (**Fig. 3.03**). The experiment is related to the selHSQMBC-TOCSY IPAP experiment described in the previous Publication 2.

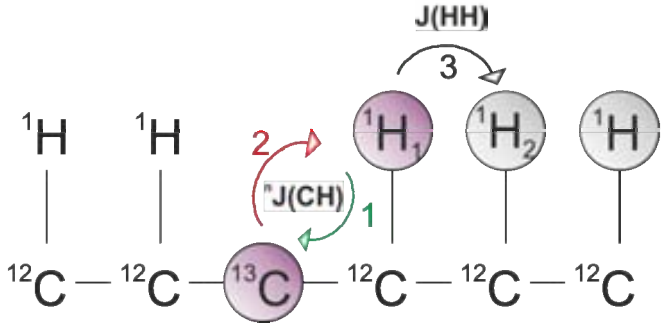

Figure 3.03. Basic magnetization transfer scheme for the selHSQMBC-COSY experiment.

Taking into account that the intensity of a relayed $^{3}J(C\text{-}H2)$ cross-peak only depends on the initial $^{2}J(C\text{-}H1)$ value and the efficiency of the proton-proton transfer, one can conclude that:

- If the initial transfer step is a 2-bonded correlation ($^{2}J(C\text{-}H1)$), the COSY transfer to the most adjacent proton (from H1 to H2) would give us a $^{3}J(C\text{-}H2)$ cross-peak.
- If the initial transfer step is a 3-bonded correlation ($^{3}J(C\text{-}H2)$), the COSY transfer would give us information of a $^{4}J(C\text{-}H3)$ or $^{2}J(C\text{-}H1)$ connectivity.

The paper presents an alternative way to measure the magnitude and the sign of small proton-carbon coupling constants for protonated and non-protonated carbon atoms, being its main advantage that a more simple and shorter pulse sequence than the selHSQMBC-TOCSY experiment is used and a sensitivity penalty due to additional relaxation losses is highly reduced.

With a slightly modification in the original selHSQMBC pulse sequence, which consists to change the selective 180º ^{1}H by a hard pulse in the R-INEPT period, a COSY transfer is successfully achieved. In this way, simultaneously evolution of J(HH) and $^{n}J(CH)$ takes place causing the appearance of AP contributions in the resulting multiplets. However, it is demonstrated that the IPAP methodology equally preserves such distortions for the α- and β-cross-peaks making possible an easy extraction of the magnitude of the coupling constant by analysing their relative displacements. Besides that, the experiment preserves all the benefits of the selHSQMBC-TOCSY experiment.

Research Article

Magnetic Resonance in Chemistry

Received: 9 March 2012 Revised: 4 July 2012 Accepted: 6 August 2012 Published online in Wiley Online Library: 4 September 2012

(wileyonlinelibrary.com) DOI 10.1002/mrc.3867

Efficient measurement of the sign and the magnitude of long-range proton-carbon coupling constants from a spin-state-selective HSQMBC-COSY experiment

Josep Saurí[a,b] and Teodor Parella[a,b]*

A spin state-selective Heteronuclear Single-Quantum Multiple-Bond Connectivities (HSQMBC-COSY) experiment is proposed to measure the sign and the magnitude of long-range proton-carbon coupling constants (^nJ(CH); $n > 1$) either for protonated or for non-protonated carbons in small molecules. The simple substitution of the selective 180° ^{1}H pulse in the original selHSQMBC pulse scheme by a hard one allows the simultaneous evolution of both proton-proton and proton-carbon coupling constants during the refocusing period and enables a final COSY transfer between coupled protons. The successful implementation of the IPAP principle leads to separate mixed-phase α/β cross-peaks from which ^nJ(CH) values can be easily measured by analyzing their relative frequency displacements in the detected dimension. Copyright © 2012 John Wiley & Sons, Ltd.

Keywords: HSQMBC; HSQMBC-COSY; long-range proton-carbon coupling constants; IPAP

Introduction

It has always been a wide interest in the design of NMR methods directed to the measurement of heteronuclear coupling constants in small molecules. In the particular case of ^{13}C, it was not an easy task because the signals corresponding to the active ^{13}C isotopomers appear below the ^{1}H–^{12}C signal in the conventional proton spectrum that is about 200 times more intense because of the low ^{13}C natural abundance (~1.1%). The strong ^{1}H–^{12}C signal is efficiently suppressed in modern NMR spectroscopy by applying pulsed field gradients as a method of coherence selection, and nowadays a multitude of NMR methods is available for the proper measurement of long-range proton-carbon coupling constants (^nJ(CH); $n > 1$).[1,2] Accepting that the problem to determine the magnitude and the sign of ^nJ(CH) is already solved for protonated carbons mainly using HSQC-TOCSY-type experiments,[3–5] some relevant aspects on ^nJ(CH) are still under study and discussion, namely, the accuracy of their measurements and how we can measure small values and also their signs on quaternary carbons.

Recently, our group has reported an efficient and straightforward in-phase and anti-phase (IPAP) approach to accurately measure ^nJ(CH) on both protonated and non-protonated carbons.[6–8] As a first advantage, the tedious analysis of typical anti-phase cross-peaks obtained from Heteronuclear Single-Quantum Multiple-Bond Connectivities (HSQMBC) experiments is avoided. Second, the main limitations associated with other commonly used experiments such as J-resolved methods (an elevated number of t_1 increments are required, the measurement of small values is not affordable and they are not sign-sensitive) are overcome. These new IPAP methods are based on the separate acquisition of complementary In-Phase (IP) and Anti-Phase (AP) HSQMBC data that after suitable linear combination affords spin state-selective HSQMBC spectra. Interestingly, the magnitude and the sign of ^nJ(CH) are determined measuring the relative left/right displacement between α/β cross-peaks in the detected dimension. First, a broadband version based on a G-BIRD-HSQMBC-IPAP experiment was suggested.[6] This and other related approaches using CPMG-based schemes can lead α/β cross-peaks with mixed phases due to residual proton-proton coupling, J(HH), evolution during the INEPT-like periods. A further development makes use of 180° proton selective pulses to completely remove the problems associated with J(HH) evolution and, therefore, pure-phase data are obtained that greatly facilitates the measurement.[7] However, the measurement of small values from this selHSQMBC-IPAP experiment remained a challenge while the sign information was not available. Recently, it has been reported that the addition of a TOCSY propagation period after the selHSQMBC block affords a general and unique tool to measure the sign and the magnitude of ^nJ(CH) for both protonated and non-protonated centers.[8] This selHSQMBC-TOCSY-IPAP method proves to be highly useful even for molecules showing overlapped resonances, complex multiplets and, very importantly, to measure very small ^nJ(CH) coupling values because the intensity of relayed cross-peaks is independent of their ^nJ(CH) values.

Herein, we describe a long-range optimized HSQC-COSY pulse scheme[9] that allows the measurement of the sign and the magnitude of ^nJ(CH) in a similar way to the selHSQMBC-TOCSY experiment. This new selHSQMBC-COSY method has better

* Correspondence to: Teodor Parella, Servei de Ressonància Magnética Nuclear, Universitat Autònoma de Barcelona, E-08193, Bellaterra, Barcelona, Spain. E-mail: teodor.parella@uab.cat

a Servei de Ressonància Magnética Nuclear, Universitat Autònoma de Barcelona, E-08193-Bellaterra, Barcelona, Spain

b Departament de Química, Universitat Autònoma de Barcelona, E-08193-Bellaterra, Barcelona, Spain

sensitivity while most of the reported features are still retained: (i) the magnitude and the sign of $^{n}J_{CH}$ are directly determined from the analysis of the relative displacement of α/β multiplets avoiding the need of complex and time-consuming analysis using individualized fitting procedures; (ii) they can be measured for both protonated and non-protonated carbons; (iii) the measurement is made in the detected dimension and therefore good resolution levels can easily be attainable with a minor number of t_1 increments; (iv) although mixed-phase multiplets are obtained, extraction of ^{n}J(CH) remains easy and accurate in a multitude of conditions: broad, unresolved or highly complex multiplets, in congested areas or with the presence of mixtures of compounds; and (v) coupling values smaller than the line width can be determined. We test the applicability of the proposed method on the alkaloid strychnine, **1**.

Results and Discussion

Figure 1 shows the basic pulse scheme of the selHSQMBC-COSY-IPAP experiment. It resembles a regular HSQC pulse train with a few different details: (i) a selective 180° ^{1}H pulse is applied in the initial INEPT period to prevent J(HH) evolution, (ii) the interpulse delays are optimized to small ^{n}J(CH) values, typically 6–8 Hz, (iii) a last 90° ^{1}H pulse is appliedfrom the y axis to generate COSY cross-peaks, and (iv) proton acquisition is performed without ^{13}C decoupling because ^{n}J(CH) values want to be measured in the detected dimension. Using another analogy, the pulse sequence is a very simple modification of the original selHSQMBC experiment[7] where the selective 180° ^{1}H pulse incorporated in the refocusing INEPT period has been replaced by a hard 180° ^{1}H pulse. In this way, simultaneous J(HH) and ^{n}J(CH) evolution takes place during this period that facilitates COSY transfer, thanks to the last 90° ^{1}H pulse. In addition, better sensitivity is achieved than the selHSQMBC-TOCSY scheme because the additional TOCSY period is avoided and therefore potential relaxation losses are reduced.

The coupling pathway involved in a selHSQMBC-COSY experiment consists of two parts (Scheme 1): First, a selective out-and-back step from the selected H2 proton to long-range coupled carbons (C1) is accomplished by the HSQMBC element, and second, a non-selective COSY transfer from this same proton to other protons via J(H2–H3) executed simply by the last 90° ^{1}H

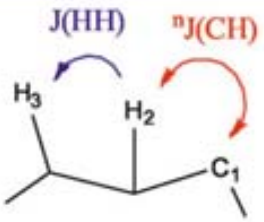

HSQMBC-COSY

Scheme 1. Coupling pathway involved in the HSQMBC-COSY experiment.

pulse. Analyzing the pulse scheme in more detail, the initial selective INEPT block for a selected H2 proton affords coherence in the form of $H_{2x}C_z * \sin(\pi {}^{n}J_{H2-C1}\Delta)$. After the simultaneous 90°$_y$(H)/90°$_x$(C) pulses, anti-phase carbon magnetization in the initial $H_{2z}C_y$ form evolves during the variable evolution t_1 period in the usual way. After that, a 90° carbon pulse creates $H_{2z}C_z$ magnetization and the purge gradient G4 removes any residual transverse magnetization. The proposed method is based on the application of the IPAP principle in a refocused HSQC scheme: Two complementary IP and AP data are separately recorded with and without the 180° ^{13}C pulse in the refocused period, respectively. Thus, IP data are generated using $\Psi = y$ and applying the 180° ^{13}C pulse:

$$\text{IP}: \; H_{2y}\sin^2(\pi J_{H2-C1}\Delta)\cos(\pi J_{H3-H2}\Delta) + 2H_{2x}H_{3z}\sin^2(\pi J_{H2-C1}\Delta)\sin(\pi J_{H3-H2}\Delta) \quad (1)$$

On the other hand, AP data are obtained using $\Psi = x$ and omitting the 180° ^{13}C inversion pulse in order to avoid $^{n}J_{CH}$ refocusing:

$$\text{AP}: \; 2H_{2y}C_z\sin(\pi J_{H2-C1}\Delta)\cos(\pi J_{H3-H2}\Delta) - 4H_{2x}H_{3z}C_z\sin(\pi J_{H2-C1}\Delta)\sin(\pi J_{H3-H2}\Delta) \quad (2)$$

The last 90°$_y$ ^{1}H pulse that was applied in the selHSQMBC experiment for purging purposes of undesired coherences now creates additional COSY cross-peaks:

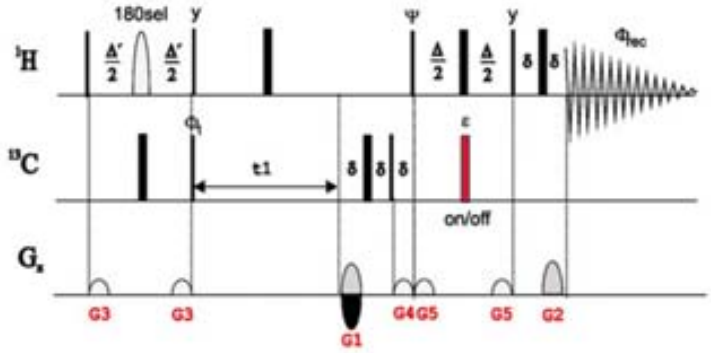

Figure 1. General pulse scheme of the proton-selective HSQMBC-COSY experiment. Thin and thick bars represent 90° and 180° non-selective pulses that are applied along the x-axis unless otherwise stated. The 180° proton pulse in the first INEPT block is applied selectively to a single frequency. The basic cycle phase was Φ_1: $x,-x$; Φ_{rec}: $x,-x$. In-phase (IP: $\Psi = y$, ε = on) and anti-phase (AP: $\Psi = x$, ε = off) data are recorded separately and combined in the time domain to provide α/β spectra. The interpulse delays are set to $\Delta = \Delta' + p_{180} = 1/(2 * {}^{n}J_{CH})$, where p_{180} is the duration of the selective 180° ^{1}H pulse. G4 gradient acts as zz-purge gradient filters, G3 and G5 are used for refocused heteronuclear gradient echo, and G1 and G2 are used for coherence selection. The sign of the G1 encoding gradient is alternated for echo/anti-echo coherence selection. δ is the duration of the gradients.

$$\text{IP}: \; H_{2y} \sin^2(\pi J_{H2-C1}\Delta) \cos(\pi J_{H3-H2}\Delta) + 2H_{2z}H_{3y} \sin^2(\pi J_{H2-C1}\Delta) \sin(\pi J_{H3-H2}\Delta) \quad (3)$$

$$\text{AP}: \; 2H_{2y}C_z \sin(\pi J_{H2-C1}\Delta) \cos(\pi J_{H3-H2}\Delta) - 4H_{2z}H_{3y}C_z \sin(\pi J_{H2-C1}\Delta) \sin(\pi J_{H3-H2}\Delta) \quad (4)$$

A key point for the IPAP principle success is the percentage of cross-talk generated in such addition/subtraction (IP ± AP) procedures due to the non-equivalent intensity between IP and AP data. Assuming that the effect of *J*(HH) modulation is exactly the same for the IP and AP data, cross-talk will be proportional to the $\sin^2(\pi J_{H2-C1}\Delta) - \sin(\pi J_{H2-C1}\Delta)$ factor and the percentage of cross-talk with respect to the overall multiplet sensitivity is defined by $[\sin(\pi J_{H2-C1}\Delta) - 1]/[\sin(\pi J_{H2-C1}\Delta) + 1]$. As similarly reported previously,[7] selHSQMBC-COSY shows to be extremely tolerable to undesired cross-talk effects over a potential mismatch between ^{n}J(CH) values and Δ optimization.

Figure 2 clearly shows the great benefits of changing the selective 180° proton pulse in the selHSQMBC experiment (Fig. 2A) by a standard hard 180° pulse (Fig. 2B). The three H14, H11a and H18a protons that appear overlapped in the conventional ^{1}H spectrum of **1** at 3.15 ppm were selectively refocused by a 20-ms Gaussian-shaped 180° pulse. A single vertical area shows the most intense long-range heteronuclear correlations from these three selected protons in the clean 8-Hz optimized selHSQMBC spectrum. In the analog selHSQMBC-COSY spectrum, a great number of additional COSY cross-peaks are available and ready to be analyzed.

The potential on the implementation of the IPAP technique into the selHSQMBC-COSY experiment is demonstrated for a non-protonated center, the carbonyl C10 carbon (Fig. 3). In addition to the initial two-bond H11a–C10 correlation (−6.2 Hz), two additional COSY cross-peaks are observed corresponding to the two-bond H11b–C10 (−7.8 Hz) and the three-bond H12–C10 (+2.1 Hz) correlations. The IPAP-HSQMBC-COSY cross-peaks (Fig. 3B and C, respectively) show mixed-phase properties, preventing any attempt to the direct extraction of coupling values. Although those mixed phases are also present in the corresponding α and β multiplets (Fig. 3D and E, respectively), this does not affect the measurement because only the displacement between α/β signals is of interest, regardless of how they are. It is important to note that no manual or automatic phase correction was applied for any of the four IP, AP, α and β multiplets. Clearly, the magnitude of all three ^{n}J(CH) couplings can be directly determined without need of any fitting process

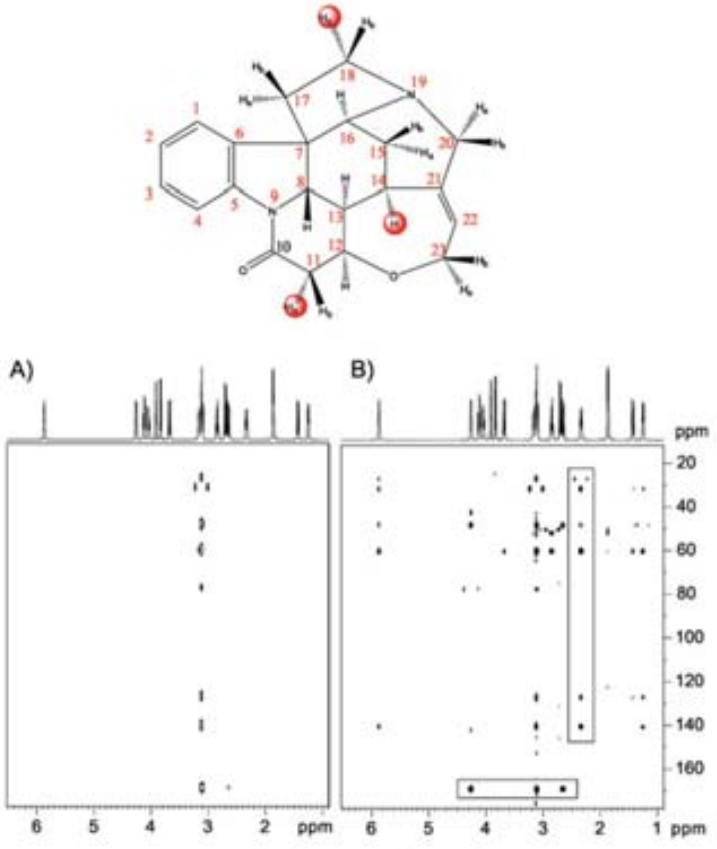

Figure 2. (A) selHSQMBC and (B) selHSQMBC-COSY spectra of **1** after selective refocusing of protons (H14/H11a/H18a) resonating at 3.15 ppm. Only the corresponding IP spectra are shown in magnitude mode. Note that additional COSY cross-peaks are originated by the simple conversion from selective to non-selective mode of the 180° ^{1}H pulse placed in the refocused period. Areas marked with a rectangle box in (B) are further discussed in Figs 3 and 4. See experimental section for more details.

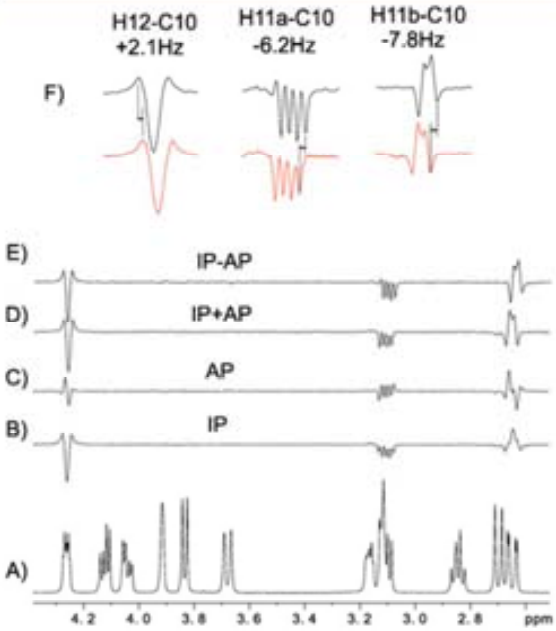

Figure 3. (A) Conventional ^{1}H and (B–E) 1D sections extracted from the ^{13}C frequency of the carbonyl C10 carbon: (B) IP and (C) AP HSQMBC-COSY data acquired as described in Fig. 2B, and (D and E) α/β HSQMBC-COSY data obtained after linear combination of B ± C. (F) Expanded 1D α and β multiplets to visualize their relative displacements.

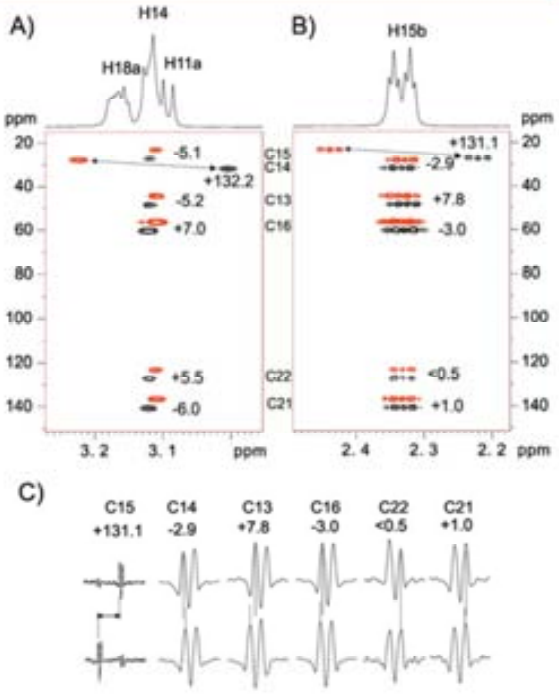

Figure 4. 2D expansions plots of the HSQMBC-COSY-IPAP spectra resulting of Fig. 2B and corresponding to the (A) excited H14 and (B) COSY H15b protons. α/β cross-peaks are shown slightly shifted in the vertical scale to visualize their mutual relative displacements. For clarity, no distinction has been made for positive and negative intensities. Note that the extraction of the relative signs from the left/right displacement analysis is only valid between cross-peaks in the same row. (C) 1D slices extracted from the different rows shown in (B).

(Fig. 3F). On the other hand, the sign is also codified from the relative left/right (negative) or right/left (positive) frequency peak displacement. The measurement of *J* from a single peak as shown in Fig. 3F is only for illustrative questions. In fact, it is more accurate to measure *J* for each resolved peak into a multiplet and obtaining an average value because multiplet distortions could introduce major errors if only a single measurement is made. The measured data are in strong agreement with those published previously.[8]

Figure 4 shows expansions corresponding to the most intense H14 proton and the COSY cross-peaks originated for its vicinal H15b proton from the selHSQMBC-COSY-IPAP spectra. All correlations involving the H14 proton with ^{n}J(CH) values ranging from 5 to 7 Hz are clearly visible and easily measured in an 8-Hz optimized experiment as a result of their sine dependence with the interpulse Δ delay (Fig. 4A). However, it is not possible to determine the sign of these ^{n}J(CH) values from the single analysis of this column. It should be emphasized that although the direct correlation presents opposite displacement because of the different magnitudes of ^{1}J(CH) *versus* ^{n}J(CH), this is not related to the relative sign. On the other hand, several features are quickly evident from the analysis of the relayed H15b column (Fig. 4B): (i) the intensity and possible cross-talks for all observed COSY cross-peaks do not depend on their ^{n}J(CH) values but the original H14 cross-peaks; (ii) the sign of ^{n}J(CH) cannot be determined analyzing only this column but they can be quickly assigned when compared the relative displacement of each cross-peak with the original H14 cross-peak (sometimes a prior knowledge of chemical shift assignment is required and it can be assumed that large three-bond connectivities present positive sign); (iii) values smaller than the line width can be measured because of almost unlimited resolution attainable in the detected dimension; and (iv) all cross-peaks belonging to the same proton show similar phase distortions because of J(HH) modulation but this does not affect the precise and reliable measurement of ^{n}J(CH) (Fig. 4C). It is very important to clarify that the extraction of relative signs is only applicable when comparing signals from the same row (the same carbon) but not for peaks of the same column but different rows (different carbons). For instance, check the correct sign from the opposite sense between H14–C16 ($^{3}J = +7.0$ Hz) and H15b–C16 ($^{2}J = -3.0$ Hz) cross-peaks. However, although H15b–C13 ($^{3}J = +7.8$ Hz) and H15b–C16 ($^{2}J = -3.0$ Hz) have the same relative displacement, they have opposite signs.

Another essential point to highlight is the relative sensitivity between equivalent selHSQMBC, selHSQMBC-COSY and selHSQMBC-TOCSY experiments. Figure 5 shows the 1D sections extracted for the C14 carbon for all these experiments acquired under the same conditions previously described in Fig. 2. Whereas in the selHSQMBC experiment only the large H14 satellites are visible, additional COSY correlations to the H22, H15a, H15b and H13 protons emerge in the selHSQMBC-COSY spectrum. Similar correlations presenting pure-phase properties are obtained from the equivalent selHSQMBC-TOCSY experiment but with a considerable penalty in sensitivity due to the additional 40-ms TOCSY mixing time. Later, the overall sensitivity will strongly depend on the duration of mixing time and also on the existing spin topologies.

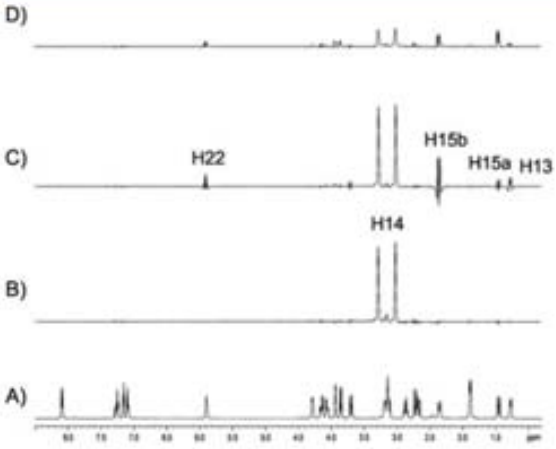

Figure 5. (A) 1D sections extracted at the C14 carbon chemical shift (45 ppm) of the IP version of (B) selHSQMBC (see Fig. 2A), (C) selHSQMBC-COSY (see Fig. 2B) and (D) selHSQMBC-TOCSY (using a 40-ms mixing time) experiments. All experiments were recorded and processed using the same conditions as reported in Fig. 2 and are plotted using the same vertical scaling in order to compare the relative sensitivity of each experiment.

To conclude, we have introduced a new selHSQMBC-COSY experiment to measure the size and the sign of ^{n}J(CH) with high accuracy using the IPAP concept. The experiment retains the simplicity of the original selHSQMBC experiment and, as an additional bonus, an increased number of coupling values and sign information can be extracted. On the other hand, the experiment also retains most of the features and benefits associated to the powerful selHSQMBC-TOCSY experiment with an important added value: ^{1}H–^{1}H COSY transfer is achieved at the same time that ^{n}J(CH) evolution and therefore superior sensitivity is achieved because an additional TOCSY period is not necessary, even considering the potential signal cancelation due to the anti-phase character associated to COSY cross-peaks. The method can be applied to a myriad of different structural and conformational aspects, shows extreme simplicity in both set-up and data interpretation and can be combined with multiple-frequency and band-selective excitation in order to obtain a complete ^{n}J(CH) data set with only a few experiments. Of course, the method might also have a profound impact to the measurement of any type of heteronuclear coupling constants involving other heteronuclei than ^{13}C, showing an enormous potential in the application on organometallic and inorganic molecules.

Methods and Materials

All NMR experiments have been recorded on a BRUKER DRX-500 spectrometer equipped with a three-channel 5-mm cryoprobe incorporating a *z*-gradient coil on a sample of 25 mg of strychnine, **1**, dissolved in 0.6 ml of $CDCl_3$. 2D ^{1}H–^{13}C IP and AP-HSQMBC experiments on **1** were separately recorded as described in Fig. 1 using a recycle delay of 1 s and the interpulse Δ and Δ' delays were optimized to 8 Hz ($\Delta = \tau' + p_{180} = 1/2 * {}^{n}J_{CH}$, where p_{180} is a selective 180° ^{1}H pulse). IP and AP data were recorded in a sequential mode, but acquisition in an interleaved mode can be advisable in less concentrated samples to minimize spectrometer instabilities. For selective refocusing, a Gaussian-shaped 180° pulse of duration of 20 ms (p_{180}) was applied in Fig. 2. Sine bell-shaped gradients of 1 ms duration (δ) were used, followed by a recovery delay of 200 μs. Gradient ratios for G1 : G2 : G3 : G4 : G5 were 80 : 20.1 : 33 : 50 : 11, measured as percentage of the absolute gradient strength of 5.35 G/cm. All experiments were acquired and processed using the echo/anti-echo protocol. Four scans were accumulated for each one of the real 64 t_1 increments, and the number of data points in t_2 was set to 4096. Spectral windows in both dimensions were 22 500 (F1) and 4500 (F2) Hz, respectively. The overall acquisition time for each IP and AP data was about 6 min, which was added/subtracted in the time domain without any scaling factor to provide spin state-selective data. Prior to Fourier transformation of each data, zero filling to 1024 in F1, 8192 points in F2 and a sine-squared function in both dimensions were applied.

Acknowledgements

Financial support for this research provided by MICINN (projects CTQ2009-08328 and Consolider Ingenio-2010 CSD2007-00006) and Bruker Española S.A. is gratefully acknowledged. We also thank the Servei de Ressonància Magnètica Nuclear, Universitat Autònoma de Barcelona for allocating instrument time to this project.

References

[1] B. L. Marquez, W. H. Gerwick, R. T. Williamson. *Magn. Reson. Chem.* **2001**, *39*, 499.
[2] T. Parella, 2D methods for the measurement of long-range proton-carbon coupling constants, in Multidimensional NMR Methods for the Solution State, (Eds: G. A. Morris, J. W. Emsley), John Wiley & Sons Ltd, Chichester, UK, **2010**, p. 305.
[3] P. Nolis, J. F. Espinosa, T. Parella. *J. Magn. Reson.* **2006**, *180*, 39.
[4] W. Kożmiński. *J. Magn. Reson.* **1999**, *137*, 408.
[5] K. Kobzar, B. Luy. *J. Magn. Reson.* **2007**, *186*, 131.
[6] S. Gil, J. F. Espinosa, T. Parella. *J. Magn. Reson.* **2010**, *207*, 312.
[7] S. Gil, J. F. Espinosa, T. Parella. *J. Magn. Reson.* **2011**, *213*, 145.
[8] J. Saurí, J. F. Espinosa, T. Parella. *Angew. Chem. Int. Ed.* **2012**, *16*, 3919.
[9] W. Willker, D. Leibfritz, R. Kerssebaum, W. Bermel. *Magn. Reson. Chem.* **1993**, *31*, 287.

2. Extension of the results

Strychnine molecule has been largely used as a standard compound to test our experiments because it displays a very interesting ^{1}H NMR spectrum in terms of peak dispersion and complexity. Nonetheless, an example of a more complex system is also presented as an extension of our results, and to show how the proposed experiments properly works even for molecules presenting high overlapped regions in their ^{1}H NMR spectrum, like, for instance, the steroid progesterone.

Fig. 3.04 compares the analogues α/β- selHSQMBC-COSY and the selHSQMBC-TOCSY spectra after selective inversion of all the non-mutually coupled protons resonating at 1.7-2.1 ppm in progesterone. For a better visualization, an expanded area containing the quaternary C3 and C5 carbons is presented. Despite distorted cross-peaks are obtained in selHSQMBC-COSY spectrum, the measurement of both the magnitude and the sign of $^{n}J(CH)$ can be made with high accuracy and simplicity, and with a strong agreement with the results obtained from the equivalent selHSQMBC-TOCSY experiment.

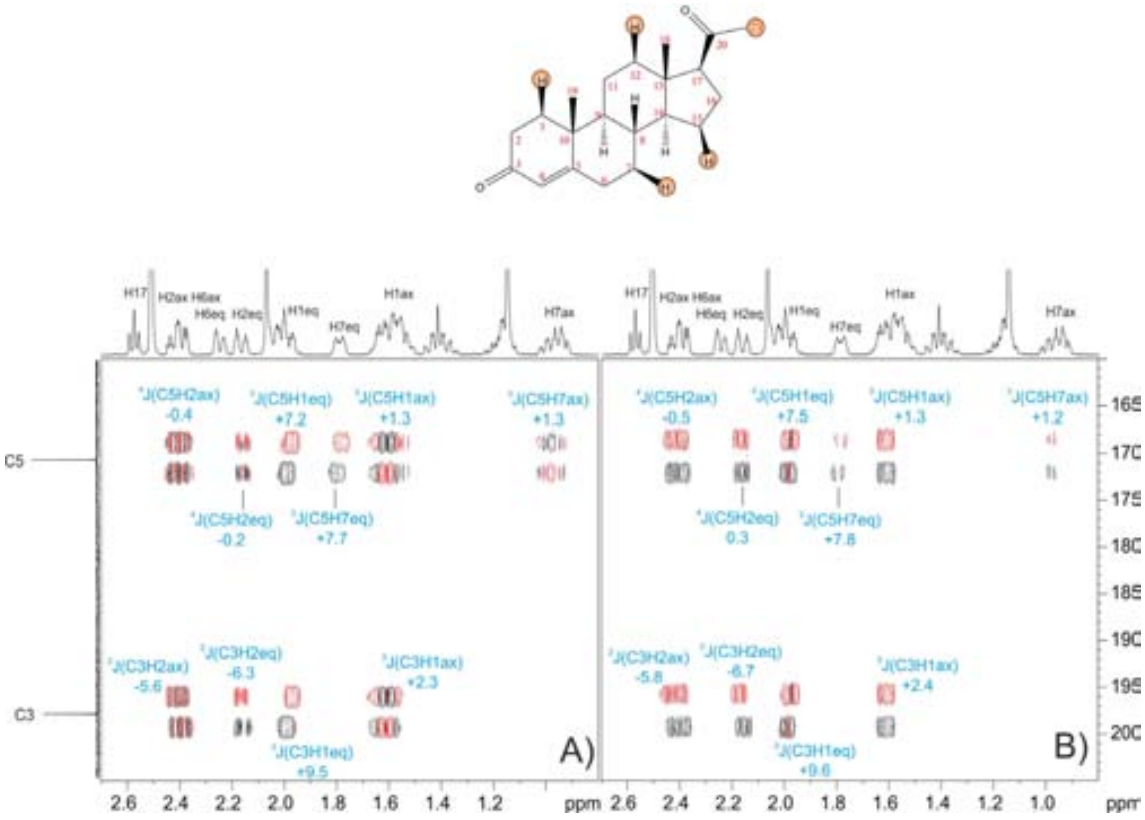

Figure 3.04. A) Expanded area of the α/β- selHSQMBC-COSY and B) α/β- selHSQMBC-TOCSY spectra in progesterone.

PUBLICATION 4

Efficient and fast sign-sensitive determination of heteronuclear coupling constants

J. Saurí, P. Nolis, T. Parella. *J. Magn. Reson*. 2013, 236, 66–69

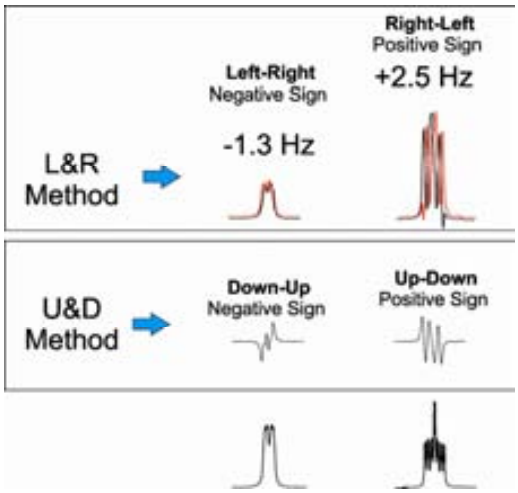

1. Introduction

In this publication, different versions of the selHSQMBC-TOCSY experiment are proposed for the fast an easy determination of the relative sign of heteronuclear coupling constants in other heteronuclei than ^{13}C and examples are provided for ^{19}F, ^{29}Si, ^{31}P, ^{77}Se and ^{119}Sn. A TOCSY block properly inserted at the end of selHSQMBC pulse sequence is able to extend $^{n}J(CH)$ information through a complete spin system via J(HH) transfer, preserving the α/β- spin state information of the heteronucleus in such a way that the relative sign can be easily extracted.

A 1D mode version of the experiment is proposed for those compounds having only one single heteronucleus of interest. Additionally, another version without PFGs for coherence selection is introduced for those compounds containing high natural abundance nuclei.

A non-refocused version of the selHSQMBC experiment leads to AP multiplets with respect to the active J(XH). Thanks to the application of the selective 180º ^{1}H pulses any J(HH) modulation is efficiently removed , and therefore pure-phase signals without undesired J(HH) contributions are obtained. We denoted this method as Up&Down (U&D) technique since the extraction of the relative sign information is achieved by analysing the relative up/down or down/up of the AP multiplet pattern.

For an accurate measurement of the $^{n}J(XH)$ value, two different 1D versions of the refocused selHSQMBC-TOCSY IPAP experiment are also proposed. One of them uses PFGs for coherence gradient selection, whereas the second omits them. We termed this method as Left&Right (L&R) technique since the measurement of the magnitude and the sign is achieved by analysing the relative left/right or right/left displacement of the pure IP α/β- multiplets.

Journal of Magnetic Resonance 236 (2013) 66–69

Contents lists available at ScienceDirect

Journal of Magnetic Resonance

journal homepage: www.elsevier.com/locate/jmr

Efficient and fast sign-sensitive determination of heteronuclear coupling constants

Josep Saurí, Pau Nolis, Teodor Parella *

Servei de Ressonància Magnètica Nuclear, Universitat Autònoma de Barcelona, E-08193 Bellaterra, Barcelona, Spain

ARTICLE INFO

Article history:
Received 26 July 2013
Revised 16 August 2013
Available online 3 September 2013

Keywords:
Heteronuclear coupling constants
IPAP
HSQMBC-TOCSY
Sign of coupling constants

ABSTRACT

Two complementary 1D NMR approaches for the fast and easy determination of the magnitude and the sign of heteronuclear *J*(XH) coupling constants are proposed: The *Up&Down* technique relies on the direct analysis of anti-phase multiplets whereas the *Left&Right* technique is based on the relative displacement between separate IPAP components.

1. Introduction

The determination of the magnitude of heteronuclear spin–spin coupling constants (*J*) plays a fundamental role in the structural and conformational characterization of organic and organometallic molecules in solution [1]. Unfortunately no much attention has been paid to the determination of the positive/negative sign of a coupling [2], and this is essential to derive theoretical and experimental correlations with structural parameters such as dihedral angles, pattern of bonds connecting the coupling nuclei, pattern substitutions along the coupling pathway and others. The theoretical calculation of coupling constants has become an important tool for the interpretation of experimentally determined data, and also for the prediction of coupling constants that are not available experimentally. Specifically, the knowledge of the sign is mandatory for the proper measurement and use of residual dipolar coupling constants (RDCs) in molecules weakly oriented in anisotropic media [3] or to get more insight about the through-bond and through-space contributions in hydrogen-bonding interactions [4].

Herein we introduce NMR methodologies that address some remaining challenges in the measurement of heteronuclear *J*(HX) coupling constants: (i) the general application on any type of high (^{31}P and ^{19}F are 100%), medium (^{119}Sn (8.6%), ^{77}Se (7.6%...)) or low natural-abundance (^{13}C (1.1%), ^{15}N (0.3%)) ½-spin NMR heteronuclei; (ii) the measurement of small *J* values, including couplings between remote spins separated for more than the conventional two- and three-bond connectivities; (iii) the *J* measurement on multiplets with different pattern complexity; and (iv) special emphasis for the easy determination of the relative *J* sign. Many small molecules only contain a single *X* heteronucleus of interest, and therefore it could become more convenient to acquire the corresponding spectra in a 1D mode, improving simplicity, resolution and data collection speed up.

2. Results and discussion

Fig. 1 shows two related approaches, referred to Up&Down (U&D) and Left&Right (L&R) methods, for the fast, easy and accurate determination of *J*(HX). They are based on a family of HSQMBC experiments that have been proposed to determine small proton–carbon coupling constants [5–7]. All these experiments use selective ^{1}H refocusing to ensure the absence of any HH modulation, making the experimental extraction of *J* extremely easy from the direct analysis of pure-phase signals. In the U&D-technique, a ^{1}H–^{1}H TOCSY transfer is inserted into the last zz-period of the basic HSQMBC pulse train to extend the measurement to other protons belonging to the same spin system (Fig. 1A). The duration of the TOCSY transfer period can be optimized for each spin system under study as usual. The resulting multiplets will present pure in-phase (IP) patterns with respect to all HH couplings and anti-phase (AP) pattern with respect to the active HX coupling. This aspect of the data allows the extraction of the relative sign of *J*(XH) by comparing the relative up/down or down/up phase between multiplets because the α/β spin-state of the heteronucleus is not affected by the mixing TOCSY process. On the other hand, the magnitude of *J*(HX) can be measured analyzing the AP pattern in cases of well resolved

* Corresponding author.
E-mail address: teodor.parella@uab.cat (T. Parella).

1090-7807/$ - see front matter © 2013 Elsevier Inc. All rights reserved.
http://dx.doi.org/10.1016/j.jmr.2013.08.013

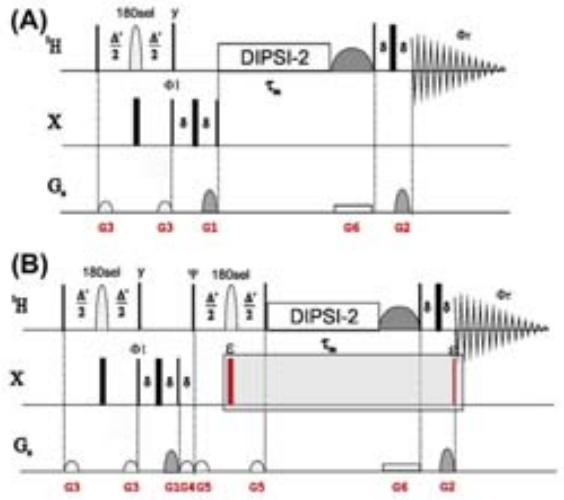

Fig. 1. (A) Non-refocused (*Up&Down* or *U&D*) and (B) refocused (*Left&Right* or *L&R*) versions of the 1D ^{1}H–X selHSQMBC-TOCSY experiment. The interpulse delays are optimized to $\Delta = \Delta' + p_{180} = 1/(2 \cdot J_{XH})$, where p_{180} is the duration of the selective 180° ^{1}H pulse. The TOCSY transfer consists of a z-filtered DIPSI-2 pulse train of duration τ_m with an additional G6 gradient simultaneously applied to an adiabatic smoothed *CHIRP* pulse to remove unwanted 2Q contributions. In (B) Two independent IP and AP datasets are separately collected as a function of the pulses marked with ε: IP (Ψ = *y* and ε = on) and AP (Ψ = *x* and ε = off). Separate α/β data are obtained after time-domain addition/subtraction data (AP ± IP). A minimum two-step phase cycle is applied: $\phi_1 = x, -x$ and $\phi_{rec} = x, -x$. The ratio between gradients (with a duration δ) G1:G2:G3:G4:G5:G6 were set to *x*:*y*:33:50:17:3, where $x/y = \gamma_H/\gamma_X$. Gradients G1 and G2 are used for coherence pathway selection and they can be omitted when working with high-abundant nuclei. The experiments can be also run in 2D mode. See details on pulse sequence timing of these non-gradient selected 1D and 2D experiments in the Supporting information.

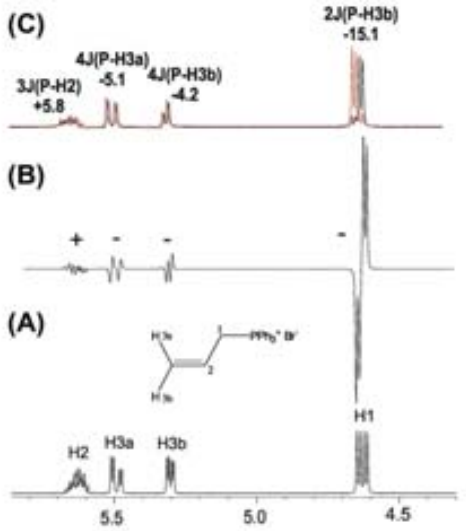

Fig. 2. 1D ^{1}H–^{31}P (B) U&D and (C) L&R spectra of 0.1 M allyltriphenylphosphonium bromide (**1**) in $CDCl_3$ acquired with the pulse sequences of Fig. 1A and 1B, respectively, without gradient coherence selection (see Fig. S1 in the Supporting information). The H1 proton was selectively excited with a 20 ms Gaussian-shaped 180° ^{1}H pulse and the inter-pulse delay and mixing times were optimized to 60 ms and 40 ms, respectively. 4 scans were collected with a relaxation delay of 1 s, giving an experimental time of only 16 s for each 1D spectrum.

multiplets or using a fitting procedure. Importantly, the intensity of a relayed H3–X signal does not depend of the *J*(H3–X) value but the cumulative *J*(H2–X) + *J*(H2–H3) pathway in the form of $2H_{3y}X_z\sin(\pi J_{H2X}\Delta)\cos(\pi J_{H2H3}\tau_m)$, and therefore small *J*(H3–X) values can be efficiently measured whenever TOCSY transfer is sufficiently effective.

Fig. 1B shows the refocused L&R version where IPAP selection is achieved by recording the experiment twice with modified refocusing conditions: when the X pulses marked with ε are applied, *J*(HX) is refocused to IP nature prior to acquisition whereas that AP magnetization is retained if they are omitted. Time-domain IP ± AP data combination followed by a conventional Fourier transformation afford the separate α- and β-spectra that allow the measurement of small *J*(HX) values by analyzing their relative signal frequency displacement. The sense of this displacement also provides the relative sign of *J*(HX) although that of a reference peak is needed to assign the absolute positive/negative value.

For low-abundance heteronuclei, the use of the G1 and G2 gradients for coherence selection (G1:G2 = γ_H/γ_X) is required to obtain high-quality U&D and L&R spectra. For high-abundance nucleus, such as ^{19}F or ^{31}P, gradients are not really needed, rendering the pulse sequences much more simple and sensitive (see Fig. S1 in the Supporting information for the corresponding pulse timing). In all cases, only H–X couplings that can be measured from a single 1D measurement are for those protons which are part of the same sequence of coupled protons as the selectively excited proton.

Several examples on standard molecules are shown here to illustrate the main features of the proposed experiments. For instance, although the magnitude of proton–phosphorus coupling constants, *J*(HP), can often be measured directly from the conventional ^{1}H multiplets or from simplified multiplets obtained from equivalent ^{31}P-decoupled 1D proton spectra of organophosphorus

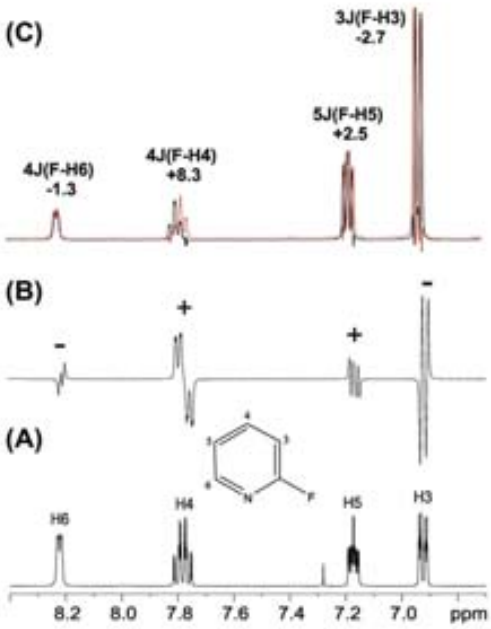

Fig. 3. 1D ^{1}H–^{19}F (B) U&D and (C) L&R spectra of 0.1 M 2-fluoropyridine (**2**) in $CDCl_3$ acquired with the pulse sequences of Fig. 1A and 1B, respectively, without gradient coherence selection. The H3 proton was selectively excited with a 20 ms Gaussian-shaped 180° ^{1}H pulse and the inter-pulse delay and mixing times were optimized to 60 ms and 40 ms, respectively. 4 scans were collected with a relaxation delay of 1 s, giving an experimental time of only 33 s for each 1D spectrum.

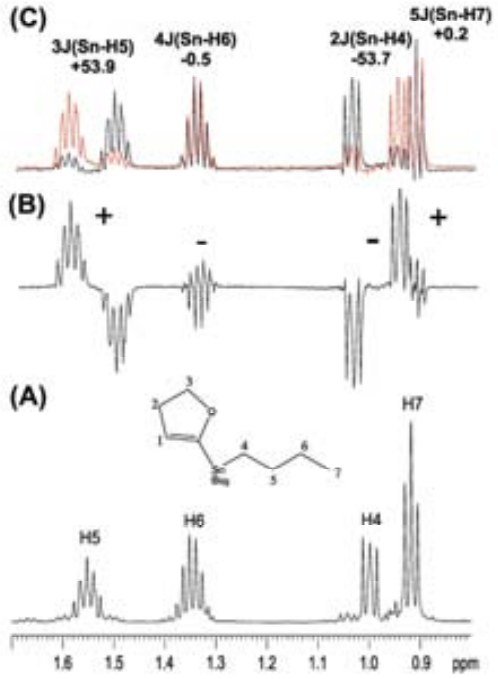

Fig. 4. 1D ^{1}H–^{119}Sn (B) U&D and (C) L&R spectra of 0.1 M tributyl(4,5-dihydrofuran-2-yl)stannane, **3**, in $CDCl_3$ acquired with the pulse sequences of Fig. 1A and 1B, respectively. The H5 proton was selectively excited with a 20 ms Gaussian-shaped 180° ^{1}H pulse and the inter-pulse delay and mixing times were optimized to 50 ms and 40 ms, respectively. 32 scans were collected with a relaxation delay of 1 s, giving an experimental time of 1 m 40 s for each 1D spectrum.

compounds (Fig. 2), the information about the sign is not directly available. The relative sign of J(HP) can be quickly ascertained from the relative U&D peak pattern (Fig. 2B) taking the relative up/down phase of the ^3J(HP) connectivity as a reference for positive signs. Although the analysis of the AP structure can also provide the magnitude of J(HX), partial cancellation of multiple lines or the displacement of peak maxima can complicate the measurement and a further fitting peak analysis/simulation can be required to minimize possible errors in the measurement. For the accurate measurement of J values irrespective of multiplet complexity or partial signal cancellation, the use of the refocused L&R method can be most suitable. Fig. 2C shows how the relative L&R displacement becomes a simple, fast and powerful way to directly extract the information of both the magnitude and the sign of J(HP) coupling constants [8].

In a similar way, Fig. 3 shows the fast determination of all proton–fluorine coupling constants, J(HF), in 2-fluoropyridine, **2** [9,10]. It is shown that the effective TOCSY transfer facilitates the straightforward and sensitive determination even for the four- and five-bond proton–fluorine coupling constants in the same experimental time required for a conventional ^{1}H spectrum. Whereas the relative sign can be readily obtained from the U&D multiplet pattern (Fig. 3B), both the magnitude and the sign are obtained from the L&R version (Fig. 3C). The H6 proton can be used as an example to compare the main features of L&R vs. U&D analysis. The small ^4J(H6–F) value causes its AP multiplet presents reduced intensity although that the relative U&D pattern evidences a negative value compared with the reference H3 proton. Note how an accurate value of −1.3 Hz is easily determined from the direct L&R analysis of the pure in-phase α/β multiplets.

Fig. 4 shows the U&D and L&R spectra of an organotin compound, **3**, acquired with gradient coherence selection [11]. Whereas the clean U&D spectrum (Fig. 4B) clearly reveals the opposite sign between the large ^2J(H–Sn) and ^3J(H–Sn) couplings, the additional small J(H–Sn) couplings can make difficult a clear visualization of coupling patterns and the accurate determination of their sizes. The analysis of the L&R multiplet patterns (Fig. 4C) allows and accurate measurement of the tiny ^4J(H–Sn) and ^5J(H–Sn) (<1 Hz) couplings along with their absolute signs. Other examples describing the challenge to measure the sign and the small magnitude of long-range J(H–Se) and J(H–Si) coupling constants in organoseleno [12] and organosilicon [13] compounds, respectively, are available as a Supplementary material (see Figs. S2 and S3 in the Supporting information).

3. Conclusions

In summary, we have proposed an efficient NMR technique for the general and easy determination of both the magnitude and the relative sign of heteronuclear coupling constants in a wide range of conditions and different heteronuclei. The measurement relies in the direct analysis of resulting pure-phase multiplets, without any further data treatment. The U&D method is recommended when short T2 relaxation times are present or when only the sign information is of interest. On the other hand, the inconvenience to manage AP multiplets makes the L&R method highly amenable to measure very small coupling constants even for complex and non-resolved multiplets by considering only the relative signal frequency displacement. 2D versions of the method are also applicable to molecules having many different active heteronuclei (see Figs. S4 and S5 in the Supporting information) and the concept can be extrapolated to measure other type of couplings involving other heteronuclei than ^{1}H for detection.

4. Methods and materials

NMR experiments were recorded on different spectrometers: a BRUKER 600 AVANCE II+ equipped with a 5-mm broadband probehead incorporating a z-gradient coil and a BRUKER AVANCE III 400 MHz spectrometer equipped with a BBFO broadband probehead incorporating a z-gradient coil. The interpulse delay $\Delta' = (\Delta + p_{180°sel}/2) = 1/(4 \times J(XH))$, where the selective 180° ^{1}H pulse ($p_{180°sel}$) with a duration of 20 ms had a Gaussian-shape in all cases. The recycle delay was set at 1 s. Gradient G4 acted as a zz-filter whereas gradients G3 and G5 flanked the inversion proton pulses to generate pure selective refocusing elements. The TOCSY transfer consisted of a z-filtered DIPSI-2 pulse train of duration τ_m (40 ms) with an additional G6 gradient simultaneously applied to a 30 ms adiabatic smoothed *CHIRP* pulse to remove unwanted ZQ contributions. G1 and G2 were used for coherence selection. All data were acquired and processed with the TOPSPIN v2.1 software package.

The test samples used in this work were: 30 mg of allyltriphenylphosphonium bromide dissolved in 0.6 ml of $CDCl_3$, 25 mg of 2-fluoropyridine dissolved in 0.6 ml of $CDCl_3$, and 30 mg of tributyl(4,5-dihydrofuran-2-yl)stannane (3) dissolved in 0.6 ml of $CDCl_3$.

Details for spectra of Fig. 2: 1D ^{1}H–^{31}P zz-selHSQMBC-TOCSY and selHSQMBC-TOCSY-IPAP experiments were recorded at 600 MHz. The interpulse Δ delay was optimized to 8 Hz. 4 scans were accumulated, the number of data points was set to 16,384 and the spectral window was 6009 Hz. The overall acquisition time was 16 s. The acquisition time in t_2 was 1.360 s with a FID resolution of 0.733 Hz.

Details for spectra of Fig. 3: 1D $^{1}H-^{19}F$ zz-selHSQMBC-TOCSY and selHSQMBC-TOCSY-IPAP experiments were recorded at 400 MHz. The interpulse Δ delay was optimized to 8 Hz. 4 scans were accumulated, the number of data points was set to 16,384 and the spectral window was 2000 Hz. The overall acquisition time was 33 s. The acquisition time in t_2 was 4.09 s with a FID resolution of 0.122 Hz.

Details for spectra of Fig. 4: 1D $^{1}H-^{119}Sn$ zz-selHSQMBC-TOCSY and 1D-selHSQMBC-TOCSY-IPAP experiments were recorded at 600 MHz. The interpulse delay was optimized to 10 Hz. 32 scans were accumulated, the number of data points was set to 16,384 and the spectral window was 8417.5 Hz. The overall acquisition time was 1 min, 40 s. The acquisition time in t_2 was 0.487 s with a FID resolution of 2.050 Hz.

All pulse program codes are available from our web server at http://sermn.uab.cat.

Acknowledgments

Financial support for this research provided by MICINN (Project CTQ2012-32436) and Bruker Española S.A. is gratefully acknowledged. We also thank to the Servei de Ressonància Magnètica Nuclear, Universitat Autònoma de Barcelona, for allocating instrument time to this project.

Appendix A. Supplementary material

Supplementary data associated with this article can be found, in the online version, at http://dx.doi.org/10.1016/j.jmr.2013.08.013.

References

[1] (a) R.H. Contreras, J.E. Peralta, Prog. NMR Spectr. 37 (2000) 321;
(b) R.H. Contreras, V. Barone, J.C. Facelli, J.E. Peralta, Ann. Rep. NMR Spectrosc. 51 (2003) 167;
(c) L.B. Krivdin, R.H. Contreras, Ann. Rep. NMR Spectrosc. 61 (2007) 133.
[2] (a) B. Wrackmeyer, E. Kupce, A. Schmidpeter, Magn. Reson. Chem. 29 (1991) 1045;
(b) M.G. Partridge, B.A. Messerle, L.D. Field, Organometallics 14 (1995) 3527;
(c) G. Otting, B.A. Messerle, L.P. Soler, J. Am. Chem. Soc. 119 (1997) 5425;
(d) G. Otting, L.P. Soler, B.A. Messerle, J. Magn. Reson. 137 (1999) 413.
[3] G. Kummerlöwe, B. Luy, Ann. Rep. NMR Spectrosc. 68 (2009) 193.
[4] (a) I.D. Rae, J.A. Weigold, R.H. Contreras, R.R. Biekofsky, Magn. Reson. Chem. 31 (1993) 836;
(b) M. Pietrzak, H.H. Limbach, M.P. Torralba, D. Sanz, R.M. Claramunt, J. Elguero, Magn. Reson. Chem. 39 (2001) 5100;
(c) I. Alkorta, J. Elguero, H.H. Limbach, I.G. Shenderovich, T. Winkler, Magn. Reson. Chem. 47 (2009) 585.
[5] S. Gil, J.F. Espinosa, T. Parella, J. Magn. Reson. 213 (2011) 145.
[6] J. Saurí, T. Parella, Magn. Reson. Chem. 50 (2012) 717.
[7] J. Saurí, J.F. Espinosa, T. Parella, Angew. Chem. Int. Ed. 51 (2012) 3919.
[8] (a) V. Sklenar, A. Bax, J. Am. Chem. Soc. 109 (1987) 1525;
(b) N. Bampos, L.D. Field, B. Messerle, Organometallics 12 (1993) 2529;
(c) W.H. Hersh, S.T. Lam, D.J. Moskovic, A.J. Panagiotakis, J. Org. Chem. 77 (2012) 4968;
(d) G.M. Clore, E.C. Murphy, A.M. Gronenborn, A. Bax, J. Magn. Reson. 134 (1998) 164;
(e) T. Carlomagno, M. Hennig, J.R. Williamson, J. Biomol. NMR 22 (2002) 65.
[9] (a) Y.G. Gakh, A.A. Gakh, A.M. Gronenborn, Magn. Reson. Chem. 38 (2000) 551;
(b) J. Battiste, R.A. Newmark, Prog. NMR Spectr. 48 (2006) 1;
(c) W.R. Dolbier Jr., Guide to Fluorine NMR for Organic Chemists, Wiley, 2009.
[10] (a) M. Hennig, M.L. Munzarova, W. Bermel, L.G. Scott, V. Sklenar, J.R. Williamson, J. Am. Chem. Soc. 128 (2006) 5851;
(b) B. Luy, J.J. Barchi Jr., J.P. Marino, J. Magn. Reson. 152 (2001) 179;
(c) B. Luy, J.P. Marino, J. Biomol. NMR 20 (2001) 39.
[11] J.C. Martins, M. Biesemans, R. Willem, Prog. NMR Spectr. 36 (2000) 271.
[12] (a) K.E. Kövér, A.A. Kumar, Y.Yu. Rusakov, L.B. Krivdin, T.Z. Illyés, L. Szilágyi, Magn. Reson. Chem. 49 (2011) 190;
(b) Y.Yu. Rusakov, L.B. Krivdin, A.A. Kumar, L. Szilágyi, K.E. Kövér, Magn. Reson. Chem. 50 (2012) 488.
[13] (a) J. Ambati, S.E. Rankin, J. Phys. Chem. A. 114 (2010) 12613;
(b) Y.Yu. Rusakov, L.B. Krivdin, V.M. Nosova, A.V. Kisin, V.G. Lakhtin, Magn. Reson. Chem. 50 (2012) 665.

Efficient and fast sign-sensitive determination of heteronuclear coupling constants

Josep Saurí, Pau Nolis and Teodor Parella*

Supporting Information

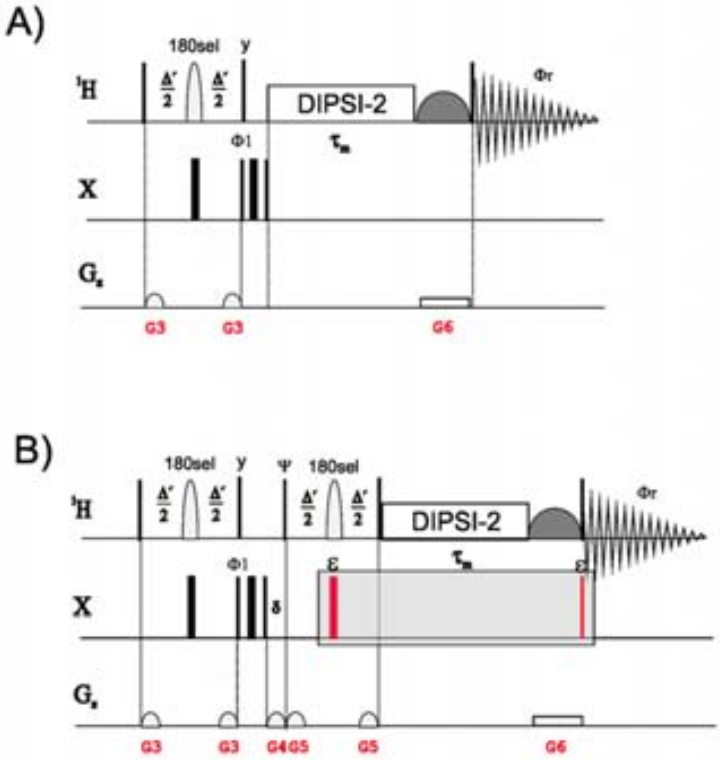

Figure S1: 1D versions of the A) U&D and B) L&R ^{1}H-X selHSQMBC-TOCSY experiments without gradient coherence selection. All experimental details are exactly the same as described in the original sequences described in Fig. 1, except that the G1 and G2 gradients and their related delays have been removed.

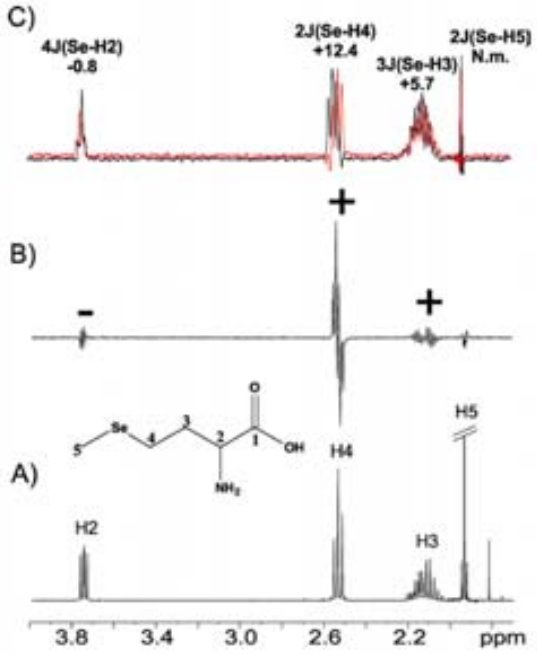

Figure S2: 1D ^{1}H-^{77}Se B) U&D and C) L&R spectra of 0.1M selenomethionine (4) in D_2O acquired with the pulse sequences of Fig. 1A and 1B, respectively. The H4 proton was selectively excited with a 20ms Gaussian-Shaped 180° ^{1}H pulse and the inter-pulse delays (Δ') and mixing time (τ_m) were optimized to 50ms and 40ms, respectively. 128 scans were collected with a relaxation delay of 1s, giving an experimental time of 10 minutes for each 1D spectrum.

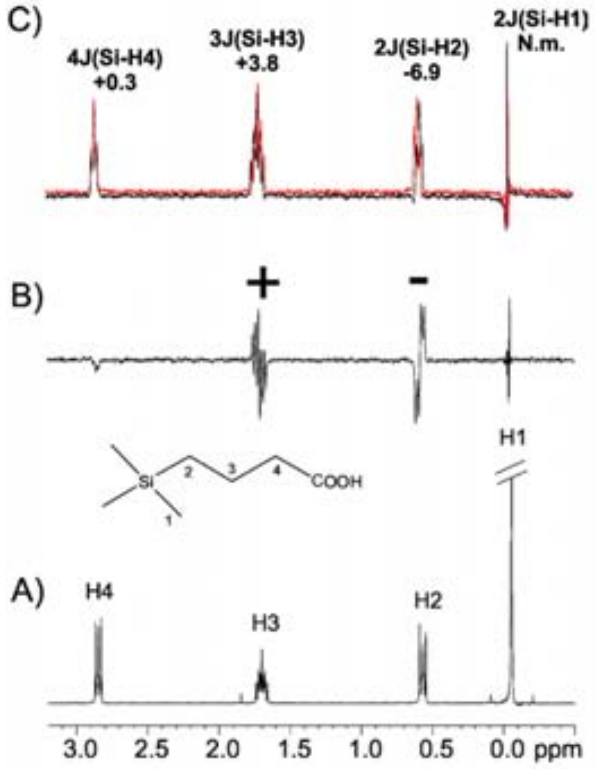

Figure S3: 1D ^{1}H-^{29}Si A) U&D and B) L&R spectra of 20mg of DSS in 0.5ml D_2O acquired with the pulse sequences of Fig. 1A and 1B, respectively. The H2 proton was selectively excited with a 20ms Gaussian-Shaped 180° ^{1}H pulse and the inter-pulse delays (Δ') and mixing time (τ_m) were optimized to 42ms and 40ms, respectively. 64 scans were collected with a relaxation delay of 1s, giving an experimental time of 3min 30s for each 1D spectrum.

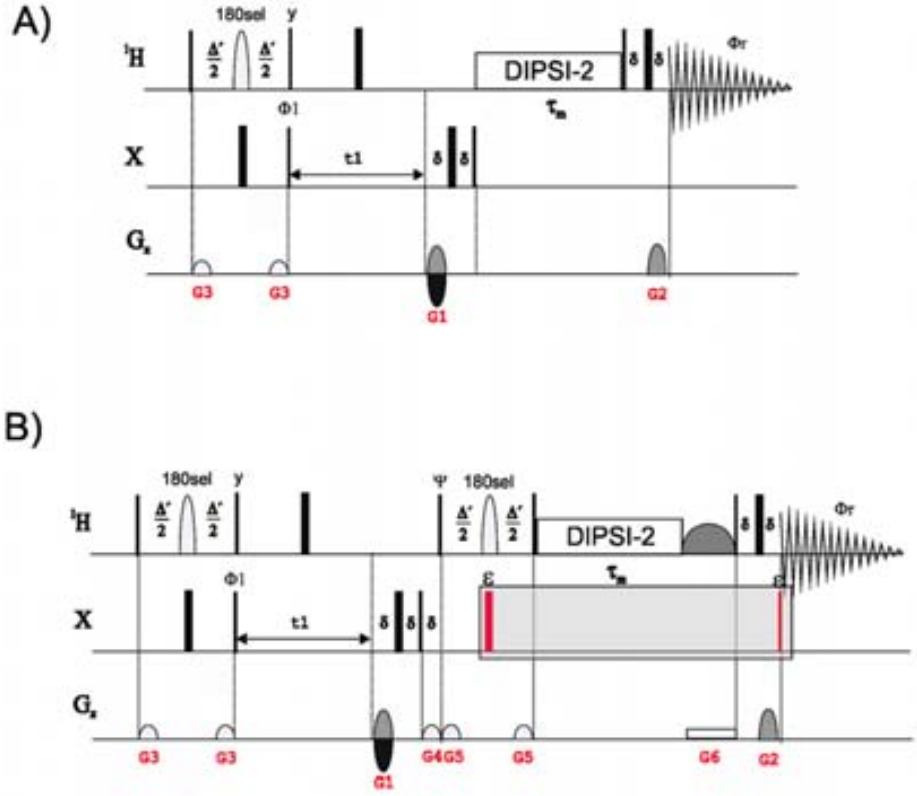

Figure S4: 2D versions of the A) U&D and B) L&R ^{1}H-X HSQMBC-TOCSY experiments with gradient coherence selection using the echo-anti/echo protocol. All experimental parameters are exactly the same are optimized as described for the 1D versions.

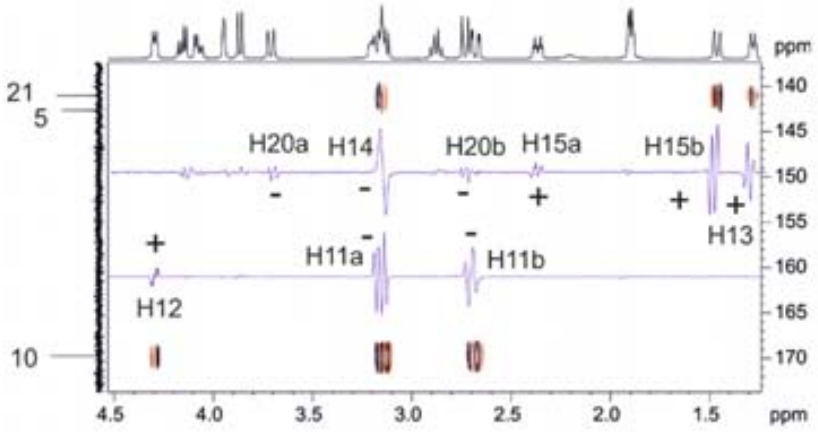

Figure S5: Expanded area of the 2D ^{1}H-^{13}C U&D spectra of a sample of 0.1M strychnine dissolved in $CDCl_3$. The pulse sequence of Fig. S4A was applied with a 40ms Gaussian-shaped 180 ^{1}H pulse applied on protons (H14, H11a and H18a) resonating at 3.15ppm. The experiment was optimized to 8 Hz. 1D slices taken at the chemical shift of the quaternary C10 and C21 carbons are shown to illustrate the relative up/down relative phase of each individual cross-peak. 4 scans for each one of the 128 t_1 increments were collected giving an experimental time of 10 min.

PUBLICATION 5

On the interference of J(HH) modulation in HSQMBC-IPAP and HMBC-IPAP experiments

J. Saurí, T. Parella. *Magn. Reson. Chem*. 2013, 51, 509–516

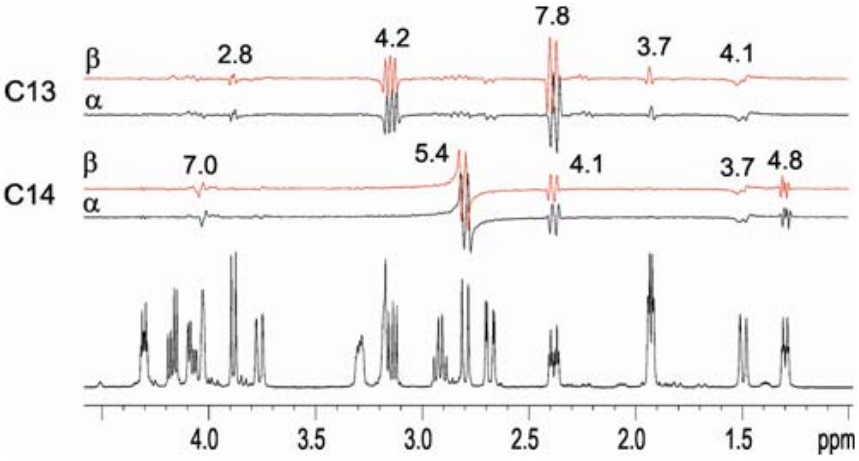

1. Introduction

In this publication, the effects of J(HH) modulation into the phase multiplet pattern of cross-peaks obtained in HSQMBC-like and HMBC-like pulse sequences are evaluated. It is shown how the IPAP methodology is able to equally preserves the undesired effects of J(HH) evolution in α- and β- selHSQMBC spectra, because the distorted cross-peaks obtained in both IP and AP data are equivalent[1]. J(HH) modulation effects are first tested by simultaneously inversion of two mutually coupled protons, and then the IPAP methodology is implemented into broadband versions of the regular HSQMBC and HMBC experiments in order to extrapolate the obtained results for the entire proton signals.

It is also shown how, with a slightly modification in the pulse schemes, an hybrid HMBC-COSY experiment can be easily designed, becoming a good complementary tool to the analogue HMBC counterpart, with the aim to obtain new cross-peaks that might be missing in the regular HMBC experiment due to the intensity dependence with respect to the magnitude of $^{n}J(CH)$ value. Such strategy is also performed for a broadband version of the HSQMBC pulse sequence. One the other hand, an assessment on the J cross-talk effects using the IPAP methodology is also presented.

The main goal of this publication was to design NMR methodologies for the measurement of heteronuclear coupling constants that could work in a broadband manner, avoiding thus the use of selective pulses and reducing spectrometer time. In addition, the proposed methods can be recorded with minimum set-up calibration under full automation conditions.

[1] See Publication 3 in this thesis work

Research Article

Magnetic Resonance in Chemistry

Received: 23 January 2013 Revised: 22 March 2013 Accepted: 19 May 2013 Published online in Wiley Online Library: 18 June 2013

(wileyonlinelibrary.com) DOI 10.1002/mrc.3977

On the interference of *J*(HH) modulation in HSQMBC-IPAP and HMBC-IPAP experiments

Josep Saurí and Teodor Parella*

The effects of phase modulation due to homonuclear proton–proton coupling constants in HSQMBC-IPAP and HMBC-IPAP experiments are experimentally evaluated. We show that accurate values of small proton–carbon coupling constants, $^nJ_{CH}$, can be extracted even for phase-distorted cross-peaks obtained from a selHSQMBC experiment applied simultaneously on two mutually *J*-coupled protons. On the other hand, an assessment of the reliability of $^nJ_{CH}$ measurement from distorted cross-peaks obtained in broadband IPAP versions of equivalent HMBC and HSQMBC experiments is also presented. Finally, we show that HMBC-COSY experiments could be an excellent complement to HMBC for the measurement of small $^nJ_{CH}$ values.

Keywords: selHSQMBC; proton–carbon coupling constants; HSQMBC; HMBC; IPAP

Introduction

It is known that the evolution of homonuclear proton–proton coupling constants (J_{HH}) during the long defocusing/refocusing periods in long-range heteronuclear correlation experiments, commonly referred as HMBC[1–3] or HSQMBC[4] experiments, causes important intensity and phase signal modulation effects. The resulting complex cross-peak shapes generally make difficult a simple data analysis that often prevents an accurate and direct extraction of small proton–carbon coupling constant values ($^nJ_{CH}$; $n > 1$). Several approaches have been proposed to solve it. The first is post-processing techniques trying the optimal matching between experimental and simulated shapes using a fitting procedure from a reference cross-peak.[2–4] This solution has been widely applied, but it strongly depends on the perfect complementarity between the reference and the experimental signals to be fitted. Other proposals are based on modified pulse sequences with the aim to minimize or avoid the unwanted evolution of J_{HH}. Improved HSQMBC experiments based on the use of simultaneous CPMG-XY16 pulse trains in both ^{1}H and ^{13}C channels have been proposed, but it has also recognized some associated inconvenience such as sample heating, offset dependence and imperfect removing of J_{HH} effects under strong coupling conditions.[5–7] A simpler approach should be the use of selective 180° ^{1}H pulses to prevent any J_{HH} evolution,[8] with the EXSIDE[9] and selHSQMBC[10] experiments being two powerful examples of this class of selective experiments for the straightforward measurement of $^nJ_{CH}$.

On the other hand, it has been shown that the incorporation of the IPAP principle in HSQMBC experiments affords a powerful technique for the measurement of $^nJ_{CH}$ with simplicity and accuracy from the analysis of the relative displacement between two separate α/β components.[10–14] In particular, the referred 2D selHSQMBC experiment has been proposed for the fast and direct measurement of $^nJ_{CH}$ coupling values from pure absorption phase multiplets along the detected F2 dimension.[10] A broadband HSQMBC-IPAP version was also proposed, where $^nJ_{CH}$ could be extracted from distorted cross-peaks and independent of their complexities.[12,13]

In this work, the effects of phase modulation due to J_{HH} in HSQMBC-IPAP experiments are experimentally evaluated. We want to clarify if $^nJ_{CH}$ can be efficiently measured from the resulting phase-distorted cross-peaks of a selHSQMBC experiment applied simultaneously on two mutually *J*-coupled protons. On the other hand, we want to extrapolate these rules in the evaluation of distorted cross-peaks obtained from broadband IPAP versions of equivalent HMBC and HSQMBC pulse trains. Finally, a discussion on the usefulness of complementary HMBC-COSY and HSQMBC-COSY experiments is made in order to detect and quantify $^nJ_{CH}$ in a variety of conditions and especially when some expected cross-peaks are absent in original HMBC/HSQMBC spectra.

Results and Discussion

The pulse sequence of the 2D selHSQMBC experiment is basically a refocused long-range optimized HSQC experiment where the central 180° ^{1}H pulses were applied on a single ^{1}H resonance to avoid any interference from other J_{HH} coupling constants.[10] The IPAP methodology is based on the acquisition of two separate in-phase (IP) and anti-phase (AP) data resulting from the evolution/no evolution of $^nJ_{CH}$ during the last refocusing period. In principle, for a fixed Δ delay optimization, it would not be possible to obtain a perfect signal refocusing in IP experiments for the complete range of existing $^nJ_{CH}$ values. Thus, for an isolated long-range coupled C_1–H_2 two-spin system, a mixture of IP and AP magnetization components is obtained after the last refocusing INEPT period that usually would result in mixed-phase cross-peaks:

* *Correspondence to: Teodor Parella, Servei de Ressonància Magnètica Nuclear, Universitat Autònoma de Barcelona, E-08193, Bellaterra, Catalonia, Spain. E-mail: teodor.parella@uab.cat*

Servei de Ressonància Magnètica Nuclear, Universitat Autònoma de Barcelona, E-08193, Bellaterra, Catalonia, Spain

$$2H_xC_z\sin(\pi^nJ_{CH}\Delta) \rightarrow 2H_xC_z\sin(\pi^nJ_{CH}\Delta)*\cos(\pi^nJ_{CH}\Delta) + H_y\sin^2(\pi^nJ_{CH}\Delta) \quad (1)$$

In the original selHSQMBC experiment,[10] the unwanted AP H_xC_z contribution was removed by converting it into non-detectable H_zC_z magnetization using a 90° ^{1}H pulse applied from the *y*-axis:

$$\rightarrow 2H_zC_z\sin(\pi^nJ_{CH}\Delta)*\cos(\pi^nJ_{CH}\Delta) + H_y\sin^2(\pi^nJ_{CH}\Delta) \quad (2)$$

However, this last 90° ^{1}H pulse could provide ^{1}H–^{1}H COSY transfer if some J_{HH} modulation is present, as reported in the analogous selHSQMBC-COSY experiment.[14] An equivalent way to achieve this same goal that lead to the same experimental results when applied to an isolated ^{1}H resonance is shown in Fig. 1(A). A 90° ^{13}C pulse is applied prior to acquisition to convert the AP contribution to non-detectable multiple-quantum coherences:

$$\rightarrow 2H_xC_y\sin(\pi^nJ_{CH}\Delta)*\cos(\pi^nJ_{CH}\Delta) + H_y\sin^2(\pi^nJ_{CH}\Delta) \quad (3)$$

The complementary AP data are recorded in the same way as reported previously (by omitting the last 90° and 180° ^{13}C pulses marked with ε in Fig. 1), and signal intensity will present a sin $(\pi^nJ_{CH}\Delta)$ intensity dependence. One preliminary experimental

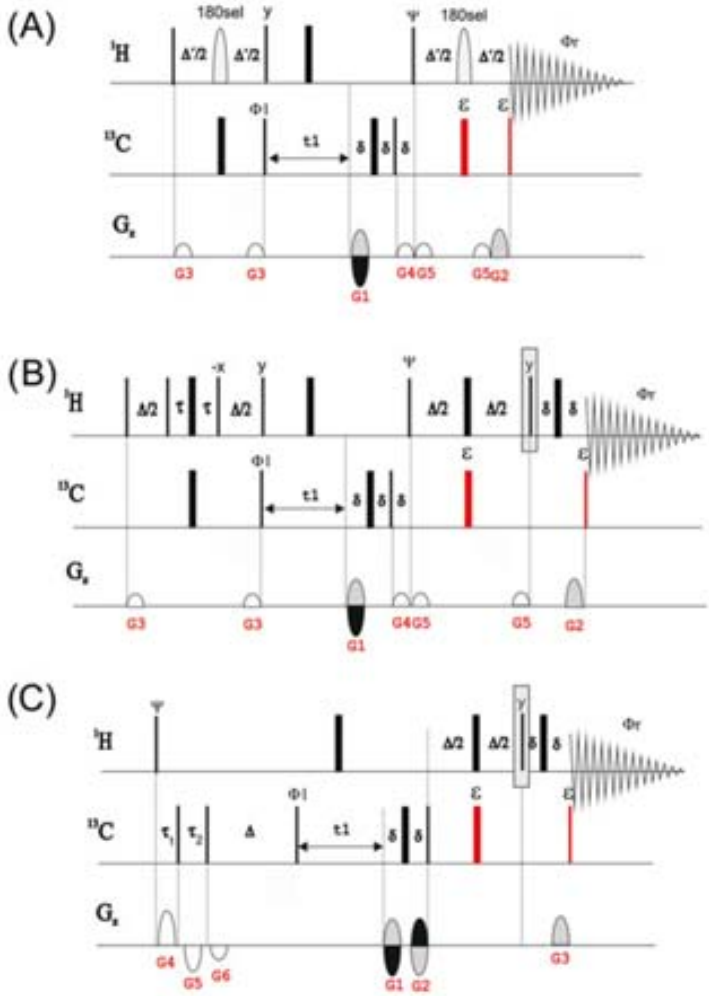

Figure 1. Pulse sequences for the IPAP versions of the 2D (A) selHSQMBC, (B) broadband HSQMBC and HSQMBC-COSY and (C) broadband HMBC and HMBC-COSY experiments. Rectangular 90° and 180° pulses are indicated by thin and thick black bars, respectively, and ^{1}H-selective 180° pulses as shaped bars. Phases are indicated above the pulses (where no phase is given, the pulse is applied along *x*). The basic phase cycle was Φ_1: *x*,−*x*; Φ_{rec}: *x*,−*x*. In-phase (IP: $\Psi = y$, ε = on) and anti-phase (AP: $\Psi = x$, ε = off) data are recorded separately and combined in the time-domain (AP ± IP) to provide α/β spectra. The interpulse delays are set to $\Delta = \Delta' + p_{180} = 1/(2^{*n}J_{CH})$, where p_{180} is the duration of the selective 180° ^{1}H pulse. In (B), a BIRD element is inserted during the initial INEPT period to suppress direct $^1J_{CH}$ correlations ($\tau = 1/(2^{*1}J_{CH})$). In (C), direct correlations are attenuated by a two-step low-pass filter (τ_1 and τ_2) optimized as described in Ref. [15]. The optional 90° ^{1}H pulse inserted into a box in (B) and (C) stands for the obtention of COSY-like spectra.

condition established for an optimal performance of the selHSQMBC experiment was that when multiple protons were excited, they must not be mutually coupled in order to avoid any J_{HH} evolution that would generate phase-distorted multiplets. First, we have used the pulse sequence of Fig. 1(A) to study the practical effects associated with the J_{HH} evolution on $^{n}J_{CH}$ measurements when two *J*-mutually coupled protons are simultaneously excited by the selective 180° ^{1}H pulse. Figure 2 (A) and (B) shows the separate selHSQMBC-IPAP spectra after individual selection of the geminal H15a and H15b protons in strychnine (1), respectively. Importantly, all observed cross-peaks present excellent pure phase multiplets from which a very accurate measurement of $^{n}J_{CH}$ along the F2 dimension can be easily made. As a comparison, Fig. 2(C) shows that the simultaneous selection of both signals using a shifted laminar pulse in a single selHSQMBC experiment produce the same results in terms of sensitivity and performance. Logically, the evolution of their large mutual coupling ($^{2}J_{H15a-H15b}$ = 14.5 Hz) generates distorted phase cross-peaks. Thus, considering a three-spin system giving a long-range cross-peak H2–C1 ($^{n}J_{C1-H2}$) and where the H2 proton is also coupled to a third H3 proton spin with J_{H2-H3}, the cross-peak intensity in IP-selHSQMBC and AP-selHSQMBC data will depend basically on Eqns (4a) and (4b), respectively:

$$H_{2y}\sin^2(\pi^{n}J_{C1-H2}\Delta)*\cos^2(\pi J_{H2-H3}\Delta) + 2H_{2x}H_{3z}\sin^2(\pi^{n}J_{C1-H2}\Delta)\cos(\pi J_{H2-H3}\Delta)*\sin(\pi J_{H2-H3}\Delta) \quad (4a)$$

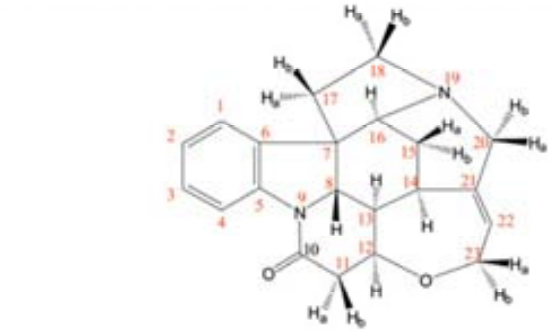

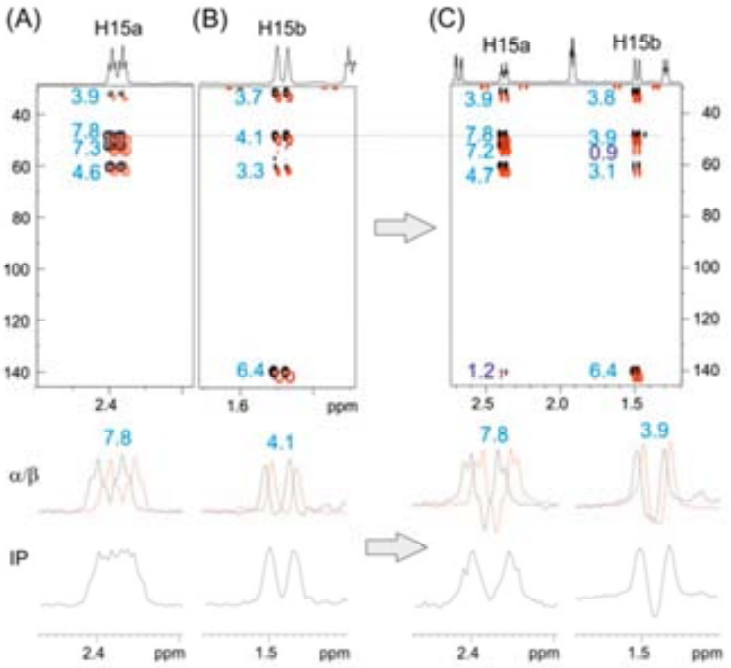

Figure 2. Effect of J_{HH} modulation in selHSQMBC experiments: (A,B) single-frequency excitation and (C) simultaneous dual-site excitation of H15a and H15b proton resonances in strychnine. Below each 2D spectrum appears 1D traces taken at the C13 carbon frequency. Whereas pure-phase IP and α/β components are obtained in (A) and (B), distorted multiplets are obtained in (C) due to the evolution of its mutual J_{HH}. Even so, the extraction on $^{n}J_{CH}$ can be made for these distorted α/β cross-peaks and with the same accuracy than the original one-site spectra.

$$H_{2y}C_z\sin(\pi^nJ_{C1-H2}\Delta)*\cos^2(\pi J_{H2-H3}\Delta) + 2H_{2x}H_{3z}C_z\sin(\pi^nJ_{C1-H2}\Delta)\cos(\pi J_{H2-H3}\Delta)*\sin(\pi J_{H2-H3}\Delta) \quad (4b)$$

Although both IP and AP signals contain an additional mixture of in-phase and anti-phase contributions from the homonuclear J_{HH} coupling, the α/β cross-peaks resulting from the IP ± AP combination will present the same relative shift displacement as found in the separate experiments, and therefore, the extraction of $^nJ_{CH}$ coupling values will be equally feasible showing a strong agreement with the values extracted from individual spectra. The main explanation for such an observation is that IP and AP data only differ in the eventual application of ^{13}C pulses, and this does not produce a differential J_{HH} modulation between them. Thus, IP and AP data will present the same multiplet structure and phase with respect to J_{HH} and the resulting α/β multiplets will retain equivalent J_{HH} distortions that will allow a reliable comparison.

Figure 3 shows a practical example of band-selective HSQMBC-IPAP experiment when only all resonances appearing at the region between 3.7 and 4.4 ppm are simultaneously refocused. $^nJ_{CH}$ values up to six different signals can be extracted from this single NMR experiment acquired in the same experimental conditions and overall acquisition time as described in the spectra of Fig. 2. Whereas pure phase multiplets are obtained for the non-mutually coupled H20a, H8, H16 and H12 protons, distorted cross-peaks are obtained for the geminal H23a/H23b pair that forms a two-spin AB spin system with a mutual coupling of $^2J_{H23a-H23b} = 13.8$ Hz. As shown from the 1D traces and despite these phase distortions, the magnitude of $^nJ_{CH}$ can be equally extracted by matching the relative α/β displacement.

A broadband version of the 2D HSQMBC-IPAP experiment where the effects of J_{HH} were more pronounced was also reported.[12,13] As discussed earlier for the selective version, the sequence proposed in Ref. [13] used a last 90°(y) ^1H pulse to remove AP contributions due to $^nJ_{CH}$ in the IP data. Strictly speaking, this proposed sequence was an HSQMBC-COSY experiment because this pulse also acts as a homonuclear ^1H–^1H COSY transfer. Here, the possibilities of this experiment are revisited by proposing IPAP versions of the HSQMBC and HSQMBC-COSY experiments (Fig. 1(B)). In addition, new pulse schemes for analog HMBC and HMBC-COSY experiments are also described (Fig. 1(C)). Specifically, the only difference between HSQMBC/HMBC and the relayed COSY counterparts rely in the application of the last 90° ^1H pulse from the *y*-axis, whereas all other experimental details remain exactly the same.

As described in Eqns (4a) and (4b), the intensity of a H2–C1 cross-peak in HSQMBC or HMBC experiments will depend basically on its $^nJ_{C1-H2}$ value. Otherwise, if a final 90$_y$(^1H) pulse is applied, COSY transfer between the two protons can be accomplished if AP J_{HH} components are available. Thus, the intensity and phase of a theoretical H2–C1 cross-peak in IP-HSQMBC-COSY experiments will depend on the additive $^nJ_{C1-H2}$ and $^nJ_{C1-H3}$ coupling mechanisms:

$$\rightarrow H_{2y}\sin^2(\pi^nJ_{C1-H2}\Delta)*\cos^2(\pi J_{H2-H3}\Delta) + 2H_{2x}H_{3z}\sin^2(\pi^nJ_{C1-H3}\Delta)*\cos(\pi J_{H2-H3}\Delta)\sin(\pi J_{H2-H3}\Delta) \quad (5)$$

The complementarity between these two approaches is based on the fact that whereas the intensity of a H2–C1 cross-peak in the HSQMBC experiment basically depends on the $\sin^2(\pi^nJ_{C1-H2}\Delta)$ function, some missing cross-peaks can become observable in HSQMBC-COSY spectra even when $^nJ_{C1-H2}$ values are close to 0. As in HSQMBC, the same main conclusions can be extracted when analyzing the analog HMBC counterpart, where the main difference relies in the additional evolution of J_{HH} during the variable t_1 period. The evolution of multiple-quantum coherences introduces additional distortions into multiplet shapes in both F2 and F1 dimensions although, in practice, this does not affect the $^nJ_{CH}$ measurement via the IPAP principle.

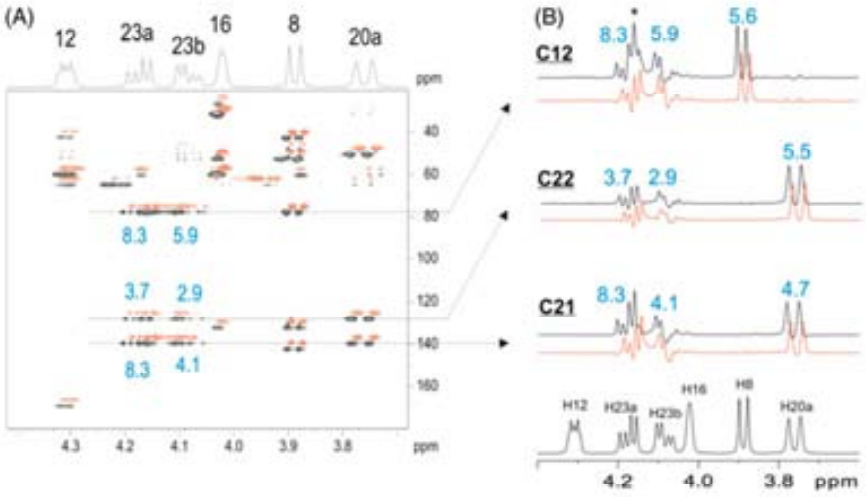

Figure 3. (A) 2D selHSQMBC-IPAP spectra after selective refocusing (with a 12-ms REBURP 180° ^1H pulse) of the region centered at 4.0 ppm comprising six different resonances; (B) corresponding 1D slices taken at the C12, C22 and C21 carbon chemical shifts of α/β selHSQMBC spectra. The optimal fitting between relative shifted α/β cross-peaks allows the measurement of $^nJ_{CH}$ independently of the phase distortion and multiplet complexity. The mark * stands for the residual $^1J_{CH}$ satellite signal arising from H12 proton.

Figure 4 shows the IP spectrum of the 2D broadband HMBC and HMBC-COSY spectra of **1** acquired with the pulse schemes described in Fig. 1(C). Basically, we can observe that some cross-peaks are present in only one of the two spectra. As discussed before, the evolution of all J_{HH} produces high distorted multiplets that prevent a direct multiplet analysis. However, the application of the IPAP principle yields two complementary IP and AP data that after linear time-domain data combination (AP ± IP) followed by conventional processing afford two equally distorted α/β multiplets that can be directly analyzed. Figure 5 shows several 1D traces extracted from different carbon frequencies in the spectra of Fig. 4(A) to demonstrate that $^{n}J_{CH}$ can be efficiently determined in a variety of situations, for different multiplet complexities and for a wide range of $^{n}J_{CH}$ values provided that the peak is observed with reasonable sensitivity. Figure 6 shows an expanded area corresponding to the H15a proton, where five different correlations can be visualized in the IP and AP spectra. Note that independent of the degree of distortion and multiplet complexity, $^{n}J_{CH}$ coupling values in the range of 3–8 Hz can be easily extracted by comparing the relative shift displacement between α/β multiplets in an 8-Hz optimized experiment.

The percentage of cross-talk obtained from the IPAP procedure follows the same general $[\sin(\pi\,^{n}J_{CH}\Delta) - 1]/[\sin(\pi\,^{n}J_{CH}\Delta) + 1]$ dependence as described earlier.[13] In practical terms, this percentage is not affected by the presence of J_{HH} modulation, and reliable measurement of $^{n}J_{CH}$ can be made over a wide range of values. For instance, for a typical 8-Hz optimized experiment (Δ = 62.5 ms), the normalized intensity (and percent of cross-talk) of an isolated CH cross-peak having a coupling of $^{n}J_{CH}$ = 8 Hz (cross-talk = 0%) should be theoretically 1 in comparison with 0.3 for a cross-peak with $^{n}J_{CH}$ = 3 Hz (cross-talk = 28%). This relatively high level of cross-talk percentage is not an impediment for a reliable measurement as shown, for instance, for the 3.3 Hz value measured experimentally from the tiny H15a–C12 cross-peak that is in good agreement with the measurement made from pure-phase α/β selHSQMBC multiplets. In practice, the major hindrance to experimentally measure a coupling of 3 Hz is the very low sensitivity of the corresponding cross-peak. The theoretical relative intensity of two peaks with $^{n}J_{CH}$ = 8 and 3 Hz on a 6-Hz optimized experiment (Δ = 83.3 ms) should be 0.75 (7% cross-talk) and 0.5 (17% cross-talk), respectively, providing a more average behavior in terms of sensitivity and cross-talk over the complete range between 3 and 9 Hz. Very importantly, J_{HH} modulation can severely affect the intensity of cross-peak, and this can prevent some measurements. For instance, a signal having a large $^{n}J_{CH}$ = 8 Hz and a single homonuclear coupling of J_{HH} = 8 Hz would give a null intensity in an 8-Hz optimized experiment. For this reason, sometimes the acquisition of an additional experiment optimized to another $^{n}J_{CH}$ value can be helpful to enhance the observation of tiny or missing cross-peaks provided that the use of longer periods do not affect the overall sensitivity by the major effects on T_2 relaxation.

An alternative to record a second different optimized experiment should be to take profit of the excellent complementarity between HMBC and HMBC-COSY experiments (Fig. 4(A) vs (B)), as clearly demonstrated for the different correlations observed for the H13 proton (Fig. 7). Four cross-peaks are clearly visible and quantifiable in the HMBC-IPAP spectra. They correspond to two ^{2}J and two ^{3}J connectivities showing large J values because of their sine function intensity dependence. On the other hand, the HMBC-COSY-IPAP spectra afforded five different correlations, all showing similar coupling pattern shape. These missed correlations in HMBC corresponding to one ^{2}J, two ^{3}J and two ^{4}J connectivities are due to the additive $^{n}J_{CH} + J_{HH}$ transfer mechanism. It is very important to highlight that accurate determination of very small $^{n}J_{CH}$ values, even smaller than the line width, is possible, thanks to the IPAP approach. As pointed before, the intensity of

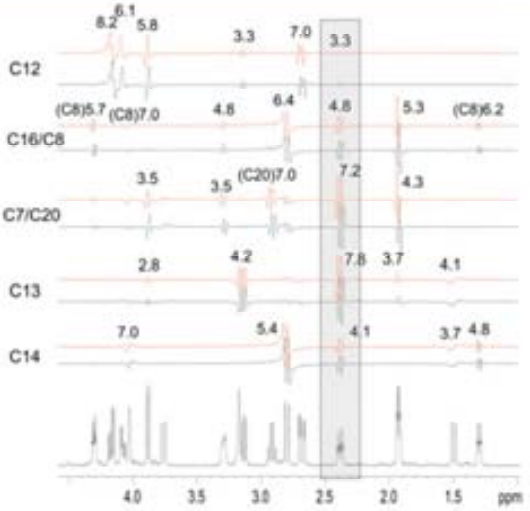

Figure 5. Selected 1D slices extracted from different carbon frequencies in the HMBC-IPAP (Fig. 4(A)). Note that, in general, a global extraction of $^{n}J_{CH}$ values can be made for all cross-peaks showing optimum signal-to-noise ratio, independent of their complexity. The marked box covers the multiplets presented in Fig. 6.

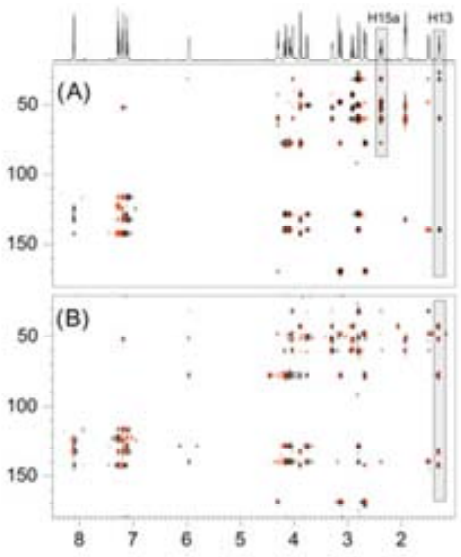

Figure 4. (A) HMBC and (B) HMBC-COSY spectra of **1** acquired using pulse scheme of Fig. 1(C) (without and with the last 90° ^{1}H pulse, respectively). Only the refocused IP data, optimized to 8 Hz, are displayed to visualize the presence of different cross-peaks in both spectra. Highlighted boxes are discussed in more detail in Figs. 5, 6 and 7.

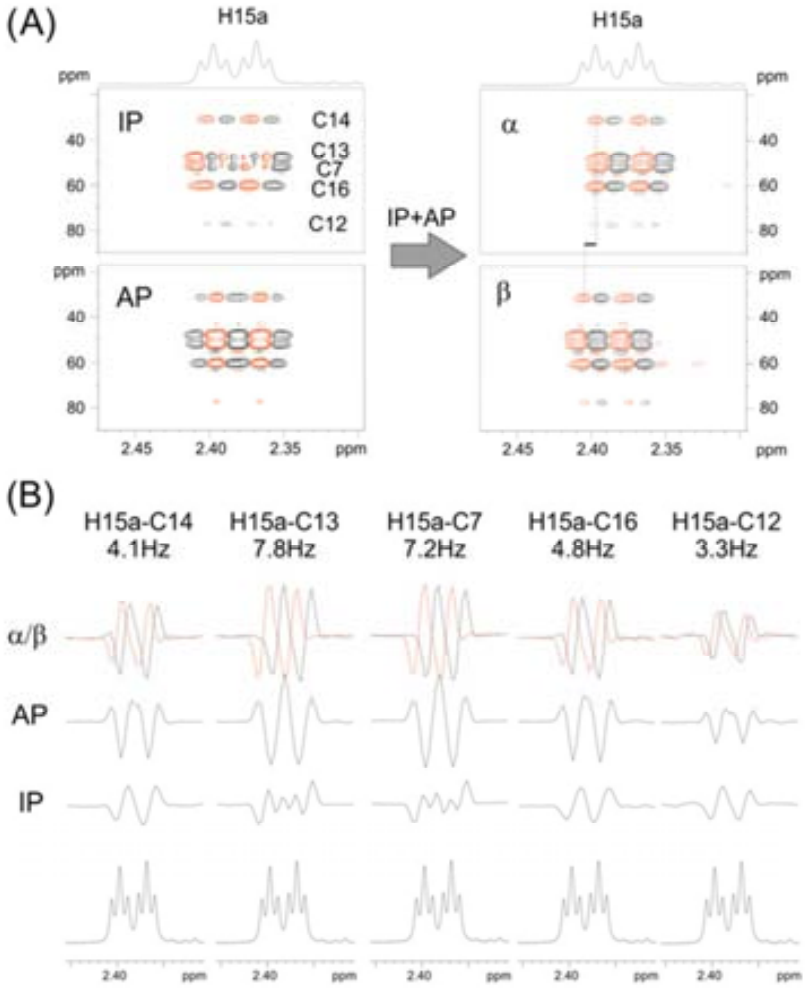

Figure 6. (A) Expanded 2D areas corresponding to the H15a proton in IP/AP and α/β HMBC spectra, and (B) 1D phase-twisted cross-peaks taken at different five carbon frequencies. Despite IP and AP data are too difficult to try a simple multiplet analysis, the relative displacement along the F2 dimension between α/β multiplets allows a direct, fast, simple and accurate measurement of $^{n}J_{CH}$. Note that all coupling constant values fall within the range 3–8 Hz, and they can be measured without the presence of pronounced cross-talking.

these COSY H13–C_x cross-peaks does not depend on its direct $^{n}J_{H13Cx}$ coupling but on the additive J_{HBCx} and $^{3}J_{HB-H13}$ (equal to 10.5 Hz) coupling pathway. Note that from the combined information of these two spectra, a total of nine different correlations are observed and efficiently quantified although the method is not sign sensitive. The concerted use of HMBC and HMBC-COSY experiments can be a reliable alternative to other proposed approaches such as the use of different delay-optimized experiments[15,16] or the use of accordion spectroscopy.[17–21]

Figure 8 compares the different relative sensitivity of the HMBC/HMBC-COSY with that of HSQMBC/HSQMBC-COSY experiments. In general, it can be stated that HMBC spectra showed a slightly better general sensitivity than HSQMBC spectra. In addition, we can say that both approaches show similar complementarity, and the measured $^{n}J_{CH}$ values are in good agreement between them. However, the intensity and phase distortions for each individual cross-peak will depend on the different J_{HH} modulation, and they will show a different partial signal cancellation due to AP contributions in HMBC-like and HSQMBC-like experiments.

In summary, it has been shown that the phase distortion caused by J_{HH} modulation in selHSQMBC experiments is not a serious impediment for their successful performance on mutually coupled protons. This reinforces its applicability because a single selHSQMBC experiment is not exclusively limited to a single ^{1}H resonance. This particularity makes the selHSQMBC far superior to the analog EXSIDE experiment where the absence of mutual J_{HH} is a requirement when multiple protons are excited. It has been shown that the IPAP technique can be successfully applied in both selective and non-selective versions, providing two equally distorted spin-state selective multiplets from which $^{n}J_{CH}$ can be made measured along the F2 dimension irrespective of multiplet complexity and phase distortion. In addition, broadband HMBC-COSY (or HSQMBC-COSY) experiment proves to be

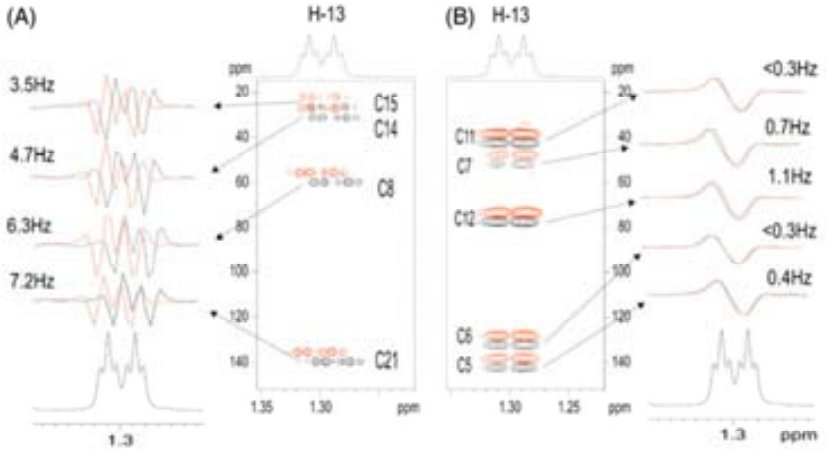

Figure 7. 2D expanded areas demonstrating the excellent complementarity between (A) 2D HMBC-IPAP and (B) 2D HMBC-COSY-IPAP experiments. Whereas in HMBC, only the largest couplings from the H13 proton are observed and measured, very small $^{n}J_{CH}$ values can be extracted in the analog HMBC-COSY spectra because cross-peak intensities depend on the additional COSY J_{HH} transfer and not for the direct $^{n}J_{CH}$ coupling. The excellent resolution achieved in the detected dimension allows the extraction of $^{n}J_{CH}$ values smaller than line width.

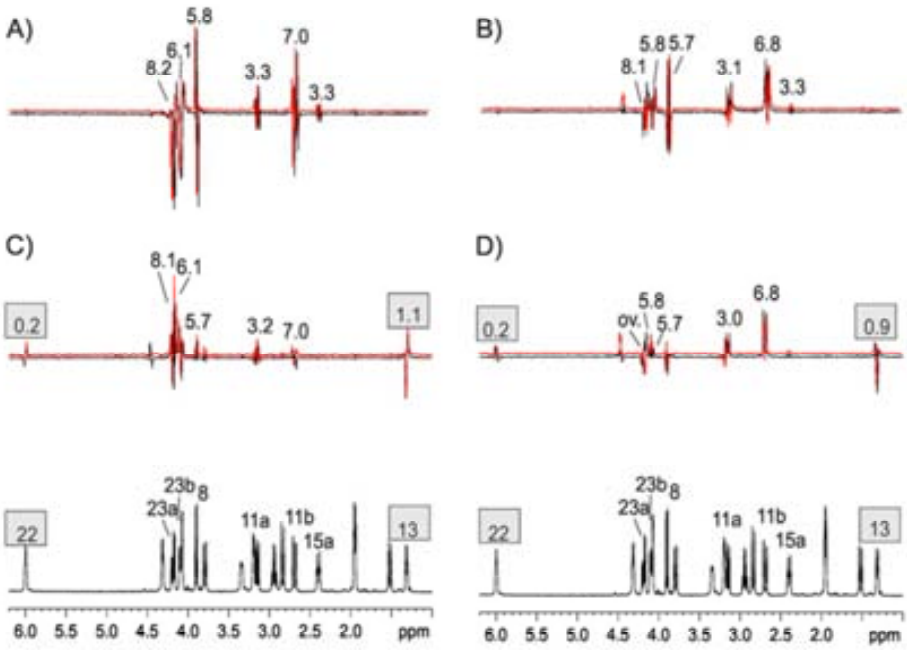

Figure 8. Comparison of the same 1D slice taken at C12 chemical shift in (A) HMBC, (B) HSQMBC, (C) HMBC-COSY and (D) HSQMBC-COSY IPAP experiments. Note that reliable $^{n}J_{CH}$ values can be measured for all cross-peaks presenting good sensitivity.

a helpful complementary tool to the conventional HMBC (or HSQMBC) experiment because it can highlight some low-intensity and/or missing cross-peaks. The only difference between both approaches relies in the single application of a final 90° ^{1}H pulse, and this does not mean an additional penalty on global sensitivity or additional set-up. The concerted use of HMBC/HMBC-COSY experiments allows the detection and quantification of a complete set of $^{n}J_{CH}$, and particularly, HMBC-COSY can be a powerful method to measure very small $^{n}J_{CH}$ values in quaternary carbons. All the described methods can be successfully applied to other heteronuclei making them a powerful and general approach to measure other heteronuclear coupling constants.

Methods and Materials

All NMR experiments were recorded on a Bruker DRX-500 spectrometer (Bruker, Rheinstetten, Germany) equipped with a

three-channel 5-mm cryoprobe incorporating a *z*-gradient coil on a 0.1 M solution of strychnine, **1**, in $CDCl_3$. 2D ^1H–^{13}C IP-ximHSQMBC and AP-HSQMBC experiments were separately recorded as described in Fig. 1 by using a repetition delay of 1 s between the subsequent transients and the interpulse delays that were optimized to 8 Hz ($\Delta = \Delta + p_{180} = 1/2^{*n}J_{CH}$, where p_{180} is the duration of the selective 180° ^1H pulse). For selective refocusing in selHSQMBC experiments, a Gaussian-shaped 180° pulse of 20 ms duration (p_{180}) and a REBURP-shaped pulse of 12 ms were applied in Figs 2 and 3, respectively.

Sine bell-shaped gradients of 1 ms duration (δ) were used, followed by a recovery delay of 100 μs. The gradient ratios described later are measured as percentage of the absolute gradient strength of 53.5 G/cm. In selHSQMBC and broadband HSQMBC/HSQMBC-COSY experiments, the gradients were optimized to G1 : G2 : G3 : G4 : G5 = 80 : 20.1 : 11 : 50 : 17. In broadband HMBC/HMBC-COSY experiments, the gradients were optimized to G1 : G2 : G3 : G4 : G5 = 40 : −40 : 20.1 : 15 : −10 : −5. To minimize direct response cross-peaks, a BIRD element (optimized to 140 Hz; $\tau = 1/(2^{*1}J_{CH}) = 3.6$ ms) was placed into the initial INEPT block of HSQMBC experiments (Fig. 1(B)), whereas a dual-step low-pass *J*-filter element (delays τ and τ' were optimized as described in Ref. [15] setting $^1J_{CHmax}$ and $^1J_{CHmin}$ to 160 and 130 Hz, respectively) was used in HMBC experiments (Fig. 1(C)).

All experiments were acquired and processed using the echo/anti-echo protocol. Four scans were accumulated for each one of the 128 t_1 increments, and the number of data points in the acquisition dimension was set to 4096. The overall acquisition time for each IP and AP data was about 12 min, which were added/subtracted in the time-domain to provide spin-state selective data. Prior to Fourier transformation of each data, zero filling to 1024 in F1, 8192 points in F2 and a squared-cosine-bell function in both dimensions were applied. Spectral windows of 22 500 Hz in the F1 dimension and 2000 Hz in selective experiments and 4500 Hz in broadband versions in the detected F2 dimension were used.

Acknowledgements

Financial support for this research provided by MICINN (projects CTQ2009-08328 and CTQ2012-32436) and Bruker Española S.A. is gratefully acknowledged. We also thank the Servei de Ressonància Magnètica Nuclear, Universitat Autònoma de Barcelona, for allocating instrument time to this project.

References

[1] A. Bax, M. Summers. *J. Am. Chem. Soc.* **1986**, *108*, 2093–2094.
[2] J. M. Richardson, J. J. Titman, J. Keeler, D. Neuhaus. *J. Magn. Reson.* **1991**, *93*, 533–553.
[3] R. A. E. Edden, J. Keeler. *J. Magn. Reson.* **2004**, *166*, 53–68.
[4] R. T. Williamson, B. L. Márquez, W. H. Gerwick, K. E. Kövér. *Magn. Reson. Chem.* **2000**, *38*, 265–273.
[5] H. Koskela, I. Kilpelainen, S. Heikkinen. *J. Magn. Reson.* **2003**, *164*, 228–232.
[6] K. Kövér, G. Batta, K. Fehér. *J. Magn. Reson.* **2006**, *181*, 89–97.
[7] S. Boros, K. E. Kövér. *Magn. Reson. Chem.* **2011**, *49*, 106–110.
[8] A. Bax, K. A. Farley, G. S. Walker. *J. Magn. Reson. A* **1996**, *119*, 134–138.
[9] V. V. Krishnamurthy. *J. Magn. Reson. A* **1996**, *121*, 33–41.
[10] S. Gil, J. F. Espinosa, T. Parella. *J. Magn. Reson.* **2011**, *213*, 145–150.
[11] J. Sauri, J. F. Espinosa, T. Parella. *Angew. Chem. Intl. Ed.* **2012**, *51*, 3919–3922.
[12] D. Uhrín, V. Varma, J. R. Brisson. *J. Magn. Reson. A* **1996**, *119*, 120–124.
[13] S. Gil, J. F. Espinosa, T. Parella. *J. Magn. Reson.* **2010**, *207*, 312–313.
[14] J. Sauri, T. Parella. *Magn. Reson. Chem.* **2012**, *50*, 717–721.
[15] A. Meissner, O. W. Sørensen. *Magn. Reson. Chem.* **2000**, *38*, 981–984.
[16] T. Schulte-Herbrüggen, A. Meissner, A. Papanikos, M. Meldal, O. W. Sørensen. *J. Magn. Reson.* **2002**, *156*, 282–294.
[17] R. Wagner, S. Berger. *Magn. Reson. Chem.* **1998**, *36*, S44–S46.
[18] G. E. Martin, C. E. Hadden, R. C. Crouch, V. V. Krishnamurthy. *Magn. Reson. Chem.* **1999**, *37*, 517–528.
[19] K. Furihata, H. Seto. *Tetrahedron Lett.* **1998**, *39*, 7337–7340.
[20] C. E. Hadden, G. E. Martin, V. V. Krishnamurthy. *J. Magn. Reson.* **1999**, *140*, 274–280.
[21] C. E. Hadden, G. E. Martin, V. V. Krishnamurthy. *Magn. Reson. Chem.* **2000**, *38*, 143–147.

2. Extension of the results

To demonstrate the reliability we show the results obtained in a more complex molecule like progesterone.

In **Fig. 3.05** it is shown the magnitude of $^{n}J(CH)$ coupling constants belonging to quaternary carbons C3 and C5 from the selHSQMBC-TOCSY IAPAP experiment after selective inversion of all the protons resonating at 1.7-2.1 ppm. Below (Fig. 3.06B) it is shown the same expanded area using the HMBC IAPAP experiment. Despite the fact that some small values are missing in the HMBC IAPAP due to the direct signal intensity dependence with the $^{n}J(CH)$ value, it is clearly visible an excellent agreement between both experiments.

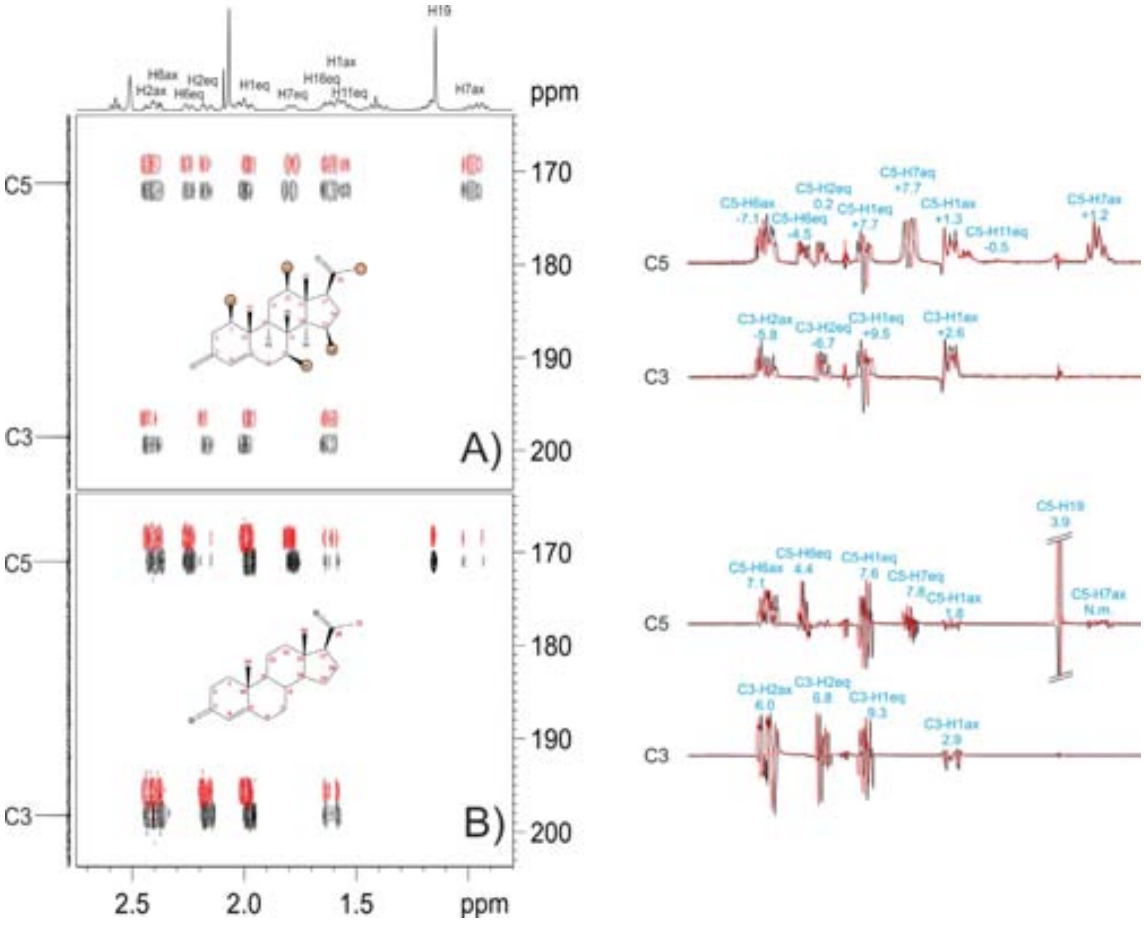

Figure 3.05. Expanded areas and 1D traces corresponding to C3 and C5 carbons of progesterone showing the A) α/β- selHSQMBC-TOCSY and B) α/β- HMBC IPAP spectra after selective inversion of all the protons resonating at 1.7-2.1 ppm. For clarity, cross-peaks in B) appear in magnitude mode and their twisted-phase lineshapes are clearly distinguished in the corresponding 1D projections.

The complementarity between HMBC and HMBC-COSY IPAP experiment is also evaluated. While HMBC IPAP experiment only shows correlations with high $^{n}J(CH)$ values, three new cross-peaks appeared in the HMBC-COSY IPAP experiment (highlighted with a grey box) at the C5 carbon frequency, corresponding to very small $^{n}J(CH)$ values (<1.5 Hz) (**Fig. 3.06**).

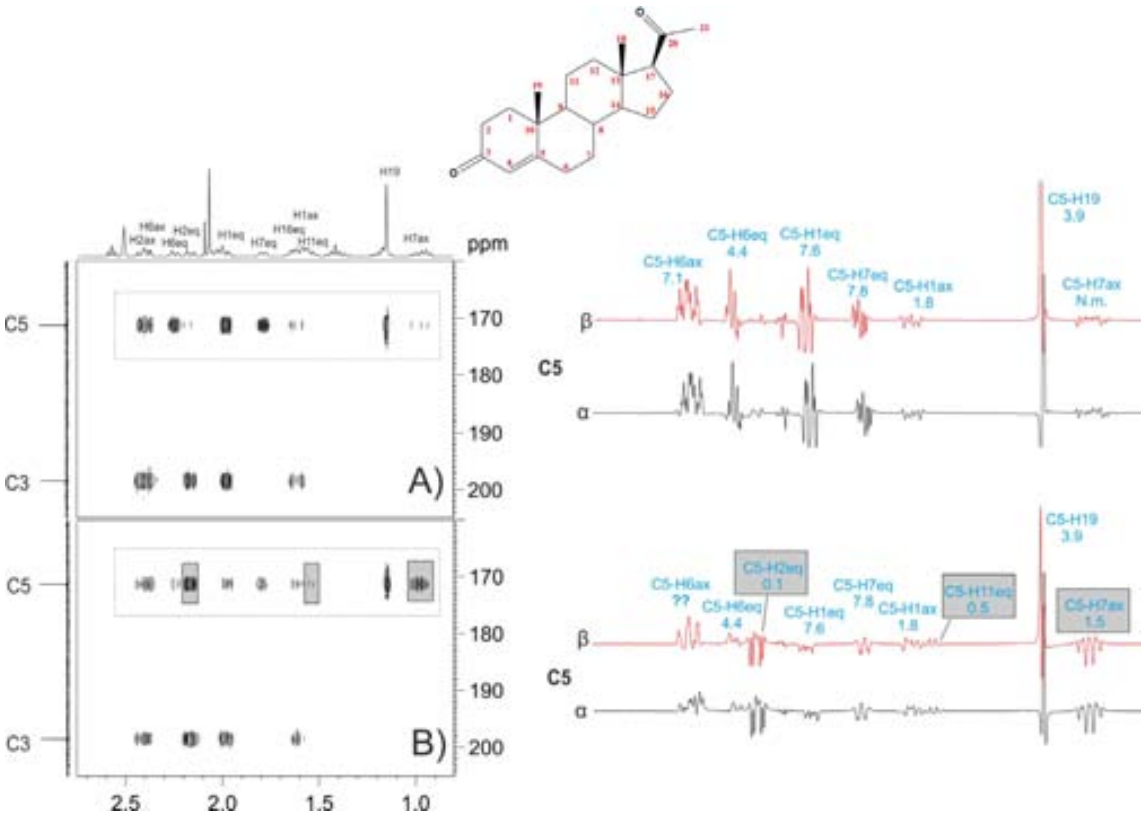

Figure 3.06. Expanded areas and 1D traces corresponding to C3 and C5 carbon frequencies showing the A) α/β-HMBC IPAP and B) α/β- HMBC-COSY IPAP spectra. 1D slices from C5 are shown on the right. Grey boxes stands to highlight the new COSY cross-peaks.

Another example to demonstrate the excellent complementarity between the HSQMBC-IPAP and the HSQMBC-COSY-IPAP experiments is given in **Fig. 3.07** but this time using a silvered compound to measure long-range ^{1}H-^{109}Ag coupling constants.

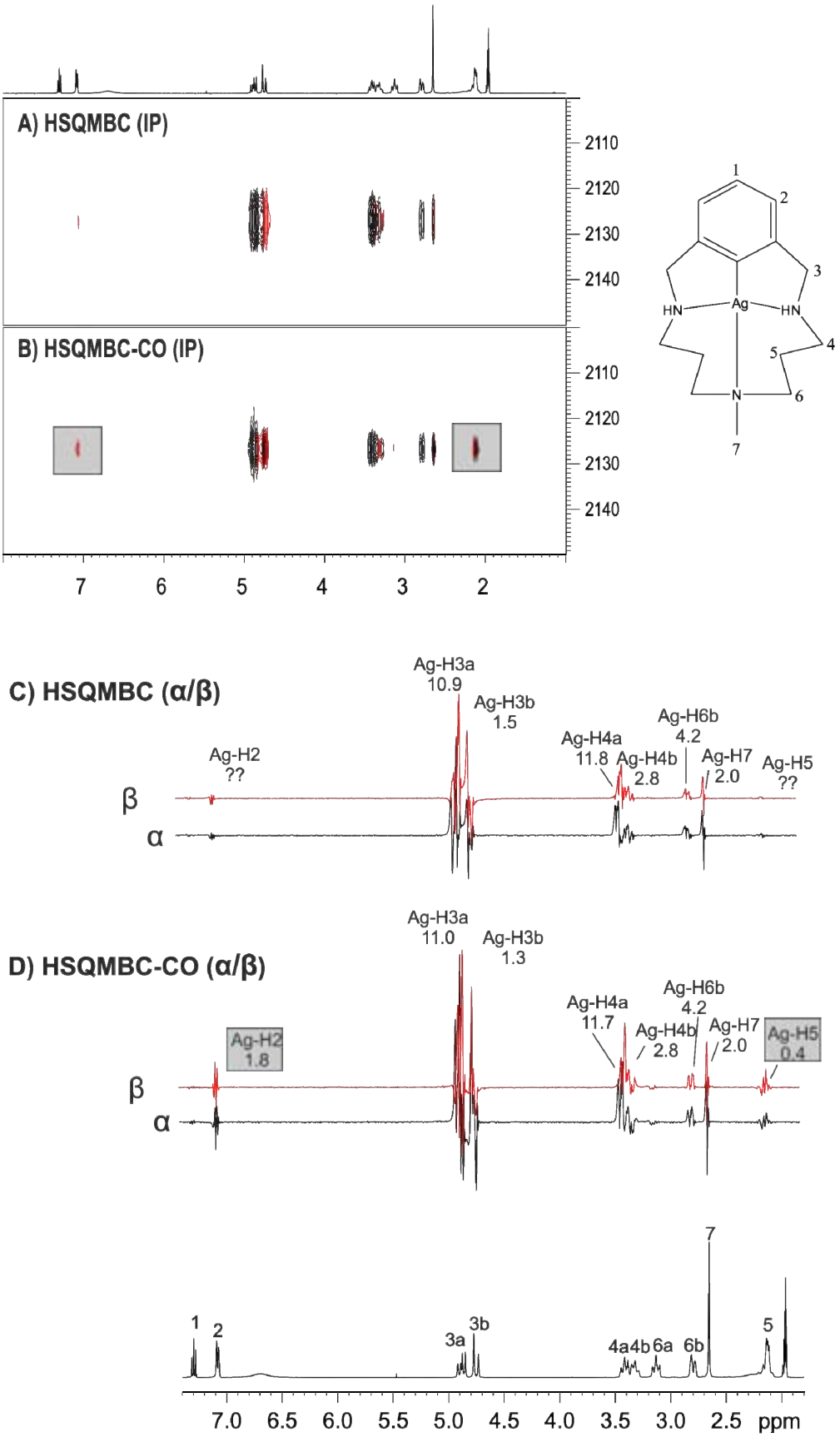

Figure 3.07. A) HSQMBC IP data, B) HSQMBC-COSY IP data, C) α/β- 1D slices from HSQMBC IPAP, and D) α/β- 1D slices from HSQMBC-COSY IPAP. At the bottom of the figure it is shown the conventional ^{1}H NMR spectrum. Grey boxes stands to highlight the new appeared cross-peaks

PUBLICATION 6

P.E.HSQMBC: Simultaneous measurement of proton-proton and proton-carbon coupling constants

J. Saurí, P. Nolis, L. Castañar, A. Virgili, T. Parella. *J. Magn. Reson.* 2012, 224, 101–106

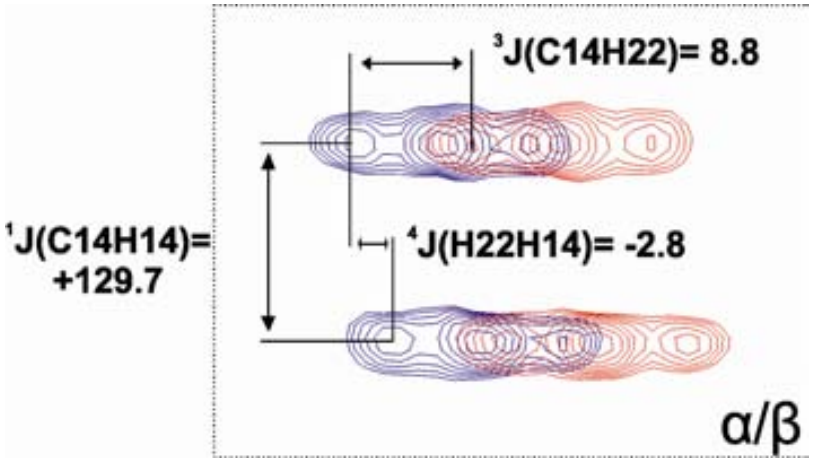

1. Introduction

In this publication, a new proton-selective NMR experiment, denoted as Pure Exclusive or P.E.HSQMBC, is presented to measure simultaneously J(HH), ^{1}J(CH) and ^{n}J(CH) coupling constants in a three ^{1}Ha-^{1}Hb-C spin-system. In addition, the experiment is also able to extract the relative sign of the J(HH) coupling constants.

The pulse scheme is based on the existing P.E.HSQC experiment, but optimized to long-range proton-carbon correlations instead of one-bond correlations. The experiment uses selective proton pulses to avoid any unwanted J(HH) modulation during the evolution periods. It is shown how the concepts of J-resolved spectroscopy as well as the E.COSY principle can be fully complementary to the IPAP technique. In this way, several coupling constants can be simultaneous measured from a single 2D cross-peak.

The main goal of the P.E.HSQMBC experiment is to take profit of the large ^{1}JC(H) value, which is used as a passive coupling constant, to generate an additional splitting in the indirect dimension of a 2D cross-peaks. The E.COSY pattern, which is generated by a 36º ^{1}H pulse, allows extract the magnitude and the relative sign of J(HH). The method also uses the IPAP technique along the detected dimension to get an accurate measurement of ^{n}J(CH), as described originally in the selHSQMBC experiment.

Journal of Magnetic Resonance 224 (2012) 101–106

Contents lists available at SciVerse ScienceDirect

Journal of Magnetic Resonance

journal homepage: www.elsevier.com/locate/jmr

P.E.HSQMBC: Simultaneous measurement of proton–proton and proton–carbon coupling constants

Josep Saurí [a], Pau Nolis [a], Laura Castañar [a,b], Albert Virgili [b], Teodor Parella [a,b,*]

[a] Servei de Ressonància Magnètica Nuclear, Universitat Autònoma de Barcelona, E-08193 Bellaterra, Barcelona, Spain
[b] Departament de Química, Universitat Autònoma de Barcelona, E-08193 Bellaterra, Barcelona, Spain

ARTICLE INFO

Article history:
Received 12 July 2012
Revised 10 September 2012
Available online 25 September 2012

Keywords:
HSQMBC
E.COSY
Proton–proton coupling constants
Long-range proton–carbon coupling constants
IPAP

ABSTRACT

A long-range optimized P.E.HSQC experiment, named P.E.HSQMBC, is proposed for the simultaneous measurement of a complete set of homonuclear and heteronuclear coupling constants from a single 2D cross-peak. The sign and the magnitude of proton–proton coupling constants are measured along the direct dimension from the relative E.COSY-type multiplet pattern displacement due to the passive one-bond coupling constant splitting generated in the indirect dimension. On the other hand, long-range proton–carbon coupling constants are independently determined in the detected dimension from a traditional fitting analysis of antiphase multiplet patterns or, more conveniently, from the IPAP multiplet displacement obtained from extended HSQMBC experiments.

1. Introduction

The determination of homonuclear and heteronuclear coupling constants is of prime importance in the structural and conformational studies of molecules in solution. Not only do *J*-couplings contain information about chemical connectivity, they also contain structural information as known for the typical Karplus-like dependence that exhibits ^3J vs dihedral angles. In addition, it has well been recognized during the last years that residual dipolar couplings (RDCs), as measured by solution state NMR, carry important structural information regarding internuclear vector orientation relative to the principal axis system of the molecule's alignment tensor [1].

Homonuclear proton–proton coupling constants, *J*(HH), can usually be determined by a variety of simple NMR methods, but the precise measurement of heteronuclear small long-range (^nJ(CH); $n > 1$) has not been so evident [2,3]. HSQC-TOCSY experiments becomes a sensitive and accurate approach to provide both the sign and the magnitude of ^nJ(CH) for protonated carbons [4–6]. On the other hand, NMR pulse schemes mainly based on the HMBC and HSQMBC experiments have been widely accepted to determine them on quaternary carbons [6–8]. However, the major inconvenient of this latter approach is the need for a post-processing fitting procedure by using the shape and intensity of signals simultaneously [6,9] to analyze the anti-phase nature of each multiplet pattern and the accuracy of the measurement is often questioned. Recently, IPAP versions have been suggested to avoid this fitting analysis by recording a series of refocused HSQMBC experiments to obtain complementary In-Phase (IP) and Anti-Phase (AP) data that are suitable to provide simplified spin-state selective multiplets after data addition/subtraction [10–13]. In this way, accurate and direct measurement of ^nJ(CH) can be made with simplicity even for complex multiplets. This IPAP approach has been also proposed to measure carbon–carbon coupling constants [14,15].

In addition to the IPAP technique, other different NMR approaches have been proposed to extract homo- and heteronuclear coupling constants from heteronuclear correlations experiments as, for instance, the elegant E.COSY (Exclusive Correlation SpectroscopY) principle [16]. The major advantages to analyze E.COSY-type multiplets are: (i) very easy interpretation; (ii) are suited equally well for the measurement of small and large coupling values, (iii) it provides information about the sign analyzing the relative slope of cross peaks components, (iv) works well even for coupling constants smaller than the NMR line width, (v) *J* values are measured from the direct dimension where good resolution requirements are more easily reached. Several E.COSY-type methods have been proposed for the simultaneous measurement of different scalar and residual dipolar couplings in small molecules. For instance, a simple and sensitive P.E.HSQC experiment, closely related to a fully coupled non-refocused HSQC pulse scheme, has been proposed to determine the sign and the magnitude of one-bond proton–carbon

* Corresponding author at: Servei de Ressonància Magnètica Nuclear, Universitat Autònoma de Barcelona, E-08193 Bellaterra, Barcelona, Spain.
E-mail address: teodor.parella@uab.cat (T. Parella).

1090-7807/$ - see front matter © 2012 Elsevier Inc. All rights reserved.
http://dx.doi.org/10.1016/j.jmr.2012.09.007

(^1J(CH) and ^{1}D(CH)) and two-bond proton–proton (^2J(HH) and ^{2}D(HH)) coupling constants from a single 2D spectrum [17]. Recently a spin-flip HSQC experiment has also been proposed for the simultaneous measurement of J(HH) and $^n J$(CH) [18]. Although this later technique is a proton-selective method that only works for protonated carbons, it has been proved that the addition of accurate long-range CH RDCs can significantly improve the structural discrimination power in complex small molecules with multiple stereogenic centers.

In what follows, we show a variant of the mentioned P.E.HSQC experiment, referred here as P.E.HSQMBC, for the simultaneous and accurate measurement of multiple J(HH), ^1J(CH) and $^n J$(CH) coupling constants. In this long-range ^{1}H–^{13}C correlation experiment, the large heteronuclear ^1J(CH) coupling constant is employed for separating two multiplet patterns along the indirect F_1 dimension while homonuclear HH couplings can be accurately measured from their relative E.COSY-type displacements in the detected F_2 dimension. The experiment closely relates to the XLOC experiment, a long-range correlation experiment designed to measure J(HH) in a similar E.COSY way [19–21]. Furthermore, we also present and discuss several options to extract $^n J$(CH) values at the same time and it will be shown that both E.COSY and IPAP principles can be implemented into the same pulse scheme to simultaneous measure different coupling constants from the same 2D multiplet with an extreme simplicity.

2. Results and discussion

Three different NMR pulse sequences suitable for an E.COSY version of the HSQMBC experiment are presented in Fig. 1. They combine the main features of three different older methods in a single experiment: (a) the accurate measurement of ^1J(CH) along the indirect dimension from F1-coupled HSQC schemes [22–25]; (b) the sign-sensitive measurement of ^1J(CH) and ^2J(HH) in E.COSY multiplets as reported in the P.E.HSQC experiment [17], and (c) the precise measurement of $^n J$(CH) using the IPAP technology in selHSQMBC experiments [11]. For the present work, we have chosen the general application of selective 180° ^{1}H pulses as a refocusing element in the INEPT block because this affords pure-phase multiplets and completely avoids any signal modulation due to J(HH).

The simplest pulse sequence is essentially a small-flip-angle non-refocused HSQC experiment where all CH coupling constants evolve freely during the entire t_1 period and the read ^{1}H pulse before acquisition is set to $\beta = 36°$ to achieve simplified multiplet structure. As described in the original P.E.HSQC experiment [17], instead of the long phase cycling schemes used in classical experiments, a simple small-angle pulse is used to generate the E.COSY-like pattern (Fig. 1A). In order to explain how pulse sequences work and describe the nature of multiplets generated in the proposed P.E.HSQMBC experiment, we concentrate the description on a heteronuclear three-spin system involving two active (H2 and C1) and a single passive (H1) spins (Scheme 1). These active spins having a long-range $^n J$(H2–C1) coupling determine the position of the cross-peak multiplet at (δ(H2), δ(C1)) which consists of two different components separated by the large ^1J(H1–C1) splitting along the F1 dimension. The magnitude and the sign of the J(H2–H1) coupling constant can be easily extracted comparing the relative displacement and the slope, respectively, between these two different rows in the detected F2 dimension (Fig. 2A). On the other hand, each row component of these E.COSY multiplets will present the characteristic antiphase pattern with respect to $^n J$(H2–C1) and pure in-phase character with respect all passive J(HH) couplings. The magnitude of $^n J$(H2–C1) must be extracted using well-established fitting algorithms that will not be discussed in detail here [6–9].

A modified P.E.HSQMBC version in where a BIRD^r cluster is incorporated into the carbon evolution period to suppress unwanted $^n J$(CH) contributions in the indirect dimension is shown in Fig. 1B. This option also offers the possibility to scale the ^1J(CH) splitting by a scaling factor k that strongly minimizes the resolution requirements and the number of t_1 increments to be acquired. This approach becomes particularly useful to obtain well defined multiplets in the indirect dimension that lead to precise measurement of scalar ^1J(CH) and/or dipolar ^{1}D(CH) values for weakly aligned samples. In analogy to the above description, this version also provides two separate cross peaks separated by $k * {}^1J$(CH) in the F1 dimension whereas $^n J$(CH) present the same AP features described above (Fig. 2B).

Finally, a refocused P.E.HSQMBC version has been developed to facilitate the measurement of $^n J$(CH) using the IPAP technique (Fig. 1C). Filtering the downfield and upfield doublet components into separate spectra is a successful concept to avoid the tedious analysis of anti-phase multiplets. This version can be understood as a F1-coupled analog of the recently proposed selHSQMBC experiment and although it suffers of a worse sensitivity due to the additional refocusing period, the magnitude of $^n J$(CH) can be extracted more accurately by the analysis of relative displacement of α/β cross-peaks in the detected dimension (see Fig. 2C). This more user-friendly method combines the principles of E.COSY and IPAP methodologies into a single NMR experiment whereas retains all the benefits described for the original selHSQMBC experiment [11].

Several details about sensitivity, multiplet patterns and relative pulse phases must be highlighted in order to explain the observed experimental data. Very importantly, two different mechanisms are present in the basic pulse scheme of Fig. 1A. First, the traditional pathway generated from the initial ^{1}H Boltzmann magnetization through the initial proton-selective INEPT transfer leads to two observable terms at the end of the t_1 period:

$$2H_{2y}C_{1z}\ \sin(\pi J_{H2-C1}\Delta)\ \cos(\pi J_{H2-C1}t_1)\ \cos(\pi J_{H1-C1}t_1) \tag{1a}$$

$$2H_{1y}C_{1z}\ \sin(\pi J_{H2-C1}\Delta)\ \sin(\pi J_{H2-C1}t_1)\ \sin(\pi J_{H1-C1}t_1) \tag{1b}$$

Thus, two different cross-peaks at δ(C1) appear showing pure anti-phase character with respect to J(H2–C1) in the F2 dimension: (i) a long-range H2–C1 correlation showing in-phase ^1J(CH) pattern and (ii) a direct H1–C1 cross-peak showing anti-phase ^1J(CH) pattern in the F1 dimension. The number of lines in the indirect dimension will depend on carbon multiplicity: CH appears as doublets, CH_2 as triplets and CH_3 as quartets with their intensities as described previously whereas quaternary carbons will not show splitting.

On the other hand, the original magnetization belonging to ^{13}C Boltzmann distribution also contributes to the final spectrum independently of the Δ delay and the selective proton pulse, in the form of the following term:

$$2H_{1y}C_{1z}\ \sin(\pi J_{H1-C1}t_1) \tag{2}$$

This pathway provides all direct correlations showing anti-phase pattern with respect to ^1J(CH) in both dimensions independently of the selective nature of the INEPT block and therefore, the measurement of the sign and the magnitude of all ^1J(CH) and ^2J(HH) couplings can be performed as exactly described for the regular P.E.HSQC experiment [17].

These two different pathways can be separately obtained by a proper phase cycling of the 90° proton pulse labeled with ϕ_2 phase. Thus, the separate acquisition of two complementary data acquired with the pulse scheme of Fig 1A and with $\phi_2 = y$ and $\phi_2 = -y$ afford the same spectrum but with inverted phase for components coming from INEPT transfer (Fig. 3A and B, respectively). Conventional data addition/subtraction affords independent

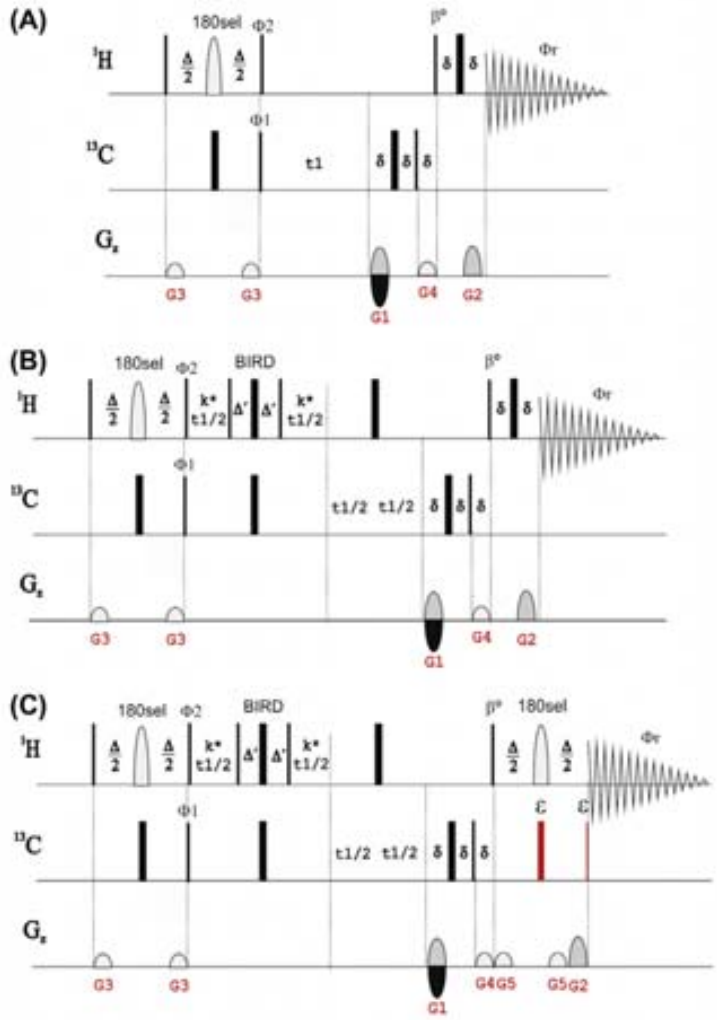

Fig. 1. Pulse sequences for the simultaneous determination of J(HH) and ^nJ(CH). Narrow and wide filled bars represent 90° and 180° pulses (unless the flip angle $\beta = 36°$ is indicated), respectively, while half-ellipsoids denote ^{1}H-selective 180° pulses (p_{180}): (a) non-refocused fully-coupled P.E.HSQMBC sequence; (b) non-refocused fully-coupled P.E.HSQMBC sequence incorporating an ^1J(CH)-scalable BIRD′ module (scaling factor k) that allows the selective evolution of ^1J(CH) whereas refocuses all ^nJ(CH) components during the variable evolution t_1 period; (c) refocused IPAP version based on the separate acquisition of In-Phase (IP:ε = on) and Anti-Phase (AP:ε = off) data that are further combined to provide separate α- and β-P.E.HSQMBC spectra. The interpulse delays are optimized to $\Delta = p_{180} + 1/[2 \cdot {}^nJ(CH)]$ and $\Delta' = 1/[2 \cdot {}^1J(CH)]$. δ stands for the duration of each gradient and the recovery delay. The minimum phase cycle is $\phi_1 = x,-x$ and $\phi_3 = x,-x$. See text for the importance of the phase ϕ_2: it is set to $\phi_2 = y$ for non-editing and $\phi_2 = y,y,-y,-y$ for editing of P.E.HSQC and P.E.HSQMBC data. Gradients G1 and G2 are used for coherence selection using echo-antiecho protocol, G3 and G5 are used for proper refocusing and G4 for zz-selection.

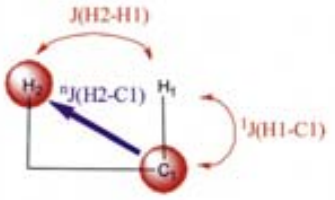

Scheme 1. Schematic representation of the spin-coupling networks involved in the simultaneous determination of ^1J(CH), J(HH) and ^nJ(CH). The blue arrow indicates the active H2–C1 coupling which is essential for coherence transfer. The desired E.COSY multiplet structure is caused by the large splitting of ^1J(H1C1) due to the spin passive H1 along the indirect dimension. Fig. 2 summaries the multiplet patterns obtained from each proposed experiment and how couplings can be measured. (For interpretation of the references to color in this figure legend, the reader is referred to the web version of this article.)

P.E.HSQC (Fig. 3C) and P.E.HSQMBC (Fig. 3D) spectra. Otherwise, the corresponding P.E.HSQMBC spectra could also be obtained directly by performing the subtraction during acquisition by applying a four-step phase cycling with $\phi_2 = y,y,-y,-y$. In this case, a 90°(^{13}C)-gradient element just before the initial 90° ^{1}H pulse helps to efficiently remove unwanted ^{13}C Boltzmann contribution.

P.E.HSQC data are analyzed exactly as described in the original experiment and no more details will be given here. On the other hand, Fig. 4 shows an expansion of the column corresponding to the H15b proton in the P.E.HSQMBC spectrum. The direct correlation, that is visible because the selective pulse also excites the satellite lines, shows pure in-phase character in the indirect F1 dimension. It is clearly shown that is possible to differentiate the corresponding active ^1J(H15b–C15) and the passive ^1J(H15a–C15)

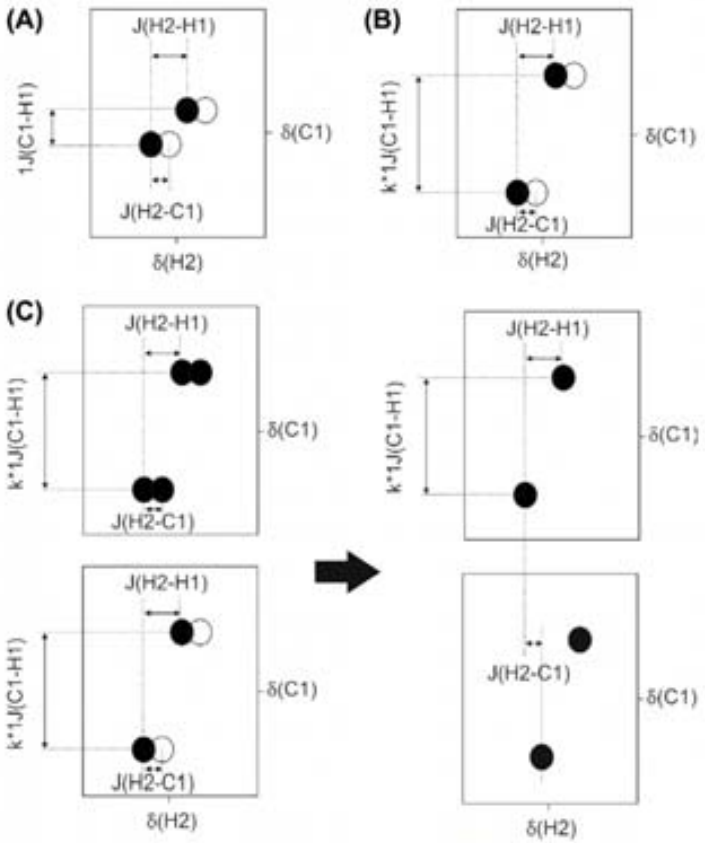

Fig. 2. (A–C) Schematics representing the expected multiplet patterns obtained from sequences of Fig. 1A, B and C, respectively. Filled and open circles represent multiplet components with opposite phase. In all cases, J(HH) is measured from the E.COSY pattern. On the other hand, $^n J$(CH) must be extracted from the analysis of anti-phase multiplet patterns in the same row (in A and B), or from the relative displacement between two components that are separated in two separate spin-state selected spectra (see C).

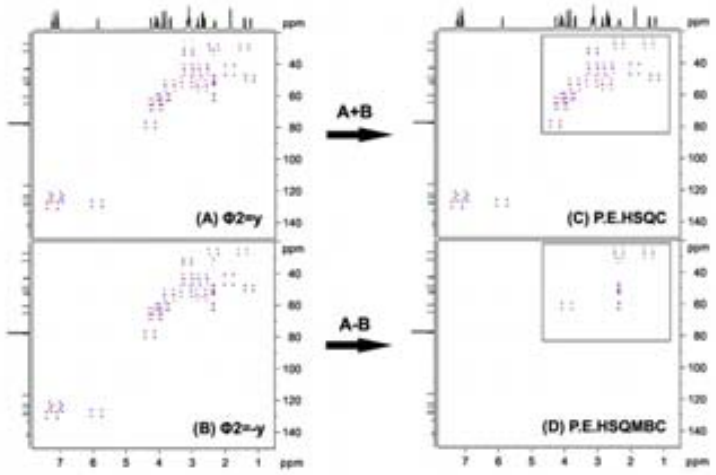

Fig. 3. General scheme to obtain separate P.E.HSQC and P.E.HSMBC spectra after selective refocusing of H15b proton (resonating at 2.35 ppm) of strychnine using the scheme of Fig. 1B. Two different data are independently acquired only changing the phase of the 90° proton pulse just applied after the t_1 period (A) using $\Phi_2 = y$ and (B) $\Phi_2 = -y$ whereas other relevant phase remain unchanged ($\Phi_1 = x, -x$ and $\Phi_r = x, -x$). After addition and subtraction of these data, two separate (C) P.E.HSQC and (D) P.E.HSQMBC spectra are obtained to determine ^1J(CH), J(HH) and $^n J$(CH). The scaling factor was set to $k = 3$ and the experiment optimized to 8 Hz.

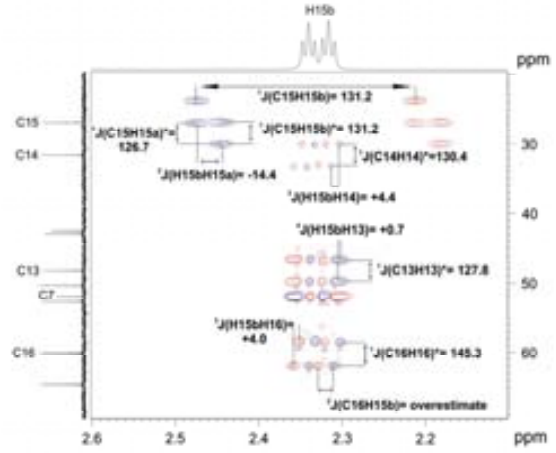

Fig. 4. Expanded region of the P.E.HSQMBC spectrum showing the column corresponding to the H15b proton (see Fig. 3D). Note that from the direct correlation, the relative sign between ^2J(HH) and ^1J(CH) can be obtained. From the other cross-peaks the sign and magnitude of ^3J(HH) can be extracted. The analysis of an specific row for the direct determination of ^nJ(CH) is not advisable due to an overestimation and a conventional fitting procedure is required.

in diastereotopic CH_2 spin systems as well as to the sign and magnitude of the geminal and passive J(H15b–H15a) coupling value. Additional H15b cross-peaks are also observed for the methines C14, C13 and C16 carbons and for the quaternary C7 carbon. The well-resolved doublets in F1 for each CH cross-peak evidences the relative displacement between them along the F2 dimension, allowing the measurement of both magnitude and sign of the corresponding J(HH) as a function of the observed signal tilting. On the other hand, each individual row displays a pure anti-phase pattern with respect to the active ^nJ(CH) that can be analyzed accordingly. The anti-phase nature structure of cross-peaks can cause partial intensity losses when the active scalar coupling is within the line width.

For this reason, a refocused version that uses the IPAP principle is proposed (Fig. 1C) for a much better and more user-friendly measurement on ^nJ(CH). Fig. 5 illustrates the experimental protocol to acquire, to process and to analyze these P.E.HSQMBC data taking the H15b–C16 cross-peak as an example. Two complementary IP and AP data are separately acquired as shown in Fig. 5A and B, respectively. Although J(HH) could already be measured in any of these spectra from the E.COSY pattern, the extraction of ^nJ(CH) would usually require an individual fitting analysis for each cross-peak. Sum and difference data (Fig. 5C and D) contain only the upfield and downfield components of the active doublet which makes it possible the straightforward measurement of ^nJ(CH) by analyzing the relative displacement between them. However, in analogy to the regular selHSQMBC experiment the sign information of ^nJ(CH) is not available from this analysis. In our hands, the use of a scaling factor of $k = 3$ is a good compromise to clearly resolve ^1J(CH) multiplet components in the indirect dimension using 256 t_1 increments. On the other hand, the non-equivalence between IP and AP data can afford undesired J-cross talk contributions that can introduce some error in the measurement. The use of an individualized scaling k' factor in the form of AP ± k' * IP can be used to correct them. The tolerance on these cross-talk effects has already been discussed previously [10,11].

A limitation of the proposed experiments is its ^{1}H-selective nature and therefore multiple experiments should be needed for a global determination of coupling values in a molecule. However, the extraction of ^nJ(CH) from multiple protons can be simultaneously obtained by applying the principles of multiple-site or band-selective excitation. Fig. 6 shows an example after selective refocusing of several protons that are not mutually coupled and acquired under the same experimental conditions as described in Fig. 3.

In summary, it has been shown that the concepts of J-resolved, E.COSY and IPAP principles can be mixed all together into the same pulse scheme in order to measure multiple coupling constants from a single 2D cross-peak analysis. We have developed a method that leads to the accurate measurement of both J(HH) and ^nJ(CH)

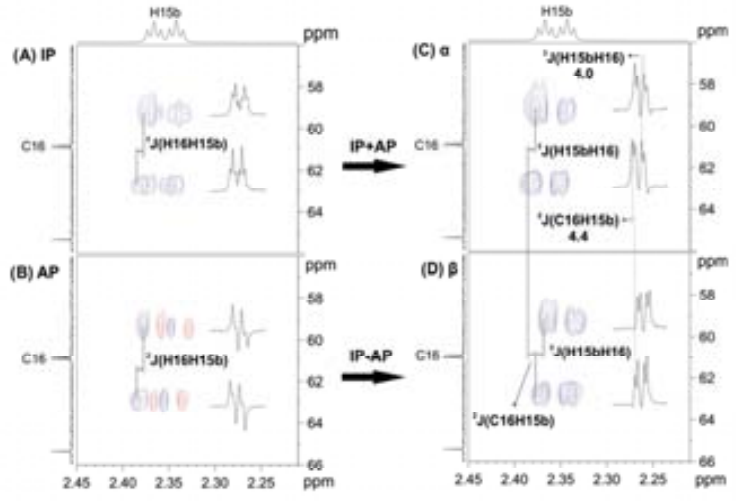

Fig. 5. Expanded areas corresponding to the H15b–C16 cross peak in the IPAP-selHSQMBC-E.COSY experiment acquired with the same experimental conditions as discussed in Fig. 3 and using pulse scheme of Fig. 1C. Two different data are acquired using the IPAP principle: (A) IP with the phase of β' pulse set to y and applying the pulses labeled with ε (on); (B) AP with the phase of β' pulse set to x and omitting the pulses ε (off). Time-domain data addition/subtraction followed by conventional processing afford complementary (C) α- and (D) β-selHSQMBC-E.COSY spectra from which the ^nJ(CH) value can be directly extracted in a simple way by analyzing the relative left/right displacement of signals in the F2 dimension.

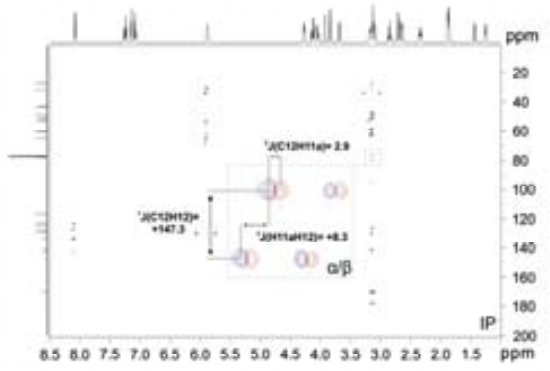

Fig. 6. Example showing the advantage to use multiple-site selective excitation in the P.E.HSQMBC experiment using shifted laminar pulses of non-mutually coupled protons. Different protons (H4 (8.15 ppm), H22 (5.9 ppm) and H11a/H18a/H14 (all three resonating near to 3.15 ppm)) were simultaneously refocused using a 40 ms Gaussian-shaped 180° proton pulse. The 2D spectrum corresponds to the In-Phase (IP) data and the inset shows the separate α/β data corresponding to the H11a–C12 cross peak.

from the high resolution obtained in the detected dimension whereas ^1J(CH) is precisely resolved in the indirect dimension. The proper combination of multiple proton excitation and non-uniform sampling can allow a faster measurement of all these couplings in small and medium size molecules. Alternatively, the experiment could be also implemented in a broadband mode, using for instance a CPMG-BIRD element instead of the selective INEPT block [26–28]. However, complete suppression of proton–proton coupling evolution and undesired sample heating remains to be solved. Much work is in progress to extrapolate all these concepts to the simultaneous measurement of the sign and magnitude of different types of heteronuclear coupling constants.

3. Methods and materials

All NMR experiments have been recorded on a BRUKER DRX-500 spectrometer equiped with a 3-channel 5-mm cryoprobe incorporating a *z*-gradient coil on a sample of 25 mg of strychnine, **1**, dissolved in 0.6 ml of $CDCl_3$. All experiments were optimized to 8 Hz, that means that ^nJ(CH) evolves during a period of $\Delta + p_{180} = 1/(2 * {}^nJ_{CH})$; where p_{180} is a selective 180° ^{1}H pulse. A Gaussian-shaped 180° pulse of duration of 20 ms (p_{180}) was used as a selective refocusing. The recycle and the interpulse BIRD′ ($\Delta' = 1/(2 * {}^1J(CH))$ delays were set to 1 s and 3.6 ms, respectively. An scaling factor $k = 3$ were used. Sine bell shaped gradients of 1 ms duration (δ) were used, followed by a recovery delay of 100 μs. Gradient ratios for G1:G2:G3:G4:G5:G6 were 80:20.1:33:50:11:17, measured as percentage of the absolute gradient strength of 5.35 G/cm.

All experiments were acquired and processed using the echo/anti-echo protocol. Quadrature detection is achieved inverting the G1and G2 gradient pulses for every second FID. Four scans were accumulated for each one of the 256 t_1 increments and the number of data points in t_2 was set to 4096. Spectral windows in both dimensions were 22500 (F1) and 4500 (F2) Hz, respectively. Prior to Fourier-transformation of each data, zero filling to 1024 in F1, 8192 points in F2 and a sine squared function in both dimensions were applied.

2D ^{1}H–^{13}C IP and AP-HSQMBC experiments of Fig. 5 were separately recorded using the same experimental conditions described in Fig. 4. The overall acquisition time for each individual IP and AP data was about 26 min which were added/subtracted in the time-domain without any scaling factor to provide spin-state selective data. Finally, the same conditions were applied for the spectra shown in Fig. 6 except for the selective refocusing. A 40 ms multiple-site pulse applied to three different frequencies was automatically generated using the shape tool package included into Tospin software (see captions for more details).

Acknowledgments

Financial support for this research provided by MICINN (Projects CTQ2009-08328 and Consolider Ingenio-2010 CSD2007-00006) and Bruker Española S.A. is gratefully acknowledged. We also thank to the Servei de Ressonància Magnètica Nuclear, Universitat Autònoma de Barcelona, for allocating instrument time to this project.

References

[1] C. Thiele, Eur. J. Org. Chem. (2008) 5673–5685.
[2] B.L. Márquez, W.H. Gerwick, R.T. Williamson, Magn. Reson. Chem. 39 (2001) 499–530.
[3] T. Parella, 2D methods for the measurement of long-range proton–carbon coupling constants, in: G.A. Morris, J.W. Emsley (Eds.), Multidimensional NMR Methods for the Solution State, vol. 305, John Wiley & Sons Ltd., Chichester, UK, 2010.
[4] P. Nolis, J.F. Espinosa, T. Parella, J. Magn. Reson. 180 (2006) 39–50.
[5] W. Kożmiński, J. Magn. Reson. 137 (1999) 408–412.
[6] K. Kobzar, B. Luy, J. Magn. Reson. 186 (2007) 131–141.
[7] M.J. Thrippleton, J. Keeler, Angew. Chem., Int. Ed. 42 (2003) 3938–3941.
[8] R.T. Williamson, B.L. Márquez, W.H. Gerwick, K.E. Kövér, Magn. Reson. Chem. 38 (2000) 265–273.
[9] L. Verdier, P. Sakhaii, M. Zweckstetter, C. Griesinger, J. Magn. Reson. 163 (2003) 353–359.
[10] S. Gil, J.F. Espinosa, T. Parella, J. Magn. Reson. 207 (2010) 312–321.
[11] S. Gil, J.F. Espinosa, T. Parella, J. Magn. Reson. 213 (2011) 145–150.
[12] J. Saurí, J.F. Espinosa, T. Parella, Angew. Chem., Int. Ed. 51 (2012) 3919–3922.
[13] D. Uhrín, V. Varma, J.R. Brisson, J. Magn. Reson. A 119 (1996) 120–124.
[14] K.E. Kövér, M. Lenoir, D. Uhrín, J. Magn. Reson. 190 (2008) 171–182.
[15] L. Jin, D. Uhrín, Magn. Reson. Chem. 45 (2007) 628–633.
[16] C. Griesinger, O.W. Sørensen, R.R. Ernst, J. Am. Chem. Soc. 107 (1985) 6394–6396.
[17] P. Tzvetkova, S. Simova, B. Luy, J. Magn. Reson. 186 (2007) 193–200.
[18] P. Trigo-Mouriño, A. Navarro-Vázquez, J. Ying, R.R. Gil, A. Bax, Angew. Chem., Int. Ed. 50 (2011) 7576–7580.
[19] M.D. Sørensen, J.J. Led, O.W. Sørensen, J. Biomol. NMR 4 (1994) 135–141.
[20] A. Meissner, O.W. Sørensen, Magn. Reson. Chem. 39 (2001) 49–52.
[21] A. Meissner, J.ø Duus, O.W. Sørensen, J. Magn. Reson. 128 (1997) 92–97.
[22] C. Thiele, W. Bermel, J. Magn. Reson. 216 (2012) 134–143.
[23] J. Furrer, M. John, H. Kessler, B. Luy, J. Biomol. NMR 37 (2007) 231–243.
[24] K. Fehér, S. Berger, K.E. Kövér, J. Magn. Reson. 163 (2003) 340–346.
[25] K.E. Kövér, K. Fehér, J. Magn. Reson. 168 (2004) 307–313.
[26] H. Koskela, I. Kilpeläinen, S. Heikkinen, J. Magn. Reson. 164 (2003) 228–232.
[27] K.E. Kövér, G. Batta, K. Fehér, J. Magn. Reson. 181 (2006) 89–97.
[28] S. Boros, K.E. Kövér, Magn. Reson. Chem. 49 (2011) 106–110.

PUBLICATION 7

Simultaneous measurement of J(HH) and two different ^{n}J(CH) coupling constants from a single multiply-edited 2D cross-peak

J. Saurí, T. Parella. *Magn. Reson. Chem*. 2013, 51, 397–402

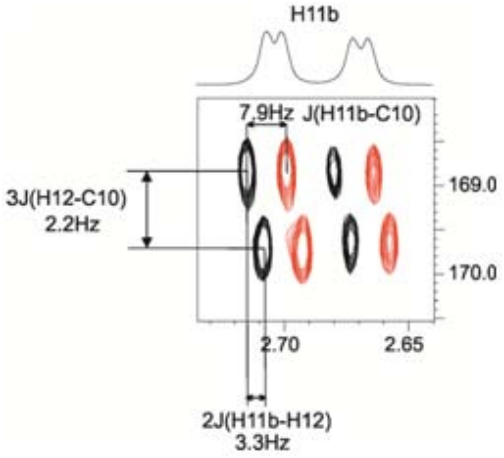

1. Introduction

After the successful implementation of P.E.HSQMBC experiment, we thought that the same idea could be implemented using $^{n}J(CH)$ instead $^{1}J(CH)$ as a passive spin. To achieve this, a selective 180º ^{1}H pulse has to be inserted during the evolution of the transverse ^{13}C magnetization. The idea is to select a different proton (H2) from which is initially selected during the INEPT transfer period (H1). In this way, cross peak will appear as a doublet in the indirect dimension due to the passive $^{n}J(C\text{-}H2)$ coupling. In addition, by using a selective 90º ^{1}H pulse over the passive H2 instead of a 90º pulse in the last INEPT, an E.COSY pattern cross-peak is obtained allowing us to measure the magnitude and the relative sign of the resolved J(H1H2) coupling constant.

It is shown show how three different editing methodologies can be combined in a single NMR experiment: the IPAP principle, J-resolved spectroscopy and the E.COSY pattern. This can be understood as a successful combination of two different concepts, one coming from the selHSQMBC IPAP experiment, and the other one from the EXSIDE experiment. EXSIDE and selHSQMBC experiments are based on a very similar concept but in the first one the active $^{n}J(CH)$ is measured along the indirect dimension as a doublet, while in the second one is measured along the direct dimension using IPAP. We denoted such experiment as J-selHSQMBC IPAP.

Research Article

Magnetic Resonance in Chemistry

Received: 28 January 2013 Revised: 2 April 2013 Accepted: 3 April 2013 Published online in Wiley Online Library: 6 May 2013

(wileyonlinelibrary.com) DOI 10.1002/mrc.3960

Simultaneous measurement of J(HH) and two different ^{n}J(CH) coupling constants from a single multiply edited 2D cross-peak

Josep Saurí and Teodor Parella*

Three different J-editing methods (IPAP, E.COSY and J-resolved) are implemented in a single NMR experiment to provide spin-state-edited 2D cross-peaks from which a simultaneous measurement of different homonuclear and heteronuclear coupling constants can be performed. A new J-selHSQMBC-IPAP experiment is proposed for the independent measurement of two different ^{n}J(CH) coupling constants along the F2 and F1 dimensions of the same 2D cross-peak. In addition, the E.COSY pattern provides additional information about the magnitude and relative sign between J(HH) and ^{n}J(CH) coupling constants.

Keywords: NMR; HSQMBC; E.COSY; long-range proton–carbon coupling constants; IPAP

Introduction

Homonuclear and heteronuclear coupling constants provide a wealth of structural and conformational information on molecules in solution.[1] In particular, during the last decades, many research groups have contributed to the development of NMR methods capable for the measurement of long-range proton–carbon coupling constants (^{n}J(CH); $n > 1$) in small molecules at natural abundance.[2] However, these determinations have posed a challenge in terms of data analysis and interpretation, which has often hindered a quick and accurate measurement of ^{n}J(CH) with simplicity.

Many years ago, the concept of J-resolved spectroscopy was introduced to separate the information of chemical shifts and J-multiplet structure in different dimensions of a multidimensional NMR spectrum. This was successfully applied in the pioneering ^{13}C-detected spin-flip experiment, where ^{n}J(CH) values were clearly determined from clean doublets that originated in the indirect F1 dimension of a heteronuclear 2D selective J-resolved experiment.[3] Recently, this selective heteronuclear echo has been introduced into the HSQC pulse train to measure the sign and the magnitude of scalar and residual dipolar HH and long-range CH coupling constants in weakly aligned media.[4] Several J-resolved versions of the 2D HMBC and heteronuclear single-quantum multiple-bond connectivity (HSQMBC) experiments have also been proposed to measure ^{n}J(CH) from the splitting that originated in the F1 dimension,[5] the popular excitation sculptured indirect detection experiment (EXSIDE) experiment being one of the most accepted methods.[6] Spin-state selective methods based on the E.COSY and in-phase/anti-phase (IPAP) principles are also important NMR approaches applied in the determination of heteronuclear couplings from simplified multiplet structures. E.COSY uses the editing features of a passive spin to spread out the J information into the F1 dimension, allowing the measurement of small magnitudes as well as of the sign of different coupling values from the same multiplet.[7] On the other hand, the IPAP methodology is an elegant solution to clearly distinguish the α/β components of a multiplet in separate spectra.[8] Recently, it has been demonstrated that the IPAP implementation into selective HSQMBC (selHSQMBC) experiments facilitates a rapid and very simple determination of ^{n}J(CH) values from high-quality spectra, without interference of homonuclear couplings.[9] A suite of related selHSQMBC-IPAP experiments have been designed by us to expand the powerful and applications of such promising methodologies even for complex, broad and low-resolved proton multiplets.[10,11] Thus, selHSQMBC-IPAP and EXSIDE experiments are analog tools because they can measure the same ^{n}J(CH) parameter along the F2 and F1 dimensions, respectively. With this in mind, we propose a new J-selHSQMBC-IPAP experiment (Fig. 1) that includes the main features offered in both selHSQMBC-IPAP and EXSIDE experiments into the same multiplet pattern (Fig. 2). It will be demonstrated that the concerted implementation of IPAP, E.COSY and J-resolved concepts into the same experiment allows the simultaneous measurement of several HH and CH coupling constants from simplified multiply edited 2D cross-peaks.

Results and Discussion

We show here that the incorporation of the selective J-resolved concept into the selHSQMBC-IPAP experiment, where ^{n}J(CH$_A$) from a selected H$_A$ proton is measured along the F2 dimension, allows the independent and simultaneous measurement of an additional ^{n}J(CH$_B$) coupling value from a different H$_B$ proton

* *Correspondence to: Teodor Parella, Servei de Ressonància Magnètica Nuclear, Universitat Autònoma de Barcelona, E-08193, Bellaterra, Barcelona, Spain. E-mail: teodor.parella@uab.cat*

Servei de Ressonància Magnètica Nuclear, Universitat Autònoma de Barcelona, 08193 Bellaterra, Catalonia, Spain

along the orthogonal F1 dimension. Experimental details such as ^{13}C frequency labeling, coherence selection using pulsed-field gradients (PFGs), interpulse delays optimization, further IPAP combination to obtain separate α/β data or the alternative use of multiple-site or region selective excitation are exactly performed as in the original selHSQMBC experiment, and not many additional comments will be included. The pulse sequence starts with a selective INEPT transfer where the central 180° ^1H pulse is applied selectively to a chosen H_A proton resonance.[12] In this way, any undesired J(HH) evolution is avoided, and only $^nJ(CH_A)$ evolution takes place in the form of $\sin(\pi\,^nJ(CH_A)\Delta')$. As an essential feature, a $^nJ(CH)$-scaling element (marked with a box in Fig. 1) is applied on a different selected H_B proton during the evolution of the transverse ^{13}C magnetization.[4,13] Thus, whereas ^{13}C chemical shift is codified in the usual way during the subsequent t_1 period, signal is also modulated by a cos $(\pi\,^nJ(CH_B)kt_1)$ factor that will cause an IP splitting because of $k\,^nJ(CH_B)$ in the F1 dimension. The last step is a reverse INEPT applied under the same conditions as the initial step but employing selective 90° and 180° pulses on H_A proton to provide characteristic E.COSY-like transfer.[14]

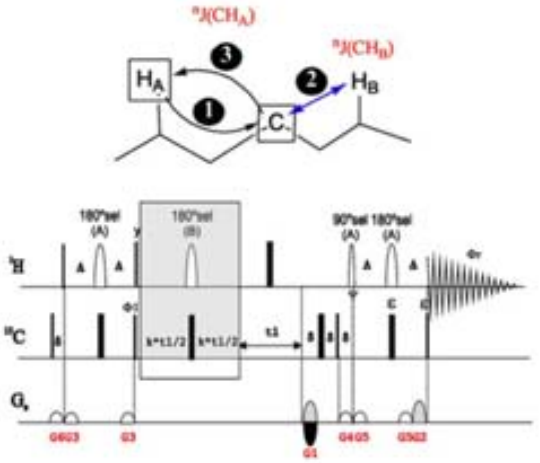

Figure 1. Schematic magnetization transfer pathway and pulse scheme for the 2D J-selHSQMBC-IPAP experiment. ^1H-selective 90° and 180° pulses were applied on different H_A or H_B protons as indicated. Acquired in-phase (IP: Ψ = y, ε = on) and anti-phase (AP: Ψ = x, ε = off) data are combined (AP ± IP) to provide α/β spectra. Interpulse delays are set to $\Delta' = 2\Delta + p180(sel) = 1/(2\,^nJ(CH_A))$. The $^nJ(CH_B)$-scaling factor during the t_1 period is given by k. More details in the experimental section.

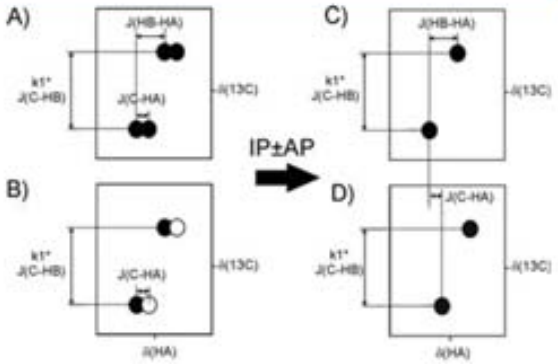

Figure 3. Schematic illustration on the multiplet patterns obtained in J-selHSQMBC experiments. (A) IP and (B) AP data are acquired and combined to provide separate (C) α- and (D) β-edited J-selHSQMBC spectra from which the measurement of $^nJ(CH_A)$ can be accurately made along the detected dimension, whereas $^nJ(CH_B)$ and $J(H_AH_B)$ are extracted from the E.COSY pattern.

The IPAP principle relies on the acquisition of two complementary in-phase (IP) and anti-phase (AP) data (Fig. 3). The acquired 2D cross-peak would show pure IP properties along the direct F2 dimension with respect to all J(HH) and IP (Fig. 3A) or AP (Fig. 3B) patterns with respect to the active $^nJ(CH_A)$ as a function of the two ^{13}C pulses marked with ε in the last INEPT period. Subsequent time-domain data combination (AP ± IP) affords two separate α/β subspectra (Figs. 3C and 3D) from which $^nJ(CH_A)$ can be easily extracted by analyzing the relative left/right displacements along the F2 dimension where resolution is not critical. In addition, each correlation can also show an additional doublet with an apparent $k^{*n}J(CH_B)$ splitting in the F1 dimension. Thus, two independent $^nJ(CH_A)$ and $^nJ(CH_B)$ coupling constants on the same carbon can be independently measured from the analysis of a single 2D cross-peak. Moreover, additional information about $J(H_AH_B)$ and the relative sign between $J(H_AH_B)$ and $^nJ(CH_B)$ can also be extracted from the E.COSY pattern generated by the passive H_B proton.

Figure 4 shows the experimental IP, AP and α/β J-selHSQMBC spectra after selective refocusing of the H_{15a} proton of strychnine, **1**, in both defocusing/refocusing periods and inverting its geminal H_{15b} proton during the independent k^*t_1 period. Fig. 4A shows pure IP multiplets with respect to both J(HH) and $^nJ(CH)$, whereas Fig. 4B shows multiplets with complex phase because of the AP nature with respect to $^nJ(CH_{15a})$ in the F2 dimension. The measurement of different $^nJ(C_aH_{15a})$ values along the F2 dimension is easily performed by analyzing the relative

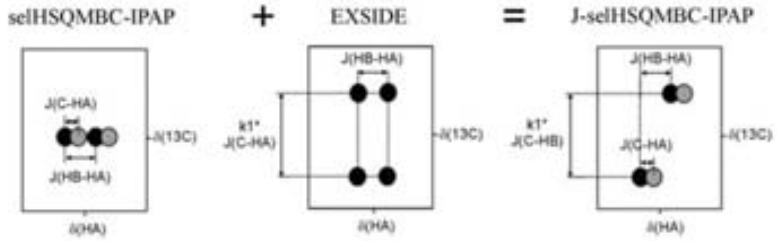

Figure 2. Multiplet patterns obtained in (A) selHSQMBC-IPAP, (B) EXSIDE and (C) J-selHSQMBC-IPAP experiments. Black and grey contours in IPAP experiments stands for separate α and β subspectra.

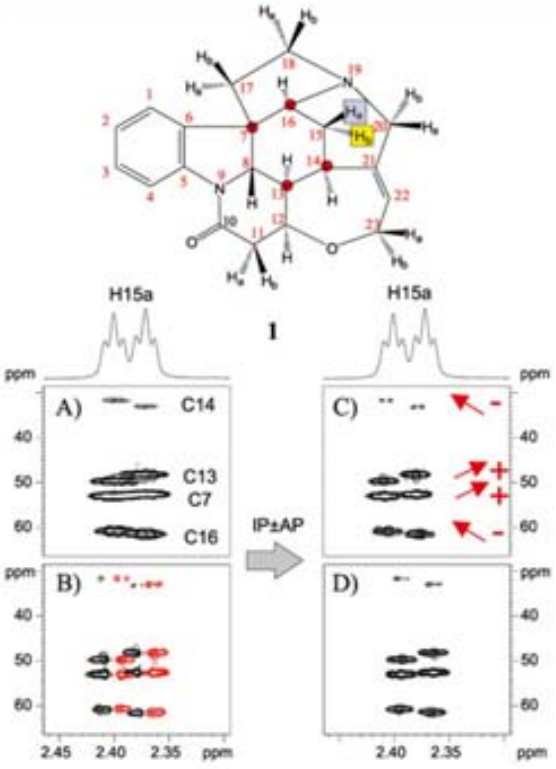

Figure 4. Expanded column corresponding to the 2D J-selHSQMBC-IPAP spectra after selection of H_{15a} proton and using the geminal H_{15b} proton as a passive spin. (A) IP and (B) AP data, which were co-added/subtracted in the time domain and further processed using conventional parameters to yield spin-state selected (C) α and (D) β spectra. The arrows indicate the relative sign of the passive $^{n}J(C_aH_{15b})$ coupling taking the negative geminal $J(H_{15a}H_{15b})$ coupling as reference.

frequency displacement between α/β cross-peaks in Figs. 4C and 4D, respectively. It is worth mentioning that α/β spectra yield more simplified multiplet structures with characteristic positive/negative E.COSY tilts that facilitate the direct measurement of the magnitude and the relative sign of the involved $^{n}J(C_aH_{15b})$ and $^{2}J(H_{15a}H_{15b})$ couplings.

The improved editing and the additional information obtained with the extended J-selHSQMBC-IPAP *versus* the original selHSQMBC-IPAP experiment when a third H_B spin comes in are illustrated in Fig. 5. The advantages of the IPAP principle are fully retained in both experiments, and $^{n}J(CH_{15a})$ values in the range of 3–8 Hz can directly be measured with minor cross-talk effects from the high-resolved F2 dimension in 8-Hz optimized experiments (see fig. 8 in ref. 9). IPAP measurements along the F2 dimension do not require a great number of t_1 increments, and selHSQMBC data of Fig. 5A have been obtained in a relatively short acquisition time using only 64 t_1 increments. In contrast, an increased number of t_1 increments are usually required for the measurement of small $^{n}J(CH)$ coupling values along the F1 dimension in the J-selHSQMBC experiment (Fig. 5B), lengthening experiment time. The excellent dispersion originated by the large $^{2}J(H_{15a}H_{15b}) = -14.5$Hz coupling allows additional measurements of small $^{n}J(C_aH_{15b})$ splittings in the range of 1–4 Hz using a scaling factor of k = 50 and 256 t_1 increments. Note that these small couplings, ranging from 1.5 to 3.9 Hz obtained, are difficult to be measured from traditional HMBC/HSQMBC experiments, mainly because signal intensities depend on the sine function. As an important feature of the J-selHSQMBC experiment, not only the magnitude but also the sign can be obtained with optimum sensitivity.

The excellent multiplet dispersion achieved by the double J-editing along the ^{1}H dimension is evidenced analyzing 1D traces (Fig. 6). For instance, the complex pure IP multiplet obtained from the original selHSQMBC experiment (Fig. 6B) for both resolved (H15a) and non-resolved (H16) ^{1}H multiplets can be efficiently spread out to four well-defined components (Figs. 6C–6F) from which $^{n}J(CH)$ and J(HH) values can be accurately measured along

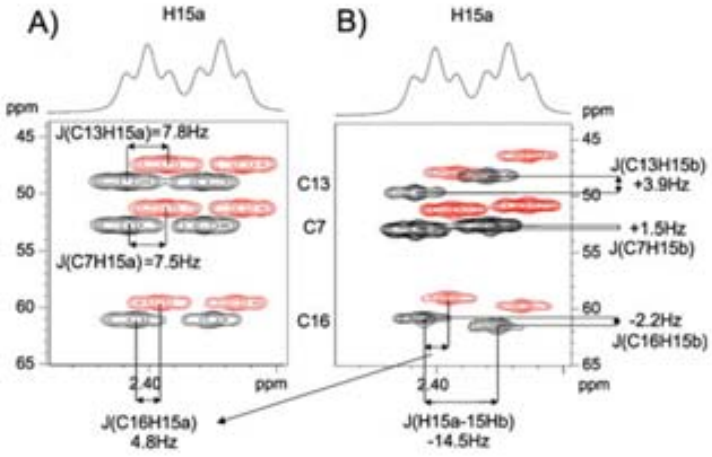

Figure 5. Comparison between 8-Hz optimized (A) 2D selHSQMBC *versus* (B) 2D J-selHSQMBC experiments after selective refocusing of H_{15a} proton. The different α/β spectra are vertically shifted to visualize the relative shift along the horizontal dimension. $^{n}J(C_aH_{15a})$ coupling values between 3 and 8 Hz are easily measured with excellent accuracy along the F2 dimension. In panel (B), the geminal H_{15b} proton was selected as a passive spin. The large J(HH) causes very good dispersion of the E.COSY pattern that allows the measurement of small $^{n}J(C_aH_{15b})$ values along the F1 dimension.

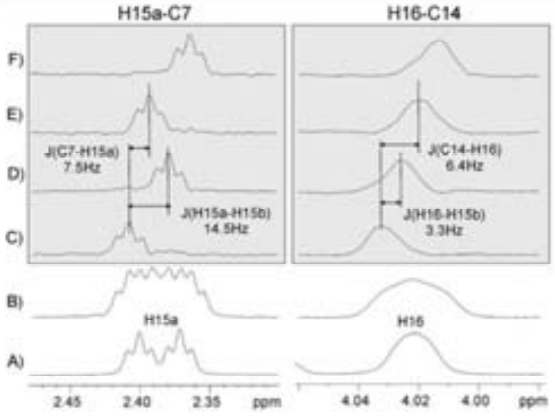

Figure 6. (A) Conventional ^{1}H, (B) IP from the selHSQMBC and (C–F) the four edited J-selHSQMBC multiplets extracted from H15–C7 and H16–C14 correlations.

the detected dimension. On the other hand, Fig. 7 shows some 2D J-selHSQMBC-IPAP cross-peaks corresponding to the three-bond H16–C14 correlation after selection of several passive H_x protons. It is a good example showing how accurate measurements of J(HH) and ^{n}J(CH) can be performed even from poorly resolved ^{1}H multiplets. Whereas IPAP works fine in all cases to determine $^3J(C_{14}H_{16}) = 6.4$Hz, the efficient measurement of additional $J(C_{14}H_x)$ values along the F1 dimension in the range of 2–10 Hz is also performed using a moderate number of t_1 increments (256 in this case) even in cases with small HH dispersion. In addition, the E.COSY pattern allows the measurement of J(HH) values even smaller than the line width and the determination of the relative sign between $^nJ(C_{14}H_x)$ and $J(H_{16}H_x)$ when comparing relative positive/negative slopes within the same column.

For small molecules, the differential relaxation between IP and AP data can be considered minimum, and the major cross-talk contribution is mainly due to the mismatch between the optimized Δ' delay and the experimental ^{n}J(CH) values. A detailed discussion and a theoretical prediction on the percentage of cross-talk have been already described in the original selHSQMBC-IPAP experiment.[9] Alternatively, two different options were proposed to certify the accuracy in such measurements: (i) the use of individualized scaling factors (AP + k*IP) and (ii) a data validation process from the individual analysis of the acquired IP and AP data and further comparison with the IPAP results. To demonstrate the accuracy of our measurements, Table 1 compares the values extracted from the IPAP, J-resolved and E.COSY patterns in Figs 4–7 with those measured from the selHSQMBC-IPAP and selHSQMBC-TOCSY-IPAP experiments previously published by our group, and also with other experimental data.[17–23] It is shown that the IPAP technique provides values of the same order as those published by all these other methods. Moreover, the largest uncertainties come from the J-resolved technique because of the lower resolution achieved in the indirect dimension, as recognized for the EXSIDE and J-HMBC experiments.

In summary, a new NMR experiment that incorporates all the features and advantages described for the popular selHSQMBC and EXSIDE experiments has been proposed to obtain multiple and accurate information about small homonuclear and heteronuclear coupling constants. Two different ^{n}J(CH) values are determined from the independent IPAP and J-splitting analysis along the direct and indirect dimensions, respectively, without any additional post-processing step. In addition, the simple doublet splitting and the features associated to the E.COSY pattern facilitate the analysis and expand the possibility to obtain additional information about the magnitude and relative signs of J(HH) and ^{n}J(CH). The most demanding experimental requirement is the high resolution needed along the F1 dimension, but this could be partially relieved and improved by the use of several techniques such as spectral folding and carbon-selective excitation[15] or the use of non-linear sampling in the indirect dimension as demonstrated for the fast and precise measurement of ^{1}J(CH) in weakly aligned samples.[16] The multiple J-editing principle described here could be also applied in an equivalent 2D J-selHSQMBC-TOCSY experiment where a homonuclear ^{1}H-^{1}H TOCSY transfer is appended just prior to acquisition. Thus, an important amount of additional and highly valuable information about the magnitude and the sign of new J(HH) and ^{n}J(CH) coupling constants should be available, maintaining all the advantages of the recently proposed selHSQMBC-TOCSY experiment.[10] TOCSY transfer retains spin-state selection properties, and therefore, the magnitude and the sign of J(HH) can be obtained from the relative positive/negative tilt of relayed E.COSY cross-peaks with respect to the initial target. It is expected that the method can find

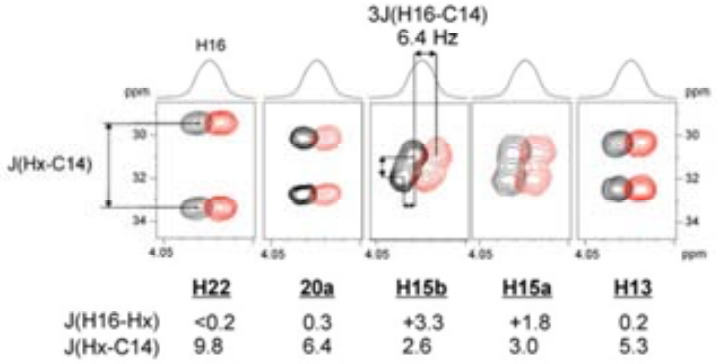

Figure 7. Several 2D H16-C14 cross-peaks extracted from J-selHSQMBC-IPAP spectra after selection of different passive H_x protons. Separate α- and β-multiplets are represented as overlayed contour plots.

Table 1. Values of several proton–proton and proton–carbon coupling constants (in Hz) in strychnine measured using different NMR methods

	J-selHSQMBC	selHSQMBC IPAP	selHSQMBC-TOCSY IPAP	HSQC-TOCSY		HMBC (AP Analysis)		selEXSIDE (J-Resol)	ACCA
	This work	Ref. 9	Ref. 10	Ref. 17	Refs. 18,19	Ref. 20	Ref. 21	Ref. 22	Ref. 23
^3J(C13H15a)	7.8 (IPAP)	7.8	+8.1	—	—	7.9	8.0/8.1	8.0	
^3J(C7H15a)	7.5 (IPAP)	7.4	+7.4	—	—	7.3	7.2/7.3	7.3	
^2J(C16H15a)	4.8 (IPAP)	4.7	−4.6	−4.6	—	—	4.5/4.3	4.0	
^3J(C13H15b)	+3.9 (J-res)	3.9	+3.6	—	—	4.6	3.3/3.5	3.0	
^3J(C7H15b)	+1.0 (J-res)	1.2	+1.2	—	—	—	—	—	
^2J(C16H15b)	−1.7 (J-res)	3.1	−2.6	−2.8	—	—	2.7/3.0	1.4	
^2J(H15aH15b)	−14.5 (E.COSY)								14.4
^3J(C14H16)	6.4 (IPAP)	6.4	+6.7	+6.4	+6.3/+6.9	6.4	—	—	
^3J(C14H22)	9.8 (J-res)	8.8	+8.9	+6.6	+8.9	8.9	7.9/8.5/8.6	8.4	
^3J(C14H20b)	6.4 (J-res)	5.4	+5.0	+5.4	+5.3	5.5	5.4/5.3	5.1	
^2J(C14H15a)	2.7 (IPAP) −2.6 (J-res)	2.7	−3.0	−2.7	−2.7/−2.6	3.2	1.8/2.8/2.8	2.0	
^2J(C14H15b)	−3.0 (J-res)	4.0	−4.0	−3.3	−3.2/−3	4.4	3.2/3.6	2.8	
^2J(C14H13)	5.3 (J-res)	5.1	−5.1	−5.4	−4.8/−4.5	4.7	4.6/4.7	4.5	
^3J(H16H15b)	1.8 (J-res)								1.82/2.1
^3J(H16H15a)	3.3 (E.COSY)								3.8

particular interest in the determination of relative conformation/configuration properties of specific sites where a complete set of local scalar and/or residual dipolar HH and CH coupling constants can be necessary.

Methods and Materials

All NMR experiments have been recorded on a BRUKER DRX-500 spectrometer equiped with a three-channel 5-mm cryoprobe incorporating a z-gradient coil on a sample of 20 mg of strychnine dissolved in 0.6 ml of $CDCl_3$. Phases are indicated above the pulses (where no phase is given, the pulse is applied along x). The basic cycle phase was Φ_1: x,-x; Φ_{rec}: x,-x. 2D ^1H–^{13}C in-phase (IP: Ψ=y, ε=on) and anti-phase (AP: Ψ=x, ε=off) J-selHSQMBC data were recorded separately and combined in the time domain (AP ± IP) to provide α/β spectra. The recycle and the interpulse delays were set to 1 s and 60 ms (optimized to 8 Hz; $2\Delta + p_{180} = 1/2^{*n}J_{CH}$, where p_{180} is a selective 180° ^1H pulse). For selective excitation/refocusing, gaussian-shaped 90° and 180° pulses of 10- and 20-ms duration (p_{180}) was applied, respectively. Sine bell-shaped gradients of 1-ms duration (δ) were used, followed by a recovery delay of 100 μs. Gradient ratios for G1:G2:G3:G4:G5:G6 were 80:20.1:17:50:11:33, measured as percentage of the absolute gradient strength of 53.5 G/cm. All experiments were acquired and processed using the echo/anti-echo protocol. Broadband adiabatic pulses were used for all inversion and refocusing 180° ^{13}C pulses. For the selHSQMBC spectrum of Fig. 5A, two scans were accumulated for each one of the 64 t_1 increments. For the J-selHSQMBC spectra of Figs 4 and 6, four scans were accumulated for each one of the 256 t_1 increments using a scaling factor of k=50. In all experiments, the number of data points in t_2 was set to 4096, the spectral windows in both dimensions were 20 000 (F1) and 2000 (F2) Hz, respectively, and the digital resolutions were set to 0.49 and 78.12 Hz, respectively. The overall acquisition time for each IP and AP J-selHSQMBC data was about 22 min, which were added/subtracted in the time domain to provide spin-state selective α/β spectra. Prior to Fourier-transformation of each data, zero filling to 1024 in F1, 8192 points in F2 and a sine squared function in both dimensions were applied. The accuracy of coupling constant magnitudes is limited by the final digital resolution achieved after processing. In the present case, the magnitudes measured from IPAP and E.COSY measurements along the detected F2 dimension are estimated to be ca. ±0.25 Hz. On the other hand, J-resolved measurements made along the indirect F1 dimension are estimated to be ±0.39 Hz, which is calculated from the 19.64-Hz resolution after zero filling and considering the scaling amplification factor.

Acknowledgements

Financial support for this research provided by MICINN (projects CTQ2009-08328 and CTQ2012-32436) is gratefully acknowledged. We also thank Servei de Ressonància Magnètica Nuclear, Universitat Autònoma de Barcelona, for allocating instrument time to this project.

References

[1] a) W. A. Thomas, *Prog. NMR Spec.* **1997**, *30*, 183–207; b) R. H. Contreras and J. E. Peralta, *Prog. NMR Spec.* **2000**, *37*, 321–425.
[2] a) R. T. Williamson, B. L. Márquez, W. H. Gerwick, K. E. Kövér, *Magn. Reson. Chem.* **2000**, *38*, 265–273; b) T. Parella, 2D Methods for the Measurement of Long-Range Proton-Carbon Coupling constants, Multidimensional NMR Methods for the Solution State, Morris, G. A. and Emsley, J. W. (eds). John Wiley & Sons Ltd, Chichester, UK, **2010**, p. 305.
[3] A. Bax, R. Freeman, *J. Am. Chem. Soc.* **1982**, *104*, 1099–1100.
[4] P. Trigo-Mouriño, A. Navarro-Vázquez, J. Ying, R. R. Gil, A. Bax, *Angew. Chem. Intl. Ed.* **2011**, *50*, 7576–7580.
[5] a) K. Furihata and H. Seto, *Tetrahedron Lett.* **1999**, *40*, 6271–6275; b) C. H. Gotfredsen, A. Meissner, J. Ø. Duus and O. W. Sørensen, *Magn. Reson. Chem.* **2000**, 692–695; c) A. Meissner and O. W. Sørensen, *Magn. Reson. Chem.* **2001**, *39*, 49–52; d) R. T. Williamson, B. L. Marquez, W. H. Gerwick, G. E. Martin and V. V. Krishnamurthy, *Magn. Reson. Chem.* **2001**, *39* 127–132; e) K. Furihata, M. Tashiro and H. Seto, *Magn. Reson. Chem.* **2009**, *47*, 814–818.
[6] V. V. Krishnamurthy, J. Magn. *Reson. A* **1996**, *121*, 33–41.
[7] C. Griesinger, O. W. Sørensen, R. R. Ernst. *J. Am. Chem. Soc.* **1985**, *107*, 6394–6396.

[8] a) D. Uhrín, V. Varma, J. R. Brisson, J. Magn, *Reson.* **1996**, *A 119*, 120–124; b) S. Gil, J. F. Espinosa, T. Parella, *J. Magn. Reson.* **2010**, *207*, 312–321.
[9] S. Gil, J. F. Espinosa, T. Parella, *J. Magn. Reson.* **2011**, *213*, 145–150.
[10] J. Sauri, J. F. Espinosa, T. Parella. *Angew. Chem. Intl. Ed.* **2012**, *51*, 3919–3922.
[11] a) J. Sauri and T. Parella, *Magn. Reson. Chem.* **2012**, *50*, 717–721; b) J. Sauri, L. Castañar, P. Nolis, A. Virgili and T. Parella, *J. Magn. Reson.* **2012**, *224*, 101–106.
[12] A. Bax, K. A. Farley, G. S. Walker. *J. Magn. Reson. A* **1993**, *119*, 134–138.
[13] J. R. Tolman, J. H. Prestegard, J. Magn. *Reson. B* **1996**, *112*, 269–274.
[14] Y. Kumaki, K. Hikichi. *Magn. Reson. Chem.* **1999**, *37*, 413–417.
[15] C. Butts, B. Heise, G. Tatolo. *Org. Lett.* **2012**, *14*, 3256–3259.
[16] C. Thiele, W. Bermel. *J. Magn. Reson.* **2012**, *216*, 134–143.
[17] M. Misiak, W. Koźmiński. *Magn. Reson. Chem.* **2009**, *47*, 205–209.
[18] T. Fäcke, S. Berger, J. Magn. *Reson. A* **1996**, *119*, 260–263.
[19] T. Parella, J. Belloc. *J. Magn. Reson.* **2001**, *148*, 78–87.
[20] V. Blechta, F. Del Rio-Portilla, R. Freeman. *Magn. Reson. Chem.* **1994**, *32*, 134–137.
[21] R. A. E. Edden, J. Keeler. *J. Magn. Reson.* **2004**, *166*, 53–68.
[22] C. P. Butts, B. Heise, G. Tatolo. *Org. Letters* **2012**, *14*, 3256–3259.
[23] J. C. Cobas, V. Constantino-Castillo, M. Martín-Pastor, F. del Río-Portillo. *Magn. Reson. Chem.* **2005**, *43*, 843–848.

2. Extension of the results

The experiment has been also tested in the peptide Cyclosporin A (**Fig. 3.08**). Such compounds are very interesting because they usually contain areas in their ^{1}H NMR spectra that are easily recognizable. For instance, all the Hα protons appear in a clearly distinguished region and well differentiated from all the other protons. Furthermore, and very interestingly, such protons are not-mutually coupled. In this way, one can selectively invert all the Hα protons by using a band selective proton pulse, and then selectively invert a specific N-Hβ proton of interest that will evolve along the indirect dimension during the t_1 period.

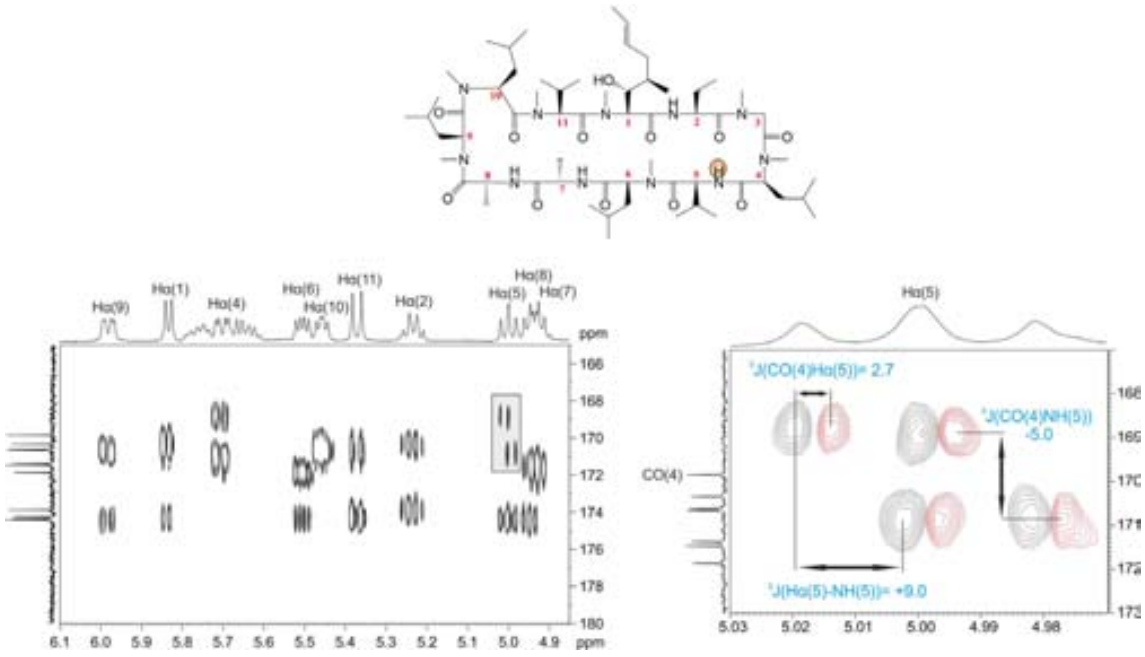

Figure 3.08. On the left it is shown the J-selHSQMBC IP data after selective inversion of all the Ha protons as Hα, and selective inversion of NH-5 as Hb. On the right it is shown and expanded area showing the α/β- spectra corresponding to the Hα5-CO4 cross-peak.

PUBLICATION 8

Straightforward measurement of individual $^{1}J(CH)$ and $^{2}J(HH)$ in diastereotopic CH_2 groups

J. Saurí, L. Castañar, P. Nolis, A. Virgili, T. Parella. *J. Magn. Reson.* 2014, 242, 33–40

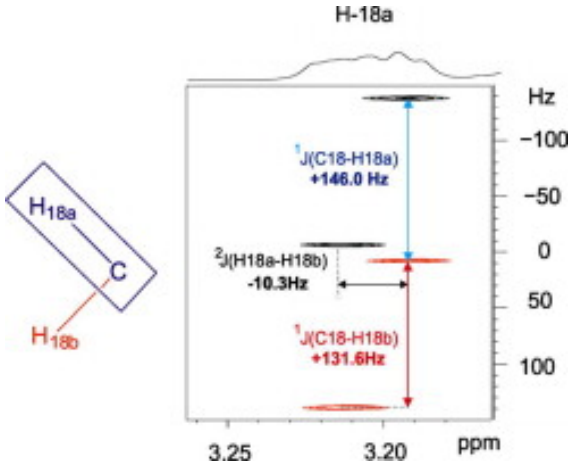

1. Introduction

This publication, unlike the other ones, is based on the HSQC-pulse scheme. Here, a new scheme is proposed for the measurement of individual $^{1}J(CH)$ as well as the magnitude and the sign of geminal proton-proton coupling constants ($^{2}J(HH)$) in diastereotopic methylene groups. The method is based on a F1-coupled HSQC spectra that uses the initial ^{13}C Boltzmann polarization instead of the conventional INEPT transfer. The experiment presented here is able to resolve some of the most important downsides regarding the measurement of coupling constants in such spin systems.

During the last years there has been a significant increase for the measurement of RDCs. In high-resolution NMR spectroscopy under solution conditions (isotropic media) only the information about the chemical shift and the scalar coupling constant is obtained. On the contrary, dipolar and quadrupolar couplings are cancelled over the entire volume of the isotropic sample due to its high translational and vibrational mobility. However, in an ideal anisotropic media (solid), where the sample is slightly aligned with respect to B_0, dipolar couplings can be detected and more structural information obtained. Typically, structural information is obtained from chemical shift, coupling constants and from NOE parameters. However, RDCs can serve as additional tool and, in some cases, they can be a key factor for structural elucidation purposes in bio-molecules[1] and organic compounds[2]. RDCs give information about molecular geometry, like for instance inter-atomic distances, obtaining conformational structure information as well as information about the relative configuration of its diastereotopic centers[3].

Experimentally, RDC's appear as an additional contribution to the conventional signal splitting due to the scalar coupling constant (J) so that, in order to extract them, two different experiments must be acquired: one in an isotropic media (extraction of J), and the other one in an anisotropic media (extraction of J+D). The magnitude of the RDC (D) is measured using the following expression:

$$\mathbf{T = J + D}$$

where T is the total coupling constant measured in the anisotropic sample, J is the scalar coupling constant measured in the isotropic sample, and D is the dipolar coupling constant determined from the above equation. It will be shown that, when the sample is aligned in an anisotropic media, the resulting pulse scheme works very nicely for the measurement of RDCs, such as $^{1}D(CH)$ and $^{2}D(HH)$, in diastereotopic CH_2 groups.

[1] N. Tjandra, A. Bax. *Science*. **1997**, 278, 1111.

[2] C.M. Thiele, S. Berger. *Org. Lett*. **2003**, 5, 705.

[3] V.M. Marathias, G.J. Tawa, I. Goljer, A.C. Bach. *Chirality*. **2007**, 19, 741.

Journal of Magnetic Resonance 242 (2014) 33–40

Contents lists available at ScienceDirect

Journal of Magnetic Resonance

journal homepage: www.elsevier.com/locate/jmr

Straightforward measurement of individual $^1J(CH)$ and $^2J(HH)$ in diastereotopic CH_2 groups

Josep Saurí, Laura Castañar, Pau Nolis, Albert Virgili, Teodor Parella *

Servei de Ressonància Magnètica Nuclear and Departament de Química, Universitat Autònoma de Barcelona, E-08193 Bellaterra, Catalonia, Spain

ARTICLE INFO

Article history:
Received 17 December 2013
Revised 31 January 2014
Available online 12 February 2014

Keywords:
E.COSY
One-bond proton–carbon coupling constants
Two-bond proton–proton coupling constants
Methylene spin systems
Inverse INEPT
Residual dipolar couplings

ABSTRACT

The C–H_A cross-peak corresponding to a diastereotopic CH_AH_B methylene spin system exhibits a characteristic 1:0:1 multiplet pattern along the indirect dimension of a ω_1-coupled HSQC spectrum. It is shown here that the use of the initial ^{13}C Boltzmann polarization instead of the regular INEPT-based ^1H Boltzmann polarization makes visible the central lines of this multiplet pattern. A spin-state-selective method is proposed for the efficient measurement of both $^1J(CH_A)$ and $^1J(CH_B)$ along the indirect dimension of a 2D spectrum as well as to the magnitude and the sign of the geminal $^2J(H_AH_B)$ coupling constant from the straightforward analysis of a single four-component E.COSY cross-peak. Additionally, the extraction of $^1J(CH)$ values for CH and CH_3 multiplicities can be also performed from the same spectrum. The success of the method is also illustrated for the determination of residual dipolar $^1D(CH)$ and $^2D(HH)$ coupling constants in a small molecule weakly aligned in a PMMA swollen gel.

1. Introduction

In recent years, it has appeared an enormous interest for the measurement of scalar and residual dipolar (RDC) one-bond proton–carbon coupling constants ($^1J(CH)$ and $^1D(CH)$, respectively) in small molecules dissolved in weakly aligned anisotropic media [1–3]. HSQC-based pulse schemes have been generally chosen for this purpose and the accuracy and the simplicity on the experimental measurement of $^1J(CH)$ are subjects of discussion. Some topics of recent interest have been (i) the design of general and robust NMR methods that works efficiently for all multiplicities, (ii) the discussion about whether the $^1J(CH)$ splitting should be measured from the direct ω_2 (^1H) or the indirect ω_1 (^{13}C) dimension, (iii) the accurate measurement of $^1J(CH)$ for individual protons in diastereotopic CH_2 or NH_2 groups, or (iv) the simultaneous determination of additional coupling constants from the analysis of the same cross-peak, being the maximum interest the sign-sensitive determination of geminal $^2J(HH)$ values.

The measurement of $^1J(CH)$ from the detected dimension is relatively easy and high levels of digital resolution are readily available. For instance, the CLIP-HSQC experiment prove to be an efficient tool to determine the $^1J(CH)$ value from the resulting clean in-phase doublets [4]. However, strong J(HH) coupling effects can generate a high degree of asymmetry between the high- and low-field multiplet lines in ω_2-coupled HSQC spectra, which can preclude reliable determination of $^1J(CH)$ coupling constants values. In addition, broad signals and/or the large contributions of RDCs can generate poorly defined multiplets that make difficult accurate measurements. These drawbacks have already been described, particularly for CH spin systems in carbohydrates or on the typical strong geminal interaction found in diastereotopic CH_2 spin systems, and some practical solutions have been proposed [5–9]. To avoid such inconveniences, the measurement of $^1J(CH)$ along the ω_1 dimension have been advisable [9,10] although this requires the need for a large number of t_1 increments, and therefore longer acquisition times. The successful use of non-linear uniform sampling, J scaling factors or spectral folding can speed up data acquisition and/or increase the digital resolution in the ω_1 dimension [10].

The accurate measurement of $^1J(CH)$ for individual protons in diastereotopic CH_AH_B (or NH_AH_B) groups is one of the most challenging tasks in this field. Several methods have been proposed that measure them from the ω_1 or ω_2 dimension, but they all present some drawback that can prevent their general use [11–25]. For instance, the passive $^1J(C–H_B)$ value can be separately measured into the active H_A cross-peak, and vice versa, along the ω_1 dimension of a J-resolved HMQC experiment [11]. In addition, the large doublet is further split by the $^2J(H_AH_B)$ coupling yielding a double-doublet. The disadvantage is that additional experiments can

* Corresponding author.
E-mail address: teodor.parella@uab.cat (T. Parella).

http://dx.doi.org/10.1016/j.jmr.2014.02.003
1090-7807/

be needed to measure $^1J(CH)$ for CH or CH_3 spin systems. ^{13}C-edited versions of the 2D ^1H J-resolved experiment have been proposed to resolve enantiomeric derivatives dissolved in anisotropic media by visualizing their different $^1J(CH)$ splitting sizes along the indirect dimension [12,13]. Other related J-resolved HSQC experiments have been also described but they can require time-consuming 3D data acquisition [14] or the collection of multiple 2D J-modulated data [15,16]. An important group of NMR experiments are those based on spin-state selection specifically designed for methylene groups [8,17–25]. Some reported examples should be the P.E.HSQC [8] SPITZE [17] or CH_2-TROSY [19,20] experiments that yield simplified coupling patterns, and where the sign and the magnitude of the geminal $^2J(HH)$ can be additionally extracted. In all these cases, the central lines of the ω_1-multiplet corresponding to a CH_2 group are not observed, and therefore only the sum of the two $^1J(CH)$ can be determined from the indirect dimension.

In the present study, a new 2D ω_1-coupled inverse INEPT experiment (referred to as ω_1-iINEPT) is proposed for the observation of the missing central lines in diastereotopic CH_2 cross-peaks. The resulting cross-peak present a characteristic E.COSY multiplet pattern that facilitates the straightforward measurement of both individual $^1J(CH_A)$ and $^1J(CH_B)$ values, as well as the sign and magnitude of the geminal $^2J(HH)$ coupling. The method starts exclusively from ^{13}C Boltzmann polarization, it is driven with broadband ^{13}C decoupling during ^1H acquisition and, very importantly, also works for CH and CH_3 multiplicities. The experiment is easily adapted for a J-resolved presentation (referred to as ω_1-iINEPT-J) which allows obtain higher levels of resolution within the same experimental time by the use of a reduced spectral width in the indirect dimension [11–13,26,27]. The success of the method is illustrated for several samples and particular cases and as well as for the measurement of small residual coupling constants in small molecules dissolved in a weakly aligned media.

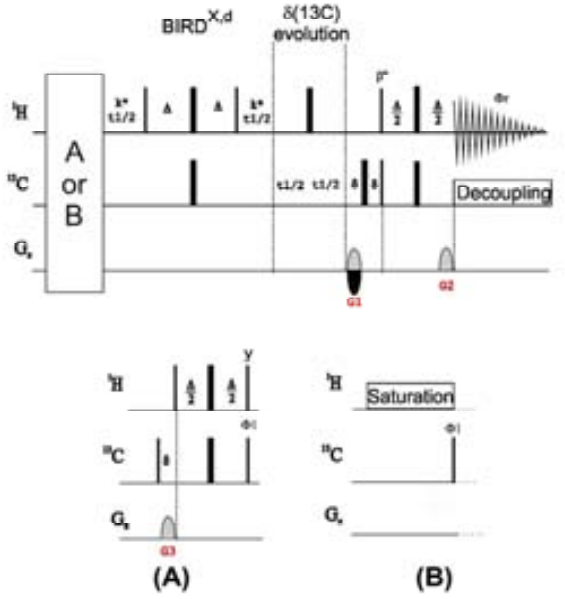

Fig. 1. Pulse sequences for the (A) ω_1-HSQC and (B) ω_1-iINEPT experiments. Thin and thick rectangles represent 90° and 180° rectangular pulses, respectively, applied along the x axis unless indicated differently. A basic two-step phase cycling is applied: $\varphi_1 = x,-x$; $\varphi_{rec} = x,-x$. A small flip angle ($\beta = 36°$) generates E.COSY cross-peaks. Inversion and refocusing 180° ^{13}C pulses can be applied as adiabatic pulses and the element labeled as $\delta(^{13}C)$ evolution period is optional. The inter-pulse delays in INEPT and BIRD elements are optimized according to $\Delta = 1/(2 * {}^1J(CH))$. The echo/anti-echo encoding of ω_1 frequencies was achieved by changing the sign of G1 between successive t_1 increments. The ratio between G1:G2:G3 were 80:20.1:13. The duration of a pulse-field gradient (PFG) and of the subsequent recovery delay amounts to δ.

2. Results and discussion

The idea to develop the ω_1-iINEPT experiment was born from the recent P.E.HSQMBC experiment, which was devised to measure three different $^1J(CH)$, $^2J(HH)$ and a $^nJ(CH)$ coupling constants from a single 2D cross-peak [28]. Other related works that have inspired us were the P.E.HSQC [8] and the BIRD-HSQC [9] experiments, this latter being further refined and evaluated by Thiele and Bermel (see Fig. 1c in Ref. [10]). The basic pulse scheme of the reference ω_1-coupled HSQC (ω_1-HSQC) experiment uses the traditional ^1H Boltzmann polarization as a starting point (Fig. 1A). In the following, we consider an isolated diastereotopic CH_AH_B spin system defined with three different $^1J(CH_A)$, $^1J(CH_B)$ and $^2J(H_AH_B)$ coupling constants. The sequence starts with an initial 90° (^{13}C)-gradient element to remove any contribution coming from the ^{13}C Boltzmann polarization. After the ^1H-to-^{13}C INEPT transfer, anti-phase ^{13}C magnetization is present as a mixture of $2H_{A_z}C_y + 2H_{B_z}C_y$, which evolve under the effects of $^1J(CH)$ and $\delta(^{13}C)$ in a sequential mode, by using separated and synchronously incremented time periods. Thus, the magnetization evolves first under the effect of a $BIRD^{d,X}$ element [29,30] flanked by a variable J-scaled t_1 evolution period (defined by a scaling factor k) to allow the exclusive evolution of $^1J(CH)$ whereas ^{13}C chemical shift and long-range CH contributions are refocused, and then ^{13}C chemical shift can evolve from an optional t_1 evolution period as usual. In the subsequent analysis, the scaling factor, which is set arbitrarily within the limits set by relaxation and/or signal overlapping, the effects of the labeling G1 gradient and the optional ^{13}C chemical shift t_1 evolution period are neglected for the sake of clarity. Thus, for a single H_A spin, the evolution during the variable t_1 BIRD-based period ($k = 1$) is described as:

$$2H_{A_z}C_y[\cos(\pi^1J(CH_A)t_1)\cos(\pi^1J(CH_B)t_1) - \sin(\pi^1J(CH_A)t_1) \times \sin(\pi^1J(CH_B)t_1)] \quad (1)$$

Applying the trigonometric relationship $\cos A\cos B - \sin A\sin B = \cos(A + B)$, we obtain

$$2H_{A_z}C_y\cos(\pi^1J(CH_A + {}^1J(CH_B))t_1) \quad (2)$$

meaning that only the outer lines of the theoretical triplet or double-doublet coupling pattern of the methylene proton cross-peak would be observed and, therefore, only the sum of the both couplings ($^1J(CH_A + {}^1J(CH_B)$) will be observed as an in-phase doublet along the indirect dimension (Fig. 2A) [15]. This dependence with respect to the cosine function makes that multiplet patterns with relative intensities of 1:1 for CH, 1:0:1 for CH_2, and 3:1:1:3 for CH_3 will be displayed along the ω_1 dimension [8,34]. A key feature introduced in the last refocusing INEPT block is the small-flip ^1H pulse angle ($\beta = 36°$) which generates simplified E.COSY multiplet patterns for non-equivalent protons in CH_2 and CH_3 spin systems (Fig. 2B) [8,31–33].

To improve the appearance and usefulness of cross-peaks obtained from ω_1-iINEPT experiments, we propose to start the experiment with the initial ^{13}C Boltzmann polarization instead of the INEPT-based ^1H Boltzmann polarization because this leads to interesting changes in the central lines of methylene cross-peaks, as known for the analogous old ^{13}C-detected heteronuclear J-resolved 2D experiment [35]. The initial 90° ^{13}C pulse, applied after an

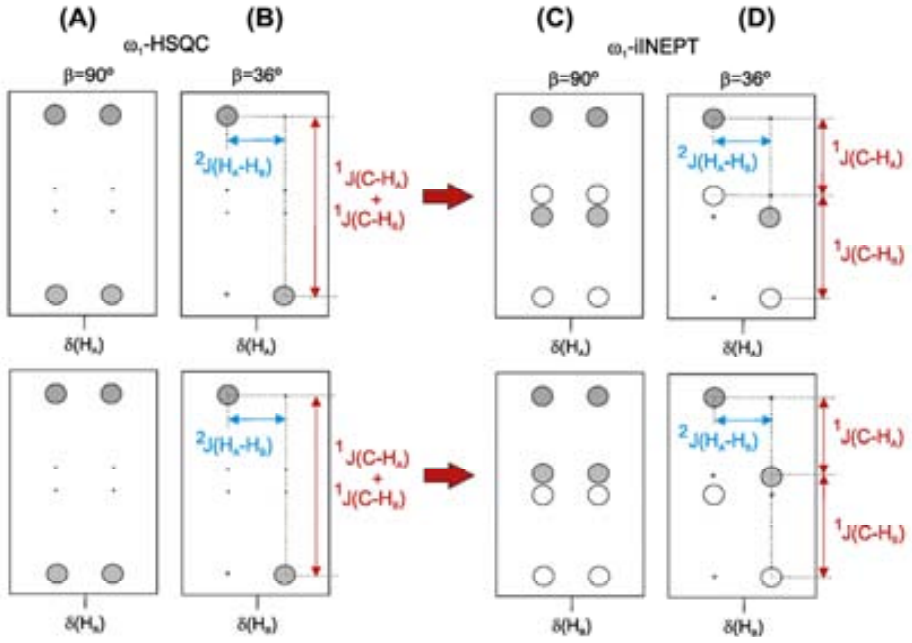

Fig. 2. Schematic representation of the 2D multiplet pattern of each individual H_A and H_B proton belonging to a methylene CH_AH_B group. (A and B) ^{1}H-Boltzmann polarization driven (ω_1-HSQC) experiments using $\beta = 90°$ and 36°, respectively, and (C and D) ^{13}C-Boltzmann polarization driven experiments (ω_1-iINEPT) using $\beta = 90°$ and 36°, respectively. In (D), the magnitude and the sign of all involved couplings (defined as $^2J(H_AH_B)$ and assuming $^1J(CH_A) < {}^1J(CH_B)$) can be readily extracted. Open and dotted circles represent peaks with opposite phase.

heteronuclear NOE enhanced pre-scan period by means of a ^{1}H WALTZ-16 pulse train saturation, generates in-phase $-C_y$ magnetization (Fig. 1B) which evolves under the effect of $^1J(CH)$ during the variable t_1 BIRD-based period:

$$-2H_{Az}C_x[\sin(\pi^1J(CH_A)t_1)\cos(\pi^1J(CH_B)t_1)] - 2H_{Bz}C_x[\cos(\pi^1J(CH_A)t_1)\sin(\pi^1J(CH_B)t_1)] \quad (3)$$

The result is a pure absorptive 2D ω_1-iINEPT spectra displaying double-doublet coupling patterns along the ω_1 dimension for each individual H_A or H_B cross-peaks, that initially would consist of eight different components as shown in Fig. 2C. Analyzing only the H_A spin, it will show an anti-phase doublet pattern with respect to $^1J(CH_A)$ (sine modulated) and an additional in-phase doublet pattern with respect to $^1J(CH_B)$ (cosine modulated) along the ω_1 dimension. As discussed before, the effect to apply a small flip angle ($\beta = 36°$) will generate a simplified four-component cross-peak with a characteristic E.COSY multiplet pattern due to the mutual $^2J(H_AH_B)$ (Fig. 2D), which facilites both the multiplet interpretation and analysis (see Fig. S1; supporting information). Thus, the active $^1J(CH_A)$ coupling is directly extracted from the anti-phase 1:−1 pattern along the same column in ω_1, whereas the passive $^1J(CH_B)$ coupling can be also extracted directly by measuring the in-phase components in each part of the E.COSY pattern. Otherwhise, the sign and the magnitude of $^2J(HH)$ is easily extracted from the frequency separation between tilted peaks along the w2 dimension. Fig. 2 summarizes the expected cross-peak pattern for a single diastereotopic CH_AH_B proton using the different ω_1-HSQC and ω_1-iINEPT approaches with $\beta = 90°$ and 36°. For CH groups, a doublet with relative 1:−1 intensities is obtained whereas a 1:1:−1:−1 coupling pattern will be displayed for a CH_3 group.

As a first example, Fig. 3A and B shows the equivalent ω_1-HSQC and ω_1-iINEPT correlation spectra, respectively, of strychnine (**1** in Scheme 1) acquired with the pulse schemes of Fig. 1, under the same experimental conditions and using a scaling factor of $k = 8$. The general coupling pattern for individual CH and CH_2 groups are marked with highlighted boxes. CH cross-peaks present the same doublet structure in both approaches. On the other hand, whereas the central lines for each individual CH_2 cross-peak are absent in the ω_1-HSQC spectrum, they are clearly distinguished in the ω_1-iINEPT version. A close inspection of the multiplet patterns for CH_2 cross-peaks in both spectra reveals the simplified E.COSY multiplet structure as described in other related experiments [8,19]. Also note the different in-phase *vs* anti-phase pattern behavior along the indirect dimension, although this is not relevant for the measurement. In cases where chemical shift assignment is already known and/or signal overlapping is not severe, the proposed method can be recorded in a J-resolved mode by simple omission of the ^{13}C chemical shift evolution period ($t_{1/2} - 180°(^1H) - t_{1/2}$). In this way the spectral width in the indirect dimension could be reduced by a factor of about 40, from 20,000 Hz (160 ppm at 500 MHz) to 500 Hz, and therefore the spectral resolution in ω_1 should be improved by a similar factor if all other experimental conditions remain the same. Fig. 3C and D shows the equivalent ω_1-HSQC-J and ω_1-iINEPT-J spectra, respectively, acquired with the same number of t_1 increments and using an scaling factor of $k = 1$. It can be observed that the absence of ^{13}C chemical shift signal dispersion does not introduce a serious problem on severe signal overlapping in a small molecule like **1**. where all cross-peaks can be succesfully analyzed. All the discussion and conclusions described in Ref. [10] about the application of non-linear sampling to accelerate data acquisition and/or to increase digital resolution in the indirect dimension could

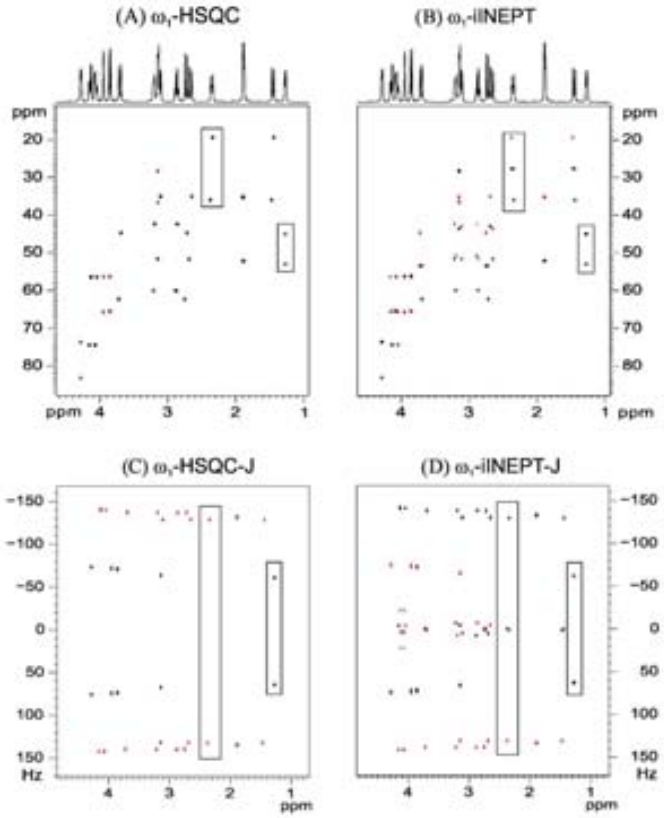

Fig. 3. 2D ^{1}H–^{13}C spectra of **1** acquired with the pulse sequences of Fig. 1. (A) ω_1-HSQC and (C) ω_1-HSQC-J spectra were obtained starting from ^{1}H Boltzmann magnetization, and (B) ω_1-ilNEPT and (D) ω_1-ilNEPT-J spectra were achieved starting from ^{13}C Boltzmann magnetization. (A) and (B) are heteronuclear correlation maps (acquired with an scaling factor of $k = 8$) whereas (C) and (D) are the corresponding J-resolved versions (scaling factor $k = 1$ and omission of the ^{13}C chemical shift t_1 evolution period). All spectra were acquired and processed under the same experimental conditions. 2 scans were collected for each one of the 256 t_1 increments using a pre-scan delay of 3 s. Squared boxes mark specific CH and diastereotopic CH_2 cross-peak as examples in each spectrum.

be extrapolated here for the proposed methods. Further increase of resolution by a factor of 3 can be additionally achieved by allowing signal folding in the indirect dimension (see Fig. S2 in the supporting information for an example provided using a reduced spectral width of 180 Hz).

Fig. 4 shows an expanded area of the 2D ω_1-ilNEPT-J spectrum, where the clean tilt, the straightforward analysis and the excellent resolution of the resulting peak patterns can be quickly observed. Note the perfect equivalence between the cross peaks of diastereotopic protons (for instance H-18a *vs* H-18b or H-11a *vs* H-11b) which permit the easy and direct measurement of the same three different involved couplings (^{1}J(CH$_A$) and ^{1}J(CH$_B$) as well as the geminal ^{2}J(HH)) from two independent cross-peaks. The comparison of the experimental J values extracted from these two different measurements evaluates the accuracy of the measurement, and also ensures the measurement of all couplings even in the case of accidental signal overlapping of one of the two diastereotopic proton prevents its analysis. For well resolved ^{2}J(HH) values, the difference between diastereotopic ^{1}J(CH) values is quickly ascertained from the relative displacement between the two central lines and accurate ^{1}J(CH) values can be easily measured even in the case of minor differences between ^{1}J(CH$_A$) and ^{1}J(CH$_B$). For instance, whereas a small difference smaller than 2 Hz is measured for the H-15a/H-15b pair, a big difference about 14.5 Hz is found for H-18a/H-18b. Experimental ^{1}J(CH) and ^{2}J(HH) data extracted from these spectra for compound **1** are in agreement with those reported previously in other works (see Table S1 in the supporting information) [5,36–39]. Even in the case of signal overlapping, CH cross-peaks can be easily distinguished from those of CH_2 groups by their different doublet or double-doublet coupling patterns and also from the relative opposite phase of the anti-phase components for CH/CH_3 and CH_2 groups because the BIRD element acts as a multiplicity-editing element. For instance, note the clear distinction and straightforward measurement that can be performed for the three different protons resonating close to 3.1–3.2 ppm.

When two diastereotopic protons have similar chemical shift and ^{1}J(CH) values, the central lines can be partially or completely cancelled, as shown for the H-17a/H-17b protons resonating at 1.9 ppm in Fig. 3D. Another special case is when the geminal ^{2}J(HH) is near to 0 Hz, where the distinction of the four E.COSY components will depend of the different ^{1}J(CH) sizes. One illustrative example is the H-8a and H-8b olefinic protons belonging to the exocyclic CH_2 group in 5-methylene-2-norbornene (**2**) (Fig. 5A) which present unresolved signals in the conventional ^{1}H spectrum, and where the mutual ^{2}J(H8a–H8b) coupling can not be directly measured. The well differentiated four components observed in the ω_1-ilNEPT-J spectra allow a measurement of ^{2}J(HH) = +1.1 Hz,

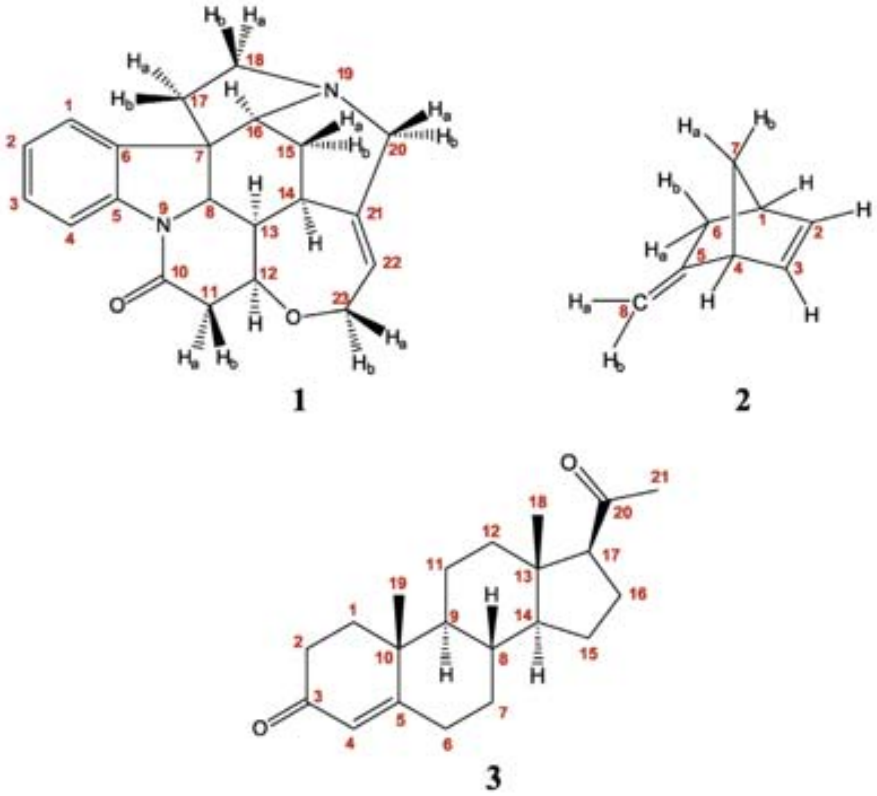

Scheme 1. Molecules used in this work.

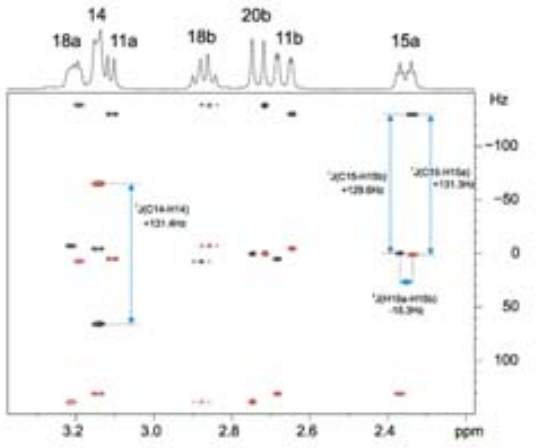

Fig. 4. Expanded area corresponding to the ω_1-iINEPT-J spectrum of Fig. 3D, where the different multiplet patterns for a CH group and several diastereotopic CH_2 spin systems can be clearly visualized and analyzed, and all $^1J(CH)$ and $^2J(HH)$ can be measured with simplicity and accuracy.

where the positive sign can be determined by comparison with the opposite E.COSY tilt presented by other diastereotopic H-6 and H-7 methylene protons, which have large negative $^2J(HH)$ values of −15.3 Hz and −8.1 Hz, respectively. Although there are small differences between the two central lines, the measurement of each individual $^1J(CH)$ (155.1 *vs* 157.1 Hz) can be performed twice, independently from each cross-peak and with a minimal deviation of ±0.1 Hz (Table S2; supporting information).

The simplicity of the proposed ω_1-iINEPT methods make them highly interesting for the measurement of small $^1D(CH)$ and $^2D(HH)$ RDCs, by comparison the difference between experimental measurements performed in isotropic *vs* anisotropic conditions ($D = T_{[aniso]} - J_{[iso]}$)). Compound **2** was weakly aligned in a poly(-methyl methacrylate) (PMMA) gel swollen in $CDCl_3$ using the reversible compression/relaxation method [40] , and $^1D(CH)$ and $^2D(HH)$ RDCs magnitudes and signs could be easily determined for all signals (see Fig. S3C; supporting information). Fig. 5 compares some cross-peaks obtained in both isotropic and anisotropic conditions. It can be seen how the relative orientation of each diastereotopic HH pair is clearly differentiated from their $^2D(HH)$ values: −0.2 Hz for H-8a/H-8b protons, −4.1 Hz for H-6a/H-6b protons and +3.1 Hz for H-7a/H-7b protons. A list of all measured scalar and residual dipolar coupling constants can be found in Table S2 of the supporting information.

The last example corresponds to a molecule having a more complex ^1H spectrum, progesterone (**3**), with high levels of signal overlapping in its aliphatic region. Fig. 6 shows an expanded area of the ω_1-iINEPT spectrum, where cross-peaks for all multiplicites can be distinguished and the corresponding $^1J(CH)$ and $^2J(HH)$ values conveniently measured (see Table S3 in the supporting information). For instance, note the excellent signal dispersion and multiplet editing for the five resonances fully overlapped in the 1.5–1.65 ppm area. Accidental overlapping of multiplet components

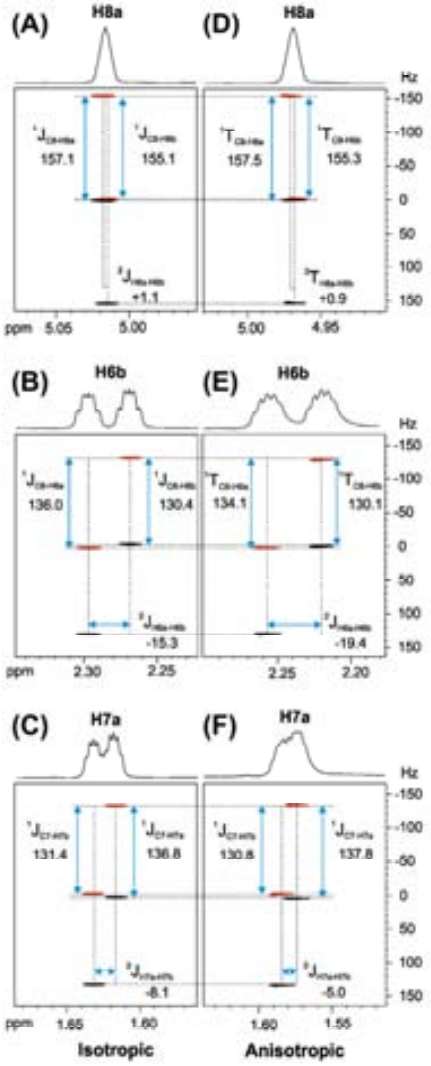

Fig. 5. Some illustrative 2D cross-peaks extracted from the ω_1-ilNEPT-J spectra of **2** showing the easy measurement of the experimental $^1J(CH)/^1T(CH)$ and $^2J(HH)/^2T(HH)$ values measured in (A–C) isotropic ($CDCl_3$) and (D–F) anisotropic (weakly aligned in PMMA gel swollen in $CDCl_3$) conditions. Similar values for the same couplings are also measured from the cross-peaks of the other diastereotopic protons (see a complete set of coupling values in Table S2 in the Supporting information).

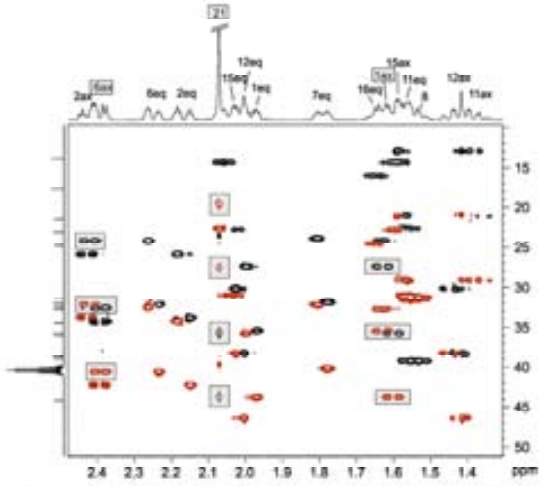

Fig. 6. Expanded area of the 2D ω_1-ilNEPT spectrum of **3** acquired with 4 scans for each one of the 256 t_1 increments, and using a pre-scan delay of 3 s. Boxes enhance the different components corresponding to the H-6ax and H-1ax protons. In addition, the 1:1:−1:−1 multiplet corresponding to the methyl group 21 (at 2.08 ppm) is also highlighted.

can be overcomed by using the J-resolved version or by changing the scaling factor. The diastereotopicity in the three protons belonging to a methyl groups is not observed and they usually appear as a singlet due to their free rotation under isotropic conditions. However, in analogy with the discussion presented here for diastereotopic CH_2 spin systems, the same conclusions could be extracted from the analysis of a hypothetical non-equivalent protons in a CH_3 group [8,41]. Whereas isotropic CH_3 cross-peaks with no distinction between equivalent protons present a typical 3:1:1:3 multiplet pattern in ω_1-HSQC experiments [34], they display a symmetrical 1:1:−1:−1 coupling pattern in the ω_1-ilNEPT, as seen for the Me-21 in Fig. 6. A modified HSQC experiment has been reported to recover the 1:2:1 and 1:3:3:1 pattern in NH_2 and NH_3^+ groups, respectively, and spin-state selected methods to study analysis have been used to study differential relaxation of the different line multiplets of methyl cross-peaks in proteins [41].

In terms of sensitivity, the ω_1-ilNEPT experiment present a sensitivity decrease when compared to the analog ω_1-HSQC experiment, because of the differential signal enhancement achieved by heteronuclear polarization transfer via INEPT or by heteronuclear NOE effects. In addition, the pre-scan delay must be optimized as a function to the longer ^{13}C T_1 values, although that protonated carbons relax relatively fast. Our experimental data confirms such theoretical prediction and signal-to-noise enhancements by a factor of about 3 and 4 can be achieved for ω_1-ilNEPT and ω_1-HSQC experiments, respectively, when compared with a reference non signal-enhanced ω_1-ilNEPT experiment acquired without proton saturation and a pre-scan delay of 3 s (see Fig. S4 in the supporting information). Although the proposed methodology could distinguish diastereotopic protons in NH_2 groups, the large difference in sensitivity enhancement achieved by polarization transfer when compared with those obtained by direct ^{15}N Boltzmann magnetization without NOE enhancement (a theoretical factor about 10) makes the experiment of limited practical use due to its very low sensitivity. In addition, the two central lines are likely to be quite broad for large molecules.

In summary, a general and simple NMR method to obtain a characteristic spin-state-selected multiplet pattern for diastereotopic CH_AH_B methylene systems has been described. The magnitude and the sign of the three involved coupling values ($^1J(CH_A)$, $^1J(CH_B)$ and $^2J(H_AH_B)$) can be measured simultaneously from the analysis of a single and clean four-component E.COSY cross-peak. The method also measures $^1J(CH)$ for all other carbon multiplicities, and it is easily adapted for a J-resolved representation that allows the use of a more reduced spectral width in the carbon dimension, obtaining higher levels of resolution within the same experimental time. We have also shown that small $^1D(CH)$ and $^2D(HH)$ RDCs can be measured for small molecules weakly aligned in anisotropic media. The proposed techniques are appropriate for routine use because require minimum set-up and afford simple data analysis and interpretation.

3. Methods and materials

The isotropic samples used in this work were 0.12 M strychnine dissolved in $CDCl_3$ (**1**), 0.14 M 5-methylene-2-norbornene dissolved in $CDCl_3$ (**2**) and 0.13 M progesterone dissolved in DMSO (**3**) (see chemical structures in Scheme 1). For the measurement of RDCs, 10 mg of **2** was aligned in a poly(methyl methacrylate) (PMMA) gel swollen in $CDCl_3$ using the reversible compression/relaxation method [40]. The ^{2}H quadrupolar splitting ($\Delta\nu Q$) for the $CDCl_3$ signal was of 24 Hz. NMR experiments on **1** and **3** were recorded on a BRUKER DRX-500 spectrometer equipped with a 3-channel 5-mm cryoprobe incorporating a z-gradient coil. NMR experiments on **2** were carried out in a Bruker Avance 600 spectrometer equipped with a TXI HCN z-grad probe. The temperature for all measurements was set to 298 K.

In all experiments, the inter-pulse Δ ($=1/(2*{}^1J(CH))$ delays were set to 3.5 ms (optimized to $^1J(CH)=145$ Hz). Gradient ratios for G1:G2:G3 were set to 80:20.1:13, measured as percentage of the absolute gradient strength of 53.5 G/cm. Sine bell shaped gradients of 1 ms of duration and followed by a recovery delay of 100 μs were used. ^{1}H saturation during the entire pre-scan delay was accomplished applying a 2.5 kHz WALTZ-16 modulated pulse train. Broadband ^{13}C decoupling during acquisition was achieved applying a 8 kHz GARP modulated pulse train. All experiments were acquired and processed using the echo/anti-echo protocol where the gradient G1 was inverted for every second FID. An scaling factor $k=8$ were used for the correlation experiments for all compounds. The J-resolved spectra were acquired omitting the $t_{1/2}-180(^1H)-t_{1/2}$ element in the pulse sequence of Fig. 1 and reducing the spectral width in the indirect ω_1 dimension to 500 Hz.

For spectra of Figs. 3, 2 scans were accumulated for each one of the 256 t_1 increments and the number of data points in t_2 was set to 2048. The recycle delay was set to 1 s for ω_1-HSQC type experiments (Fig. 3A and C) and 3 s for ω_1-ilNEPT type experiments (Fig. 3B and D). Spectra 3A and 3B were acquired with an spectral window of 5000 Hz (in ω_2) and 20,000 Hz (in ω_1) giving a FID resolution of 2.4 and 9.8 Hz, respectively. Prior to Fourier-transformation of each data, zero filling to 4096 in ω_2, 1024 in ω_1 and a π/2-shifted sine-squared window function in both dimensions were applied. After applying zero filling the digital resolution was 1.2 and 2.4 Hz, respectively. In spectra of Figs. 3C and 3D, the spectral window in ω_1 dimension was reduced to 500 Hz giving a FID resolution of 2.4 Hz (in ω_2) and 1.9 Hz (in ω_1). After applying zero filling the digital resolution was 1.2 and 0.5 Hz, respectively.

In the ω_1-ilNEPT-J experiments recorded on **2** in isotropic and anisotropic media (Fig. 5), a recycle delay of 3 s was used, 4 scans were accumulated for each one of the 256 t_1 increments and the number of data points in t_2 was set to 2048. Both of them were acquired with an spectral window of 3600 Hz (in ω_2) and 500 Hz (in ω_1) giving a FID resolution of 1.8 and 1.9 Hz, respectively. Prior to Fourier-transformation of each data, zero filling to 4096 in ω_2, 1024 in ω_1 and a π/2-shifted sine-squared window function in both dimensions were applied. After applying zero filling the digital resolution was 0.9 and 0.5 Hz, respectively. In the ω_1-ilNEPT experiment recorded on **3** (Fig. 6), a recycle delay of 3 s was used, 4 scans were recorded for each one of the 256 t_1 increments and the number of data points in t_2 was set to 2048 in all the experiments. Data were acquired with an spectral window of 2000 Hz (in ω_2) and 12,500 Hz (in ω_1) giving a FID resolution of 1.0 and 6.1 Hz, respectively. Prior to Fourier-transformation of each data, zero filling to 4096 in ω_2, 1024 in ω_1 and a π/2-shifted sine-squared window function in both dimensions were applied. After applying zero filling the digital resolution was 0.5 and 1.5 Hz, respectively.

Acknowledgments

Financial support for this research provided by MINECO (project CTQ2012-32436) is gratefully acknowledged. Authors thanks to R.R. Gil and A. Navarro-Vázquez for a sample of PMMA gel. We also thank the Servei de Ressonància Magnètica Nuclear, Universitat Autònoma de Barcelona, for allocating instrument time to this project.

Appendix A. Supplementary material

Supplementary data associated with this article can be found, in the online version, at http://dx.doi.org/10.1016/j.jmr.2014.02.003.

References

[1] C.M. Thiele, Residual dipolar couplings (RDCs) in organic structure determination, Eur. J. Org. Chem. (2008) 5673–5685.
[2] G. Kummerlowe, B. Luy, Residual dipolar couplings for the configurational and conformational analysis of organic molecules, Annu. Rep. NMR Spectrosc. 68 (2009) 193–230.
[3] G. Kummerlowe, B. Luy, Residual dipolar couplings as a tool in determining the structure of organic molecules, Trend Anal. Chem. 28 (2009) 483–493.
[4] A. Enthart, J.C. Freudenberger, J. Furrer, H. Kessler, B. Luy, The CLIP/CLAP HSQC: pure absorptive spectra for the measurement of one-bond couplings, J. Magn. Reson. 192 (2008) 314–322.
[5] C.M. Thiele, Simultaneous assignment of all diastereotopic protons in strychnine using RDCs: PELG as alignment medium for organic molecules, J. Org. Chem. 69 (2004) 7403–7413.
[6] B.W. Yu, H. van Ingen, S. Vivekanandan, C. Rademacher, S.E. Norris, D.I. Freedberg, More accurate ^{1}JCH coupling measurement in the presence of ^{3}JHH strong coupling in natural abundance, J. Magn. Reson. 215 (2012) 10–22.
[7] B.W. Yu, H. van Ingen, D.I. Freedberg, Constant time INEPT CT-HSQC (CT)-CT-HSQC) – a new NMR method to measure accurate one-bond J and RDCs with strong 1H–1H couplings in natural abundance, J. Magn. Reson. 228 (2013) 159–165.
[8] P. Tzvetkova, S. Simova, B. Luy, P.E. HSQC: a simple experiment for the simultaneous and sign-sensitive measurement of (^{1}JCH + DCH) and (^{3}JHH + DHH) couplings, J. Magn. Reson. 186 (2007) 193–200.
[9] K. Fehér, S. Berger, K.E. Kövér, Accurate determination of small one-bond heteronuclear residual dipolar couplings by F1 coupled HSQC modified with a G-BIRD(r) module, J. Magn. Reson. 163 (2003) 340–346.
[10] C.M. Thiele, W. Bermel, Speeding up the measurement of one-bond scalar (1J) and residual dipolar couplings (1D) by using non-uniform sampling (NUS), J. Magn. Reson. 216 (2012) 134–143.
[11] K.E. Kövér, K. Fehér, Measurement of one-bond heteronuclear dipolar coupling contributions for amine and diastereotopic protons, J. Magn. Reson. 168 (2004) 307–313.
[12] L. Ziani, J. Courtieu, D. Merlet, Visualisation of enantiomers via insertion of a BIRD module in X-H correlation experiments in chiral liquid crystal solvent, J. Magn. Reson. 183 (2006) 60–67.
[13] U.R. Prabhu, S.R. Chaudhari, N. Suryaprakash, Visualization of enantiomers and determination of homo- and hetero-nuclear residual dipolar and scalar couplings: the natural abundant ^{13}C edited J/D-resolved NMR techniques, Chem. Phys. Lett. (2010) 334–341.
[14] J. Furrer, M. John, H. Kessler, B. Luy, J-spectroscopy in the presence of residual dipolar couplings: determination of one-bond coupling constants and scalable resolution, J. Biomol. NMR 37 (2007) 231–243.
[15] M. Ottiger, F. Delaglio, J.L. Marquardt, N. Tjandra, A. Bax, Measurement of Dipolar Couplings for methylene and methyl sites in weakly oriented macromolecules and their use in structure determination, J. Magn. Reson. 124 (1998) 365–369.
[16] T.N. Pham, T. Liptaj, K. Bromek, D. Uhrin, Measurement of small one-bond proton-carbon residual dipolar coupling constants in partially oriented ^{13}C natural abundance oligosaccharide samples. Analysis of heteronuclear ^{1}JCH-modulated spectra with the BIRD inversion pulse, J. Magn. Reson. 157 (2002) 200–209.
[17] T. Carlomagno, W. Peti, C. Griesinger, A new method for the simultaneous measurement of magnitude and sign of ^{1}DCH and ^{1}DHH dipolar couplings in methylene groups, J. Biomol. NMR 17 (2000) 99–109.
[18] P. Permi, A spin-state-selective experiment for measuring heteronuclear one-bond and homonuclear two-bond couplings from an HSQC-type spectrum, J. Biomol. NMR 22 (2002) 27–35.
[19] E. Miclet, D.C. Williams Jr., G.M. Clore, D.L. Bryce, J. Boisbouvier, A. Bax, Relaxation-optimized NMR spectroscopy of methylene groups in proteins and nucleic acids, J. Am. Chem. Soc. 126 (2004) 10560–10570.
[20] G. Guichard, A. Violette, G. Chassaing, E. Miclet, Solution structure determination of oligoureas using methylene spin state selective NMR at ^{13}C natural abundance, Magn. Reson. Chem. 46 (2008) 918–924.

[21] T. Parella, M. Gairí, Simultaneous recording of spin-state-selective NMR spectra for different I_nS spin systems, J. Am. Chem. Soc. 126 (2004) 9821–9826.
[22] P. Permi, Two simple NMR experiments for measuring dipolar couplings in asparagine and glutamine side chains, J. Magn. Reson. 153 (2001) 267–272.
[23] E. Miclet, E. O'Neil-Cabello, E.P. Nikonowicz, D. Live, A. Bax, ^3H–^1H dipolar couplings provide a unique probe of RNA backbone structure, J. Am. Chem. Soc. 125 (2003) 15740–15741.
[24] P. Nolis, J.F. Espinosa, T. Parella, Optimum spin-state-selection for all multiplicities in the acquisition dimension of the HSQC experiment, J. Magn. Reson. 180 (2006) 39–50.
[25] P. Nolis, T. Parella, Solution-state NMR experiments based on heteronuclear cross-polarization, Curr. Anal. Chem. 3 (2007) 47–68.
[26] M. Liu, R.D. Farrant, J.M. Gillam, J.K. Nicholson, J.C. Lindon, Selective inverse-detected long-range heteronuclear *J*-resolved NMR spectroscopy and its application to the measurement of ^3JCH, J. Magn. Reson. B 109 (1995) 275–283.
[27] K. Kobzar, H. Kessler, B. Luy, Stretched gelatin gels as chiral alignment media for the discrimination of enantiomers by NMR spectroscopy, Angew. Chem. Int. Ed. 44 (2005) 3145–3147.
[28] J. Saurí, L. Castañar, P. Nolis, A. Virgili, T. Parella, P.E. HSQMBC: simultaneous measurement of proton–proton and proton–carbon coupling constants, J. Magn. Reson. 224 (2012) 101–106.
[29] J.R. Garbow, D.P. Weitekamp, A. Pines, Bilinear rotation decoupling of homonuclear scalar interactions, Chem. Phys. Lett. 93 (1982) 504–509.
[30] D. Uhrín, T. Liptaj, K.E. Kövér, Modified BIRD pulses and design of heteronuclear pulse sequences, J. Magn. Reson. A 101 (1993) 41–46.
[31] C. Griesinger, O.W. Sørensen, R.R. Ernst, Two-dimensional correlation of connected NMR transitions, J. Am. Chem. Soc. 107 (1985) 6394–6396.
[32] L. Mueller, P.E-COSY, a simple alternative to E.COSY, J. Magn. Reson. 72 (1986) 191–196.
[33] C. Griesinger, O.W. Sørensen, R.R. Ernst, Practical aspects of the E.COSY technique. Measurement of scalar spin-spin coupling constants in peptides, J. Magn. Reson. 75 (1987) 474–492.
[34] Y. Takayama, D. Sahu, J. Iwahara, Observing in-phase single-quantum ^{15}N multiplets for NH_2/NH_3^+ groups with two-dimensional heteronuclear correlation spectroscopy, J. Magn. Reson. 194 (2008) 313–316.
[35] W.P. Aue, L. Muller, R.R. Ernst, Phase separation in two-dimensional spectroscopy, J. Magn. Reson. 28 (1977) 29–39.
[36] B. Luy, K. Kobzar, H. Kessler, An easy and scalable method for the partial alignment of organic molecules for measuring residual dipolar couplings, Angew. Chem. Int. Ed. 43 (2004) 1092–1094.
[37] A. Bagno, F. Rastrelli, G. Saielli, Toward the complete prediction of the ^1H and ^{13}C NMR spectra of complex organic molecules by DFT methods: application to natural substances, Chem. Eur. J. 12 (2006) 5514–5525.
[38] M. Misiak, W. Kożmiński, Determination of heteronuclear coupling constants from 3D HSQC-TOCSY experiment with optimized random sampling of evolution time space, Magn. Reson. Chem. 47 (2009) 205–209.
[39] J.C. Cobas, V. Constantino-Castillo, M. Martin-Pastor, F. del Río Portilla, A two-stage approach to automatic determination of 1H NMR coupling constants, Magn. Reson. Chem. 43 (2005) 843–848.
[40] C. Gayathri, N.V. Tsarevsky, R.R. Gil, RDCs analysis of small molecules made easy: fast and tuneable alignment by reversible compression/relaxation of reusable PMMA gels, Chem. Eur. J. 16 (2010) 3622–3626.
[41] G. Kontaxis, A. Bax, Multiplet component separation for measurement of methyl ^{13}C–^1H dipolar couplings in weakly aligned proteins, J. Biomol. NMR 20 (2001) 77–82.

Straightforward measurement of individual $^{1}J(CH)$ and $^{2}J(HH)$ in diastereotopic CH_2 groups.

Josep Saurí, Laura Castañar, Pau Nolis, Albert Virgili and Teodor Parella*

Supporting Information

Figure S1: Effect of the β angle in ω_1-iINEPT-J experiments.

Figure S2: Spectral Folding in ω_1-iINEPT-J experiment.

Figure S3: ω_1-iINEPT and ω_1-iINEPT-J spectra of 5–methylene-2-norbornene in isotropic and anisotropic media.

Figure S4: Intensity signal dependence with respect the pre-scan delay in ω_1-iINEPT and ω_1-HSQC experiments

Table S1: $^1J(CH)$ and $^2J(HH)$ coupling constants of strychnine measured from ω_1-iINEPT-J spectra and other published methods.

Table S2: $^1J(CH)/^1T(CH)$ and $^2J(HH)/^2T(HH)$ coupling constants of 5-methylene-2-norbornene measured from ω_1-iINEPT-J spectra.

Table S3: $^1J(CH)$ and $^2J(HH)$ coupling constants of progesterone measured from ω_1-iINEPT and ω1-HSQC spectra.

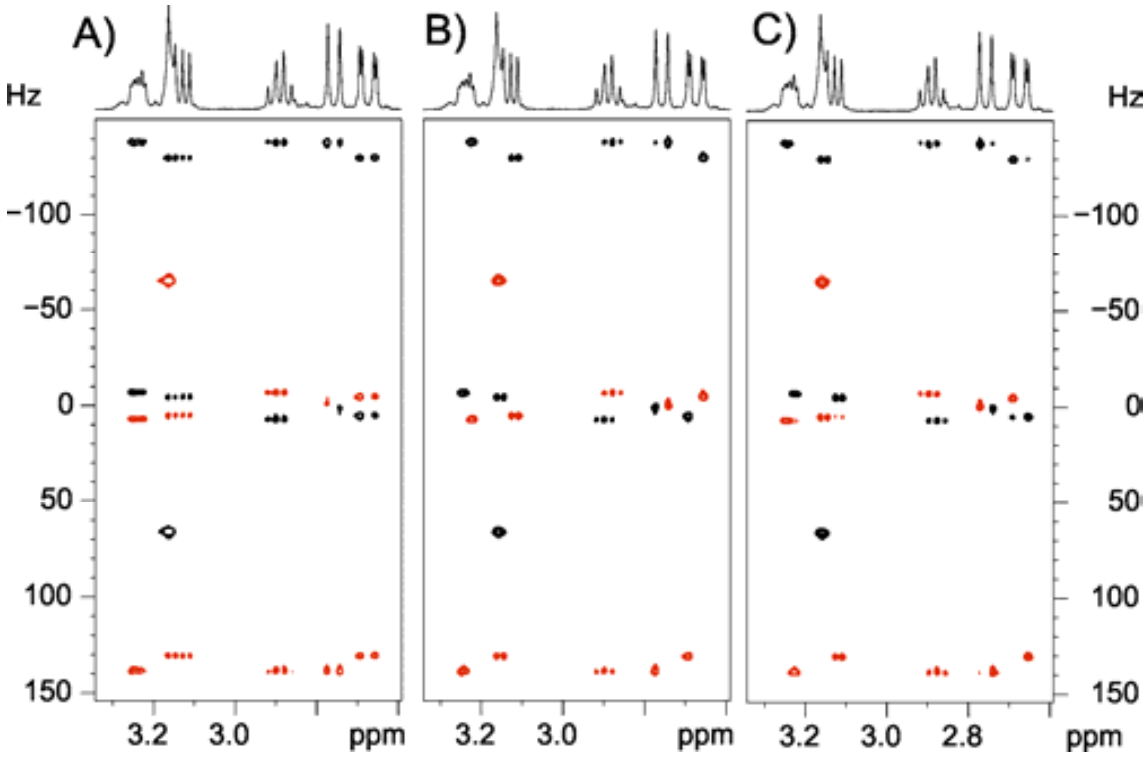

Figure S1: Effect of the β angle in ω_1-iINEPT-J experiments of **1**: A) β=90º, B) β=36º, and C) β=126º. Note the complementary spin-state selection in B *vs* C. Experimental conditions as described for Fig. 3D.

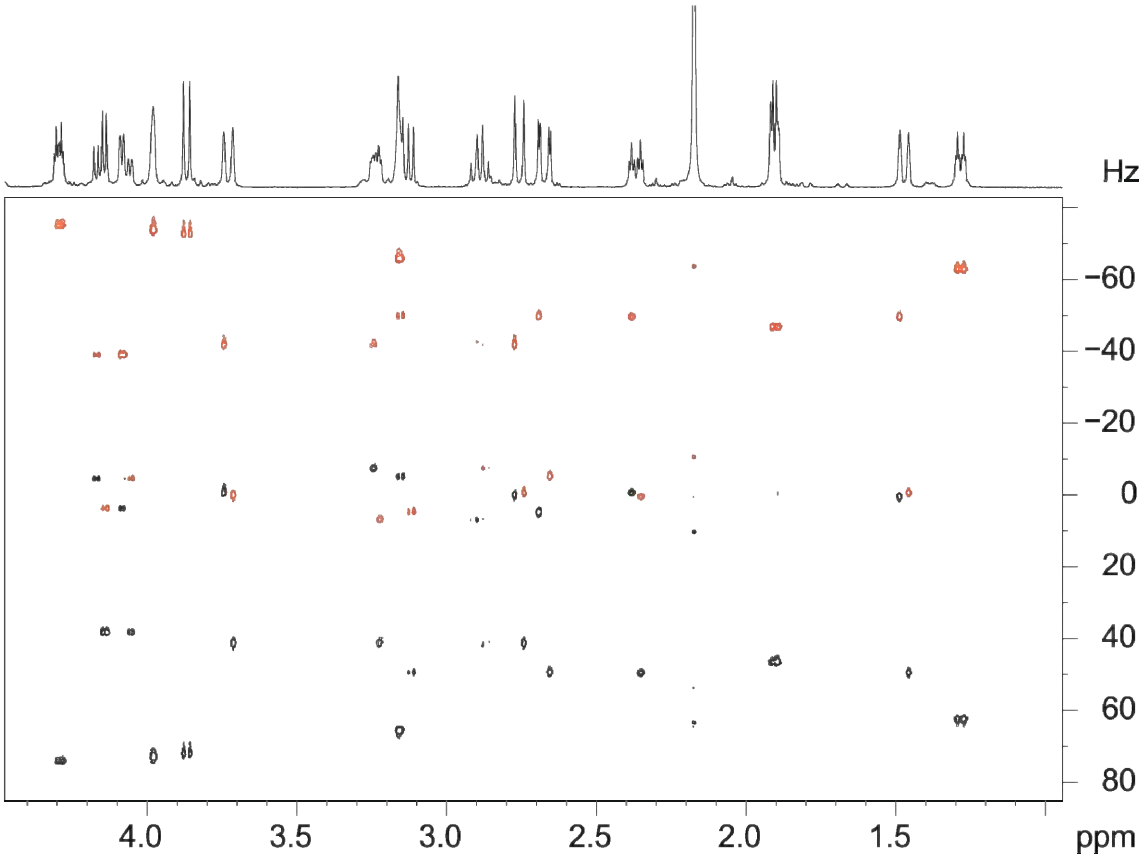

Figure S2: Spectral folding in the ω_1-iINEPT-J spectrum of **1**. 2 scans were collected for each one of the 256 t_1 increments using a spectral width (SW(F1)) of 180Hz in the indirect dimension. The digital resolution was of 0.18 Hz in the indirect dimension. All other experimental conditions as described in the Fig. 3D. ^{1}J(CH) coupling values are extracted from the relationship SW(F1)-$\Delta\nu(\omega_1)$, where $\Delta\nu(\omega_1)$ is the distance measured between individual components of a given cross-peak along the indirect dimension. Similarly, the distance between outer components allows to obtain the sum of the two coupling values, according to $^1J(CH_A)+{}^1J(CH_B)=2*SW(F1)-\Delta\nu(F1)$.

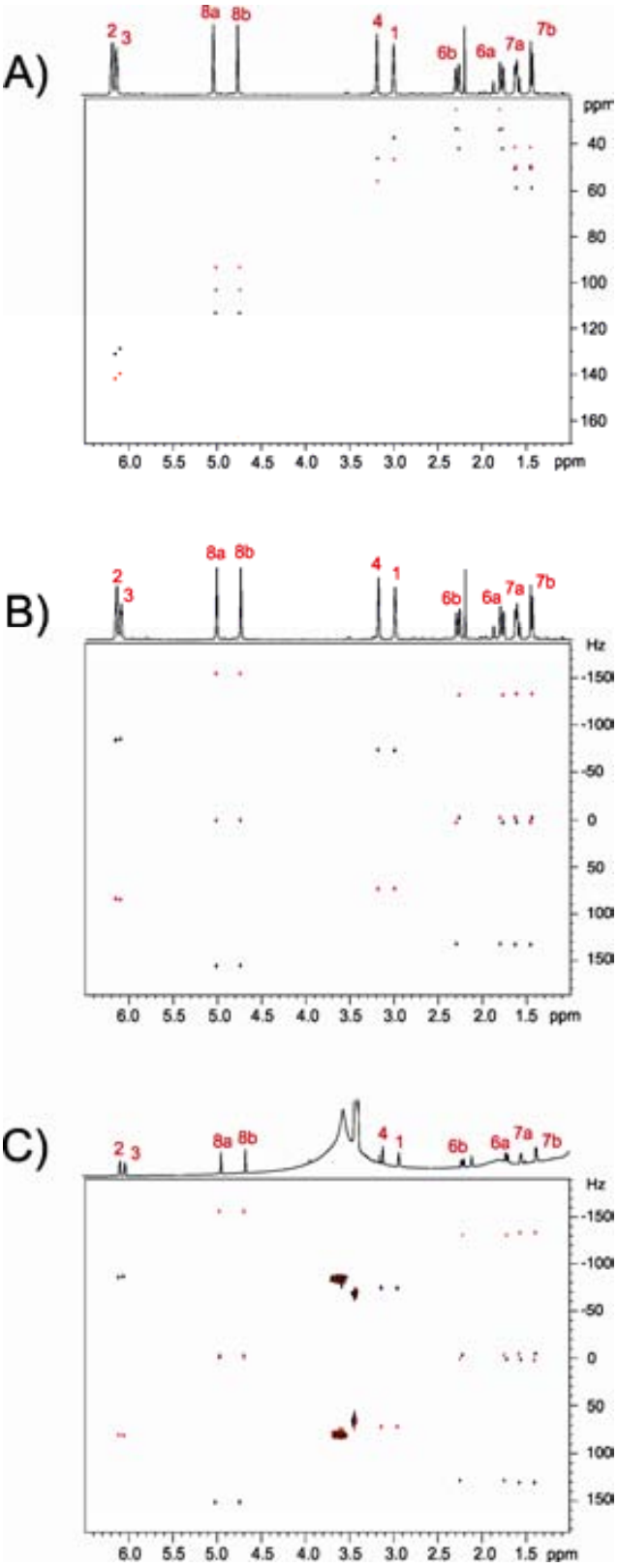

Figure S3: A) ω_1-iINEPT and B) ω_1-iINEPT-J spectra of **2** in isotropic $CDCl_3$ solution; C) ω_1-iINEPT spectra of **2** in anisotropic conditions (PMMA gel swollen in $CDCl_3$). ω_1-iINEPT experiment (A) was acquired with an scaling factor of k=8 whereas B) and C) used K=1. Other experimental conditions as described for Fig. 5.

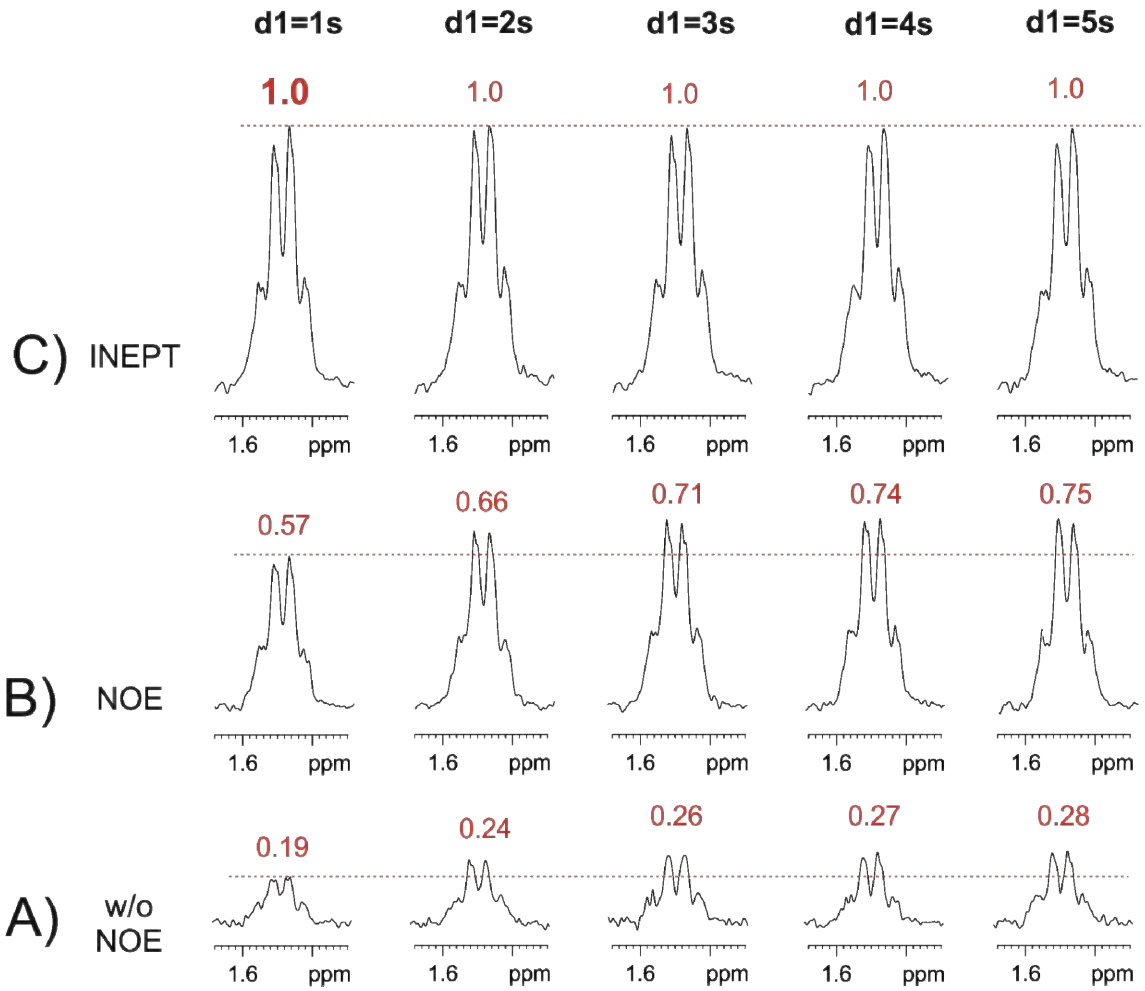

Figure S4: Signal intensity dependence of the H-8 proton in **3** as a function of the duration of the pre-scan delay: ω_1-iINEPT experiments A) without and B) with ^{1}H-saturation during the pre-scan delay, and c) ω_1-HSQC experiment using an initial INEPT transfer. As a reference, the intensity of the HSQC experiment using a recycle delay of 1 second has been normalized to 1.

Table S1: $^{1}J(CH)$ and $^{2}J(HH)$ coupling constants (in Hz) of strychnine (**1**) extracted from the ω_1-iINEPT-J spectrum.

		ω_1-iINEPT-J (This work)		**ref. [37]**	**ref. [36]**	**ref. [38]**	**ref. [5]**	**ref. [37]**	**ref. [39]**
		$^{1}J(CH)$	**$^{2}J(HH)$**	**$^{1}J(CH)$**				**$^{2}J(HH)$**	
C1	H1	158.9	-	158.0	158.8	159.0	159.0	-	-
C2	H2	161.7	-	162.0	160.7	161,3	161.56	-	-
C3	H3	160.3	-	159.0	-	159,4	159.85	-	-
C4	H4	169.1	-	168.2	168.7	168,6	168.4	-	-
C8	H8	144.9	-	145.1	144.7	144,9	144.89	-	-
C11 (from H11a)	H11a H11b	135.6 125.9	-18,1	133.8	134.9	135,3	135.06	-17,4	-17.38
C11 (from H11b)	H11a H11b	135.7 126.1	-18.3	125.2	125.8	125,5	126.08		
C12	H12	149.2	-	147.6	148.3	149,3	149.17	-	-
C13	H13	124.8	-	123.6	123.7	125,2	124.38	-	-
C14	H14	131.4	-	131.4	130.3	131,9	130.36	-	-
C15 (from H15a)	H15a H15b	131.3 129.6	-15.3	132.1	130.0	131,5	130.36	-14,5	-14.31
C15 (from H15b)	H15a H15b	130.7 129.6	-15.4	132.2	129.4	130,4	129.93		
C16	H16	146.8	-	146.9	145.9	146,3	146.6	-	-
C17	H17	133.1	-	134.0	134.2	133,1	132.93	-	-
C18 (from H18a)	H18a H18b	146.0 131.6	-10.3	139.7	147.1	147,6	146.17	-10,1	-
C18 (from H18b)	H18a H18b	146.1 131.3	-10.3	131.5	131.0	133,5	131.2		
C20 (from H20a)	H20a H20b	139.0 138.5	-15.6	137.7	138.4	139,7	138.91	-14,3	-14.74
C20 (from H20b)	H20a H20b	138.9 138.9	-15.5	137.7	138.7	139,9	138.91		
C22	H22	158.7	-	158.1	159.1	159,3	159.43	-	-
C23 (from H23a)	H23a H23b	145.1 137.3	-13.7	144.7	145.5	145,9	145.74	-13,7	-13.44
C23 (from H23b)	H23a H23b	145.6 137.2	-13.8	136.8	136.0	137,2	137.2		
Digital Resolution (Hz)		0.5	1.1	1.0	-	0.4	0.2	1.0	-

Table S2: $^{1}J(CH)$/ $^{1}T(CH)$ and $^{2}J(HH)$/$^{2}T(HH)$ coupling constants (in Hz) of 5–methylene-2-norbornene (**2**) measured from ω_1-iINEPT-J experiments in isotropic and anisotropic weakly aligned media.

		Isotropic		Anisotropic			
		$^{1}J_{CH}$	$^{2}J_{HH}$	$^{1}T_{CH}$	$^{2}T_{HH}$	$^{1}D_{CH}$ [a]	$^{2}D_{HH}$ [b]
C_1	H_1	147.2	-	147.9	-	0.7	-
C_2	H_2	168.9	-	168.2	-	-0.7	-
C_3	H_3	170.8	-	170.2	-	-0.6	-
C_4	H_4	148.3	-	148.8	-	0.5	-
C_6 (from H_{6a})	H_{6a}	136.0	-15.1	134.4	-18.9	-1.6	-3.8
	H_{6b}	130.7		130.1		-0.6	
C_6(from H_{6b})	H_{6a}	136.0	-15.3	134.1	-19.4	-1.9	-4.1
	H_{6b}	130.4		130.1		-0.3	
C_7 (from H_{7a})	H_{7a}	136.8	-8.1	137.8	-5.0	1.0	3.1
	H_{7b}	131.4		130.8		-0.6	
C_7 (from H_{7b})	H_{7a}	136.8	-8.1	137.9	-5.1	1.1	3.0
	H_{7b}	131.5		130.9		-0.6	
C_8 (from H_{8a})	H_{8a}	157.0	1.1	157.5	0.9	0.5	-0.2
	H_{8b}	155.1		155.3		0.2	
C_8 (from H_{8b})	H_{8a}	157.1	1.0	157.6	0.8	0.5	-0.2
	H_{8b}	155.1		155.4		0.3	
Digital Resolution (Hz)		0.5	0.9	0.5	0.9		

[a] RDCs ($^{1}D_{CH}$) values calculated from the different between the $^{1}T_{CH}$ values and the corresponding isotropic $^{1}J_{CH}$ values.
[b] RDCs ($^{2}D_{HH}$) values calculated from the different between the $^{2}T_{HH}$ values and the corresponding isotropic $^{2}J_{HH}$ values.

Table S3: $^{1}J(CH)$ and $^{2}J(HH)$ coupling constants of progesterone (**3**) measured from ω_1-iINEPT and ω_1-HSQC experiments.

		ω_1-iINEPT		**ω_1-HSQC**	
		$^{1}J(CH)$	**$^{2}J(HH)$**	**$^{1}J(CH)$ [a]**	**$^{2}J(HH)$**
C1 (from H1ax)	H1ax H1eq	126.8 129.9	-13.5	256.7	-13.8
C1 (from H1eq)	H1ax H1eq	126.5 127.7	-13.6	256.2	-13.3
C2 (from H2ax)	H2ax H2eq	123.9 132.1	-16.7	255.7	-16.6
C2 (from H2eq)	H2ax H2eq	124.3 132.3	-16.9	255.9	-16.9
C4	H4	158.8	-	158.7	-
C6 (from H6ax)	H6ax H6eq	124.8 130.6	-14.3	255.3	-14.5
C6(from H6eq)	H6ax H6eq	125.1 130.7	-14.4	255.1	-14.2
C7 (from H7ax)	H7ax H7eq	124.7 130.4	-13.2	254.5	-13.4
C7 (from H7eq)	H7ax H7eq	124.6 130.2	-13.3	254.5	-13.0
C8	H8	124.4	-	123.7	-
C9	H9	122.9	-	123.6	-
C11 (from H11ax)	H11ax H11eq	125.3 127.8	-9.5	253.7	-9.7
C11 (from H11eq)	H11ax H11eq	126.2 128.3	-10.8	253.8	-10.6
C12 (from H12ax)	H12ax H12eq	127.3 126.4	-13.7	256.2	-13.7
C12 (from H12eq)	H12ax H12eq	127.2 126.9	-13.5	256.1	-13.7
C14	H14	124.0	-	124.1	
C15 (from H15ax)	H15ax H15eq	130.7 132.4	-12.6	262.2	-12.9
C15 (from H15eq)	H15ax H15eq	ov 132.9	-13.7	262.1	-12.9
C16 (from H16ax)	H16ax H16eq	128.2 133.6	*	260.5	*

C16 (from H16eq)	H16ax H16eq	127.1 133.5	*	261.1	*
C17	H17	127.5	-	127.9	-
C18	H18	125.6	-	125.5	-
C19	H18	127.4	-	127.0	-
C21	H19	126.8	-	127.2	-
Digital Resolution (Hz)		1.5	0.5	1.5	0.5

[a] For diastereotopic CH_2 protons, only the sum of ^1J(CHA) and ^1J(CHB) is obtained.

IV. APPENDIXES

APPENDIX ONE

Simultaneous determination of multiple heteronuclear coupling constants

This section contains some of the work that, because of the timing problems, it has not been included as Publications. It is basically focused on the simultaneous measurement of several coupling constants in a single 2D NMR experiment by using some of the pulse sequences developed and introduced in Results and Discussion section. It will be shown how such simultaneous measurement can be achieved by using two different concepts:

- The presence of a high-abundant passive spin
- The use of Time-Shared (TS) 2D NMR experiments

Additionally, these two concepts can be combined allowing us to obtain even more information:

- TS Experiments in compounds having a high-abundant passive spin

The presence of passive spin effects in selHSQMBC-like experiments

When the original selHSQMBC pulse scheme is applied on molecules containing a passive high-abundant spin Z, such as ^{19}F or ^{31}P, the additional measurement of J(ZH) and J(XZ) is feasible from the complementary E.COSY [1] coupling pattern, independently to the measurement of J(CH) from the IPAP pattern. The selHSQMBC method is a frequency-selective experiment and, in principle, they provide J values for a single resonance, although it can be also collected for an increase number of signals by using regions-selective pulses on non-J-coupled protons. Otherwise, selHSQMBC experiments[2] involve pure in-phase magnetization, and therefore the incorporation of a TOCSY transfer allows to extend the determination of all J(ZH), J(XZ) and J(CH) coupling constants for an entire ^{1}H spin system[3] in a very easy way thanks to the pure IP nature of the cross-peaks obtained due to the use of selective proton pulses in the INEPT transfer that completely remove any J(HH) modulation.

A schematic representation showing the IPAP methodology in selHSQMBC when a high-abundant Z nucleus acts as a passive spin is shown in **Fig. 4.01**. Two complementary IP and AP data are acquired and then combined (IP±AP) to obtain α/β sub-spectra. Coupling constant values are extracted as shown in the panels. The relative tilting of the E.COSY pattern provide information about the relative signs of the involved couplings.

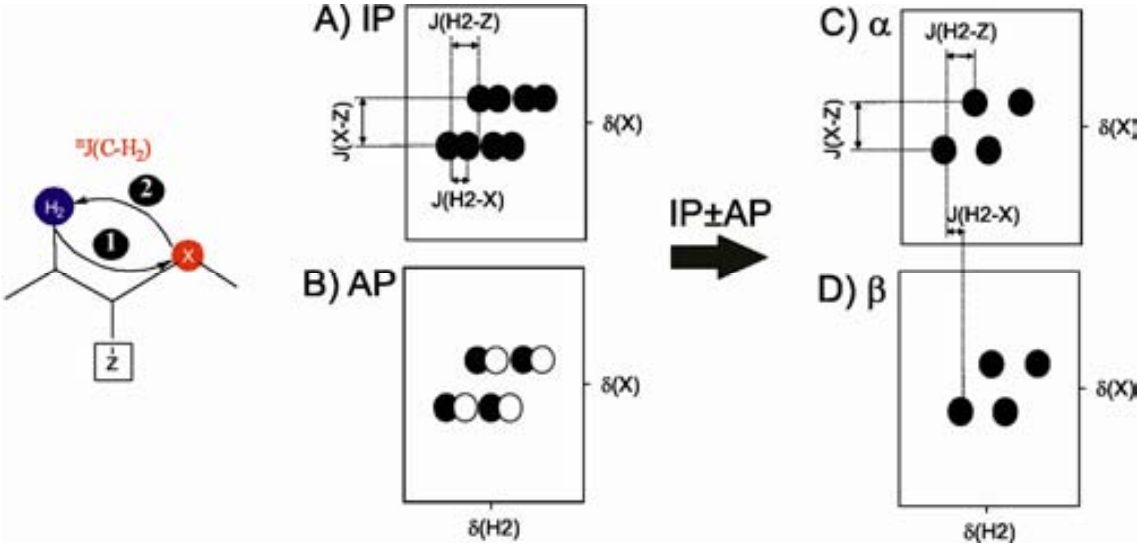

Figure 4.01. Schematic representation showing the IPAP methodology in selHSQMBC when a high-abundant nucleus acts as a passive spin

[1] C. Griesinger, O. W. Sørensen, R. R. Ernst. *J. Am. Chem. Soc*. **1986**, 107, 6394.

[2] S. Gil, J.F. Espinosa, T. Parella. *J. Magn. Reson*. **2011**, 213, 145.

[3] J. Saurí, J.F. Espinosa, T. Parella. *Angew. Chem. Intl. Ed*. **2012**, 51, 3919.

a) Passive spin in selHSQMBC IPAP experiment

A real example is shown in **Fig. 4.02** corresponding to the 2D ^{1}H-^{13}C selHSQMBC-IPAP experiment after selective excitation of the H1 proton of allyltriphenylphosphonium bromide. IP data yield ^{n}J(PH) in the detected dimension as well as J(CP) in the indirect dimension thanks to the E.COSY pattern generated by the presence of the passive ^{31}P spin. The arrows indicate the relative sign of J(CP) and the relative displacement between α/β cross-peaks allows the accurate measurement of ^{n}J(CH).

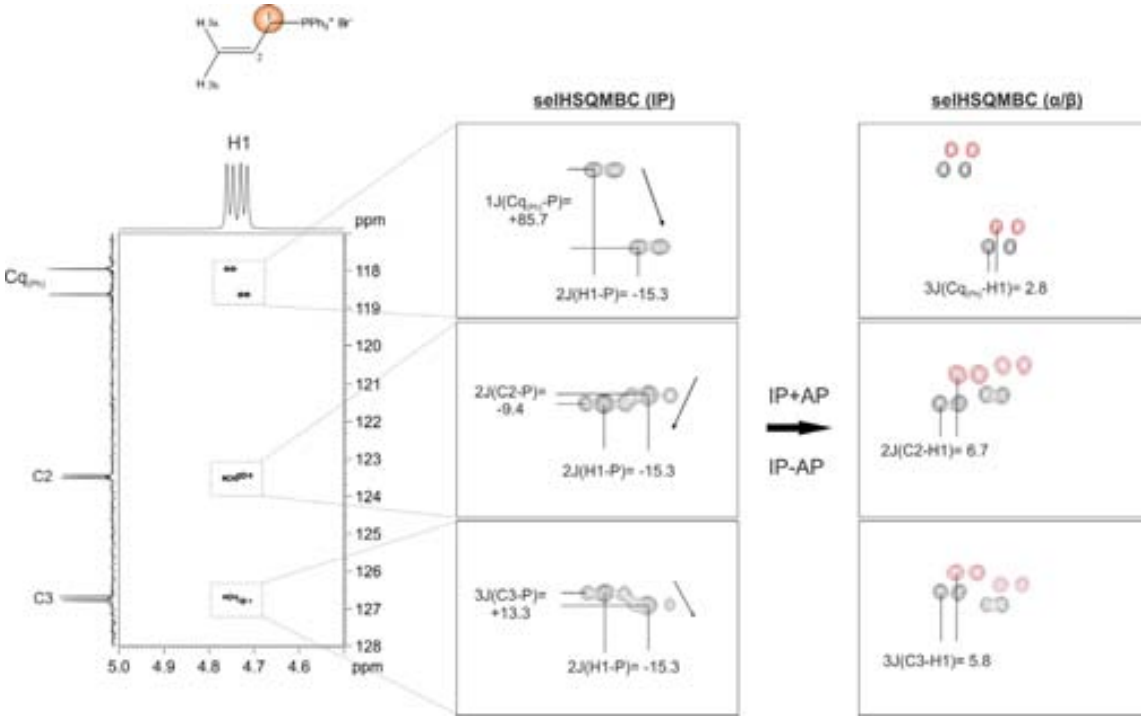

Figure 4.02. Expanded area corresponding to 2D ^{1}H-^{13}C selHSQMBC-IPAP after selective excitation of the H1 proton of allyltriphenylphosphonium bromide.

b) Passive spin in selHSQMBC-TOCSY IPAP experiment

The related selHSQMBC-TOCSY experiment allows extend all the features from selHSQMBC IPAP experiment to other protons belonging to the same spin system (**Fig. 4.03)**. Positive tilt means the same sign, while negative sign means opposite sign. Assuming that ^{3}J(PH) are positive, we can stay that ^{1}J(CP) are positive, ^{2}J(CP) negative and ^{3}J(CP) positive again.

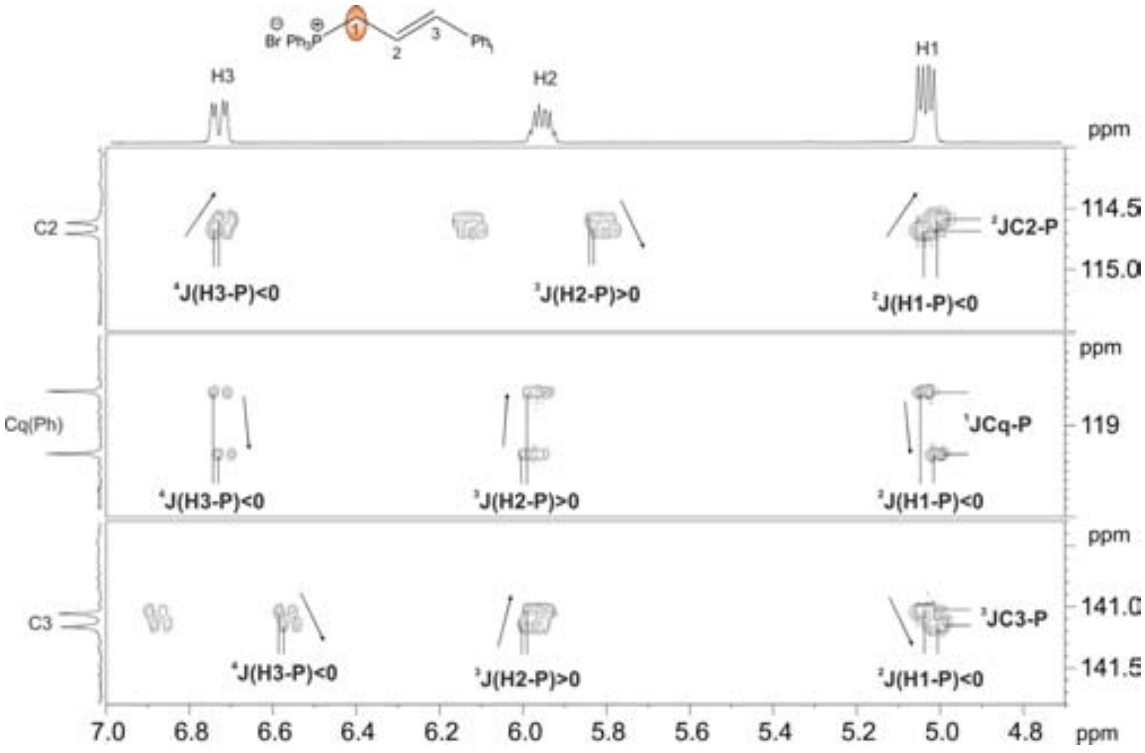

Figure 4.03. Relative E.COSY multiplet tilting in the relayed cross-peaks obtained in a pure in-phase 2D ^{1}H-^{13}C selHSQMBC-TOCSY spectrum of cinnamyltriphenylphosphonium bromide after selective excitation of the H1 proton. The passive ^{31}P nucleus allows the determination of the sign and the magnitude of from the relative E.COSY pattern generated along the indirect F1 dimension. Note that the relative sign between J(CP) and J(HP) can be easily determined taken from the relative tilt of the E.COSY pattern.

The selHSQMBC experiment can be successfully applied to other nuclei than X= ^{13}C and, for instance, the application of equivalent ^{1}H-^{15}N selHSQMBC and ^{1}H-^{15}N selHSQMBC-TOCSY counterparts on molecules containing nitrogen at natural abundance and fluorine nuclei allows the simultaneous measurement of a complete set of J(NH), J(NF), J(HF) coupling constants. For instance, the selHSQMBC-TOCSY IPAP spectrum of 2-fluoropyridine after selective excitation of the H4 proton is illustrated in **Fig. 4.04.** It is shown that under good digital resolution conditions, long-range J(NH) coupling values smaller than 2-3 Hz can be measured along the detected dimension using the IPAP technique, mainly because the intensity of the corresponding relayed cross-peaks depends of the efficiency of the starting N-H coupling.

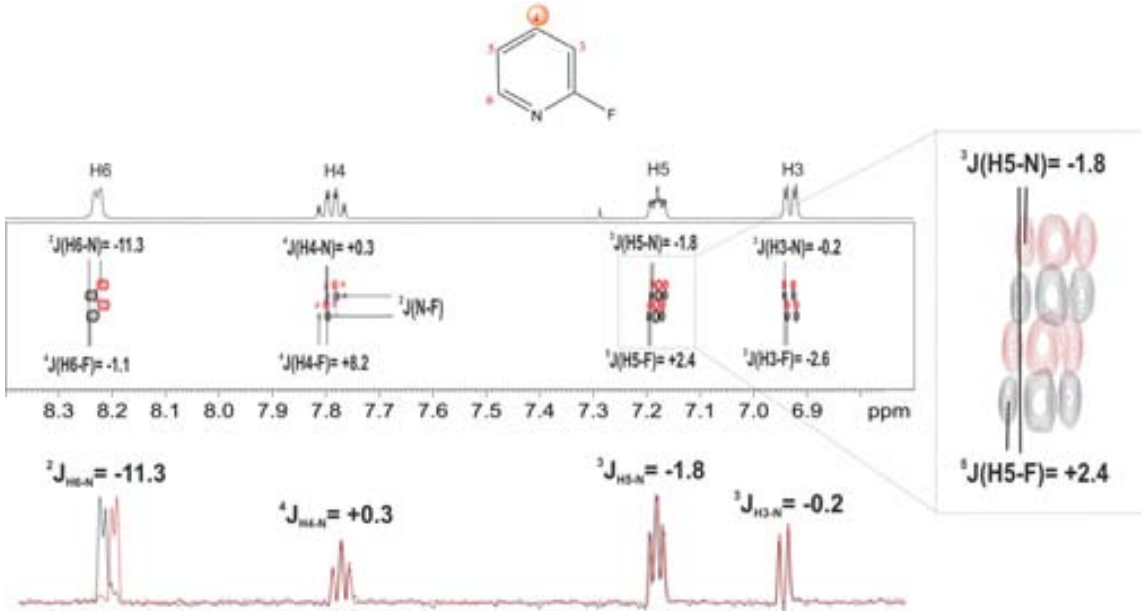

Figure 4.04. Expanded area showing α/β- spectra corresponding to 2D ^{1}H-^{15}N selHSQMBC-TOCSY IPAP experiment (pulse scheme of Fig. 1D) after selective excitation of H4 proton of 2-fluoropyridine. The passive ^{19}F nucleus allows the determination of the sign and the magnitude of J(NF) and J(HF) from the relative E.COSY pattern generated along the indirect F1 dimension, while the sign and the magnitude of ^{n}J(NH) are measured from the relative displacement of the α/β spectra as it is shown from the 1D slices.

Time-sharing selHSQMBC-like experiments

The most conventional strategies in NMR spectroscopy are based on the sequential acquisition of individual n experiments. However, the successful implementation of PFGs in 2D heteronuclear shift correlation pulse sequences allow an elegant way to select specific coherence pathways as well as purging undesired magnetization[4]. Taking profit of these advantages it is possible to simultaneously acquire information from different nuclei in a single correlation experiment. HSQC-like pulse sequences have the same coherence pathway irrespective to the nucleus (for instance ^{13}C or ^{15}N), being the optimization of the Δ delay the only real difference.

Time-shared (TS) NMR experiments[5] propose a new way to obtain information saving time by a simultaneous acquisition of n experiments that are further properly processed to separate the different information obtained (**Fig. 4.05**).

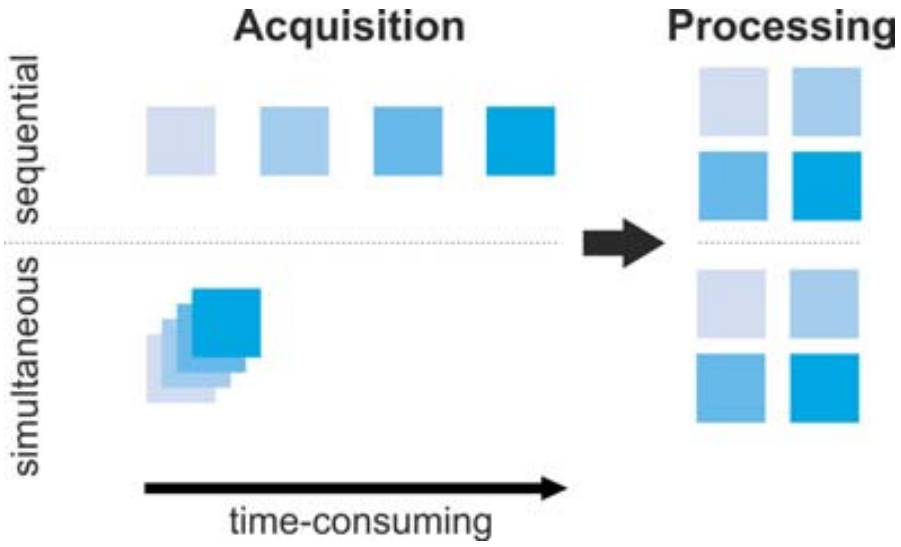

Figure 4.05. Comparison of sequential vs. simultaneous acquisition. Note that the same information is obtained in the processing step.

The concept used in TS experiments can be described as the simultaneous evolution of two different heteronuclear frequencies into the same t_1 period. For instance, an example of TS concept introduced into the selHSQMBC IPAP pulse sequence is shown in **Fig. 4.06.**

[4] a) T. Parella. *Magn. Reson. Chem.* **1998**, 36, 467, b) M. Sattler, J. Schleucher, C. Griesinger. *Prog. Nucl. Magn. Reson. Spectrosc.* **1999**, 34, 93.

[5] a) P. Nolis, T. Parella. *J. Biomol. NMR*. **2007**, 37, 65. b) M. Pérez-Trujillo, P. Nolis, T. Parella. *Org. Lett*. **2007**, 9, 29, c) P. Nolis, M. Pérez-Trujillo, T. Parella. *Angew. Chem. Int. Ed*. **2007**, 46, 7495, d) P. Nolis, M. Pérez, T. Parella. *Magn. Reson. Chem*. **2006**, 44, 1031.

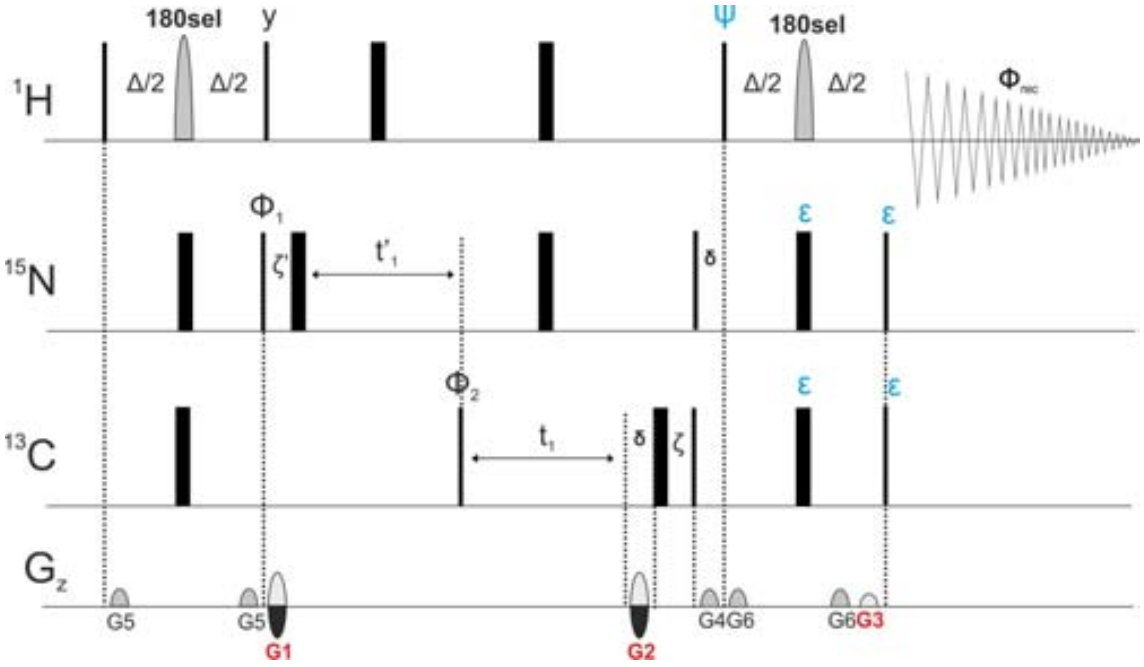

Figure 4.06. Pulse schemes of the time-shared version of the ^{1}H-^{13}C-^{15}N selHSQMBC experiment. The interpulse delays are optimized to Δ=1/(2·^{n}JXH). IP: Ψ= y, ε= on. AP: Ψ= x, ε= off. A minimum two-step phase cycle is needed: ϕ_1=x,-x, ϕ_2=-x,x and ϕ_{rec}=x,-x. Gradients G1, G2 and G3 are used for coherence pathway selection using echo-antiecho, G5 acts as a zz-filter, G4 and G6 flank the inversion proton pulses to generate pure refocusing elements. The ratios between gradients G1:G2:G3:G4:G5:G6 were set to 80:20.1:8.1:50:17:11.

Two independent IP and AP datasets are separately collected as a function of the pulses marked with ϕ: IP (Ψ=y and ε=on) and AP (Ψ=x and ε=off). α- and β- data are obtained after time-domain data addition/subtraction (AP±IP).

Several aspects should be taken into account when implementing TS in a given pulse scheme. On the one hand, spectral windows must be optimized for the independent evolution of ^{13}C and ^{15}N chemical shift during t_1 and t'_1 periods. Such periods are implemented according to $\Delta t_1 = 1/(SW(^{13}C))$ and $\Delta t'_1 = 1/(SW(^{15}N)) - 1/(SW(^{13}C))$ in order to allow ^{15}N heteronuclear evolution and to incorporate ^{13}C evolution within the period of ^{15}N evolution (**Fig. 4.07**).

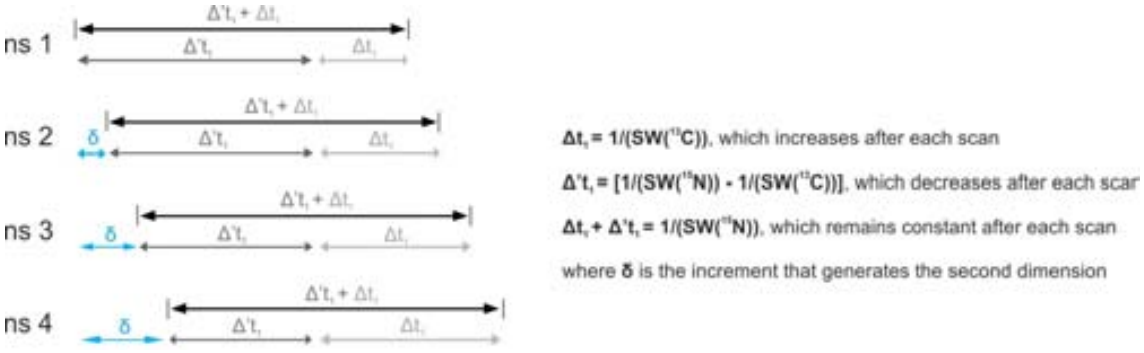

Figure 4.07.

Because ^{13}C evolution period is inserted into the ^{15}N evolution period, ζ and ζ' delays need to be reorganized for a proper setting up of the pulse sequence, so that

ζ = t_1 + δ + 180º H pulse

ζ' = t'_1 + 2(180º H pulse) + 90º C pulse + t_1 + δ + 180º C pulse + ζ

On the other hand, it is also important to consider the different values of $^{n}J(CH)$ and $^{n}J(NH)$ when optimizing the inter-pulse Δ delays. However, as these values cover the same ranges (from 0 to 12Hz) for both nucleus, concatenated ^{13}C and ^{15}N periods are not really needed.

To identify cross-peaks belonging to ^{13}C or ^{15}N, data collection must include a differential setting on the relative phase between the 90º ^{15}N and ^{13}C pulses just before t_1 (marked ϕ_1 and ϕ_2, respectively in Fig. 4.06). If the phases of the first 90º pulse are the same for both nuclei (ϕ_1=x, ϕ_2=x) the signals are acquired with the same amplitude modulation. On the contrary, if one of these phases is 180º inverted with respect to the other phase (ϕ_1=x, ϕ_2=-x) the signals of both nuclei will show inverse amplitude modulation. In order to separate the signals for each nucleus, the acquisition of two complementary spectrums in where the first one is recorded using ϕ_1=ϕ_2= x, and the second one using ϕ_1=x, ϕ_2=-x, is required. Then, by addition and subtraction of these two spectra, two new spectra providing independent ^{1}H-^{13}C and ^{1}H-^{15}N shift correlations are obtained. Additionally, IP and AP data might be also acquired in order to achieve α/β spin-selected editing. Thus, a four-step acquisition procedure is recommended to achieve this double nucleus-editing and α/β-editing procedure. Data addition/subtraction in the time-domain followed by conventional processing yield separate $^{13}C/^{15}N$ doubly-edited spectra, retaining the maximum sensitivity levels thanks to the Hadamard-type data combination (**Fig. 4.08**).

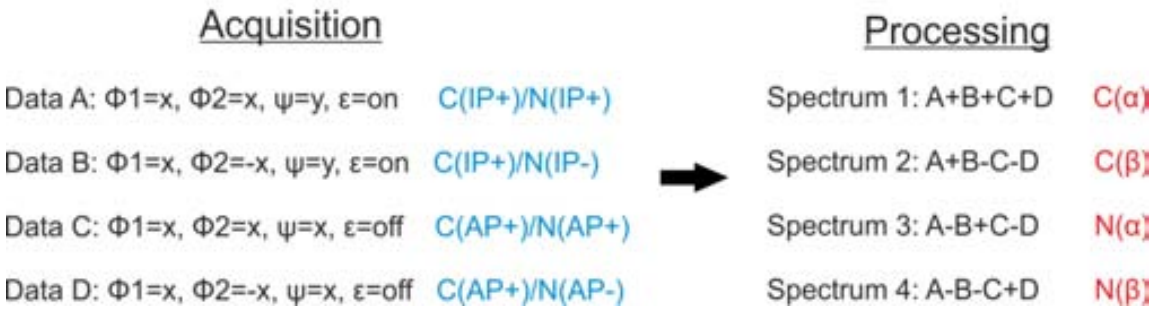

Figure 4.08. Acquisition and processing protocols followed in time-sharing experiments. Four different data are collected by setting two different variables: ϕ_1 for nuclei editing purposes and Ψ/ε for IPAP editing. These data are further combined to provide four separate data that are processed in the usual way to yield the corresponding spin-state selective α/β- spectra.

a) TS-selHSQMBC IPAP

Fig. 4.09 shows a practical example of the TS-selHSQMBC-IPAP experiment using 1,7-phenantroline as a nitrogen containing compound, for the simultaneous measurement of $^{n}J(CH)$ and $^{n}J(NH)$ of the selected H2 and H8 non-mutually coupled protons.

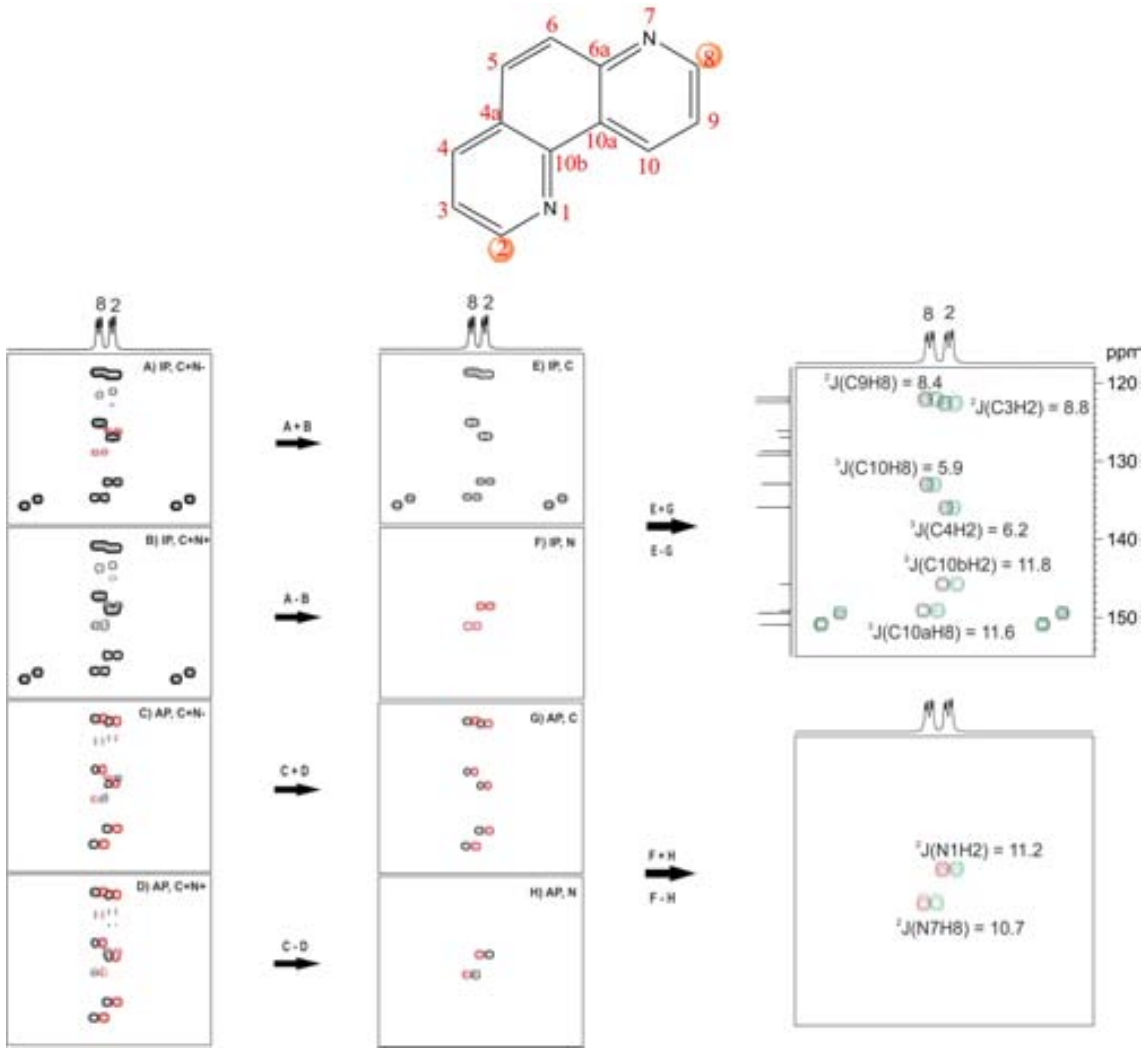

Figure 4.09. TS-selHSQMBC-IPAP spectra of 1,7-phenantroline compound after selective inversion of non-mutually coupled protons H8 and H2. A) IP data where ^{13}C and ^{15}N nuclei present opposite phase, B) IP data where both ^{13}C and ^{15}N nuclei show the same phase, C) AP data where ^{13}C and ^{15}N nuclei have opposite phase, D) AP data where both ^{13}C and ^{15}N nuclei show the same phase, E) IP data showing only ^{13}C nucleus, F) IP data showing only ^{15}N nucleus, G) AP data showing only ^{13}C nucleus, H) AP data showing only ^{15}N nucleus. At the top-right corner it is shown the α/β- spectra corresponding to ^{13}C nucleus from which the extraction on $^{n}J(CH)$ is performed. At the bottom-right corner it is shown the α/β- spectra corresponding to ^{15}N nucleus from which the extraction on $^{n}J(NH)$ is performed.

b) TS-selHSQMBC-TOCSY IPAP

The TS concept can also be implemented in selHSQMBC-TOCSY pulse sequence in where more additional information is obtained due to the efficient J(HH) transfer (**Fig. 4.10**).

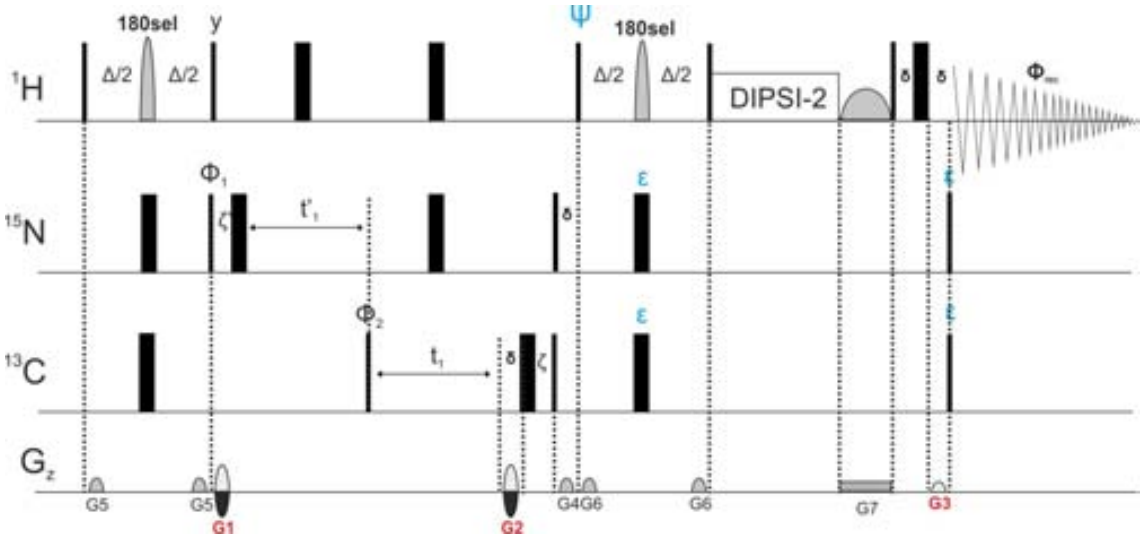

Figure 4.10. Pulse scheme of the time-shared version of the ^{1}H-^{13}C-^{15}N selHSQMBC-TOCSY experiment. The interpulse delays are optimized to Δ=1/(2·^{n}JXH). IP: Ψ= y, ε= on. AP: Ψ= x, ε= off. A minimum two-step phase cycle is needed: ϕ_1=x,-x, ϕ_2=-x,x and ϕ_{rec}=x,-x. Gradients G1, G2 and G3 are used for coherence pathway selection using echo-antiecho, G5 acts as a zz-filter, G4 and G6 flank the inversion proton pulses to generate pure refocusing elements, and G7 for ZQ suppression. The ratios between gradients G1:G2:G3:G4:G5:G6:G7 were set to 80:20.1:8.1:50:17:11:3.

Fig. 4.11 shows the resulting doubly-edited TS-selHSQMBC-TOCSY spectra that allow extend the measurement to all other protons belonging to the same ^{1}H spin system as well as to the sign information. The same procedure as described for the TS-selHSQMBC IPAP experiment has been used.

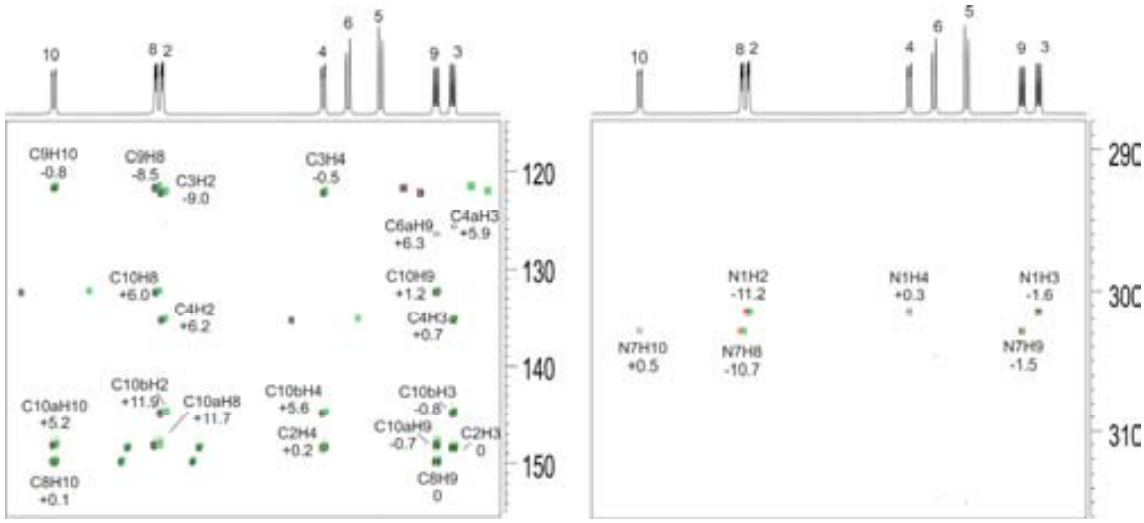

Figure 4.11. TS-selHSQMBC-TOCSY IPAP experiment in 1,7-phenantroline after selective inversion of non-mutually coupled protons H8 and H2. Left: α/β- spectra corresponding to the ^{13}C nucleus; Right: α/β- spectra corresponding to the ^{15}N nucleus.

Combining time-sharing & passive spin effects in selHSQMBC-like experiments

TS-selHSQMBC-like experiments show interest when applied to molecules containing high-abundant passive spins. For instance, the equivalent TS-selHSQMBC-TOCSY IPAP spectrum on 2-fluoropyridine compound afford an increased number of cross-peaks from which a complete set of magnitudes and signs of heteronuclear $^{n}J(CH)$, $^{n}J(NH)$, $^{n}J(CF)$, $^{n}J(NF)$ and $^{n}J(FH)$ coupling constants can be extracted from a single NMR experiment (**Fig. 4.12**).

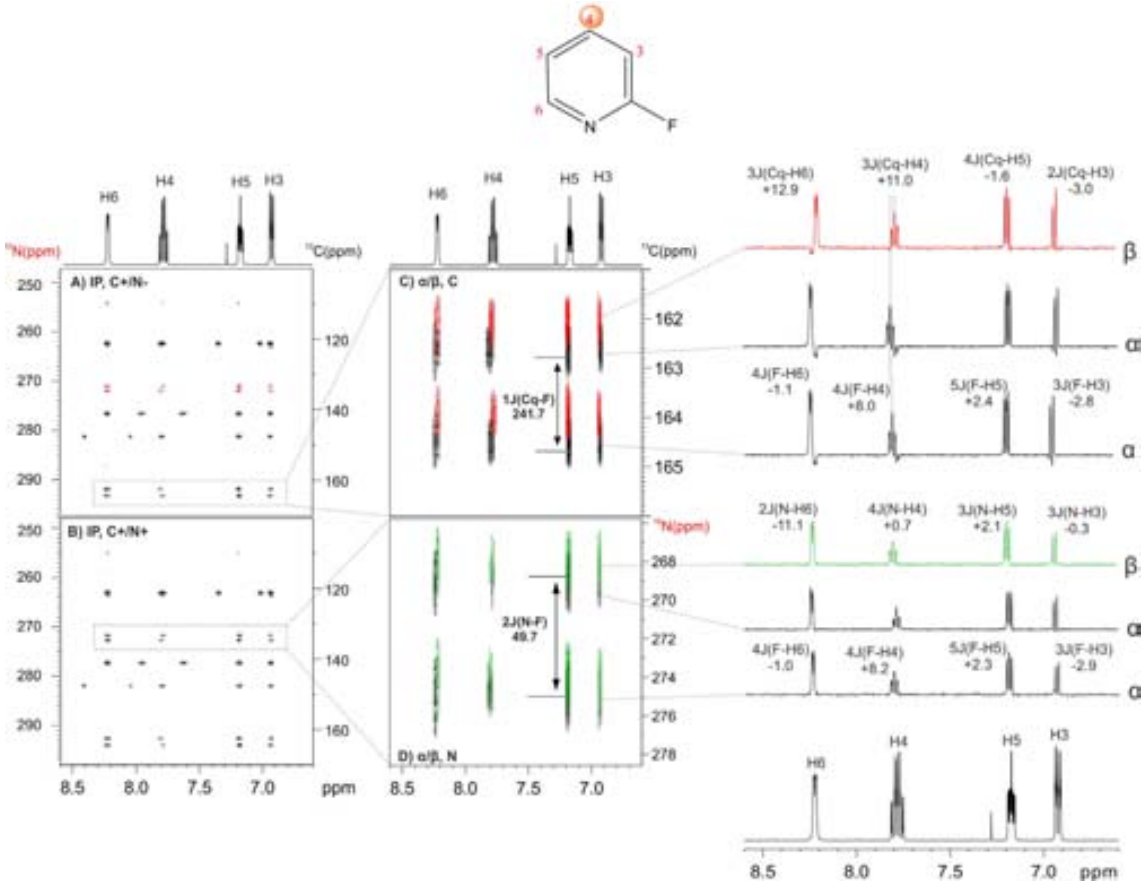

Figure 4.12. TS-selHSQMBC-TOCSY IPAP experiment in 2-fluoropyridineafter selective inversion of H4 proton. A) IP data where ^{13}C and ^{15}N nuclei have opposite phase. B) IP data where ^{13}C and ^{15}N nuclei present the same relative phase. Expanded areas corresponding to the α/β- C) ^{13}C and D) ^{15}N sub-spectra. The extraction of the magnitude and the sign of all the coupling constants measured along the detected dimension are shown from the 1D slices at the right of the figure.

APPENDIX TWO

Towards Pure-Shift NMR

This appendix contains part of the work developed during my PhD that cannot be included in Results and Discussion section because it will be used for another doctoral thesis from our research group. Nevertheless, it is presented here as a collaborative work.

It is based on a new homodecoupling technique developed by our research group, denoted as HOmonuclear Band Selective (HOBS).

Implementation of the HOmodecoupled Band Selective (HOBS) technique into the selHSQMBC experiment

Over recent years, a significant interest has emerged to develop homodecoupled ^{1}H NMR spectroscopy techniques that offer increased resolution by simplifying the homonuclear splitting pattern, and therefore reducing signal overlapping. They are known as pure-shift NMR techniques[1].

There are several methodologies to achieve homodecoupling. Most of these experiments rely in spatial encoding selection and their reliable applicability strongly depends on the experimental sensitivity. For this reason, pure-shift experiments have been mainly reported for homonuclear applications because its implementation into heteronuclear inverse-detected experiments suffers of important sensitivity success. Using a different concept, a tilted pseudo-3D HMBC experiment has been proposed to achieve a pure-shift HMBC experiment with homodecoupling along the detected dimension by incorporating a J-resolved dimension into the HMBC pulse scheme.

Based on a real-time homodecoupling scheme propose by Zangger et al., our research group has recently developed a new pure-shift technique denoted as HOmodecoupled Band Selective (HOBS)[2] in where homodecoupling is achieved during detection by applying a pair of hard/semiselective 180º ^{1}H pulses (represented as solid and shaded shapes) at the middle of $2\Delta=AQ/n$ periods, in which AQ is the acquisition time and n the number of concatenated loops, Δ is the duration of gradients and δ the recovery delay (**Fig. 4.13**).

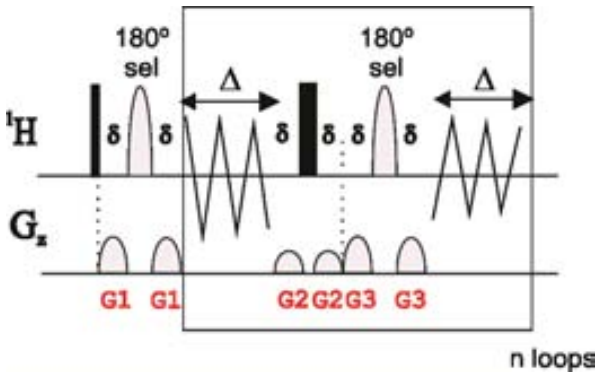

Figure 4.13. Schematic representation of the 1D homodecoupling band-selective (HOBS).

The HOBS method incorporates a number of advantages, such as: a) a good spectral quality related to the use of selective gradient echoes, b) real-time data collection without need of additional reconstruction methods that also allows conventional FID data processing and c) an easy implementation in multidimensional band-selective NMR experiments. On the

[1] a) A.J. Pell, J. Keeler. *J. Magn. Reson*. **2007**, 189, 293, b) Luy. *J. Magn. Reson*. **2009**, 201,18, c) K. Zangger, H. Sterk. *J. Magn. Reson*. **1997**, 124, 486, d) N.H. Meyer, K. Zangger. *Angew. Chem. Intl. Ed*. **2013**, 52, 7143, e) M. Nilsson, G.A. Morris, *Chem. Comm*. **2007**, 9, 933, f) J.A. Aguilar, S. Faulkner, M. Nilsson, G.A. Morris. *Angew. Chem. Intl. Ed*. **2010**, 49, 3901, g) G.A. Morris, J.A. Aguilar, R. Evans, S. Haiber, M. Nilsson. *J. Am. Chem. Soc.* **2010**, 132, 12770, h) J.A. Aguilar, A.A. Colbourne, J. Cassani, M. Nilsson, G.A. Morris. *Angew. Chem. Intl. Ed*. **2012**, 51, 6460, i) A. Lupulescu, G.L. Olson, L. Frydman. *J. Magn. Reson*. **2012**, 218 , 141, j) J.A. Aguilar, M. Nilsson, G.A. Morris. *Angew. Chem. Intl. Ed*. **2011**, 50, 9716.

[2] L. Castañar, P. Nolis, A. Virgili, T. Parella. *Chem. Eur. J.* **2013**, 19, 17283.

contrary important requirements are that i) proton-proton magnetization must be acquired as in-phase magnetization for a successful homodecoupling and ii) the selective pulse must be applied on non-mutually J-coupled protons.

For that reasons we thought that the HOBS methodology could be implemented into pure IP selHSQMBC experiments to obtain pure-shift band-selective heteronuclear correlation spectra, offering a considerable enhancement in terms of resolution and sensitivity[3] (**Fig. 4.14**).

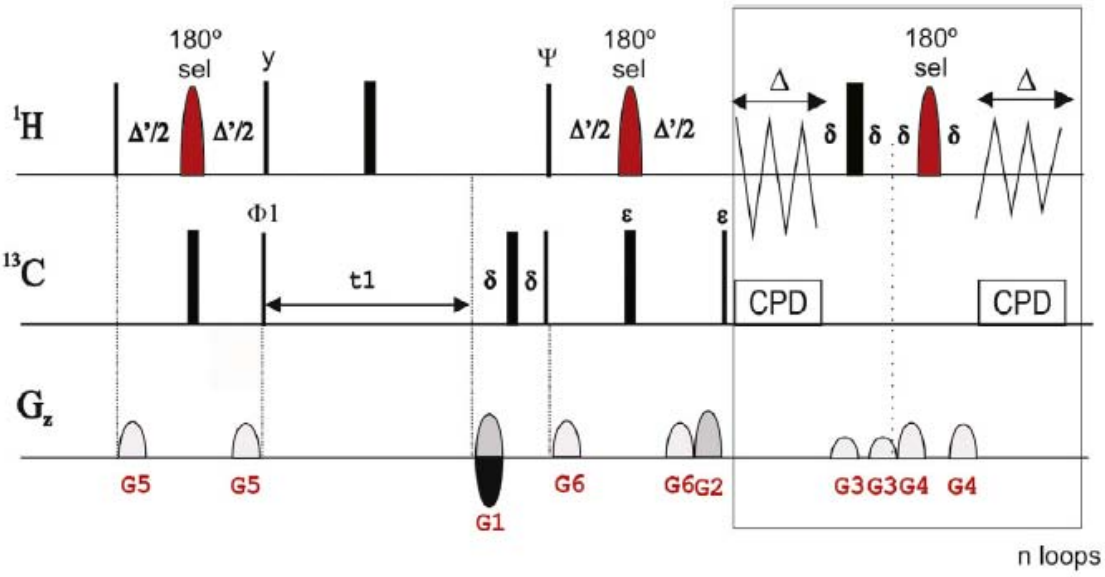

Figure 4.14. Experimental pulse schemes for the HOBS-selHSQMBC experiment. Thin and thick bars represent broadband 90º and 180º pulses, respectively, whereas shaped pulses are region-selective 180º pulses. The selective 180º ^{1}H pulse applied at the middle of INEPT periods and during detection have the same shape and duration and we found that REBURP pulses in the order of 3–10 ms provides the best result as a function of the required selectivity. The INEPT delays are set to 8 Hz. The basic phase cycling is ϕ1 = x, -x and ϕ(receiver) = x, -x; all other unlabeled pulses are from the x-axis. Optional heteronuclear decoupling (CPD) during data collection can also be applied as shown in the scheme. For the measurement of proton-carbon coupling constants, the IPAP methodology can be applied: two different IP and AP data are recorded without heteronuclear decoupling as a function of the last 90º and 180º ^{13}C pulses (IP: Ψ= y, ε = on; AP: Ψ = x, ε = off) and then they are added/subtracted to afford two separate α/β- subspectra.

We propose a completely new way to measure coupling constants in where all cross-peaks would appear homodecoupled from other protons resonating outside of the selected area, only displaying the active ^{n}J(CH) splitting. As the acquisition is made in the detected dimension high levels of spectral resolution can be easily reached and if the multiplet is resolved enough the extraction can be made by direct analysis of the cross-peak. In cases of poor resolved cross-peaks the technique is fully compatible with the IPAP methodology.

As the HOBS technique uses band selective pulses to reach an homodecoupled spectrum, peptides and proteins are good targets for evaluating the efficiency of band-selective NMR spectroscopy experiments because a set of equivalent spins (amide NH, Hα or

[3] L. Castañar, J. Saurí, P. Nolis, A. Virgili, T. Parella. *J. Magn. Reson.* **2014**, 238, 63.

aliphatic side-chain protons) appear in well-separated areas, and very importantly, they are not mutually coupled. An example of the HOBS-selHSQMBC experiment using the cyclic peptide cyclosporine A is presented in **Fig. 4.15** in where all the Hα protons have been selectively inverted.

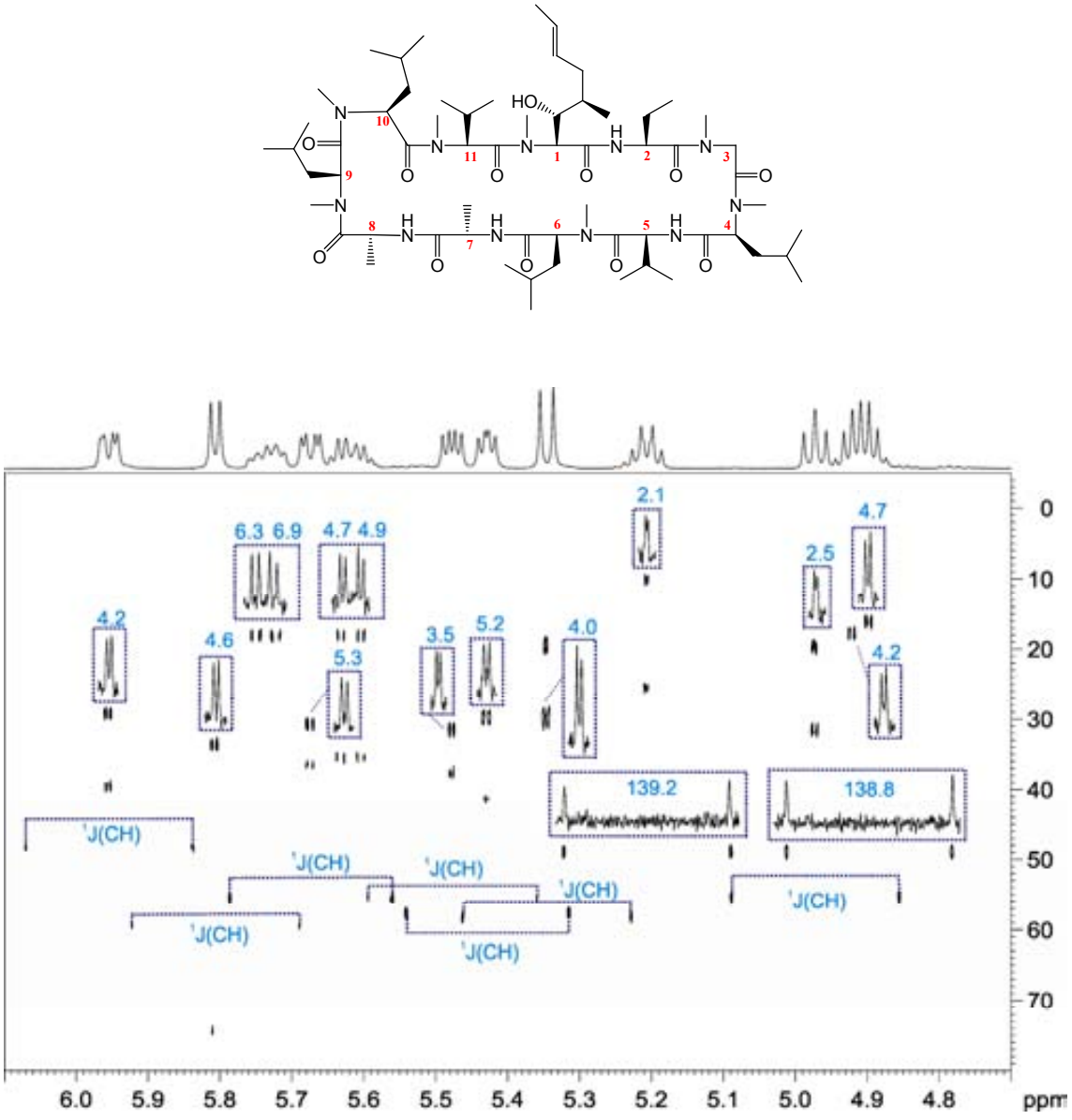

Figure 4.15. In-phase HOBS-selHSQMBC spectra of cyclosporine after applying a 5 ms ReBURP 180º pulse as a band-selective 180º H pulse on its Hα proton region. The value of J(CH) for all direct and long-range cross-peaks can be extracted directly from the analysis of the clean doublet along the detected dimension (see the extracted value in each individual 1D inset). Note that only the AB spin system (protons resonating at 5.62 and 5.73 ppm) appears as a double of doublets due to their mutual J(HH).

V. CONCLUSIONS

A. It has been demonstrated that the use of the CLIP technique in selHSQMBC-like experiments…

i. … offers the possibility to obtain pure IP multiplets exhibiting an extra splitting, so that the relevant $^{n}J(CH)$ value can be measured directly along the detected dimension as the difference in frequency between two peaks in resolved multiplets.
ii. … allows the easy extraction of $^{n}J(CH)$ even in complex and non-resolved cross-peaks by a fitting analysis.
iii. … avoids the tedious analysis of twisted-phase multiplets and also the uncertainty on the percentage of unwanted cross-talk related to IPAP experiments

B. It has been demonstrated that the IPAP methodology…

i. … Is a powerful technique for the accurate measurement of small heteronuclear coupling constants.
ii. … can be successfully applied in both selective and broadband HSQMBC and HMBC- based experiments, providing two equally distorted spin-state selective multiplets from which $^{n}J(CH)$ can be measured along the F2 dimension, irrespective of multiplet complexity and phase distortion.
iii. … represents a good alternative tool to extract coupling constants, avoiding fitting/matching procedures of AP or IP data.
iv. … can be simultaneously implemented together with other editing blocks, such as J-resolved spectroscopy and/or E.COSY pattern in a single NMR experiment, facilitating cross-peak analysis and expanding the possibility to obtain additional information about the magnitude and relative signs of J(HH) and $^{n}J(CH)$

C. It has been demonstrated that a TOCSY/COSY block inserted at the end of the pulse sequence in HSQMBC-like and HMBC-like experiments…

i. …extends the information into a given spin system via J(HH) transfer, offering thus an increased number of cross-peaks to be analysed and a complete set of J(CH) to be measured.
ii. … offers an excellent versatility to clean overlapped regions and make reliable measurements in congested areas.
iii. … offers the possibility to extract coupling values smaller than the line width because the intensity of a relayed cross-peaks only depends of the initial large long-range correlation and the efficiency of the TOCSY/COSY transfer.
iv. … preserves the α/β spin-state information of the heteronucleus, allowing the extraction of the relative sign of the coupling constant by applying the IPAP technique.
v. … proves to be a very powerful tool to show up some low-intensity and/or missing cross-peaks

D. It has been shown that the presence of a high-abundant passive spin in selHSQMBC-like experiments…

   i. … offers the possibility to simultaneously measure both the magnitude and the relative sign of different coupling constants thanks to the E.COSY patter generated along the indirect dimension.

E. It has been shown that the concept of Time-Shared NMR experiments…

   i. … can be successfully implemented in selHSQMBC-like experiments, allowing the simultaneously measurement of different coupling constants
   ii. … can be applied on compounds having high-abundant passive spins, extending even more the possibility to simultaneously measure both the magnitude and the sign of a complete set of homo- and heteronuclear coupling constants.

F. It has been shown that the homodecoupling HOBS technique…

   i. … can be successfully implemented into selHSQMBC experiment, offering a completely new way to measure heteronuclear coupling constants from simplified pure-shift multiplet patterns
   ii. … is able to retain the maximum sensitivity and offers enhanced resolution.

G. It has been demonstrated that the use of ^{13}C Boltzmann polarization as initial polarization transfer instead of the conventional INEPT transfer in F1-coupled HSQC related experiments…

   i. … allows observe the central lines of a diastereotopic CH_2 multiplet, which appear now resolved along the indirect dimension of a 2D spectrum, faciliting the measurement of the sign and the magnitude of $^{1}J(CH)$ and $^{2}J(HH)$ coupling constants. In addition, $^{1}J(CH)$ values for CH and CH_3 multiplets are also measured.

PULSE PROGRAMS

AND DATA SET EXAMPLES

In the following link you can find Data Set Examples of each Publication presented in the Thesis Work, as well as the corresponding Pulse Program Code for Bruker.

A png file with ^{1}H NMR and ^{13}C NMR assignments for Strychnine and 2-Fluoropyridine compounds is also available.

http://sermn.uab.cat/2014/04/josepsauri-phdthesis

.